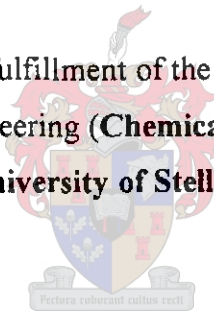


PREPARATION AND CHARACTERISATION OF PALLADIUM COMPOSITE MEMBRANES

by

JOHAN NICO KEULER

Thesis submitted in partial fulfillment of the requirements for the degree
Master in Engineering (**Chemical Engineering**)
at the **University of Stellenbosch**

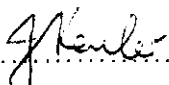


Supervisors: Prof. L Lorenzen
Prof. RD Sanderson

December 1997

DECLARATION

I, the undersigned hereby declare that the work contained in this thesis is my own original work and has not previously in its entirety or in part been submitted at any university for a degree.


.....
Signature

..... 02 / 10 / 97
Date

ABSTRACT

This study focuses on the preparation and characterization of palladium-silver-nickel composite membranes. Electroless plating was used to deposit thin metal films on alumina-zirconia membrane supports. Palladium conversion, in the electroless palladium plating process, was optimized with the aim of minimizing expensive palladium losses. The effect of deposition order on alloy composition and heat treatment on structural characteristics of the composite membrane was investigated.

The inorganic support membranes were thoroughly cleaned and pretreated prior to plating to catalyze the surface. Factorial designs were used to obtain the maximum palladium conversion. Tetra amine palladium nitrate gave better solution stability and resulted in higher conversions than tetra amine palladium chloride. Buffer pH values of 9 to 11 caused little variation in palladium conversion. Moving outside this range resulted in a sharp decline in palladium conversion. At a pH of 9 to 11 the stabilizer is in the correct ionic form (EDTA^{3-} and EDTA^{4-}) to best stabilize the palladium ions, and hydrazine acts as a proper reducing agent. Significant interactions existed between the EDTA concentration (stabilizer) and hydrazine concentration (reducing agent) and between EDTA and temperature. The EDTA concentration was the most sensitive variable. A 27.5 g 10% tetra amine palladium nitrate solution per liter plating solution was used. Conversions exceeding 80% were obtained after three hours plating with 20 ml plating solution at the following conditions: temperatures from 71 to 77 °C, 40-60% molar excess hydrazine, EDTA:Pd-salt molar ratios between 30:1 and 40:1 and buffer pH = 11.

Silver plating rates for two hours plating of up to 2 mg/cm² were obtained using a dilute silver nitrate solution with hydrazine as reducing agent. Electroless nickel plating was performed in a low temperature bath (40 °C) with nickel sulphate as source of metal ions and sodium hypophosphite as reducing agent.

Metal films were fully characterized before and after heat treatment for 5 hours in a hydrogen atmosphere at 650 °C. Scanning electron microscopy (SEM) was used to analyze the surface structure. X-ray diffraction (XRD) patterns were taken to examine alloying and detect

changes in the crystal structure after heating. Energy dispersive X-ray maps (EDS) were used to visualize the diffusion process and particle induced X-ray emission (PIXE) was used to construct concentration profiles across the thickness of the metal films.

Palladium deposits were dense, but columnlike, with a purity of 99.75%. Silver deposits were non-homogeneous, in other words it did not cover the entire substrate. The purity of the silver films was 99.5%. The nickel films were about 97% pure, very dense and defect free. When silver was deposited on palladium, the alloy penetrated more than 3 microns into the support and the palladium and silver concentrations varied across the thickness of the film after heating. By depositing palladium on silver, there was very little penetration into the support membrane pores (about 1 micron) and the palladium to silver ratio remained constant across the thickness of the film after heating.

Silver-palladium-nickel alloy films can be prepared by first depositing silver, then palladium and finally nickel. During heat treatment, a counter diffusion process took place and the smaller nickel atoms penetrated into pores and defects that might be present in the palladium-silver solid solution. By adding more than 3% nickel, dense defect free films can be prepared, which is much thinner than conventional palladium-silver films. This method makes it possible to reduce the film thickness of dense, non-porous films to less than 5 microns, reducing fabrication cost and increasing the hydrogen flux through the film. Dense, non-porous palladium-silver films are usually in the range of 10-15 microns.

OPSOMMING

Hierdie studie fokus op die bereiding en karakterisering van palladium-silwer-nikkel saamgestelde membrane. Dun films is deur die proses van elektrodelse platering neergeslaan op alumina-zirkonia membraanbasisse. Palladium omsetting in die elektrodelse palladium plateringsproses is geoptimeer met die doel om duur palladium verliese te minimeer. Onderzoek is ingestel na die effek van neerslag volgorde op allooï samestelling en na die uitwerking van hittebehandeling op die struktuur karakteristieke van die saamgestelde membraan.

Die anorganiese basismembrane is deeglik skoongemaak en vooraf behandel om die oppervlak te kataliseer en platering te versnel. Optimum palladium omsettings is bepaal deur gebruik te maak van faktoriaal ontwerpe. Tetra amien palladium nitraat lei tot beter stabiliteit van die plateringsoplossing en hoër omsettings as tetra amien palladium chloried. Buffer pH waardes van 9-11 het geen beduidende invloed op die palladium omsetting. Waardes buite hierdie gebied het 'n skerp afname in omsetting tot gevolg, want by 'n pH van 9 tot 11 is die stabiliseerder in die korrekte ioniese vorm (EDTA^{3-} en EDTA^{4-}) om die palladium ione die beste te stabiliseer en die reduseermiddel baie doeltreffend. Beduidende interaksies bestaan tussen EDTA konsentrasie (stabiliseerder) en hidrasien konsentrasie (reduseermiddel) en tussen EDTA en temperatuur. Die EDTA konsentrasie is die sensitiefste parameter. Die konsentrasie van die palladiumsout was 27.5 g 10% tetra amien palladium nitraat oplossing per liter plateringsoplossing. Omsettings van meer as 80% is behaal na drie ure platering met 20 ml oplossing by die volgende toestande: temperatuur tussen 71 °C en 77 °C, 40-60% oormaat hidrasien, EDTA: Pd-sout molêre verhouding van 30:1 tot 40:1 en buffer pH=11.

Silwer plateringstempo's vir twee ure platering van so hoog as 2 mg/cm² is verkry met 'n verdunde silwernitraat oplossing en hidrasien as reduseermiddel. Elektrodelse nikkel platering is uitgevoer in 'n lae temperatuur bad (40 °C) met nikkelsulfaat as bron van metaalione en natriumhipofosfiet as reduseermiddel.

Hittebehandeling is uitgevoer in 'n waterstofatmosfeer by 650 °C vir 5 ure. Metaalfilms is volledig gekarakteriseer voor en na hittebehandeling. Die oppervlak topografie is geanaliseer met behulp van 'n skanderings elektron mikroskoop. X-straal diffraksie patrone is geneem

om allooivorming te ondersoek en veranderinge in die kristalstruktuur na verhitting te identifiseer. Die diffusieproses is visueel ondersoek deur die energieverspreiding van X-strale te analiseer en partikel geïnduseerde X-straal emissie is gebruik om konsentrasieprofiel oor die dikte van die film te konstrueer.

Neergeslaande palladium films was dig en die struktuur kolomagtig. Film suiwerheid was 99.75%. Silwerneerslae was nie-homogeen en het nie die volle basismembraan bedek nie. Silwer suiwerheid was 99.5%. Nikkel films was 97% suiwer, baie dig en met geen sigbare defekte nie. Wanneer silwer op palladium gedeponeer word, penetreer die allooï ten minste 3 mikron in die basis se porieë in en palladium en silwer konsentrasies wissel oor die dikte van die film na hittebehandeling. Deponering van palladium op silwer lei tot slegs geringe penetrasie in die basismembraan in (ongeveer 1 mikron) en die palladium tot silwer verhouding bly konstant oor die dikte van die film na hittebehandeling.

Silwer-palladium-nikkel allooï films kan berei word deur eers silwer te deponeer, daarna palladium en laastens nikkel. Nikkel en silwer diffundeer in teenoorgestelde rigtings verby mekaar gedurende hittebehandeling. Die kleiner nikkel atome vul enige gapings en defekte wat in die palladium-silwer soliede oplossing gevorm word. Deur meer as 3% nikkel by te voeg, word 'n nie-poreuse, defek vrye membraan verkry wat dunner is as die konvensionele palladium-silwer membrane. Hierdie metode kan gebruik word om nie-poreuse films se dikte te verminder na minder as 5 mikron. Gevolglik is vervaardiging aansienlik goedkoper en kan 'n groter waterstofvloed deur die film verkry word. Die dikte van nie-poreuse palladium-silwer films is gewoonlik in die orde van 10-15 mikron.

ACKNOWLEDGEMENTS

I wish to express my gratitude to:

The **FRD** for financial contribution towards the project.

Prof. **VM Linkov** (from University of Western Cape) for supplying the membrane supports.

Prof. **L Lorenzen** for guidance and leadership during the project.

The **Microscope Unit** (especially Dane and Miranda) at the University of Cape Town for assisting with SEM work.

Mnr. **HS Pienaar** (US Geology Department) for helping with X-ray diffraction experiments.

Dr **V Prozesky** and Dr **WJ Przybylowicz** (both from the National Acceleration Centre) who assisted with PIXE experiments.

Prof. **RD Sanderson** for motivation and encouragement.

SASOL for sponsoring the project.

Dr **TJ v W. Kotze** (US Department of Statistics) for introducing me to statistical analysis and use of his computer packages.

Miss **EJ van Wyk** for proof-reading the thesis.

TABLE OF CONTENTS

| | |
|---|-----------|
| TABLE OF CONTENTS | I |
| LIST OF FIGURES | VI |
| LIST OF TABLES | XI |
| CHAPTER 1: INTRODUCTION | 1 |
| CHAPTER 2: BACKGROUND AND LITERATURE SURVEY | 4 |
| 2.1. SEPARATION PROCESSES | 4 |
| 2.2. INORGANIC MEMBRANES | 4 |
| 2.2.1. Types of inorganic membranes | 5 |
| 2.2.2. Preparation techniques for porous inorganic membranes | 7 |
| 2.2.2.1. Anodic oxidation | 7 |
| 2.2.2.2. Pyrolysis | 7 |
| 2.2.2.3. Phase separation and leaching | 8 |
| 2.2.2.4. Sol-gel process | 8 |
| 2.2.2.5. Slip casting | 8 |
| 2.2.2.6. Other methods | 9 |
| 2.2.3. Advantages of inorganic membranes | 9 |
| 2.2.4. Disadvantages and problems of inorganic membranes | 10 |
| 2.2.5. Applications | 10 |
| 2.3. PALLADIUM BASED CATALYTIC MEMBRANES | 12 |
| 2.3.1. Hydrogen permeation through palladium membranes | 12 |
| 2.3.2. Palladium alloy membranes | 13 |
| 2.3.2.1. Effect of alloying on hydrogen permeation | 13 |
| 2.3.2.2. Increasing membrane stability through alloying | 15 |
| 2.3.2.3. Alloying for catalytic purposes | 15 |

| | | |
|---|---|-----------|
| 2.3.3. | Applications for palladium based membranes | 15 |
| 2.3.3.1. | Hydrogenation | 16 |
| 2.3.3.2. | Dehydrogenation | 17 |
| 2.3.3.3. | Reaction coupling and decomposition reactions | 19 |
| 2.3.4. | Preparation techniques for palladium and palladium alloy membranes | 19 |
| 2.3.4.1. | Physical vapor deposition (PVD) | 20 |
| 2.3.4.2. | Quenching and rolling | 21 |
| 2.3.3.2. | Chemical vapor deposition (CVD) | 21 |
| 2.3.4.4. | Sol-gel process | 22 |
| 2.3.4.5. | Wet impregnation | 23 |
| 2.3.4.6. | Other solution based methods | 24 |
| 2.3.4.7. | Electroplating | 24 |
| 2.3.4.8. | Electroless plating | 25 |
| 2.3.4.8.1. | Substrate cleaning | 26 |
| 2.3.4.8.2. | Surface activation | 27 |
| 2.3.4.8.3. | General electroless plating solution compositions | 28 |
| 2.3.4.8.4. | Electroless silver plating | 29 |
| 2.3.4.8.5. | Electroless nickel plating | 30 |
| 2.3.4.8.6. | Electroless palladium plating | 31 |
| 2.3.4.8.7. | Palladium silver co-deposition | 33 |
| 2.3.5. | Palladium alternatives for hydrogen transport | 35 |
| 2.4. | MEMBRANE CHARACTERISATION | 36 |
| 2.4.1. | Particle induced X-ray emission (PIXE) | 37 |
| 2.4.2. | Scanning electron microscopy (SEM) | 38 |
| 2.4.3. | X-ray diffractometry (XRD) | 39 |
| 2.5. | GAS SEPARATION | 40 |
| CHAPTER 3: EXPERIMENTAL PROCEDURES | | 41 |
| 3.1. | INTRODUCTION | 41 |

| | | |
|---|---|-----------|
| 3.2. | MEMBRANE FABRICATION | 41 |
| 3.2.1. | Membrane characteristics | 42 |
| 3.3. | MEMBRANE CLEANING | 42 |
| 3.4. | MEMBRANE PRETREATMENT | 42 |
| 3.5. | ELECTROLESS PLATING | 44 |
| 3.5.1. | Safety procedures | 44 |
| 3.5.2. | Electroless palladium plating | 44 |
| 3.5.3. | Electroless silver plating | 45 |
| 3.5.4. | Electroless palladium-silver co-deposition | 46 |
| 3.5.5. | Electroless nickel plating | 47 |
| 3.6. | HEAT TREATMENT FOR CREATING PALLADIUM ALLOYS | 47 |
| 3.7. | ANALYTICAL TECHNIQUES | 49 |
| 3.8. | SUMMARY | 50 |
| CHAPTER 4: ELECTROLESS PALLADIUM PLATING | | 51 |
| 4.1. | INTRODUCTION | 51 |
| 4.2. | PROCESS VARIABLES | 51 |
| 4.3. | CHOICE OF CHEMICALS | 52 |
| 4.4. | FACTORIAL DESIGNS | 54 |
| 4.5. | KINETIC STUDY | 61 |
| 4.6. | EFFECT OF BUFFER pH ON PALLADIUM CONVERSION | 63 |
| 4.7. | COMBINED EFFECT OF TEMPERATURE AND EDTA CONCENTRATION ON Pd CONVERSION | 67 |
| 4.8. | COMBINED EFFECT OF HYDRAZINE AND EDTA ON Pd CONVERSION | 70 |
| 4.9. | SOLUTION STABILITY AND OPTIMUM PLATING CONDI-TIONS | 73 |
| 4.10. | MODELLING ELECTROLESS PALLADIUM PLATING | 75 |
| 4.11. | SUMMARY | 82 |
| CHAPTER 5: ELECTROLESS SILVER AND NICKEL PLATING | | 83 |
| 5.1. | INTRODUCTION | 83 |

| | | |
|-------------|--|-----------|
| 5.2. | PALLADIUM-SILVER CO-DEPOSITION | 83 |
| 5.2.1. | Dynamics of co-deposition | 85 |
| 5.2.2. | Non-ideal co-deposition behavior | 85 |
| 5.2.2. | Suggested palladium-silver co-deposition mechanism | 87 |
| 5.2.3. | Problems of palladium-silver co-deposition | 88 |
| 5.3. | ELECTROLESS SILVER PLATING | 88 |
| 5.3.1. | Plating on an activated substrate | 89 |
| 5.3.1. | Plating on a predeposited palladium film | 90 |
| 5.4. | ELECTROLESS NICKEL PLATING | 93 |
| 5.5. | PALLADIUM PLATING ON SILVER DEPOSITS | 95 |
| 5.6. | SUMMARY | 96 |

CHAPTER 6: SURFACE CHARACTERISATION USING SEM AND PIXE 97

| | | |
|--------------|--|------------|
| 6.1. | INTRODUCTION | 97 |
| 6.2. | REPRESENTATIVE SAMPLES | 97 |
| 6.3. | MEMBRANE SUPPORT | 98 |
| 6.4. | PURE PALLADIUM (a) | 99 |
| 6.5. | PURE SILVER (b) | 101 |
| 6.6. | PURE NICKEL (c) | 102 |
| 6.7. | Pd-Ni COMPOSITE MEMBRANE (94.6:5.4) (d) | 104 |
| 6.8. | Ag ON Pd COMPOSITE MEMBRANE (78:22) (e) | 105 |
| 6.9. | Pd ON Ag COMPOSITE MEMBRANE (24:76) (f) | 107 |
| 6.10. | Pd ON Ag COMPOSITE MEMBRANE (18:82) (j) | 108 |
| 6.11. | Pd ON Ag COMPOSITE MEMBRANE (10:90) (i) | 111 |
| 6.12. | Ag-Pd-Ni COMPOSITE MEMBRANE (26.4:67.9:5.7) (g) | 112 |
| 6.13. | SUMMARY | 113 |

CHAPTER 7: STRUCTURAL CHARACTERISATION USING XRD 115

| | | |
|-------------|--------------------------------------|------------|
| 7.1. | INTRODUCTION | 115 |
| 7.2. | PALLADIUM COATED MEMBRANE (a) | 115 |

| | | |
|-------|--|-----|
| 7.3. | SILVER COATED MEMBRANE (b) | 117 |
| 7.4. | NICKEL COATED MEMBRANE (c) | 118 |
| 7.5. | PALLADIUM-NICKEL COATED MEMBRANE (d) | 119 |
| 7.6. | PALLADIUM-SILVER COATED MEMBRANE (e) | 120 |
| 7.7. | SILVER-PALLADIUM (24:76) COATED MEMBRANE (f) | 121 |
| 7.8. | SILVER-PALLADIUM-NICKEL COATED MEMBRANE (g) | 123 |
| 7.9. | SILVER-PALLADIUM COATED MEMBRANES | 123 |
| 7.10. | SUMMARY | 126 |

CHAPTER 8: METAL DIFFUSION 127

| | | |
|------|---|-----|
| 8.1. | INTRODUCTION | 127 |
| 8.1. | DATA PROCESSING | 127 |
| 8.3. | HEAT TREATMENT | 129 |
| 8.4. | CONCENTRATION PROFILES FOR Pd-Ni (d + HEAT) | 129 |
| 8.5. | CONCENTRATION PROFILES FOR Pd-Ag (e + HEAT) | 131 |
| 8.6. | CONCENTRATION PROFILES FOR Ag-Pd (24:76) (f + HEAT) | 133 |
| 8.7. | CONCENTRATION PROFILES FOR Ag-Pd (18:82) (j + HEAT) | 134 |
| 8.8. | CONCENTRATION PROFILES FOR Ag-Pd-Ni (g + HEAT) | 137 |
| 8.9. | SUMMARY | 139 |

CHAPTER 9: CONCLUSIONS 141

REFERENCES 144

| | | |
|-------------|--|-----|
| APPENDIX A: | List of chemicals used in this study | 153 |
| APPENDIX B: | Electroless plating data | 155 |
| APPENDIX C: | Concentration profiles for simultaneous Ag and Pd deposition | 174 |
| APPENDIX D: | PIXE spectra for various metal films | 183 |
| APPENDIX E: | PIXE data from line scans after heating | 199 |
| APPENDIX F: | List of publications resulting from this thesis | 202 |

LIST OF FIGURES

CHAPTER 2

- Figure 2.1: Commercial silicon carbide and alumina membranes from ATECH
- Figure 2.2: Solubility of hydrogen in palladium-silver alloys
- Figure 2.3: Diffusion coefficients in palladium and palladium-silver alloys
- Figure 2.4: Permeability of hydrogen through palladium alloys at 350 °C and 2.2 Mpa
- Figure 2.5: Hydrogen permeabilities for various materials

CHAPTER 3

- Figure 3.1: Schematic representation of the set up for performing heat treatment

CHAPTER 4

- Figure 4.1: The effect of various Pd salts and reducing agents on mass Pd plated ($T = 64\text{ }^{\circ}\text{C}$)
- Figure 4.2: The effect of various Pd salts and reducing agents on Pd conversion
- Figure 4.3: Hydrazine-buffer pH interaction
- Figure 4.4: Hydrazine-temperature interaction
- Figure 4.5: Temperature-hydrazine interaction
- Figure 4.6: Temperature-buffer pH interaction
- Figure 4.7: Buffer pH-hydrazine interaction
- Figure 4.8: Buffer pH-temperature interaction
- Figure 4.9: The effect of EDTA concentration on Pd conversion
- Figure 4.10: Hydrazine-temperature interaction
- Figure 4.11: Hydrazine-EDTA interaction
- Figure 4.12: Temperature-hydrazine interaction
- Figure 4.13: Temperature-EDTA interaction
- Figure 4.14: EDTA-hydrazine interaction
- Figure 4.15: EDTA-temperature interaction
- Figure 4.16: The effect of buffer pH on Pd concentration profiles
- Figure 4.17: The effect of EDTA concentration on Pd concentration profiles

- Figure 4.18: The effect of temperature on Pd concentration profiles at various EDTA concentrations
- Figure 4.19: Effect of buffer pH on Pd conversion
- Figure 4.20: The effect of EDTA concentration on Pd conversion
- Figure 4.21: Distribution of ionic species of EDTA as a function of pH
- Figure 4.22: The effect of temperature on Pd conversion
- Figure 4.23: The effect of EDTA at various temperatures on Pd conversion
- Figure 4.24: The effect of EDTA at various temperatures on Pd conversion
- Figure 4.25: The effect of hydrazine on Pd conversion at different EDTA concentrations
- Figure 4.26: The effect of EDTA at various hydrazine concentrations on Pd conversion
- Figure 4.27: The effect of EDTA and hydrazine concentrations on Pd conversion
- Figure 4.28: EDTA: Pd-salt molar ratios required for stable plating solutions
- Figure 4.29: Effect of hydrazine, EDTA concentration on Pd conversion at 71 °C
- Figure 4.30: Pd conversion at hydrazine: Pd-salt molar ratio of 0.72:1
- Figure 4.31: Surface plot of hydrazine and EDTA (model 1)
- Figure 4.32: Surface plot of hydrazine and EDTA (model 2)
- Figure 4.33: Surface plot of temperature and EDTA (model 1)
- Figure 4.34: Surface plot of temperature and EDTA (model 2)
- Figure 4.35: Surface plot of hydrazine and temperature (model 1)
- Figure 4.36: Surface plot of hydrazine and temperature (model 2)
- Figure 4.37: Probability plot of residuals (model 1)
- Figure 4.38: Probability plot of residuals (model 2)

CHAPTER 5

- Figure 5.1: Concentration profiles for Pd in solution at various Ag concentrations
- Figure 5.2: Relationship between Pd in solution and Pd deposited on membrane
- Figure 5.3: Electroless Ag plating on an activated substrate
- Figure 5.4: Surface plot of Ag plating on an activated substrate
- Figure 5.5: Electroless Ag plating on a Pd film
- Figure 5.6: Surface plot of Ag plating on a Pd plated surface
- Figure 5.7: Ni plating rates on an activated substrate

CHAPTER 6

- Figure 6.1: SEM image of membrane support
- Figure 6.2: Top view of (a)
- Figure 6.3: Top view of (a + heat)
- Figure 6.4: Side view of (a)
- Figure 6.5: Side view of (a + heat)
- Figure 6.6: Side view of a palladium film before heating with pretreatment layer at the bottom of the film
- Figure 6.7: Side view of a palladium film after heating
- Figure 6.8: Top view of (b)
- Figure 6.9: Top view of (b + heat)
- Figure 6.10: Side view of (b)
- Figure 6.11: Side view of (b + heat)
- Figure 6.12: Top view of (c)
- Figure 6.13: Top view of (c + heat)
- Figure 6.14: Side view of (c)
- Figure 6.15: Side view of (c + heat)
- Figure 6.16: Top view of (d)
- Figure 6.17: Top view of (d + heat)
- Figure 6.18: Side view of (d)
- Figure 6.19: Side view of (d + heat)
- Figure 6.20: Top view of (e)
- Figure 6.21: Top view of (e + heat)
- Figure 6.22: Side view of (e)
- Figure 6.23: Side view of (e + heat)
- Figure 6.24: Top view of (f)
- Figure 6.25: Top view of (f + heat)
- Figure 6.26: Side view of (f)
- Figure 6.27: Side view of (f + heat)
- Figure 6.28: Top view of (j)
- Figure 6.29: Top view of (j + heat)
- Figure 6.30: Side view of (j)
- Figure 6.31: Side view of (j + heat)
- Figure 6.32: Side view of (i)

- Figure 6.33: Side view of (i + heat)
Figure 6.34: Top view of (g)
Figure 6.35: Top view of (g + heat)
Figure 6.36: Side view of (g)
Figure 6.37: Side view of (g + heat)

CHAPTER 7

- Figure 7.1: XRD pattern for a pure palladium film (a)
Figure 7.2: XRD pattern for a pure silver film (b)
Figure 7.3: XRD pattern for a pure nickel film (c)
Figure 7.4: XRD patterns for a Pd-Ni film (d)
Figure 7.5: XRD patterns for a Ag on Pd film (e)
Figure 7.6: XRD patterns for a Ag-Pd (24:76) film (f)
Figure 7.7: XRD patterns for a Ag-Pd-Ni film (g)
Figure 7.8: XRD patterns for a Ag-Pd (10:90) film (i)
Figure 7.9: XRD patterns for a Ag-Pd (18:90) film (j)

CHAPTER 8

- Figure 8.1: Concentration profiles for Pd+Ni (98:2) after heating
Figure 8.2: Ratio between Pd and Ni (98:2) across the film after heating
Figure 8.3: Concentration profiles for Pd+Ag (78:22) after heating
Figure 8.4: Ratio between Pd and Ag (78:22) across the film after heating
Figure 8.5: Concentration profiles for Ag+Pd (24:76) after heating
Figure 8.6: Ratio between Ag and Pd (24:76) across the film after heating
Figure 8.7: Concentration profiles for Ag+Pd (18:82) after heating
Figure 8.8: Ratio between Ag and Pd (18:82) across the film after heating
Figure 8.9: Map of silver layer
Figure 8.10: Map of palladium layer
Figure 8.11: Map of zinc layer
Figure 8.12: Map of zirconium layer
Figure 8.13: Map of yttrium layer
Figure 8.14: Concentration profiles for Ag+Pd+Ni (16:82:2) after heating

- Figure 8.15: Concentration profiles for Ag+Pd+Ni (16:82:2) after heating
- Figure 8.16: Map of Ni
- Figure 8.17: Map of Pd
- Figure 8.18: Map of Ag
- Figure 8.19: Map of Ni
- Figure 8.20: Map of Pd
- Figure 8.21: Map of Ag

LIST OF TABLES

CHAPTER 2

- Table 2.1: List of microfiltration and ultrafiltration applications currently in operation using the CARBOSEP series from TECH-SEP.
- Table 2.2: Deformation rates of palladium alloys
- Table 2.3: Pd-Ag alloy deposition parameters for magnetron sputter coating
- Table 2.4: Calculated electrode potentials (Volts)

CHAPTER 3

- Table 3.1: Solutions for pretreatment at room temperature (25 °C)
- Table 3.2: Compositions of the palladium plating solutions (values per litre plating solution) initially used
- Table 3.3: Composition per litre of palladium plating solution used for all further experiments
- Table 3.4: Composition per litre of silver plating solution used
- Table 3.5: Composition per litre of palladium-silver plating solution used at 60 °C
- Table 3.6: Composition per litre of nickel plating solution used

CHAPTER 4

- Table 4.1: Process variables used for first factorial design
- Table 4.2: Responses (palladium salt to Pd metal conversion) for variables investigated
- Table 4.3: 2³ factorial design with EDTA concentration constant
- Table 4.4: Process variables used for second factorial design
- Table 4.5: Responses (palladium salt to Pd metal conversion) for variables investigated
- Table 4.6: 2³ factorial design with buffer pH constant at pH = 11
- Table 4.7: Average conversions for buffer pH values of 9 and 11 at an EDTA: Pd-salt molar ratio of 6:1
- Table 4.8: $E_{Pd^{2+}/Pd}$ for various EDTA to Pd-salt molar ratios at 25 °C
- Table 4.9: Sequential analysis of variance (model 1)
- Table 4.10: Analysis of variance (model 1)

- Table 4.11: Parameter estimation (model 1)
 Table 4.12: Sequential analysis of variance (model 2)
 Table 4.13: Analysis of variance (model 2)
 Table 4.14: Parameter estimation (model 3)

CHAPTER 5

- Table 5.1: Percent Pd initially in solution and percent Pd deposited on membrane
 Table 5.2: Calculated electrode potentials (Volt)
 Table 5.3: Conversions for palladium deposited on silver

CHAPTER 6

- Table 6.1: Membranes used for analysis
 Table 6.2: Membrane composition in percentages, with 10 ppm = 0.001 %
 Table 6.3: Surface composition of palladium film in percentages
 Table 6.4: Surface composition of the silver film in percentages
 Table 6.5: Surface composition of the nickel film in percentages
 Table 6.6: Pd-Ni film composition before and after heating
 Table 6.7: Pd-Ag film composition before and after heating
 Table 6.8: Ag-Pd (24:76) film composition before and after heating
 Table 6.9: Ag-Pd (18:82) film composition before and after heating
 Table 6.10: Thermal expansion coefficients
 Table 6.11: Ag-Pd (10:90) film composition before and after heating
 Table 6.12: Ag-Pd-Ni film composition before and after heating

CHAPTER 7

- Table 7.1: Structural data for the palladium deposit
 Table 7.2: Structural data for the silver deposit
 Table 7.3: Structural data for the nickel deposit
 Table 7.4: XRD data before and after heating Ag-Pd (24:76)
 Table 7.5: XRD data for Ag-Pd coated membranes (samples i and j) after heating

CHAPTER 1

INTRODUCTION

Traditionally palladium tubes and foils have been used as membranes to selectively separate hydrogen, but they are about 150 microns thick and very expensive. Dense, non-porous palladium films can be deposited on inorganic supports reducing the film thickness to between 10 and 15 microns. Not only is this much cheaper, but hydrogen fluxes through the film is increased considerably. Inorganic supports, especially ceramic membranes, have the advantage of high thermal and chemical stability. Alumina based membranes can operate at temperatures up to 800 °C without any changes in their pore structure and over a wide pH range.

Between 20 and 25% silver is added to commercial palladium membranes to prevent hydrogen embrittlement of the palladium film, to extend film life and increase the hydrogen flux through the film. Palladium and palladium alloys have been successfully used, not only for hydrogen purification, but also for hydrogenation, dehydrogenation and decomposition reactions. Dehydrogenation reactions are equilibrium based and very endothermic, thus extensive temperatures are required to obtain high conversions. Palladium and palladium alloy composite membranes catalyse most dehydrogenation reactions and selectively extract hydrogen. The equilibrium is shifted to the product side, resulting in significant conversion increases. Since much higher conversions can be obtained at lower temperatures, there are large savings in energy, catalyst and equipment life and the cost of recycle equipment. The product becomes much more concentrated in the retentate stream, reducing the number of separation stages and the separation cost.

Membrane reactors are gaining a high profile in terms of new possibilities in chemical engineering, yet the material science needed to optimise their construction has not been adequately investigated. For instance only standard electroless plating solution is used without optimisation. There appears to be no defined investigation of the formation versus the various structures that can be obtained.

As this field is so new, not only is it necessary to optimise the formation of a catalytic membrane reactor, but it is also necessary to gain a full understanding of all the parameters. This includes efficiency of the electroless plating process, how homogeneous are the plated alloys, are the membranes defect free, which coatings will peel of which will not, will the plated surface be rough or smooth and what happens to the crystal structure of the alloy upon heating. If these questions can be answered in this thesis then a range of excellent membrane reactors, each with its own unique parameters, can be constructed.

This study investigates means of reducing fabrication cost of palladium alloy membranes. Electroless plating is used to prepare palladium composite membranes. This is the only technique available for producing even thickness films on the inside of a tubular membrane. Palladium conversion in the electroless palladium plating reaction has not been studied widely and solutions traditionally used, result in low palladium conversions. Since palladium salts are very expensive, any loss is costly. One of the objectives of this study was to optimise palladium conversion and to determine operating conditions for sufficient solution stability.

Electroless silver and nickel plating were investigated. A second alternative for reducing film cost is to produce thinner films. Defects and film porosity increase when films become thinner. The main function of the palladium alloy film is to selectively separate hydrogen, and thus it may not be porous. The addition of nickel to silver-palladium was investigated to determine the effect on membrane structure and porosity. Small amounts of nickel were added as an attempt to create non-porous structures and reduce film thickness to below 5 microns. All metal films were heat treated in a hydrogen atmosphere for 5 hours at 650 °C to obtain sufficient alloying and a proper distribution of film elements.

An in depth study was performed on membrane characterisation. Traditionally researchers have only investigated the membrane surface using SEM and XRD. In this work SEM and XRD was used for surface characterisation. Depth information was extracted with EDX maps and PIXE. EDX maps give a two dimensional view of element distribution in the composite film after heat treatment. The diffusion process can be visualised by comparing maps before and after heat treatment. PIXE was used to construct concentration profiles across the thickness of the film and to determine the penetration depth into the support

membrane pores. The amount of penetration is important, since it determines the metal to ceramic adhesion.

Flowing from this work a second study, where such reactors are well defined and optimal, will be performed concentrating on chemical reactions of interest inside the catalytic membrane reactor.

SEM and EDS work were performed at the Electron Microscope Unit of the University of Cape Town, XRD at the Geology Department of the University of Stellenbosch and PIXE with the Van de Graaff Accelerator at the National Acceleration Centre in Faure. All other experimental work was conducted at the Department of Chemical Engineering (University of Stellenbosch).

CHAPTER 2

BACKGROUND AND LITERATURE SURVEY

2.1. SEPARATION PROCESSES

One of the most common problems, not only in the chemical industry but also in various other disciplines, is high separation cost. Separation requires energy and has three main objectives:

- concentration, where a desired component is present in low concentration and solvent has to be removed
- purification, where undesirable impurities have to be removed and
- fractionation (separating a mixture into various desired components)

A membrane is a permselective barrier between two phases allowing some components to pass easier than others. A driving force is necessary to obtain component transport. This force can be a pressure difference, a concentration gradient or an electrostatic potential gradient. Synthetic membranes have been produced since 1860 (Mulder, 1991), because they have several benefits over other separation processes which makes them very attractive. Separation can be performed continuously and energy cost is low. Only mild separation conditions are required, scale up is easy and no additives are necessary. Some of the drawbacks are membrane fouling and a short membrane life under certain conditions.

2.2. INORGANIC MEMBRANES

Development of inorganic membranes started in the 1940's for nuclear applications (Soria, 1995) where uranium isotopes were separated by the process of gaseous diffusion applied to UF_6 . Further work on synthetic inorganic membranes was continued by CEA in France and at Oak Ridge National Laboratories in the US in the 1950's and 1960's. The emphasis started shifting to membrane development for separation processes such as reverse osmosis, ultra-filtration and microfiltration. In the early 80's inorganic membranes became commercially available with MEMBRALOX (by SCT), CERAFLOR (by SCT) and CARBOSEP (by TECH-SEP) leading the way (Soria, 1995). In the past ten years, the market in this field has grown

exponentially with ever increasing global competition between American, Japanese and European companies. In a review article regarding inorganic membrane reactors Hsieh (1989), listed fifteen major manufacturers of inorganic membranes capable of producing membranes with a wide range of pore diameters.

Porous ceramic membranes, used in cross flow, dominate the market of inorganic membranes currently. Soria (1995) reported that the surface area of installed inorganic membranes across the world is about 40 000 m² per year. This figure represented about 10% of the total surface area of membranes in cross flow mode. SCT and TECH-SEP dominate the market with 20 000 m² per year and 15 000 m² per year, respectively. Membranes can be classified into organic and inorganic membranes. In this study, only the latter will be considered.

2.2.1. TYPES OF INORGANIC MEMBRANES

Inorganic membranes are either dense or porous. Porous inorganic membranes can either be symmetric, where the pore structure is uniform across the membrane, or asymmetric where there is a change in structure. Dense membranes are made of metals (mostly palladium, silver and their alloys) or from dense zirconia, especially calcia-based. Palladium and palladium alloys are permeable for hydrogen, while silver and zirconia membranes preferentially permeate oxygen.

Dense metal-composite membranes have been studied in recent years where metals such as tantalum (Peachey et al., 1996; Buxbaum and Kinney, 1996), vanadium and niobium are coated with palladium allowing for higher hydrogen fluxes. Tantalum, vanadium and niobium have superior hydrogen permeabilities, but their poor surface properties lower the hydrogen transport significantly; thus they are coated with palladium.

A composite membrane usually consists of a support with thickness in the 100 µm or millimetre range and a selective top layer in the micron range. The materials mostly used for commercial porous inorganic membranes are: α-alumina, titania, silicon carbide, carbon, glass, porous stainless steel and porous silver. The selective layer can be made from various oxides such as alumina, titania, zirconia, molecular sieve carbon, zeolites, silicon carbide, amorphous metals or alloys etc.). Yttria is often added to zirconia to improve the thermal stability of the

zirconia membrane (Gopalan et al., 1994). Yttria retards the grain growth rate and prevents changes in the pore structure at elevated temperatures. The addition of about 2 wt% yttria results in high chemical and thermal stabilities. A list of membrane compositions can be found in Soria (1995) and Hsieh et al. (1989).

The most recent commercially available membranes have pore sizes of 40 Å. In the early 90's Lin and co-workers (Lin and Burggraaf, 1991) started breaking the sub-10 Å pore size barrier. With the introduction of zeolite and carbon coated membranes, sub-10 Å pores can now be prepared. Nanoporous (5-6 Å pore size) layers of carbon have been prepared by Rao and Sircar (1994), zirconia and titania layers with pore sizes of 6 Å and 8 Å respectively by Guizard et al. (1994), and zeolite coatings with pore size of less than 10 Å by Fan et al. (1994).

Commercialised inorganic membranes can be found in disk, tube or multichannel form. Disks, and to a lesser extent monochannel tubes, have a low packing density, limiting their industrial applications. **Figure 2.1** shows some mono- and multichannel membranes from ATECH Innovations. Gryaznov (1986a) achieved higher packing densities with thin-walled palladium tubes which are spiral wound. However, this technique is limited to metals.

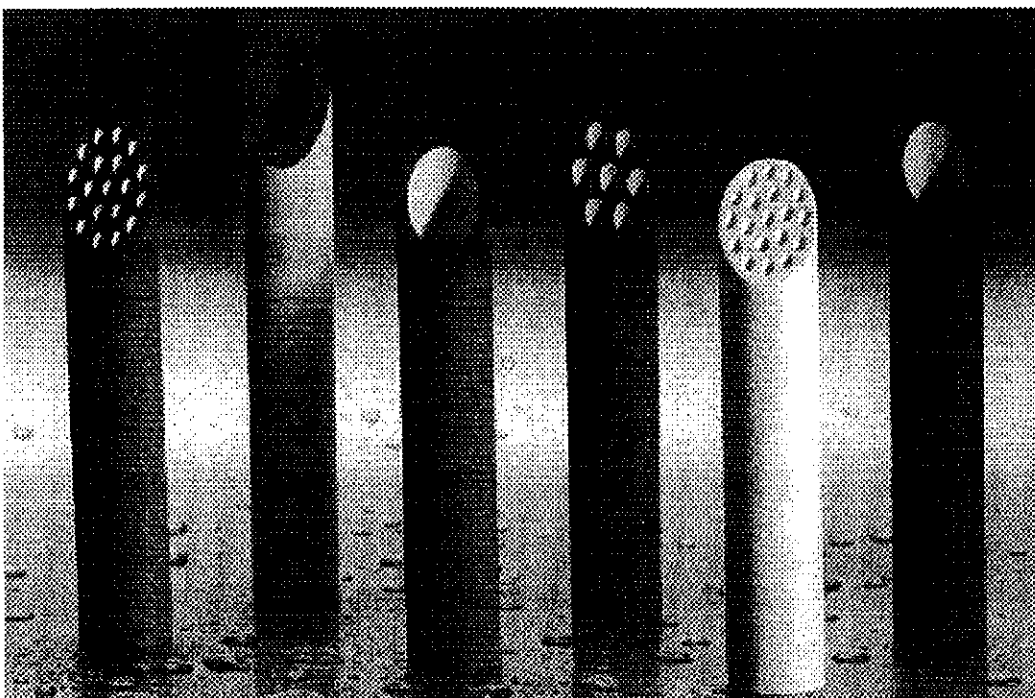


Figure 2.1: Commercial silicon carbide and alumina membranes from ATECH

Hollow fibres are an excellent alternative to achieve very high packing densities and surface areas. Linkov (1994) and Smith (1995) have successfully prepared hollow fibre carbon composite membranes. Due to the large surface area to volume ratio of hollow fibres, they prove to be excellent for creating catalytic membranes. The lack of strength, flexibility and hollow fibre sealing has prevented such membranes from becoming fully commercialised.

2.2.2. PREPARATION TECHNIQUES FOR POROUS INORGANIC MEMBRANES

The methods for preparing porous inorganic membranes are discussed in this section. Later in this chapter, methods for preparing palladium based catalytic membranes will be looked at in more detail.

2.2.2.1. Anodic oxidation

This is the oldest technique for preparing inorganic membranes. The commercial ANAPORE from Whatman is prepared in this way. High purity, thin metal foils (mainly aluminium and zirconium) are anodically oxidised in an acid electrolyte, which may comprise of chromic, oxalic, phosphoric or sulphuric acid. The unaffected metal is removed from the porous film by an etchant, mercuric chloride, dissolving compound or an electrochemical process (Hsieh, 1989).

Nourbakhsh et al. (1989) reported that anodic oxidation is the only method to produce ideal porous structures with nonintersecting pores perpendicular to the membrane and surrounded by hexagonal cells. Membrane characteristics (pore size, density and thickness) can be accurately controlled by choice of electrolyte, anodising voltage, temperature and anodising time. The pore size, for example, decreases with voltage and electrolyte strength.

2.2.2.2. Pyrolysis

Carbon and silicon carbide membranes are made using pyrolysis. Polymers are deposited on porous supports and then, through controlled pyrolysis, the inorganic membrane is formed. Polyacrylonitrile, phenolic resins, cellulose and many other materials can be used to produce carbon membranes (Linkov 1994). Pyrolysis is performed at temperatures ranging from 800 °C to 1500 °C in an inert atmosphere. All non-carbon atoms are eliminated from the original polymeric structure and a graphite coating remains. This process is used by Le

Carbone Lorraine to make their commercial carbon substrate/carbon selective layer membrane. Similarly, silicon rubber is used to make silica membranes. The membrane can be made hydrophilic or hydrophobic, depending on the degree of pyrolysis.

2.2.2.3. Phase separation and leaching

Glass membranes, like porous Vycor glass and Shiras porous glass can be prepared by phase separation and leaching. A borosilicate glass ($\text{SiO}_2\text{-Al}_2\text{O}_3\text{-B}_2\text{O}_3\text{-CaO}$ or $\text{Na}_2\text{O-B}_2\text{O}_3\text{-SiO}_2$) is heated to between 600 °C and 800 °C to bring into effect the separation into two phases: a silicon dioxide rich phase insoluble in mineral acids and a boric rich phase which can be acid or water leached. By removing the borate phase, a porous silicon dioxide structure remains. Parameters that influence the porosity are annealing time, annealing temperature and glass composition.

2.2.2.4. Sol-gel process

Most porous, inorganic composite membranes are currently prepared using sol-gel chemistry of metal alkoxides, the reason being that membranes can be made with pore sizes of a few nanometres or even as small as a few Angstrom (Guizard et al., 1994). Selective layers of zeolites, γ -alumina, titania or zirconia can be made from their respective sols. Two routes are currently employed for sol-gel, i.e. the polymeric gel route and the colloidal suspension route (Soria, 1995). The precursor, which can either be an organic metal compound or an inorganic salt, is hydrolysed while a condensation reaction is occurring simultaneously. The amount of water present determines the hydrolysis rate and the route by which the gel will be formed (colloidal or polymeric). Different routes will result in different final structures.

2.2.2.5. Slip casting

Selective layers can be deposited on inorganic supports by slip casting from a solution containing dispersed particles. Contact between a slip and a dry microporous support results in a capillary pressure drop, which forces the dispersion medium to flow into the pores of the support. The slip contains particles, plasticizers, organic binders and surfactants. It is prepared by sol-gel, precipitation, mixing or crystallisation. Unfired membranes are strengthened by organic binders, while plasticizers prevent cracking upon heating and surfactants are used to stabilise the dispersion.

Drying and calcination are necessary to obtain the desired membrane. Slip formulation and dipping time determine the membrane thickness. Pore size is a function of the particle size and the thermal treatment procedure.

2.2.2.6. Other methods

Porous membranes can be made by thin film deposition techniques such as chemical vapour deposition (Li et al., 1994; Han and Lin, 1994; Uemiya et al., 1994), physical vapour deposition, sputtering, ion plating and metal plating. Track etching (Riedel and Spohr, 1980) has been used to make porous mica membranes.

2.2.3. ADVANTAGES OF INORGANIC MEMBRANES

The exponential growth in the development of inorganic membranes rightly suggests that these membranes have definite commercial value. The major advantages can be summarised as follows (these comply to the majority of inorganic membranes):

- thermal stability at elevated temperature (up to 700-800 °C)
- chemical stability over a wide pH range (0 to 14) at any temperature
- maintain efficiency at extremely high viscosity levels
- imperviousness to the action of oxidising agents (carbon membranes are excluded here) and solvents
- do not age
- can be cleaned by steam sterilisation 消毒
- some membranes are very resistant to thermal shock and have a very high filtration flux (KERASEP)
- in many cases inorganic membranes are superior to organic membranes for gas separation due to molecular sieving
- high electrical conductivity
- allow for the making of catalytic membranes, which is used in heterogeneously catalysed processes above 200 °C



2.2.4. DISADVANTAGES AND PROBLEMS OF INORGANIC MEMBRANES

Perfect membrane materials and perfect membrane configurations or membrane modules do not exist. Every type of membrane has certain limitations and problems which can be addressed by improved development. Some of the problems encountered with inorganic membranes are (Armor, 1995):

- oxide systems suffer from instability (especially porous glass with its active surface), because they are formed from metastable phases
- commercial sub-40 Å pore size membranes are not yet available
- selective layers are still too thick and should be made thinner without any defects or pin holes
- leak free membrane sealants at high temperatures (> 250 °C) is a major problem
- composite membranes, especially catalytic metal membranes, are susceptible to fouling and poisoning
- better characterisation techniques for nanoporous membranes should be developed
- the use of large amounts of sweep gas is costly
- metal membranes tend to become brittle after repeated heating cycles
- mechanical strength is generally poor
- coatings over large areas tend to be of non-uniform thickness
- currently one of the biggest disadvantages is the cost of composite membranes; they are very expensive, especially Pd based catalytic membranes

Some other disadvantages include difficulty with adherence of selective layers to carbon membranes, oxidation of carbon membranes above 150 °C, sulphide poisoning of palladium based membranes, low oxygen diffusion rates through silver membranes below 500 °C and difficulty with scale up.

2.2.5. APPLICATIONS

Hsieh (1989) gives numerous examples of literature studies on gas and liquid separations using inorganic membranes. Applications mentioned (Table 2.1 and thereafter) are limited to those which have been implemented in industry.

Table 2.1: List of microfiltration and ultrafiltration applications currently in operation using the CARBOSEP series from TECH-SEP.

| | Recover | Concentrate | Separate | Purify | Sterilise | Clarify |
|--|---------|-------------|----------|--------|-----------|---------|
| Dairy products | | | | | | |
| milk standardisation, milk and curd concentrates | X | X | | | | |
| whey | X | X | X | X | | |
| | | | | | | |
| Beverages | | | | | | |
| fruit juices, wine | | | | X | X | X |
| | | | | | | |
| Biotechnology | | | | | | |
| membrane reactors | | X | X | | | |
| enzymes | | X | X | X | | |
| pyrogen removal | | | X | X | X | |
| large volume parenterals | | | | X | X | X |
| lactic ferments | | X | X | X | | |
| fermentation broth cultures | X | | X | | X | |
| | | | | | | |
| Other applications | | | | | | |
| vinegar | | | | X | X | X |
| egg products | X | X | X | | | |
| lysozyme recovery | X | X | | X | | |
| blood | X | X | X | X | | |

The table was taken from one of TECH-SEP's technical brochures.

- Water treatment (drinking water purification)
- Waste treatment (textile dye recovery, metal cleaning, regeneration of water-based cleaners, heavy metal waste, pulp and paper wastes)

- Gas cleanup (particulate removal, solvent vapour recovery)
- Gas/gas separation (oxygen separation, methane/nitrogen separation, hydrogen separation, CO₂ recovery, binary gas mixture separation, isotope separation and fuel cells)
- Tritium recovery
- SO_x and NO_x recovery
- Sensors

Catalytic membranes, predominantly Pd based, have been used in various hydrogenation, dehydrogenation and decomposition reactions. These will be discussed in the next section.

2.3. PALLADIUM BASED CATALYTIC MEMBRANES

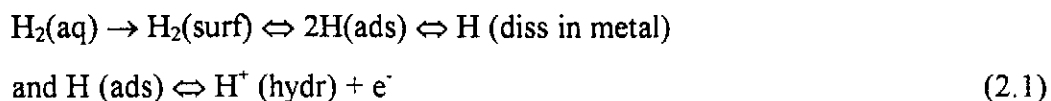
2.3.1. HYDROGEN PERMEATION THROUGH PALLADIUM MEMBRANES

Hydrogen permeates through palladium via a solution diffusion mechanism. Three steps have been identified by Barrer (1951):

1. reversible dissociative chemisorption of hydrogen on the metal surface
2. reversible dissolution of atomic hydrogen in the metal layers
3. diffusion of atomic hydrogen in the metal

Steps 1 and 2 take place on either side of the membrane surface.

Makrides (1964) suggested a similar mechanism:



Diffusion is often the rate-limiting step for palladium membranes. Hydrogen permeation is dependent on the diffusion rate and the concentration gradient across the membrane. The concentration difference at the high and low pressure sides of the membrane results from the hydrogen solubility in the metal and the pressure difference across the film. At steady state Fick's law can thus be used to describe the rate of hydrogen permeation per unit area (Uemiya et al., 1991b; Buxbaum and Kinney, 1996).

2.3.2. PALLADIUM ALLOY MEMBRANES

Pure palladium is not commercially used for hydrogen purification, but rather an alloy containing 23 wt% silver and 77 wt% palladium. In most catalytic membrane reactors this is also true (Sathe et al., 1994; Clayson and Howard, 1987; Shu et al., 1994; Uemiya et al., 1991b). The reason for this is that palladium has two hydride phases and below 300 °C and 2.0 MPa (Shu et al., 1991) the β phase nucleates from the α phase, resulting in severe lattice strains. After a few $\alpha \rightleftharpoons \beta$ transitions the pure palladium becomes brittle. The β phase is the preferred one for high hydrogen fluxes, since there is a sharp increase in hydrogen solubility in the β phase with increasing temperature and pressure.

The face centred cubic (fcc) lattice constant increases with increasing hydrogen concentration. Silver has an electron-donating role similar to the hydrogen atom in palladium and thus both compete for the filling of the electron holes in the 4d band of palladium. The 4d band is filled quicker, followed by filling of the 5s band and forming of the β -hydride phase at lower hydrogen concentrations. The result is a sharp decrease in critical pressure and temperature for the $\alpha \rightarrow \beta$ transition after forming a Pd/Ag alloy.

2.3.2.1. Effect of alloying on hydrogen permeation

The hydrogen solubility dramatically increases with increasing silver content (**Figure 2.2**). The severe increase in solubility should result in very high hydrogen permeability. However, this is not the case, because the diffusion coefficient in the alloy is significantly reduced (**Figure 2.3**), thus lowering the flux. At 350 °C and 2.2 MPa the maximum hydrogen permeability through a Pd-Ag membrane occurred at 23 wt% Ag and the value is only 1.7 times higher than that of pure palladium (**Figure 2.4**).

A Pd-Cu (94:6 wt%) alloy has been studied by Uemiya et al. (1991a) and they found the hydrogen permeation rate to be much lower than that of a similar Pd-Ag (93:7 wt%) alloy. **Figure 2.4** indicates a maximum permeation rate for Pd-Cu at 40 wt% copper. Yttrium and cerium have excellent hydrogen permeabilities. An 8:24:68 wt% Y:Ag:Pd alloy corresponds to the maximum permeability. Ce and Y are both harder than Pd-Ag (23:77 wt%) and can thus withstand higher trans-membrane pressure gradients. Binary alloys of Pd with Ni, Rh,

Ru, Cr, V and Fe have been studied (references can be found in Shu et al., 1991). In most cases the permeability is reduced, for example Pd-Ru (Armor 1995).

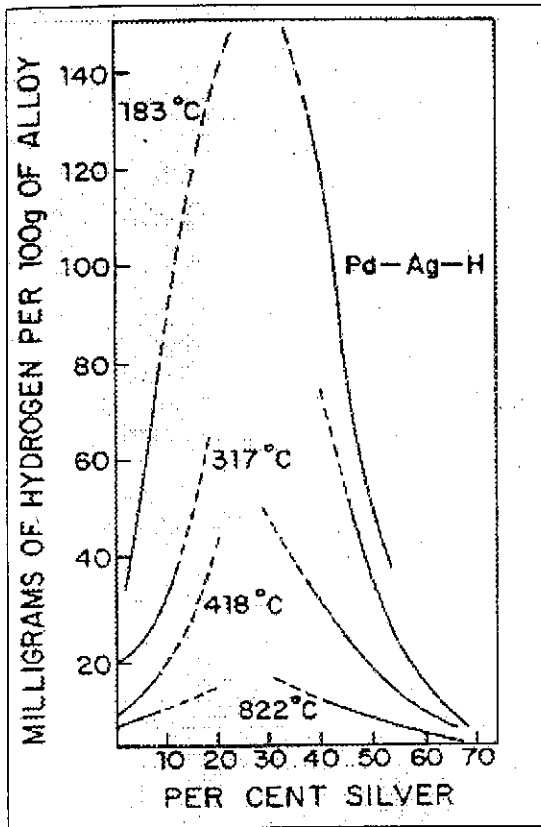


Figure 2.2: Solubility of hydrogen in palladium-silver alloys (Shu et al., 1991)

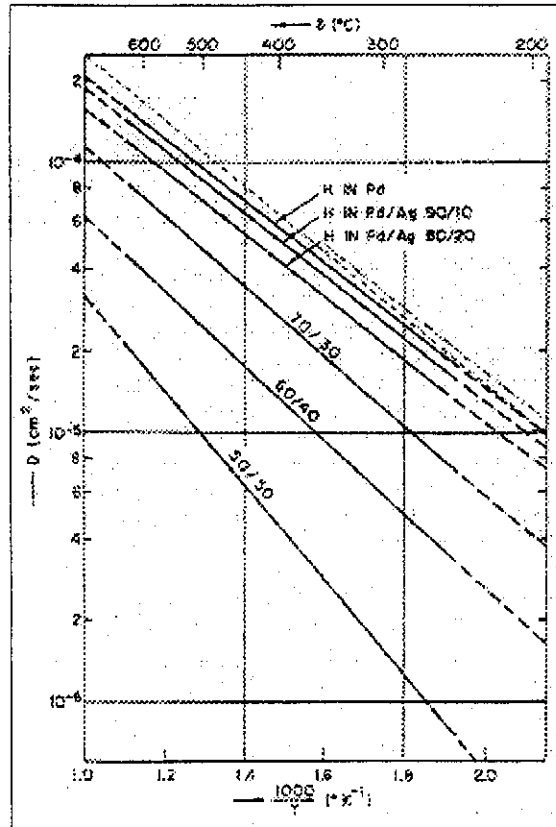


Figure 2.3: Diffusion coefficients in palladium and palladium-silver alloys (Holleck, 1970)

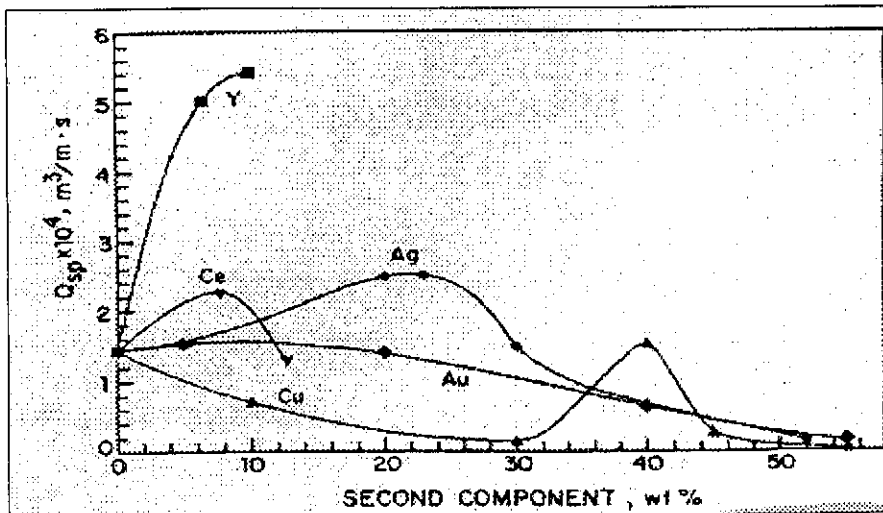


Figure 2.4: Permeability of hydrogen through palladium alloys at 350 °C and 2.2 MPa (Shu et al., 1991)

2.3.2.2. Increasing membrane stability through alloying

The major reasons for alloying are to reduce the α , β transition from 250 °C to room temperature and to increase hydrogen permeation through the metal film. Further elements can be added to the palladium alloy to improve strength. Adding Ni or Au can increase the mechanical stability and lifespan of Pd alloys. Rodina et al. (1971) measured the number of temperature cycles (20 to 520 °C) in a hydrogen atmosphere before deformation occurred. The results are listed in **Table 2.2**.

Table 2.2: Deformation rates of palladium alloys

| Elements | Composition (wt %) | Temperature cycles |
|-------------|--------------------|--------------------|
| Pd | 100 | 20-30 |
| Pd/Ag | 80:20 | 50-70 |
| Pd/Au | 92:8 | 200 |
| Pd/Ag/Au | 73:24:3 | 300 |
| Pd/Ag/Au/Ru | 73.74:20:5:1.26 | 2000 |
| Pd/Ag/Ni | 85:10:5 | 2500 |
| Pd/Ni | 94.5:5.5 | 3000 |

2.3.2.3. Alloying for catalytic purposes

Certain elements are added to enhance the catalytic activity of pure palladium. They are mainly Ni (Smirnov et al., 1978; Bulenkova et al., 1978), Ru (Gryaznov, 1986a; Skakunova et al., 1988) and Rh (Parfenova et al., 1983; Gryaznov, 1986b). Sn, Sb, Cu and Mo have also been added for some reactions.

2.3.3. APPLICATIONS FOR PALLADIUM BASED MEMBRANES

Johnson Matthey developed commercial hydrogen purification equipment, consisting of 77:23 wt% Pd/Ag tubes in the early sixties. This process is still used in small to medium scale plants for the production of high purity (< 0.1 ppm impurities) hydrogen. Since the 1970's, a lot of work has been done (initially in the Soviet Union and later in Japan) on the use of palladium and palladium alloys in membrane reactors. Palladium acts as a catalyst and also allows for

selective hydrogen diffusion. The work done in the 70's and 80's mainly used palladium and palladium alloy foils or tubes. The disadvantages of using this is cost and lower hydrogen diffusion rates, since the metal films were relatively thick ($> 100 \mu\text{m}$). Currently, thin and less expensive films ($< 20 \mu\text{m}$) are being prepared on inorganic porous supports or metals like niobium and tantalum. Palladium is being investigated more and more in catalytic membranes and they are advantageous in the following reactions:

- introduce hydrogen to the reactants for hydrogenation
- extract hydrogen from the products in dehydrogenation reactions
- allow for simultaneous hydrogenation/dehydrogenation reactions by transporting hydrogen from the product side in one reaction to the reaction side on the other side of the membrane
- gas cleanup by decomposition of unwanted gases

The literature on catalytic processes using palladium membranes is extensive (more than 80 references are cited in Shu et al., 1991), with most of the work done by Gryaznov and his co-workers using palladium and palladium alloy tubes. Only a few of the more recent investigations using palladium coated porous inorganic supports will be discussed.

2.3.3.1. Hydrogenation

Several potential benefits arise from using a palladium-based membrane.

- An impure hydrogen feed can be used on the permeate side. Pure hydrogen will diffuse to the reaction side.
- Hydrogen and reactants compete for the same adsorption sites when they are fed simultaneously in a reactor. By permeating through the membrane, the hydrogen concentration in the adsorbed layer though very low, can be continuously supplied from the reverse side, allowing for much higher hydrogenation rates per unit surface area.
- In the fine chemical and pharmaceutical industries, selectivity in hydrogenation reactions is very important. Low concentrations of dissolved hydrogen are especially selective towards triple bond and double bond hydrogenations. Most reactions are in the liquid phase and controlled hydrogen permeation can reduce unwanted side reactions.
- Catalytic membranes eliminate the process needed for hydrogen separation from products.

- Separate feeding of reagents increases safety when working with reagents restricted to explosion boundaries.
- Finally, thermal runaway can be prevented when dealing with fast, exothermic, heterogeneously catalysed gas reactions (Veldsink et al., 1992).

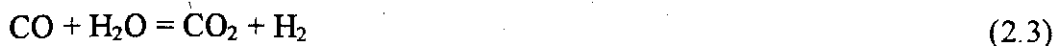
Some reactions where these advantages can be exploited are the hydrogenation of nitrobenzene (Torres et al., 1994), hydrogenation of cyclo-octadiene and octadecene as liquids (Farris and Armor, 1993) and the oxidation of carbon monoxide (Veldsink et al., 1992). The selective hydrogenation of acetylenic alcohols has been used to commercially produce the synthetic perfume linalool (Gryaznov and Smirnov, 1974).

2.3.3.2. Dehydrogenation

Dehydrogenation reactions are equilibrium based and usually very endothermic. In other words, they require excessive temperatures to achieve any appreciable conversion. The equilibrium limits the product yield. By using a hydrogen permeable membrane, the equilibrium can be shifted to the product side as hydrogen permeates the membrane. Hydrogen is continuously removed from the products. High purity hydrogen can be prepared in this manner and high conversion, exceeding the equilibrium value, can be obtained in the dehydrogenation reaction. The following advantages arise from using a palladium based catalytic membrane:

- High conversion can be obtained at much lower temperatures, thus increasing catalyst and reactor life. There are considerable energy savings by performing the reaction at lower temperatures
- The product becomes much more concentrated in the retentate stream. This reduces the number of separation stages to obtain a pure product
- Smaller recycle streams can be used, saving on pumping and compression costs
- High purity hydrogen can be produced

Two reactions of industrial importance have been studied in depth using the catalytic membrane approach. Hydrogen can be produced by the methane steam reforming reaction and the water gas shift reaction.



Thermodynamic restrictions are eliminated and high conversions can be obtained by proper choice of operating conditions (Kikuchi et al., 1989; Kikuchi, 1995; Shu et al., 1995; Shu et al., 1994).

Many authors explored the dehydrogenation of alkanes, cycloalkanes, long chain alcohols, etc. using catalytic membranes. Valuable aromatics can be produced by the dehydrogenation of paraffins or cycloparaffins with more than six carbon atoms (Clayson and Howard, 1987). One of the classic reactions used to illustrate the advantages of the palladium based membranes is the dehydrogenation of cyclohexane to produce benzene. Itoh (1987) achieved 100% conversion at 200 °C and 1 atm, compared to the equilibrium value of 18.7%.

However, it must be stressed that such improvements are achieved only with very long residence times (15 minutes for the Itoh investigation). This is problematic, since it results in very low production rates. As soon as the residence time decreases, the conversion also starts to decrease. Cannon and Hacskaylo (1992) reported conversions exceeding 75% for the cyclohexane/benzene reaction using a Pd impregnated porous Vycor glass membrane. The equilibrium value at the same conditions was 30%. Higher flow rates were used in this study, but it was still very low. In the last five years, most work has been done on the dehydrogenation of aliphatic alkanes with the aim of establishing proper reactor models. Reactions investigated include:

- ethane dehydrogenation (Gobina et al., 1995a; Gobina et al., 1995b; Champagnie et al., 1992; Tsotsis et al., 1992)
- propane dehydrogenation (Pantazidis et al., 1995; Sheintuch and Dessau, 1996)
- iso-butane and n-butane dehydrogenation (Sheintuch and Dessau, 1996; Kikuchi, 1995; Casanave et al., 1995; Gobina and Hughes, 1996a)

By dehydrogenating iso-butane iso-butene is formed, which is a raw material for producing MTBE (methyl tertiary butyl ether), an octane booster. Styrene has been produced from

ethylbenzene (Gallaher et al., 1993) as well as toluene from methylcyclohexane (Ali and Rippin, 1994).

2.3.3.3. Reaction coupling and decomposition reactions

Reaction coupling has kinetic and thermal advantages. Palladium based catalytic membranes have been used for various reaction couplings (Shu et al., 1991). Gryaznov and co-workers have been the leaders in this field. The use of oxygen on the permeate side has been studied by several people in various reactions. The atomic hydrogen on the membrane surface decreases and this accelerates the hydrogen permeation rate. Furthermore, heat is generated by the exothermic reaction between hydrogen and oxygen, which is conducted through the membrane and utilised by the dehydrogenation reaction. Cheng and Shuai (1995) simulated the oxidative coupling of methane at various temperatures and pressures, while Itoh and Govind (1989a) investigated the oxidative dehydrogenation of 1-butene and Pantazidis et al. (1995) looked at the oxidative dehydrogenation of propane.

Palladium membrane reactors have been used for gas clean up by decomposing unwanted gases. Ammonia can be removed from high temperature, high pressure synthesis gas produced during coal gasification by decomposing it to nitrogen and hydrogen using catalytic palladium membranes. Conventional techniques failed due to high nitrogen and hydrogen concentrations in the synthesis gas imposing severe equilibrium restrictions. Collins (1993) achieved ammonia conversion of over 94% at 873 K compared to a 58% equilibrium conversion. Gobina et al. (1996b) also reported very good results. Edlund and Pledger (1993) investigated hydrogen sulphide decomposition using a composite metal membrane with 25 μm Pt coating. At 973 K, 793 kPa and 1.5 mole percent hydrogen sulphide feed, 99.4% conversion was obtained compared to an equilibrium value of 13%. The decomposition of water to hydrogen and oxygen has also been achieved by Compagnie des Métaux Précieux (1976).

2.3.4. PREPARATION TECHNIQUES FOR PALLADIUM AND PALLADIUM ALLOY MEMBRANES

Many techniques exist for making palladium thin films ($< 20 \mu\text{m}$). Each has its own advantages and disadvantages. Disadvantages may be equipment cost, film thickness and film

uniformity control, purity control and alloying capabilities. In this section, only the techniques which are used on laboratory scale will be discussed, with particular emphasis on electroless plating. This technique was investigated in detail in this study.

2.3.4.1. Physical vapour deposition (PVD)

There are two basic categories for PVD: sputtering and evaporation. Deposition thicknesses can range from 10^{-10} to 10^{-3} m and deposition rates as high as 25 $\mu\text{m/s}$ can be obtained using electron beam heated sources (Ullmann, 1987). The advantages of this technique are that most metals can be deposited in this way and that complex alloys can be prepared. Very thin films can be prepared in this way ($< 1 \mu\text{m}$) and the deposition rate can be accurately controlled. Disadvantages are control of film uniformity and difficulty with depositing films on non-flat surfaces.

Evaporation can be performed with resistive heating of the crucible containing the metal to be deposited. Evaporation takes place near the fusion temperature and ejected atoms move in straight lines in all directions, condensing on cooler targets in their direct path. The heating element must have a considerably higher fusion temperature than the evaporant, must not contaminate it and must not form alloys with it. Sputter coating is more commonly used than evaporation. In the sputtering process, atoms are dislodged from the target through ion bombardment with an inert gas (usually argon) and then deposited on the substrate. Proper surface cleaning prior to deposition is essential for good adherence. Evaporation rates for various metals are quite similar, thus alloys can easily be deposited. Magnetron sputter coating is most commonly used and Gryaznov et al. (1993) have used it to prepare alloys of palladium and one or more of Ru, In, Co, Pb and Mn. System conditions for magnetron sputter coating (radio frequency glow discharge) with palladium-silver are listed in **Table 2.3** (Gobina and Hughes, 1996a).

Jayaraman et al. (1995b) have used similar conditions, but varied the substrate temperature from 80 °C to 600 °C. Optimum adhesion and gas tightness during permeation experiments were obtained at a substrate temperature of 400 °C. By varying the sputter time from 4 to 15 minutes, Jayaraman and Lin (1995a) coated to thicknesses of 250, 350 and 500 nm.

Table 2.3: Pd-Ag alloy deposition parameters for magnetron sputter coating

| | |
|---------------------------|-----------|
| System pressure | 0.67 Pa |
| Substrate temperature | < 300 °C |
| Substrate/target distance | 70 mm |
| RF (radio frequency) | 13.56 MHz |
| RF power to substrate | 110 W |
| power during deposition | 10 W |
| RF power to target | 150 W |

2.3.4.2. Quenching and rolling

This process is similar to that for producing commercial metal plates and sheets. Metals are heated to above their melting temperatures, cast, forged or pressed and repeatedly cold rolled or pressed. Contamination with trace amounts of Si, C, O and S become a severe problem when preparing thin foils in the micron range. Films prepared in this way are unsupported, thus thicker to maintain a sufficient transmembrane pressure. Thicker films are more costly and have a low hydrogen permeation rate.

The only application found for this technique was the preparation of amorphous Pd-Si alloys by Itoh et al. (1995). Amorphous Pd_xSi_{1-x} (x = 0.85, 0.825, 0.8) was prepared by rapid quenching from melts using a copper roller (300 mm diameter, 20 mm width). Amorphous ribbons of 40 µm thickness and 5 mm width were obtained.

2.3.4.3. Chemical vapour deposition (CVD)

Layers from the gas phase with thicknesses of 0.1 to 10 µm can be prepared by chemical vapour deposition. Most metal complexes can be deposited in this manner. The complex is heated by direct resistance heating, radio frequency, plasma or laser beam and deposited on a heated substrate. CVD equipment is depicted in Ullmann (1987). This process has been used for depositing SiO₂ in the pores of the substrate by reacting SiCl₄ and CO₂ entering the membrane reactor from the shell and tube side respectively (Nam and Gavalas, 1989; Illias and Govind, 1989). Deposition of palladium using CVD has been limited probably due to the lack

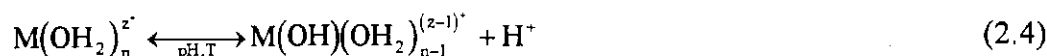
of thickness control. Wachtman and Haber (1986) have suggested thermal decomposition of Pd(acac)₂ at 350-400 °C for making thin films.

2.3.4.4. Sol-gel process

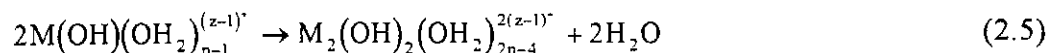
Thin palladium films can be produced using sol-gel chemistry. The technique can be divided into two routes depending on whether the precursor is a metal salt or an alkoxide (Brinker and Scherer, 1990). Inorganic polymerisation can either be done in an aqueous or in an organic medium. Hydroxylation and polymerisation of hydroxylated molecular species form polymeric oxide species. A three dimensional network of particles is formed in the gelation process. The following chemical reactions are of importance during sol-gel transition (Julbe et al., 1993):

In the aqueous phase:

Hydrolysis:

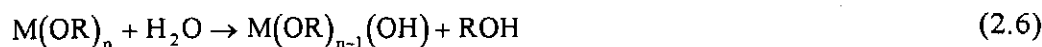


Condensation (in the case of olation):

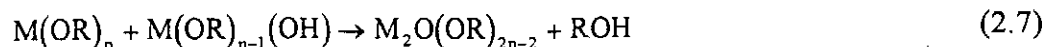


In the organic phase:

Hydrolysis:



Condensation (in the case of alcoxolation):



The reaction between a metal salt or hydrated oxide and an excess of water forms a precipitate of gelatinous hydroxide particles. Peptising with electrolytes leads to stable colloidal

suspensions. Small particles (nm range) tend to agglomerate into larger aggregates, but can be broken down to a few nanometres by appropriate treatment. Avoiding hydroxide precipitation in alkoxide derived sols results in very fine structures reaching one nanometre in size.

Many additives are added for proper process control. These include: stabilisers, binders, solvent molecules, basic or acid catalysts, organic ligands, mineral anions and plasticisers or drying control additives (Julbe et al., 1993). Livage et al. (1988) have made a detailed study of sol-gel chemistry of transition metal oxides. Hydroxylated ligand additives such as organic acids, polyols, β -diketones and allied derivatives can be used to modify the reactivity of alkoxide precursors in organic media (Laaziz et al., 1992).

The gel is applied onto tubular membrane supports by slip casting to form organic-inorganic membranes. The final step is firing of the membrane to remove any organic molecules present. The result is an inorganic support with a metal or oxide layer suspended on it.

Hongbin et al. (1995) tested the adsorption potential of various Pd^{II} -salts on $\gamma\text{-Al}_2\text{O}_3$ particles. Of $\text{Pd}^{\text{II}}\text{-Cl}$, $\text{Pd}^{\text{II}}\text{-NH}_3$ and $\text{Pd}^{\text{II}}\text{-EDTA}$ the latter two are best suited for preparing $\text{Pd}/\gamma\text{-Al}_2\text{O}_3$ membranes. With a palladium modified boehmite sol (2 wt% $\text{Pd}/\gamma\text{-Al}_2\text{O}_3$) they prepared a membrane with very narrow pore size distribution and average pore diameter of about 6.5 nm. Vitulli et al. (1995) prepared porous Pt/SiO_2 catalytic membranes on $\alpha\text{-Al}_2\text{O}_3$ supports with pore diameters < 10 nm using mesitylene solvated Pt atoms.

2.3.4.5. Wet impregnation

This technique is best suited for depositing Pd particles within the pores of the inorganic support. It is not suited for preparing dense, non-porous membranes, but rather to reduce the porosity of the membrane support and to obtain very high catalytic areas. Porosity control is difficult. Champagnie et al. (1992) prepared Pt impregnated membranes. According to them, proper uniform impregnation remains a problem. Cannon and Hacskaylo (1992) prepared palladium impregnated porous Vycor glass membranes via metal complex adsorption and metal complex decomposition.

In the adsorption method, cleaned tubes were impregnated at ambient conditions in a solution of $\text{Pd}(\text{NO}_3)_2(\text{H}_2\text{O})_x$, distilled water and denatured ethanol. Immersion was carried out for two days followed by thorough washing in distilled water, immersion in distilled water for up to 24 hours to prevent cracking in the membrane reactor and then air drying. In the metal complex deposition technique, the membrane was ultrasonically treated in hydrogen peroxide for 8 hours, rinsed in distilled water and air dried. The membrane was then placed in a solution of $[\text{Pd}(\text{C}_3\text{H}_5)\text{Cl}]_2$ and denatured ethanol for 16 hours, immersed in distilled water for 24 hours and allowed to air dry. The adsorption method had a negligible effect on the pore diameter and surface area of the untreated membrane, while the decomposition method reduced the pore diameter from 44 Å to 34 Å and increased the surface area from 187 m²/g to 227 m²/g.

2.3.4.6. Other solution based methods

Huang and He (1994) prepared polymer supported colloidal palladium catalyst. PdCl_6 was incorporated into a polymer mixture containing toluene, glutin, diallyl phtalate (DAP), n-vinylpyrrolidone (NVP), azo-bis-isobutyronitrile (AIBN) and water. PdCl_6 -bound NVP was reduced with NaBH_4 at 50 °C in a hydrogen atmosphere for 2 hours. Fritsch and Peinemann (1995) prepared non-porous polymer supported Pd-Ag membranes using various polymers, N-methyl-2-pyrrolidone and palladium acetate and/or silver acetate. The solution was casted and heated to 80 °C in a dust free atmosphere. Immersion in $\text{NaBH}_4/\text{MeOH}$, washing in methanol and drying in a vacuum completed the membrane fabrication process.

2.3.4.7. Electroplating

Metals or alloys can be plated on a substrate acting as a cathode. Metal cations, suspended in a plating solution, are reduced by means of an external current passing through the electrolyte. Deposition rate and thickness are determined by bath temperature, current density and metal ion concentration. Even thickness plating over large areas is very difficult due to variance in current density and declining metal cation concentration in the bath. Electroplating can only be performed on conducting surfaces, thus excluding untreated ceramics and plastics. Porous, Pd-Cu alloy plated membranes have been manufactured by Kikuchi (1988). The support was plated with 71-94 wt% Pd and 6-29 wt% Cu. A method for electroplating Pd or its alloys on porous ceramic supports has also been described by Itoh et al. (1989b).

2.3.4.8. Electroless plating

Electroless plating is a technique similar to electroplating except that there is no external supply of electrons. A substrate is covered by means of an autocatalytic reduction of metal ions with a reducing agent. This technique is currently the preferred one for preparing palladium based catalytic membranes. Various materials can be used as a membrane support, which include porous Vycor glass (Yeung et al., 1995a; Uemiya et al., 1991a), porous stainless steel (Shu et al., 1993) and alumina (Collins, 1993; Yeung et al., 1995b). Electroless plating has also been widely used in the electronic industry for the fabrication of printed circuit boards, low resistance ohmic contacts (Stremsdoerfer et al., 1990), chip level interconnects (Dressick et al., 1994) and selective metal deposition on silicon substrates (Cachet et al., 1992). The wide use of electroless plating is due to the many advantages it offers over other methods of metal deposition, including

- The technique is quick and simple
- No expensive equipment is required. The main cost is the palladium salt used and the material loss is small compared to the losses in other methods (PVD, CVD etc.)
- An even thickness layer can be prepared on any shape
- Dense, non-porous films can be prepared
- Good adhesion is obtained between membrane support and metal film

Some problems do, however, occur when using this method. These problems are addressed in this study and ways are found to minimise them. The problems are:

- Low deposition rates using hydrazine as reducing agent (Athavale and Totlani, 1989)
- Film impurities are deposited using certain reducing agents. Loweheim (1974) reported 1.5% phosphorus in the film using sodium hypophosphite as reducing agent, while Shipley (1984) reported that borohydride reducing agents usually result in a 3-8% boron deposit
- Thickness control causes difficulty
- Costly Pd losses might occur due to bath decomposition (Shu et al., 1991)
- A further unresolved aspect is the palladium conversion obtained in the plating reaction. Not many publications have covered this area. Pearlstein and Weightman (1969) reported 90% conversion after nineteen consecutive one hour depositions

2.3.4.8.1 *Substrate cleaning*

Proper cleaning of the area to be plated prior to activation and plating is essential. Fingerprints, dirt and particles such as ceramic dust that exist on the surface or in the pores, will cause non-uniform plating, metal film irregularities or lead to loss in adhesion.

Many cleaning procedures for ceramics and glass exist in the literature (Sasaki, 1991; Baudrand, 1984; Graham, 1971). Four cleaning steps usually precede surface activation viz. alkaline clean, rinse, etch and rinse again. Etching is optional and depends on the surface roughness of the specimen. Ultrasonic cleaning is strongly recommended when cleaning porous ceramics for removing particles and dust from the pores. When glass, plastic or non-porous ceramic are plated, etching is required. For good metal adhesion, plastics are etched with strongly oxidising chromic acid-water or chromic acid-sulphuric acid-water (Kirk-Othmer, 1980a). The etchant chemically modifies the surface making it hydrophilic and physically roughens it to ensure mechanical locking and chemical bonding of metal to plastic. Etching of ceramic and glass is done with sodium hydroxide (Lin and Jong, 1993) or fluorides (Graham, 1971; Baudrand, 1984). According to Baudrand (1984) 97% alumina can still be etched with fluorides to create microporosity, but pure alumina cannot be etched effectively and must be made microporous in the fabrication process.

Etching is usually not needed when cleaning porous materials like Vycor glass (Yeung, 1995a), porous stainless steel (Shu et al., 1993) and Membralox (Collins and Way, 1993b). A few cleaning procedures are presented below:

Porous Vycor glass (Yeung, 1995a): Clean in 30% hydrogen peroxide at 80 °C for 1 hour; rinse in deionised water; clean ultrasonically in trichloroethylene; rinse in ethanol and deionised water; store in deionised water.

Porous alumina-Membralox (Collins, 1993): Ultrasonic rinse in deionised water (5min); ultrasonic rinse in alkaline solution (5min); rinse in cold deionised water (1min); soak in 25 wt% acetic acid (5min); ultrasonic rinse in cold deionised water (3min); ultrasonic rinse in 333 K deionised water (1min); rinse in 333 K deionised water (1min); ultrasonic rinse in isopropyl alcohol (5min).

Porous stainless steel (Shu et al., 1993): Ultrasonic cleaning in carbon tetrachloride for one hour.

Non-porous alumina (96%) (Lin and Jong, 1993): Ultrasonic cleaning in acetone; cleaning in 5% NaOH (5min); etching in HNO₃; ultrasonic cleaning in distilled water between each step.

2.3.4.8.2. Surface activation

Plating on most metals does not require catalytic activation (Kirk-Othmer, 1980a). Exceptions are stainless steels and titanium, which need to be etched first. These exceptions, as well as non-conductors (ceramics, plastics) must be pre-treated in order to ensure the catalytic surface required for controlled electroless plating. The catalysts for electroless plating not only act as plating initiators, but have a considerable effect on the smoothness, coverage, adhesion and surface quality of the deposited metal film.

Catalysing the inactive surface is done using a combination of tin and palladium. Two processes are commonly used (Feldstein, 1974):

1. The older two step immersion procedure consisting of a sensitising step (SnCl₂/HCl) followed by an activation step with PdCl₂/HCl.
2. The "exchange process" requiring a catalysation step with PdCl₂/SnCl₂/HCL (colloids) and then acceleration with NaOH, HCl, H₂SO₄, ammonium fluoroborates or fluoboric acid (Cohen and Meek, 1976).

In the two step process the tin chloride solution acts as a sensitiser and the palladium salt solution as an activator. After immersion into the SnCl₂ solution, the Sn(II)-ions are adsorbed onto the substrate. Palladium atoms are then deposited around the tin ions according to the following reaction:



Tin acts both as a reducing agent for palladium ions and it stabilises the formed Pd nuclei, via strong specific Sn⁴⁺ adsorption. The high positive charge density of the Sn⁴⁺ ions prevents Pd nuclei aggregation through ~~electrostatic repulsion~~ ^{静电排斥}. The excess Sn⁴⁺ ions are removed in a separate step to produce a clean catalytic Pd surface.

colloid 胶体

Cohen and West (1973) developed a model for Pd-Sn colloids (second process). A complex between Pd(II) and Sn(II) is formed after mixing their acidic chloride salts. Palladium(II) is reduced to Pd(0) within the complex, yielding a nucleus for colloid growth. The core of the colloid is a Pd-Sn alloy, Pd₃Sn or PdSn₂ (Cohen et al., 1971). A stabilising layer of Sn(II), OH⁻ and Cl⁻ complexes surrounds the core. Colloid growth rate and particle sizes are determined by the formation of Sn(II). Activators and accelerators are used to enhance the activity of the Pd/Sn catalysts by removing tin from the activated surface and exposing the catalytic Pd at the core.

Pd, Sn

In recent years, methods have been developed using organic solvents and ligands instead of tin (Van der Putten et al., 1992; Dressick et al., 1994) for stabilising the Pd colloids. These processes involve fewer steps and display superior selectivity compared to the conventional Pd/Sn catalysing processes. Furthermore, there are less adherence problems compared to that encountered with Pd/Sn catalyst on Si-OH containing surfaces (silicon, silica and glass).

Several mixed PdCl₂/SnCl₂ catalyst solutions are listed in the literature (Osaka and Takematsu, 1980; Feldstein, 1974). A method for evaluating catalyst for electroless plating is proposed by Horkans, 1983.

The two step procedure deposits more Pd on the surface than the exchange process, ensuring a very even metal film over a large surface area after plating. The two step process also deposits less tin (Horkans, 1983) which is important in obtaining a very high purity Pd film necessary for catalytic membranes. The method of SnCl₂ solution preparation plays an important role in the amount of tin coverage on the substrate. The lowest desired tin coverage is obtained by dissolving SnCl₂ in hydrochloric acid and then diluting with deionised water. The tin covering is higher when dissolving the salt in deionised water and finally adding acid.

2.3.4.8.3. General electroless plating solution compositions

The main components of a electroless plating bath are: a metal salt of the metal to be plated, a reducing agent, a stabiliser to allow for controlled release of the metal ion and a pH regulator which ensures the correct pH for proper working of the reducing agent and the stabiliser.

The oxidation potential of the reductant must be less noble than that of the metal and the metal must have sufficient catalytic activity for the anodic oxidation reaction to occur at a reasonable rate. Only a few reductants are available for electroless plating, i.e. hydrazine, sodium hypophosphite, formaldehyde, dialkylamine borane and borohydride. Electroless plating cannot be performed with all metals. Electroless plating usually accompanies hydrogen evolution and metals known to be good hydrogenation/dehydrogenation catalysts can usually be plated. An universal mechanism for electroless plating was suggested by Van den Meerakker (1981), where the first step is the dehydrogenation of the reductant.



RH represents the reductant and M the metal.

The following reducing agent-metal ion combinations exist for electroless plating according to Ohno et al., (1985). Metals in brackets indicate low possibility.

- hydrazine: Co, Ni, Pd, Pt, (Cu)
- dimethylamine borane: Ni, Co, Pd, (Pt)
- borohydride: Ni, Co, Pd, Pt, Au, Ag, (Cu)
- formaldehyde: Cu, Au, Ag, (Pt), (Pd)
- sodium hypophosphite: Au, Ni, Pd, Co

2.3.4.8.4. *Electroless silver plating*

Electroless silver plating has not received much attention. The main reason is the problem of stabilising the silver ions to allow for controlled deposition of metal atoms. Silver nitrate is used as the source of metal atoms and it can be stabilised with disodium EDTA (ethylene diamine tetra acetate) or sodium citrate. Pearlstein and Weightman (1974) successfully produced electroless silver deposits using dimethylamine borane as reducing agent. Yeung et al. (1995b) used formaldehyde as reducing agent and a very concentrated silver nitrate bath

(9.1 g/litre). This is in contrast to Shu et al. (1993), who suggests very dilute silver baths with hydrazine as reducing agent and EDTA as stabiliser. Complete compositions of silver plating solutions can be found in Yeung et al. (1995b) and Shu et al. (1993). The route of Shu was taken in this study, since lower silver concentrations make plating more controllable. The reactions which occur in the solution are:

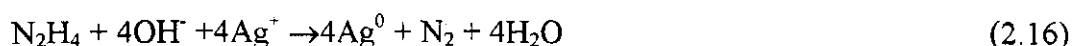
oxidation reaction:



reduction reaction:



overall:



Silver has a low activity and surface activation is required prior to plating. The silver atoms preferentially deposit on the Pd nuclei present on the substrate and not in the pores (Shu et al., 1993).

2.3.4.8.5. *Electroless nickel plating*

By far the most work done on electroless plating is in the field of electroless nickel plating. Between 1985 and 1987, Riedel (1991) reported that the world electroless nickel consumption was about 1000 tons per year. Substrates on which nickel was plated are steel and cast iron (71%), aluminium and non-ferrous (20%), tool and high-alloy steel (6%) and others (e.g. ceramics). Coatings are mainly for improved strength and for increased corrosive resistance. Deposition on alumina (Deuis et al., 1995), glass (Honma et al., 1995) and plastic require surface activation. The literature on electroless nickel plating is abundant and numerous alkaline and acidic electroless plating baths are listed (Riedel, 1991). Nickel sulphate and nickel chloride are the salts mainly used for electroless plating and although many reducing agents can be used, sodium hypophosphite is the most common. Most depositions occur at high temperatures (> 90°C), leading to fast reactions. It is very difficult to control the

deposition of small amounts of nickel (nm thickness), which was required in this study, at high temperatures. Thus a low temperature bath operating at 40 °C was chosen.

The deposition mechanism of nickel, using sodium hypophosphite as reducing agent, is as follows (Shipley, 1984):



overall:



Hydrogen ions can compete with nickel ions according to the following side reaction:

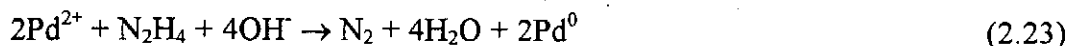


2.3.4.8.6. *Electroless palladium plating*

The two main reducing agents for electroless palladium plating are hydrazine (Rhoda, 1959) and sodium hypophosphite (Pearlstein and Weightman, 1969). In 1981, Hough et al., obtained a patent for utilising tertiary amine boranes as reducing agent. Two palladium salts can be used as source for Pd nuclei, i.e. $\text{Pd}(\text{NH}_3)_4(\text{NO}_3)_2$ and PdCl_2 which is complexed with ammonium hydroxide to form a palladium-amine complex. The first study conducted by Rhoda (1959) used tetra amine palladium nitrate as metal salt, hydrazine as reducing agent and disodium EDTA as stabiliser. Ammonium hydroxide was used to create an alkaline solution of the desired pH. The reactions occurring in the bath are:

reduction reaction:



oxidation reaction:**overall reaction:**

Hydrazine catalytically decomposes at high temperatures in the presence of a metal catalyst:



The effects of several variables (solution temperature, molar hydrazine: Pd ratio and palladium salt concentration) on palladium deposition rates are discussed in the important Rhoda (1959) publication.

A second group of researchers (Pearlstein and Weightman, 1969; Athavale and Totlani, 1989) concentrated on palladium chloride baths, complexed with ammonium hydroxide and with sodium hypophosphite as reducing agent. Pearlstein studied the effect of hypophosphite concentration, palladium chloride concentration, solution temperature, ammonium chloride concentration and ammonium hydroxide concentration on deposition rates. They also looked at the possibility of palladium alloy deposition with nickel, cobalt, zinc and rhenium. Athavale claimed that hydrazine leads to very low deposition rates, poor bath stability and poor coating quality. An in depth study on plating variables is discussed in the work of Athavale. The following mechanism (which is assumed to contain transition states of adsorbed radicals) is suggested for electroless palladium plating with sodium hypophosphite as the reducing agent:

Oxidation reactions:

Reduction reactions:

Electroless palladium plating, for creating catalytic membranes, uses only hydrazine as reducing agent and EDTA as stabiliser, because of film impurities that result when using sodium hypophosphite. Some advances have been made in the nineties on increasing deposition rates and modifying the plated Pd film density. Yeung et al. (1994, 1995a, 1995b) used osmotic pressure to change the Pd film density. Plating solution was passed through the inside of the tubular membrane while the outer surface was exposed to different solutions or air. A 6 molar sucrose solution with an osmotic pressure of about 250 bar and a 3.5 molar CaCl₂ solution with osmotic pressure of 517 bar were used, respectively, to increase palladium mass transfer to the membrane and create thicker, more dense palladium films. By using formaldehyde or air on the outer surface, zero osmotic pressure or reverse osmotic pressure was applied. The resulting films were thin, porous and discontinuous. Deposits grew radially inward leading to columnlike growth. Li et al. (1996) achieved higher palladium deposition rates by modification of the surface activation step. Instead of using the conventional sensitising and activation solutions, they used a γ -AlOOH sol modified with a PdCl₂ solution to deposit a γ -Al₂O₃ top layer with Pd particles dispersed in it.

2.3.4.8.7. Palladium silver co-deposition

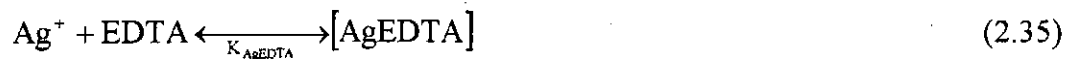
Electroless co-deposition of metals is complex and difficult to control. Individual deposition rates not only depend on the reduction rates, but also on the catalytic activity of the substrate. Further factors, which complicate the process, are hydrogen overpotentials and different degrees of complexation between the stabiliser and the metal ions. Shu et al. (1993) reports that silver inhibits palladium plating during the co-deposition process. Silver easily deposits on palladium (on the substrate) and then passivates further palladium deposition. Shu et al. (1993) offers an explanation based only on reduction potentials of silver and palladium. The most important equations are listed: $E_{\text{Ag}^+/\text{Ag}}^0 = 0.7996 \text{ (V)}$; $E_{\text{Pd}^{2+}/\text{Pd}}^0 = 0.83 \text{ (V)}$,

The Nernst equation can be used to calculate potentials in dilute solutions.

$$E_{\text{Pd}^{2+}/\text{Pd}} = E_{\text{Pd}^{2+}/\text{Pd}}^0 + \frac{RT}{2F} \ln[\text{Pd}^{2+}] \quad (\text{Volt}) \quad (2.32)$$

$$E_{\text{Ag}^+/\text{Ag}} = E_{\text{Ag}^+/\text{Ag}}^0 + \frac{RT}{F} \ln[\text{Ag}^+] \quad (\text{Volt}) \quad (2.33)$$

The co-ordination between the metal ions (Ag^+ and Pd^{2+}) and the stabiliser (EDTA) should be taken into account. The following equilibria exist:



K_{PdEDTA} and K_{AgEDTA} are stability constants with $\log K_{\text{PdEDTA}} = 18.5$ and $\log K_{\text{AgEDTA}} = 7.3$, respectively at 25 °C. The palladium and silver ion concentrations can now be written as:

$$[\text{Pd}^{2+}] = \frac{[\text{Pd}^{2+}]}{K_{\text{PdEDTA}} [\text{EDTA}]} \quad (2.36)$$

and

$$[\text{Ag}^+] = \frac{[\text{Ag}^+]}{K_{\text{AgEDTA}} [\text{EDTA}]} \quad (2.37)$$

The electrode potentials are thus:

$$E_{\text{Pd}^{2+}/\text{Pd}} = 0.2831 + \frac{RT}{2F} \ln \left[\frac{[\text{Pd}^{2+}]_0}{[\text{EDTA}]} \right] \quad (\text{Volt}) \quad (2.38)$$

and

$$E_{\text{Ag}^+/\text{Ag}} = 0.3679 + \frac{RT}{F} \ln \left[\frac{[\text{Ag}^+]_0}{[\text{EDTA}]} \right] \quad (\text{Volt}) \quad (2.39)$$

Reduction favours the higher reduction potential and from **Table 2.4** a high palladium to silver ratio bath must be used before palladium starts depositing. It must be stressed that Shu's explanation is very simplified and considers only the reduction potentials and not the other factors previously mentioned.

Table 2.4: Calculated electrode potentials (Volt)

| Electrode reaction | 25Pd-75Ag | 50Pd-50Ag | 75Pd-25Ag | 83.4Pd-16.6Ag |
|--|-----------|-----------|-----------|---------------|
| $\text{Pd}^{2+} + 2\text{e}^- \rightarrow \text{Pd}^0$ | 0.213 | 0.222 | 0.227 | 0.228 |
| $\text{Ag}^+ + \text{e}^- \rightarrow \text{Ag}^0$ | 0.256 | 0.245 | 0.228 | 0.217 |

2.3.5. PALLADIUM ALTERNATIVES FOR HYDROGEN TRANSPORT

Several low cost refractory metals, including tantalum, niobium and vanadium are stronger than palladium and have higher hydrogen permeabilities than palladium (**Figure 2.5**). They can easily be fabricated into thin walled tubes at a fraction of the cost of palladium.

Buxbaum et al. (1996, 1993) have done considerable research in this field. These metals seem to be an attractive alternative for palladium. A disadvantage is that not much is known about the ability of these metals to obtain thin films by electroless plating. The thinnest tubes available are 150 μm for niobium and 75 μm for tantalum (Buxbaum and Kinney, 1996). A further disadvantage is that these metals are much more prone to hydrogen embrittlement. Niobium membranes must operate above 420 $^\circ\text{C}$ and tantalum above 350 $^\circ\text{C}$. The permeation rates also decrease with time. Niobium and tantalum are used as alternative supports for palladium. A thin electroless palladium film is still deposited on the surface to reduce surface poisoning of niobium and tantalum.

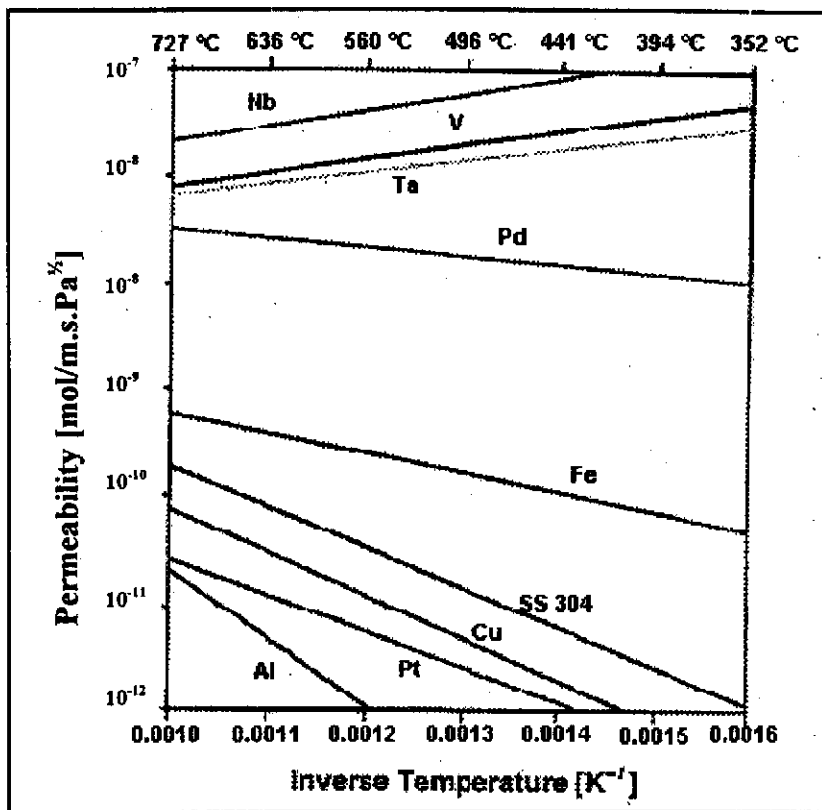


Figure 2.5: Hydrogen permeabilities for various materials

2.4. MEMBRANE CHARACTERISATION

The pores in porous membranes can be divided into three categories:

- macropores: > 50 nm
- mesopores: 2 nm < pore size < 50 nm
- micropores: < 2 nm (20 Å)

Characterisation can either be structurally related (i.e. pore size, pore size distribution, top layer thickness and surface porosity) or permeation related (i.e. actual separation parameters and cut-off value). Characterisation techniques will only be mentioned briefly and detailed descriptions can be found in Mulder (1991).

Microfiltration membranes with pore sizes ranging from 0.1 to 10 µm are characterised using scanning electron microscopy, mercury intrusion porometry, the bubble point method and by permeation measurements. Ultrafiltration membranes usually have an asymmetric structure

with selective top layer and pore sizes ranging from 20 to 1000 Å in the top layer. Difficulty is encountered when characterising these membranes with the techniques mentioned previously. The following methods can be used with greater chance of success: gas adsorption-desorption (BET), thermoporometry, permporometry, rejection measurements and scanning or transmission electron microscopy.

Transport through non-porous membranes occurs by a solution-diffusion mechanism and separation is achieved by differences in solubility and/or diffusivity. Characterisation methods include permeability measurements, differential scanning calorimetry for polymer membranes, X-ray diffraction analysis and plasma etching. The surface can be analysed using electron spectrometry, X-ray photoelectron spectrometry, secondary ion mass spectrometry or Auger electron spectrometry. The three main techniques used for membrane characterisation in this study are particle induced X-ray emission (PIXE), scanning electron microscopy (SEM) and X-ray diffractometry (XRD).

2.4.1. PARTICLE INDUCED X-RAY EMISSION (PIXE)

Particle induced X-ray emission started in 1970 and is a powerful technique for elemental analysis (Johansson and Campbell, 1988). X-ray emission analysis involves the excitation of an atom in a specific sample so that it can emit characteristic X-rays. The X-rays are then measured. The intensities can be converted back to elemental concentrations in the sample. Electron beams, filtered photons or alpha particles can be used as a means of excitation. The main advantage of protons over electrons is that protons of a much higher energy can be used (MeV energy range), thus achieving greater penetration depth (Willard et al., 1981). Depth information can easily be extracted with high energy protons, while electrons are mainly used for surface characterisation.

Lithium-drifted Si(Li) detectors are used for X-ray detection. Si(Li) spectroscopy is coupled with proton excitation to allow for a high data accumulation rate and the capability of simultaneous analysis of many elements. The main applications of PIXE are in biology, medicine, environmental analysis, oceanography, geology, material science and metallurgy. Concentrations of down to 1 ppm can be detected.

Inner shell electrons are ejected from an atom by means of a proton beam. Outer shell electrons will fill the resulting vacancies and characteristic X-rays, with specific energies for a particular element, will be emitted. Transitions in the innermost shell are called K X-rays (high energy) and those of the next shell are L X-rays (lower energy). A particle accelerator is used for supplying protons. The Van de Graaff machine was used in this study and is still used quite commonly for various analysis (Christian and O'Reilly, 1986). Protons of 2-3 MeV can be produced and twice the energy for double charged helium ions. The beam is stabilised by passing it through magnetic fields and directed by means of slits.

PIXE is a non-destructive technique and suitable for analysing valuable specimens. A resolution of 160 eV can be obtained, thus K_{α} X-rays of neighbouring elements in the transition element region of the periodic table can be fully resolved and analysed. No overlapping occurs for K-lines of palladium and silver; a problem which is encountered with electron analysis. A further advantage of PIXE is that it offers a maximum sensitivity or minimum detection limit for elements 20 to 35 and 75 to 85. These are the most common trace elements in the biological and geological sciences.

2.4.2. SCANNING ELECTRON MICROSCOPY (SEM)

The SEM can be used to extract morphological information and for analytical purposes when coupled with X-ray generation. The essential features of a scanning electron microscope are (Hearle et al., 1974):

- a source of electrons
- a method of focussing a tiny beam of electrons on the sample
- a method of scanning the electron beam across the sample
- a method of detecting the response from the sample
- a display system
- some way of transmitting response data from the sample to the displayer

The scanning electron microscope has numerous advantages over the optical and direct electron microscope. Some of the advantages include (Hearle et al., 1974):

- The focus depth is much greater than for optical microscopes, which is an important asset for extracting morphological information

- At high magnification, no complex sample preparation is required, as in the case of transmission electron microscopy
- Switching from low to very high magnification is both easy and quickly. No problems are encountered when zooming in on fine detail

Some disadvantages are:

- The high vacuum environment required for operation
- No colour response and no internal detail

Unlike with PIXE, the electron energy is much lower (between 2 and 50 keV; Goodhew, 1975) and no penetration through atomic layers occur. The resolution achieved for X-ray analysis is weak and only suitable for detecting major matrix elements.

2.4.3. X-RAY DIFFRACTOMETRY (XRD)

This subject is covered in detail in the work of Cullity, 1978. X-ray diffraction is used to determine the crystal structure of a metal or alloy. When an X-ray passes through the three dimensional array of atoms making up a crystal, a diffraction effect is produced. Each atom scatters a fraction of the beam and the scattered waves can reinforce under certain conditions to form a diffracted beam. The conditions that must be fulfilled are given by the Bragg equation (Smithells, 1992):

$$n\lambda = 2d_{hkl} \sin \theta \quad (2.40)$$

with n an integer, λ the wavelength of the incident beam, d_{hkl} the interplanar spacing of the hkl planes and θ the angle of incidence on the hkl planes.

Angular positions of diffraction peaks, shape of peaks and peak intensity give information on the physical state of the crystals and the crystal shape. Some applications include (Smithells, 1992):

- Phase analysis and quantification
- Crystal structure determination

- Texture measurement and detection of imperfections
- Macro stress and micro stress analysis

2.5. GAS SEPARATION

Gas molecules tend to diffuse from a higher pressure to a lower pressure. Several transport mechanisms exist depending on the pore size:

- bulk diffusion
- Knudsen diffusion
- viscous flow in wide pores
- surface diffusion along the pore wall

No separation can be obtained by viscous flow (pores $> 500 \text{ \AA}$), because the mean free path of the gas molecule is very small compared to the pore diameter. When the free path of the gas becomes greater than the pore diameter, the gas flow is called Knudsen flow. This takes place at pore diameters of about 50-100 \AA under pressure and 50-500 \AA in the absence of pressure. The mean free path of oxygen at 25 °C and 10 bar pressure for example is 70 \AA , thus a membrane with pores smaller than 70 \AA will result in Knudsen flow at that conditions. The separation factor is determined by the square root ratio of the molecular masses of the gases being separated. Bulk diffusion takes place when certain gases are preferentially dissolved. One gas diffuses faster through the membrane than the other, causing a difference in permeation and separation. Pore sizes required for bulk diffusion is a few Angstrom and smaller.

CHAPTER 3

EXPERIMENTAL PROCEDURES

3.1. INTRODUCTION

In this chapter the experimental procedures for each step in the electroless plating process of palladium, silver and nickel will be discussed. The composition of the solutions used, and the techniques for preparing them, will be presented. A method for heat treatment of metallic films to ensure proper alloying between palladium, silver and nickel is developed. Finally, all the characterisation techniques, as well as the sample preparation required for each instrument, are given.

3.2. MEMBRANE FABRICATION

Membranes were supplied by Prof. VM Linkov, currently from the University of the Western Cape. The membrane fabrication technique used by Linkov and co-workers is given below: γ - Al_2O_3 and ZrO_2 , stabilised with Y_2O_3 , were heated at 900°C in a vacuum furnace for two hours to remove organic pollutants. This operation was followed by separate milling of Al_2O_3 and ZrO_2 in a wet ball mill using steel balls with a diameter of 15 mm. The oxide/ball/water ratio was maintained as closely as possible to 1:2:1 throughout the whole milling operation. The dense precipitate formed in the mill was placed into a polyethylene drum, 15-20% water was added to it and the mixture was roller stirred for over 4 hours. The casting suspension was prepared by mixing milled Al_2O_3 and ZrO_2 stabilised with Y_2O_3 in the same drum for 1 hour.

The composition of the casting suspension, which resulted in the best mechanical properties and highest chemical stability of the resulting ceramic membranes, was as follows:

- Al_2O_3 70%
- ZrO_2 29%
- Y_2O_3 1%

The casting suspension was poured into specially designed tubular gypsum moulds where precursors for ceramic membranes formed during 1 minute. The moulds were drained,

membrane precursors removed and placed into a drying chamber. The drying temperature was maintained at 20 °C, the humidity at 40% and the drying time was 2-3 days. After drying, the membrane precursors were placed in an oven, heated up to 1300 °C at a heating rate of 100-110 °C per hour and calcined at this temperature for 1 hour.

3.2.1. MEMBRANE CHARACTERISTICS

The alumina-zirconia supports were analysed by the Department of Chemical Engineering at the University of Cape Town. Their results showed that the BET surface area was between 3.8 and 4.6 m²/g and the average pore diameter between 68 and 78 Å.

3.3. MEMBRANE CLEANING

The received membrane modules were 21 cm in length. They were cut into 5 cm pieces using a diamond saw. Four cleaning steps were used:

- Ultrasonic rinsing in 1 litre 0.1 wt% NaOH solution (1.0 g NaOH dissolved in 1 litre demineralised water) for 1 minute.
- Ultrasonic rinsing in 1 litre demineralised water for 2 minutes.
- Rinsing in isopropanol for 10 minutes (250 ml).
- Rinsing in demineralised water for 10 minutes (250 ml).

Rubber gloves were used for all handling. After cleaning, the membrane pieces were dried in an oven at 120 °C for at least 8 hours.

3.4. MEMBRANE PRETREATMENT

The two step procedure was used with the same solutions as used by Shu et al. (1993). For a 5 cm membrane piece, 500 ml tin chloride and 500 ml palladium salt solution were used (**Table 3.1**). The tin chloride solution was prepared by weighing the salt, adding demineralised water and then adding the hydrochloric acid. The mixing order of the palladium salt solution was the same. The tin chloride solution was used within 8 hours of preparation, since it was found that the activity of the solution started to decline after a day or two. The palladium salt solution has an infinite shelf life. The same palladium salt solution was used more than once for the activation of different membrane pieces.

Table 3.1: Solutions for pretreatment at room temperature (25 °C)

| | |
|---|-------------------------------|
| <u>Tin chloride solution</u> | |
| SnCl ₂ ·2H ₂ O | 1 g/litre |
| HCl (32%) | 1 ml/litre |
| | |
| <u>Palladium salt solution</u> | |
| (NH ₃) ₄ Pd(NO ₃) ₂ | 1.6 ml 10% solution per litre |
| HCl (32%) | 1 ml/litre |

The membranes were sealed at the ends with teflon to ensure activation on the outer membrane surface only. The following procedure was repeated ten times (the first five times in fresh solutions and the last five times in the same solutions used for the first five treatments to maximise the use of pretreatment solution):

- 2 minutes in 100 ml tin chloride solution
- 30 seconds in 100 ml demineralised water
- 2 minutes in 100 ml palladium salt solution
- 30 seconds in 100 ml demineralised water

The activation was completed with a further five treatments in the solutions used in the previous steps:

- 1 minute in 100 ml tin chloride solution
- 1 minute in 100 ml palladium salt solution

After pretreatment, an even, uniform brown layer was deposited on the white membrane support. In all cases, the above method ensured that the entire outer membrane surface was catalysed. The 50 mm pieces were then dried for 2 hours in an oven at 120 °C and cut into 8 mm pieces using a diamond saw. Latex rubber gloves were used at all times to prevent fingerprints and oil deposits on the surface. The 8 mm pieces were washed in demineralised water to remove possible ceramic dust from the cutting process and then dried again at 120 °C for at least 8 hours. Prior to electroless plating the pieces were weighed.

3.5. ELECTROLESS PLATING

3.5.1. SAFETY PROCEDURES

Hydrazine is a very toxic chemical and great care should be taken when working with it. All electroless plating experiments were performed in a fume hood with a strong extractor fan. Rubber gloves, protective clothing and a respirator must be worn at all times.

3.5.2. ELECTROLESS PALLADIUM PLATING

Initially $(\text{NH}_3)_4\text{Pd}(\text{NO}_3)_2$ (10% solution) and PdCl_2 were compared to determine which one is the more effective palladium salt (Table 3.2). The composition of the PdCl_2 bath was taken from Collins (1993) and the composition of the $(\text{NH}_3)_4\text{Pd}(\text{NO}_3)_2$ (10% solution) bath was similar to that used by Yeung et al., (1995a) except that half his concentration was used in these experiments. The effect of adding formaldehyde, which also acts as a reducing agent, was determined in the initial set of experiments.

Membranes were end-sealed with teflon plugs to ensure plating only on the outer membrane surface. The volume of plating solution was 22 ml, membrane length 8 mm and plating time 2 hours. Plating was done in glass vials pre-cleaned with 6% HNO_3 . The plating temperature was controlled to ± 0.5 °C from the setpoint temperature of the water bath.

Table 3.2: Compositions of the palladium plating solutions (values per litre plating solution) initially used

| Components of plating solutions | 1 | 2 | 3 | 4 |
|---|------|------|------|------|
| $(\text{NH}_3)_4\text{Pd}(\text{NO}_3)_2$ (ml 10% solution) | 25 | 25 | - | - |
| PdCl_2 (g) | - | - | 2.7 | 2.7 |
| NH_4OH (25 %) (ml) | 200 | 200 | 390 | 390 |
| Disodium EDTA (g) | 20 | 20 | 35 | 35 |
| Hydrazine (molar ratio to Pd) | 0.80 | 0.80 | 0.66 | 0.66 |
| pH 10 buffer (ml) | 100 | 100 | - | - |
| Formaldehyde (37 %) (ml) | - | 1.5 | - | 1.5 |
| Temperature (°C) | 64 | 64 | 64 | 64 |

The palladium salt solutions were allowed to stabilise for at least 8 hours prior to plating. The palladium salt solution and the hydrazine solution were heated separately to the reaction temperature. The sealed membrane was then added to the palladium salt solution and then the hydrazine solution was introduced.

For optimising the palladium conversion, the following solutions were used:

Table 3.3: Composition per litre of palladium plating solution used for all further experiments

| | |
|---|----------------------------|
| (NH ₃) ₄ Pd(NO ₃) ₂ (g 10 % solution) | 27.5 |
| NH ₄ OH (25 %) (ml) | 200 |
| Disodium EDTA (g) | varied from 20.6 to 171.4* |
| Hydrazine 0.02 M (ml) | varied from 258 to 405* |
| pH buffer (varied from 8 to 12) (ml) | 100 |
| Temperature (°C) | varied from 59 to 77 |

*EDTA: Pd molar ratio varied from 6 to 50 and the hydrazine: Pd molar ratio varied from 0.4 to 0.88

For these experiments the plating volume was 20 ml, plating time 3 hours and membrane length between 7 and 9 mm. After a few minutes in the plating solution, the outer membrane surface started changing from brown to dark grey. Tiny gas bubbles formed at the surface, indicating that the reaction was in progress. The plating solution was shaken every ten minutes for the duration of the experiment. When the experiment had finished, the membrane was washed in water to remove most salts present in the membrane pores and then heated at 200 °C for 2 hours to evaporate all remaining organic material present. At this point the membrane was weighed again to determine the mass increase.

3.5.3. ELECTROLESS SILVER PLATING

The pretreatment procedure for silver deposition is the same as that used for palladium deposition. The silver plating volume was 20 ml and plating time 2 hours. Solutions were

once again allowed to stabilise for at least 8 hours. **Table 3.4** gives the composition of the solutions used.

Table 3.4: Composition per litre of silver plating solution used

| | |
|--------------------------------------|----------------------------|
| AgNO ₃ (g) | 0.65 |
| NH ₄ OH (25 %) (ml) | 200 |
| Disodium EDTA (g) | varied from 28.5 to 113.9* |
| Hydrazine 0.02 M (molar ratio to Pd) | 1.3:1 (249 ml) |
| Temperature °C | Varied from 55 to 65 |

*EDTA: Ag molar ratio varied from 20 to 80

No buffer was used for silver plating, but ammonia was used to obtain the correct pH. The brown pretreated membrane surface turned white when silver was deposited on the activated substrate. When silver was deposited on a palladium film, the dark grey surface turned light grey or white. Drying was done in the same way as the palladium coated membranes. The silver deposit was uneven and in many cases did not cover the entire substrate.

3.5.4. ELECTROLESS PALLADIUM-SILVER CO-DEPOSITION

The plating volume for electroless palladium-silver co-deposition was 25 ml per experiment and the plating time was 2 hours. The composition of the plating solution is listed in **Table 3.5** and is similar to that used by Yeung (1995a).

Table 3.5: Composition per litre of palladium-silver plating solution used at 60 °C

| | |
|---|--------------------------|
| (NH ₃) ₄ Pd(NO ₃) ₂ (g 10 % solution) | 5.0 |
| AgNO ₃ (g) | varied from 0.02 to 0.10 |
| NH ₄ OH (25 %) (ml) | 200 |
| Disodium EDTA (g) | 45 |
| Hydrazine 0.02 M (molar ratio to Pd) (ml) | 250 or 500 |
| Buffer (pH 10) (ml) | 100 |

The co-deposits were generally non-uniform, uneven and did not cover the entire surface. Drying was done in the same manner as the palladium coated membranes. The deposited amounts were very small ($< 0.6 \text{ mg/cm}^2$).

3.5.5. ELECTROLESS NICKEL PLATING

Several plating baths can be used for electroless nickel plating. Most operate at temperatures above $90 \text{ }^\circ\text{C}$, making the plating reaction very fast. When preparing palladium nickel alloys, 0.4 mg/cm^2 has to be deposited for a 5 micron thickness film with 7 wt% nickel. A low temperature ($40 \text{ }^\circ\text{C}$) nickel plating bath was thus chosen according to Riedel (1991). **Table 3.6** gives the composition of the bath.

Table 3.6: Composition per litre of nickel plating solution used

| | |
|--------------------------------------|-------------------------|
| NiSO ₄ .6H ₂ O | 20 g |
| NH ₄ OH (25 %) | 200 ml |
| NaH ₂ PO ₄ | 10 g |
| Temperature | Varied from 35 to 45 °C |

The plating time was varied from 5 to 60 minutes. The membrane length was 8 to 10 mm and the plating volume was 20 ml. The nickel sulphate and the sodium hypophosphite were added in the glass vial and the solution preheated to the set point temperature. Then the membrane was added. The surface quickly turned from brown to silver grey after the membrane was placed in the plating solution. Drying was done in the same way as the palladium coated membranes.

3.6. HEAT TREATMENT FOR CREATING PALLADIUM ALLOYS

Composite membranes were prepared by separate deposition of metals on the ceramic support. When preparing palladium-nickel composites, the palladium was first deposited and then the nickel. For palladium-silver composites, both the deposition of palladium on silver and the deposition of silver on palladium were investigated. Palladium-silver-nickel composites were prepared by first depositing the silver, then the palladium and finally the nickel. The set up used for heat treatment is schematically shown in **Figure 3.1**.

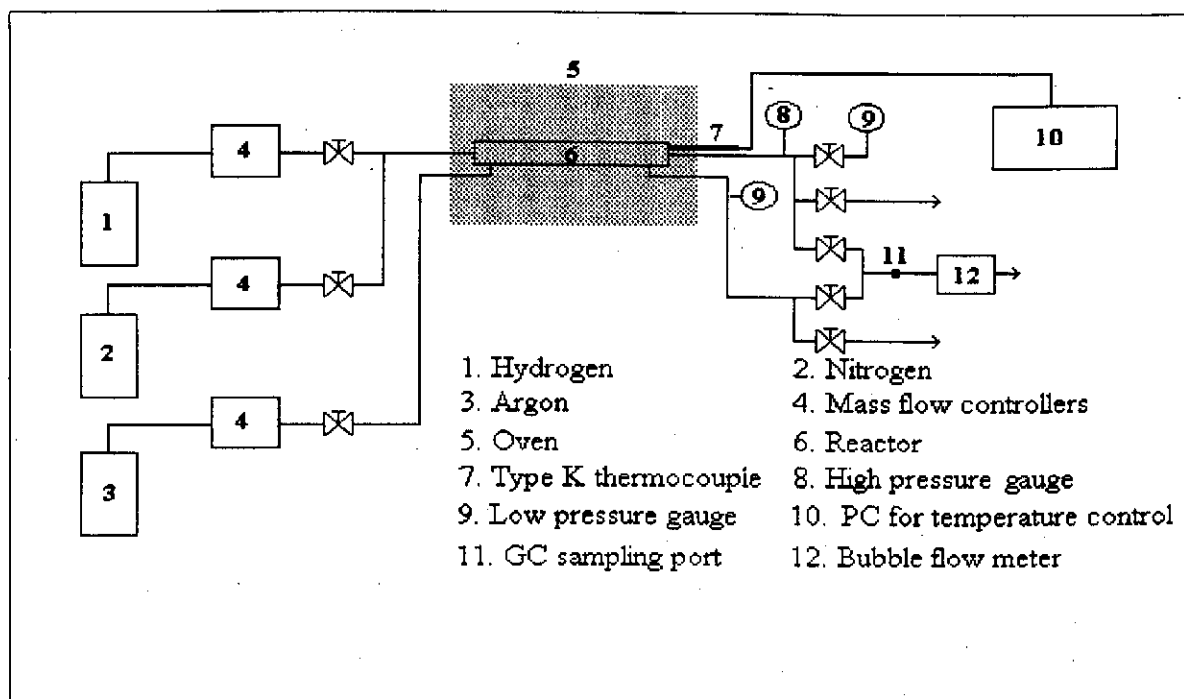


Figure 3.1: Schematic representation of the set up for performing heat treatment

The following procedure was used for the heat treatment of the composite membranes:

- The membrane pieces were put in a stainless steel reactor, which was placed inside a tubular heating oven. The system was flushed (at room temperature) with 1.5 litres of argon per minute for about 5 minutes. This was done to remove any oxygen present.
- The argon flow rate was set at 100 cm^3 per minute using a Hastings flow controller (HFC 202C) and the temperature was increased from room temperature at a rate of $100 \text{ }^\circ\text{C}$ per 30 minutes until $650 \text{ }^\circ\text{C}$ was reached.
- The argon flow was stopped when $650 \text{ }^\circ\text{C}$ was reached and replaced by a hydrogen flow. The flow rate was controlled at 50 cm^3 per minute using a Hastings flow controller (HFC 202C). Heating in a hydrogen atmosphere at $650 \text{ }^\circ\text{C}$ ($500, 600$ and $700 \text{ }^\circ\text{C}$ were used by Shu et al., 1996) continued for 5 hours.
- The hydrogen flow was stopped and replaced by an argon stream to degas the palladium film and to avoid hydrogen embrittlement. The flow rate was 100 cm^3 per minute for 2 hours.
- The oven was then switched off and the reactor allowed to cool down. After 8 hours the membranes were removed from the reactor and cut into smaller pieces for analysis.

3.7. ANALYTICAL TECHNIQUES

Inductive coupled plasma discharge (ICP) was used to analyse solutions for kinetic studies. Palladium solutions were diluted to below 100 ppm and silver solutions to below 15 ppm by adding demineralised water.

Scanning electron microscopy (SEM) was carried out at the Microscope Unit, University of Cape Town, with a Cambridge Stereoscan 440. For top view images, the samples were mounted on aluminium stubs and gold plated. For cross section views, the membranes were mounted on their sides in small round cups (about 30 mm diameter). The cups were filled with a quick setting resin that hardened completely after about five minutes. The resin disks were polished using water sanding paper of different mesh sizes (400, 800 and 1000). The final treatment consisted of polishing the disk on a polishing wheel with 0.3 and 0.05 μm alumina slurries. The disks were then carbon coated to allow for energy dispersive X-ray analysis (EDX). EDX was used for mapping palladium, silver and nickel in the film before and after heat treatment and it was done using a KEVEX SIGMA 3 analyser. SEM pictures were taken at 10 kV and a probe current of 200 pA, while EDX was done at 40 kV and a probe current of about 100 pA.

Rutherford backscattering (RBS) and proton induced X-ray emission (PIXE) were performed on the same samples as those used for SEM. The analysis was conducted at the National Acceleration Centre (Faure) with a Van der Graaff Generator. An iridium on silicon reference was used to calibrate the instrument. Two and three MeV protons were used as source of particles. A point analysis of each sample was done, firing protons into the metal film. A view of the membrane's cross-section was used for constructing maps. A single map ran for at least 6 hours to build up sufficient statistics. Line scans were taken from the outside to the inside of the membrane's cross-section. Fifteen points were selected, evenly spaced half a micron apart, and a point analysis was done at each point. By doing so, a concentration profile from the resin across the metal film into the support could be constructed. The proton beam was tuned to less than one micron in the y-direction and about 3 micron in the x-direction. The membranes were mounted in such a way that the film could be scanned in the y-direction.

X-ray diffraction patterns were used to determine the crystal structure of the alloy films. A Phillips X-ray diffractometer with Cu K α radiation and a graphite monochromator was used to take the spectrums. A silicon standard was used for calibration of the 2 θ scale. The voltage was set at 50 kV and the current at 40 mA. XRD was done at the Geology Department, University of Stellenbosch.

3.8. SUMMARY

In this chapter, the various experimental steps for preparing palladium, silver, nickel and palladium composite membranes are outlined. All the solutions used for cleaning, pretreatment and electroless plating are presented. The heating method used for creating palladium alloys is discussed and a flow chart of the set up given. All the equipment used for analysis is listed as well as the techniques used for sample preparation. Finally, the standards for calibration of the various instruments are also discussed. A list of all chemicals used can be found in **APPENDIX A**.

CHAPTER 4

ELECTROLESS PALLADIUM PLATING

4.1. INTRODUCTION

Electroless palladium (Pd) plating on alumina membranes was investigated with the aim of obtaining very high Pd conversions and pure Pd films. Interactions between operating variables including Pd source, temperature, reducing agent concentration, stabiliser concentration and buffer pH require proper choice of conditions to ensure bath stability and to maximise conversion. An investigation of the above mentioned variables readily enabled conversions exceeding 80 % to be obtained after 3 hours of plating. Near optimal values (> 95 %) were also achieved within a three hour reaction period for a very specific choice of variables. Surface uniformity and purity of the deposited film were excellent. The operating concentration of the stabiliser (Na₂EDTA) appears to be the most critical consideration in the plating process. Varying Na₂EDTA concentration, results in a optimal region of Pd conversion. Conversions quickly dropped when the system became unstable or if the system had too high a stability.

4.2. PROCESS VARIABLES

There are many variables influencing electroless palladium plating. The most important variables investigated were:

- type of reducing agent
- type of palladium salt
- concentration of reducing agent
- concentration of stabiliser
- buffer pH value
- temperature

The following variables were kept constant for all runs:

- volume of plating solution
- surface area of membrane to be plated

- concentration of palladium salt
- stirring mechanism (solution was shaken by hand every ten minutes)

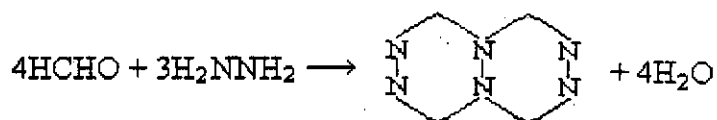
The effects of the variables were determined by factorial designs, and then the conditions for optimum palladium conversion were investigated.

4.3. CHOICE OF CHEMICALS

A limited choice of reductants are available for electroless palladium plating viz. dialkylamine borane (Hough et al., 1981), borohydride, hypophosphite (Pearlstein et al., 1969), formaldehyde and hydrazine (Rhoda, 1959). Very little has been published using borohydride and boranes for electroless Pd plating. This option was not considered, since boron is co-deposited with Pd. Formaldehyde is not a good reducing agent (Ohno et al., 1985) due to the small potential difference that acts as driving force. Hypophosphite is commonly used, but deposits usually contain in excess of 1.5 % phosphorus (Athavale et al., 1989), thus lowering the quality of the film. Problems with surface adhesion of Pd using hypophosphite can be encountered for films exceeding 5 μm (Collins, 1993). Hydrazine was judged the most suitable and chosen as reducing agent.

Both tetra amine palladium nitrate and palladium chloride were investigated as source of metal ions, with hydrazine and formaldehyde as reducing agents. The results are given in **Figure 4.1**

The conditions at which the experiments were performed are given in **Table 3.2** (see **Experimental Procedures**). An addition of between 1 and 2 ml formaldehyde per litre plating solution is claimed to produce higher quality films (Yeung et al., 1995a). In this study a white gelatinous precipitate was formed in such a solution. As seen from **Figure 4.1**, the conversion was very low with formaldehyde present and decreased to zero after two plating sessions, making it unsuitable as reducing agent when an osmotic driving force is not present. The precipitate is a polymerised form of tetraformal trisazine. The gel intermediate is formed according to the following reaction (Schmidt, 1984, p.313):



(4.1)

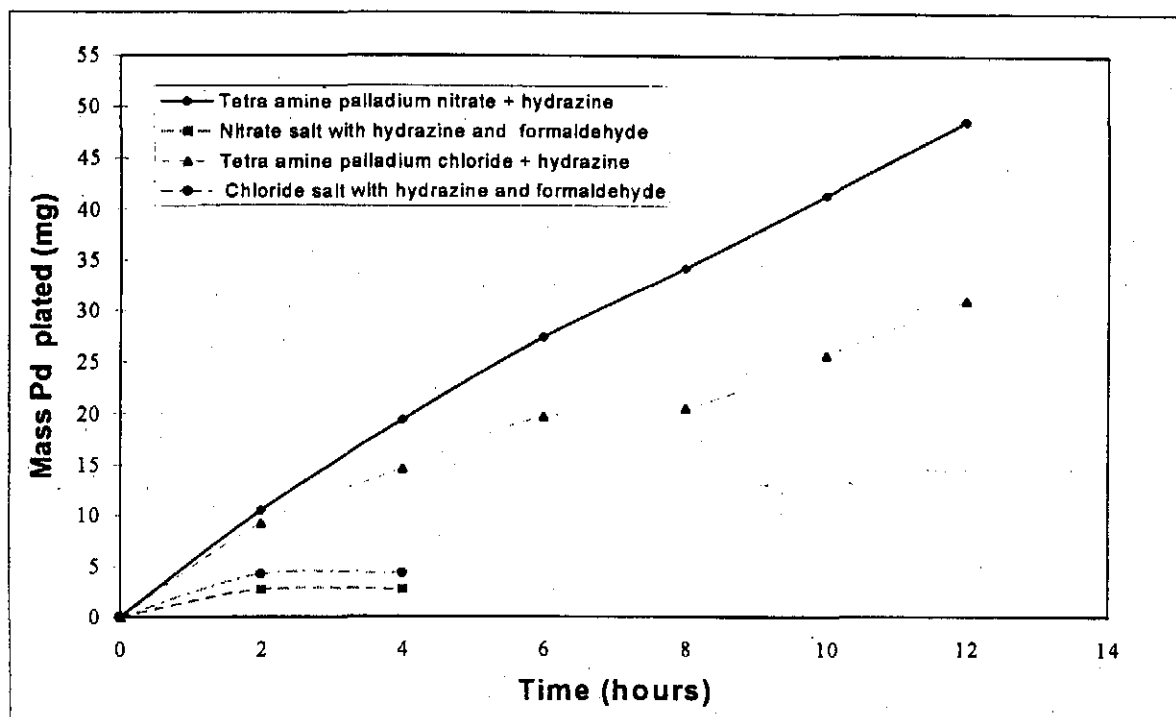


Figure 4.1: The effect of various Pd salts and reducing agents on mass of Pd plated ($T = 64\text{ }^{\circ}\text{C}$)

Membranes were plated for two hours, removed, dried and weighed. The membranes were then placed in fresh plating solution and the process repeated for six times to obtain a total plating time of twelve hours. Both the tetra amine complexes of palladium chloride and palladium nitrate produced films which increased linearly in thickness with time (see **Figure 4.1**). This quality is very suitable for controlling the film thickness. The chloride salt gave lower conversions (**Figure 4.2**) and thus the nitrate form was preferred. Hydrazine was chosen as the reducing agent.

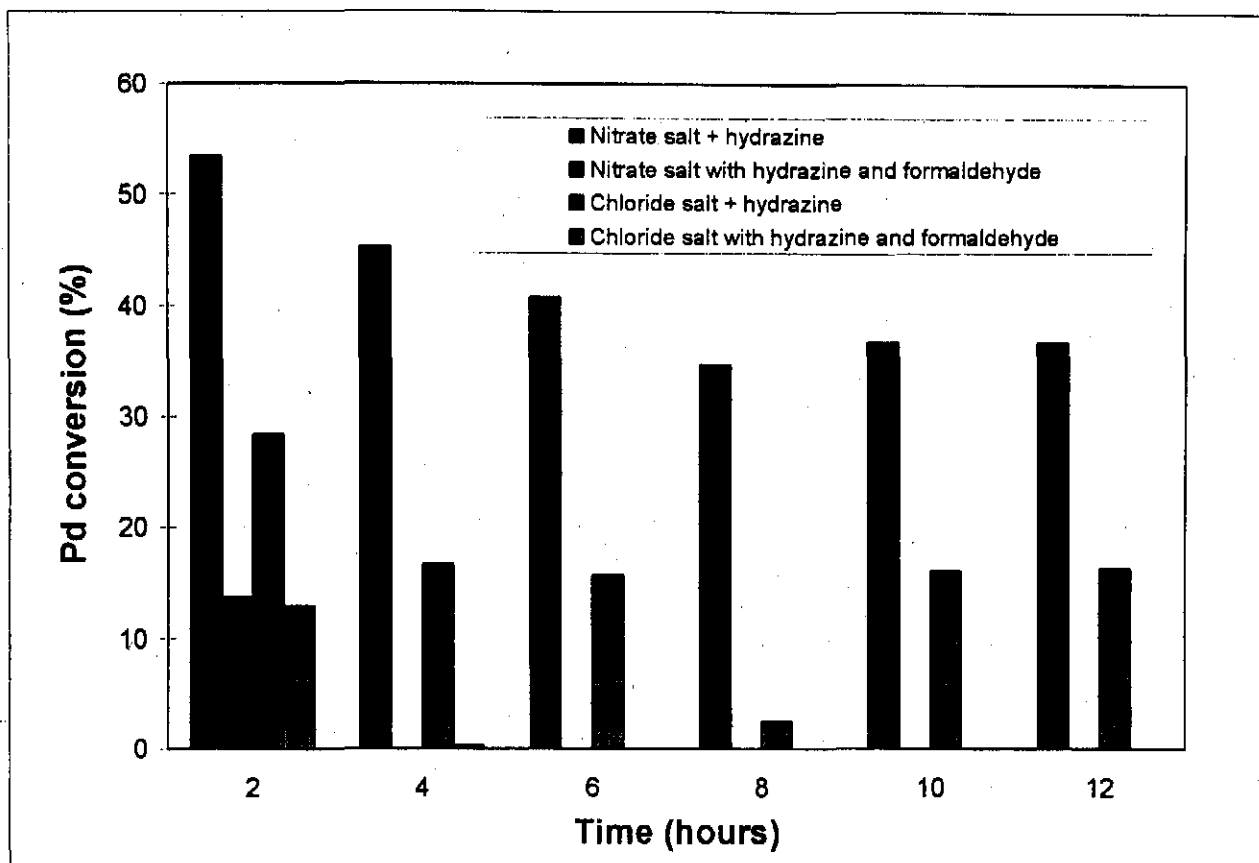


Figure 4.2: The effect of various Pd salts and reducing agents on Pd conversion

4.4. FACTORIAL DESIGNS

The factorial design is the most efficient technique to study the effects of two or more factors. The effect of a factor is the change in response produced by a change in the level of the factor. All possible combinations of the levels of the factors are investigated. Interaction occurs when the difference in response between the levels of one factor is not the same at all levels of the other factors. The principles of the factorial design are discussed in Montgomery (1991) and Davies (1978). The main advantages of the factorial design over one-factor-at-a-time experiments are:

- They are more efficient than one-factor-at-a-time experiments,
- They prevent drawing misleading conclusions when interactions are present,
- The effect of one factor can be estimated at several levels of the other factors, giving valid conclusions over a wide range.

A 2³ factorial design was performed with one replicate, keeping the EDTA concentration constant (EDTA: Pd-salt molar ratio of 6:1) and varying the temperature, hydrazine concentration and buffer pH. The process variables are given in **Table 4.1**.

Table 4.1: Process variables used for first factorial design

| Factor | Variable | Low level | High level | Unit |
|--------|--------------------|-----------|------------|------|
| A | Hydrazine: Pd-salt | 0.4:1 | 0.72:1 | - |
| B | Buffer pH | 9 | 11 | pH |
| C | Temperature | 59 | 71 | °C |

The results are presented in **Table 4.2**.

Table 4.2: Responses (palladium salt to Pd metal conversion) for variables investigated

| | Hydrazine: Pd = 0.4:1 | | Hydrazine: Pd = 0.72:1 | |
|------------------|-----------------------|-----------|------------------------|-----------|
| | T = 59 °C | T = 71 °C | T = 59 °C | T = 71 °C |
| buffer pH | | | | |
| 9 | 23.0 | 42.0 | 35.5 | 30.0* |
| | 16.5 | 44.0 | 42.0 | 39.0* |
| | | | | |
| 11 | 21.0 | 50.0 | 45.0 | 33.5* |
| | 17.0 | 41.0 | 26.5 | 35.5* |

* indicates where bath instability occurred during a 3h plating period

At high hydrazine concentrations and high temperatures, bath instability occurred. The Pd was not only deposited on the membrane, but also on Pd nuclei in the solution and on the walls of the glass vial. The solution turned black and no further plating could occur. The bath decomposition was an indication that the EDTA concentration was too low. Statistical analysis of the data in **Table 4.2** yielded the results listed in **Table 4.3**.

Table 4.3: 2³ factorial design with EDTA concentration constant

| | Effect | Sum of squares | Degrees of freedom | Mean square | F-ratio |
|---------------|--------|----------------|--------------------|-------------|--------------------|
| hydrazine (A) | 4.06 | 4.06 | 1 | 66.02 | 1.72 ^a |
| buffer pH (B) | -0.31 | -0.31 | 1 | 0.39 | 0.01 |
| T (C) | 11.06 | 11.06 | 1 | 489.52 | 12.78 ^b |
| AB | -1.19 | -1.19 | 1 | 5.64 | 0.15 |
| AC | -13.81 | -13.81 | 1 | 763.14 | 19.93 ^b |
| BC | 1.56 | 1.56 | 1 | 9.77 | 0.26 |
| ABC | -0.06 | -0.063 | 1 | 0.02 | 0.00 |
| Error | | | 8 | 38.30 | |
| Total | | | 15 | | |

^asignificant at 25%, ^bsignificant at 1%

Table 4.3 indicates that the buffer pH has little effect on palladium conversion for the values investigated. The chance that the temperature and the temperature-hydrazine concentration interaction do not have an effect on palladium conversion is less than 1%. It can thus be concluded, with high certainty, that these two effects are significant. Figures 4.3-4.9 show the interactions between the variables investigated. Lines that do not run parallel indicate interaction between variables. No interaction occurred between buffer pH and temperature or buffer pH and hydrazine concentration. The strong hydrazine-temperature interaction is clear from Figures 4.4 and 4.5.

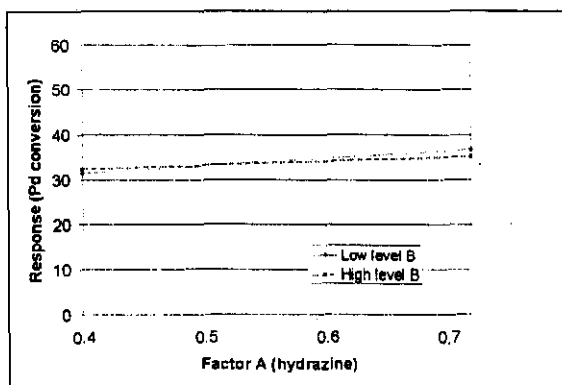


Figure 4.3: Hydrazine-buffer pH interaction

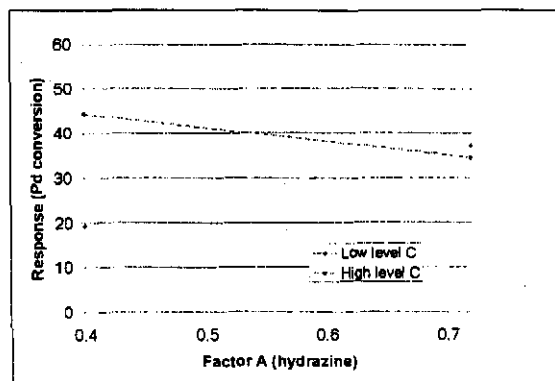


Figure 4.4: Hydrazine-temperature interaction

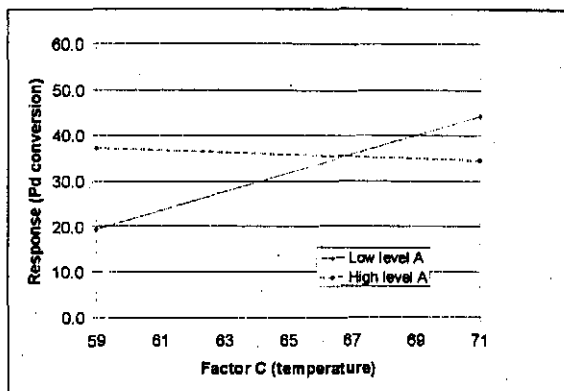


Figure 4.5: Temperature-hydrazine interaction

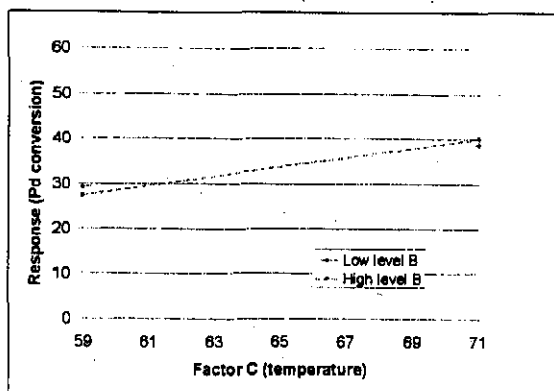


Figure 4.6: Temperature-buffer pH interaction

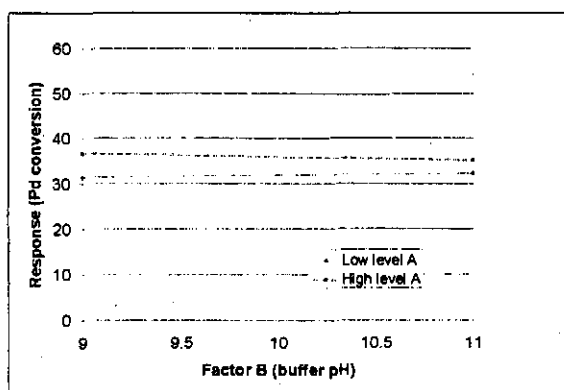


Figure 4.7: Buffer pH-hydrazine interaction

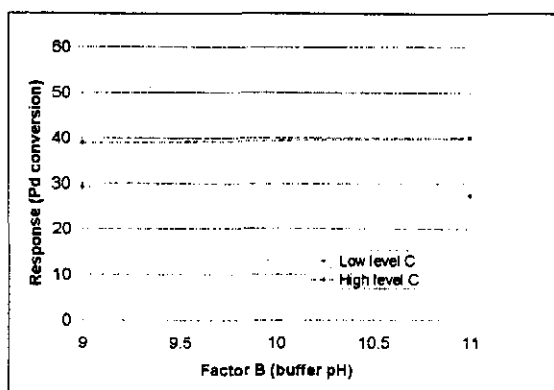


Figure 4.8: Buffer pH-temperature interaction

A one-factor-at-a-time set of experiments were done to determine suitable EDTA concentrations for a second 2^3 factorial design with buffer pH constant at pH = 11. The EDTA: Pd salt molar ratio was varied with temperature constant at 71 °C, hydrazine: Pd-salt molar ratio = 0.72:1 and buffer pH = 11. The results are summarised in **Figure 4.9**. The solution was stable for EDTA: Pd-salt molar ratios of 20:1 and greater.

A second 2^3 factorial design (**Table 4.4**) was constructed to determine the effects of EDTA, hydrazine and temperature on Pd conversion. The buffer pH was kept constant at pH = 11.

Table 4.4: Process variables used for second factorial design

| Factor | Variable | Low level | High level | Unit |
|--------|--------------------|-----------|------------|------|
| A | Hydrazine: Pd-salt | 0.56:1 | 0.72:1 | - |
| B | EDTA: Pd-salt | 14 | 30 | - |
| C | Temperature | 71 | 77 | °C |

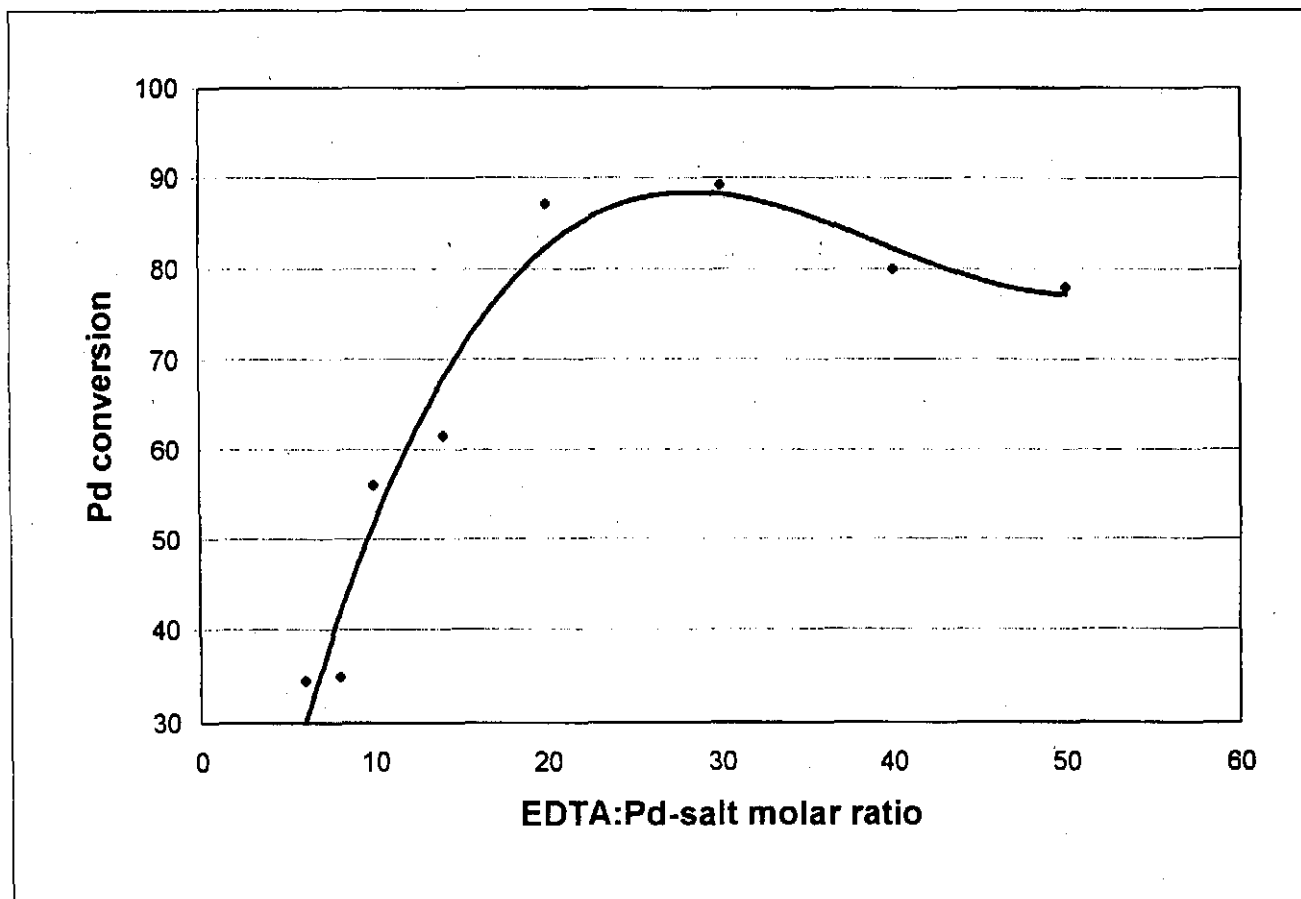


Figure 4.9: The effect of EDTA concentration on Pd conversion

The responses for the variables in Table 4.4 are listed in Table 4.5. A single experiment was done at each point. For one point there are four data values, since this point was also investigated during other sets of experiments.

Table 4.5: Responses (palladium salt to Pd metal conversion) for variables investigated

| EDTA: Pd | Hydrazine: Pd = 0.56:1 | | Hydrazine: Pd = 0.72:1 | |
|----------|------------------------|-----------|-------------------------|-----------|
| | T = 71 °C | T = 77 °C | T = 71 °C | T = 77 °C |
| 14 | 55.0* | 71.8* | 61.5* | 59* |
| 30 | 71.8 | 81.5 | 87.0; 98.3, 96.5; 93 | 99.2 |

* indicates where bath instability occurred during a 3h plating period

Bath instability was observed at the low EDTA concentration, which limited the Pd conversion. A statistical analyses of the data in Table 4.5 is given in Table 4.6.

Table 4.6: 2³ factorial design with buffer pH constant at pH = 11

| | Effect | Sum of squares | Degrees of freedom | Mean square | F-ratio |
|---------------|--------|----------------|--------------------|-------------|---------|
| hydrazine (A) | 8.27 | 136.74 | 1 | 136.74 | 0.599 |
| EDTA (B) | 24.67 | 1217.09 | 1 | 1217.09 | 5.330 |
| T (C) | 7.43 | 110.45 | 1 | 110.45 | 0.484 |
| AB | 11.42 | 260.78 | 1 | 260.78 | 1.142 |
| AC | -5.82 | 67.72 | 1 | 67.72 | 0.297 |
| BC | 0.28 | 0.16 | 1 | 0.16 | 0.001 |
| | | | | | |
| Error | | 913.33 | 4 | 228.33 | |
| Total | | 2706.26 | 10 | | |

^asignificant at 5%, no further significant effect at 25%

From Table 4.6, it is evident that EDTA is the only significant effect. The temperature and hydrazine concentrations appear to be fairly insignificant in the electroless palladium plating process. This conclusion is not true, but is a shortcoming of the factorial design. If the high and low levels of a variable are chosen too close to one another, the effect of the factor is lost. The levels of the hydrazine and temperature are very close, which lower their significance.

(Compare Table 4.1 where the distance between levels is double that of Table 4.4). The interactions are depicted in Figures 4.10 to 4.15.

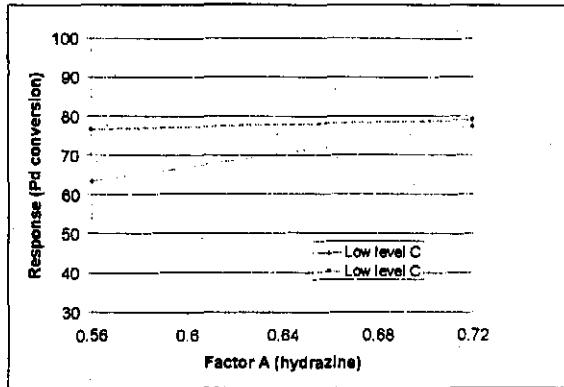


Figure 4.10: Hydrazine-temperature interaction

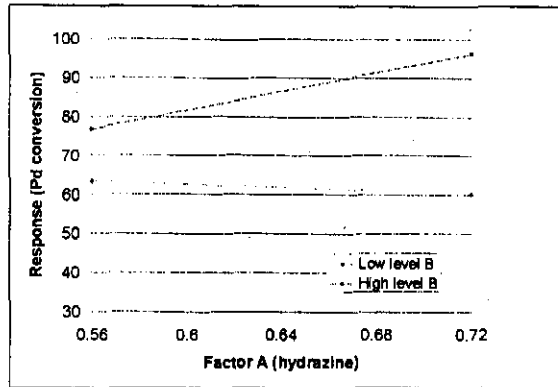


Figure 4.11: Hydrazine-EDTA interaction

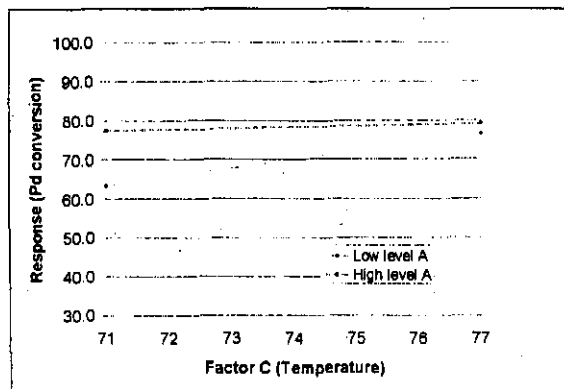


Figure 4.12: Temperature-hydrazine interaction

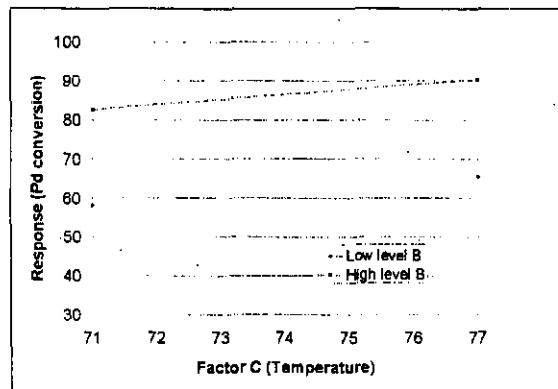


Figure 4.13: Temperature-EDTA interaction

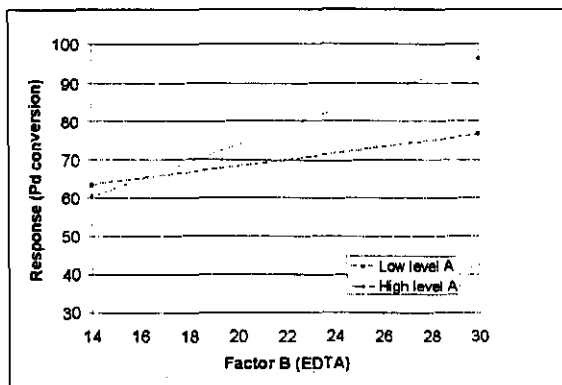


Figure 4.14: EDTA-hydrazine interaction

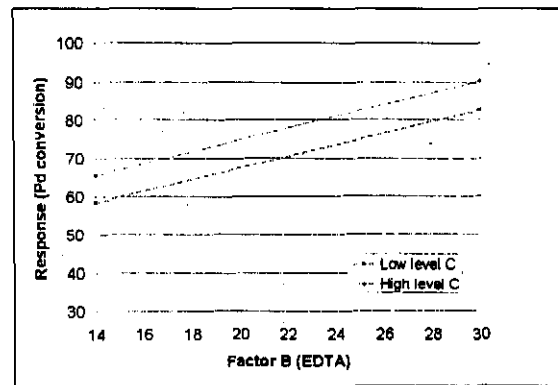


Figure 4.15: EDTA-temperature interaction

4.5. KINETIC STUDY

A kinetic study was done to determine a sufficient plating time and to obtain some insight into the reaction rate of the electroless palladium plating reaction. Small amounts of the plating solution was extracted at fixed times and analysed with ICP. **Figure 4.16** compares the reaction rate at various buffer pH values.

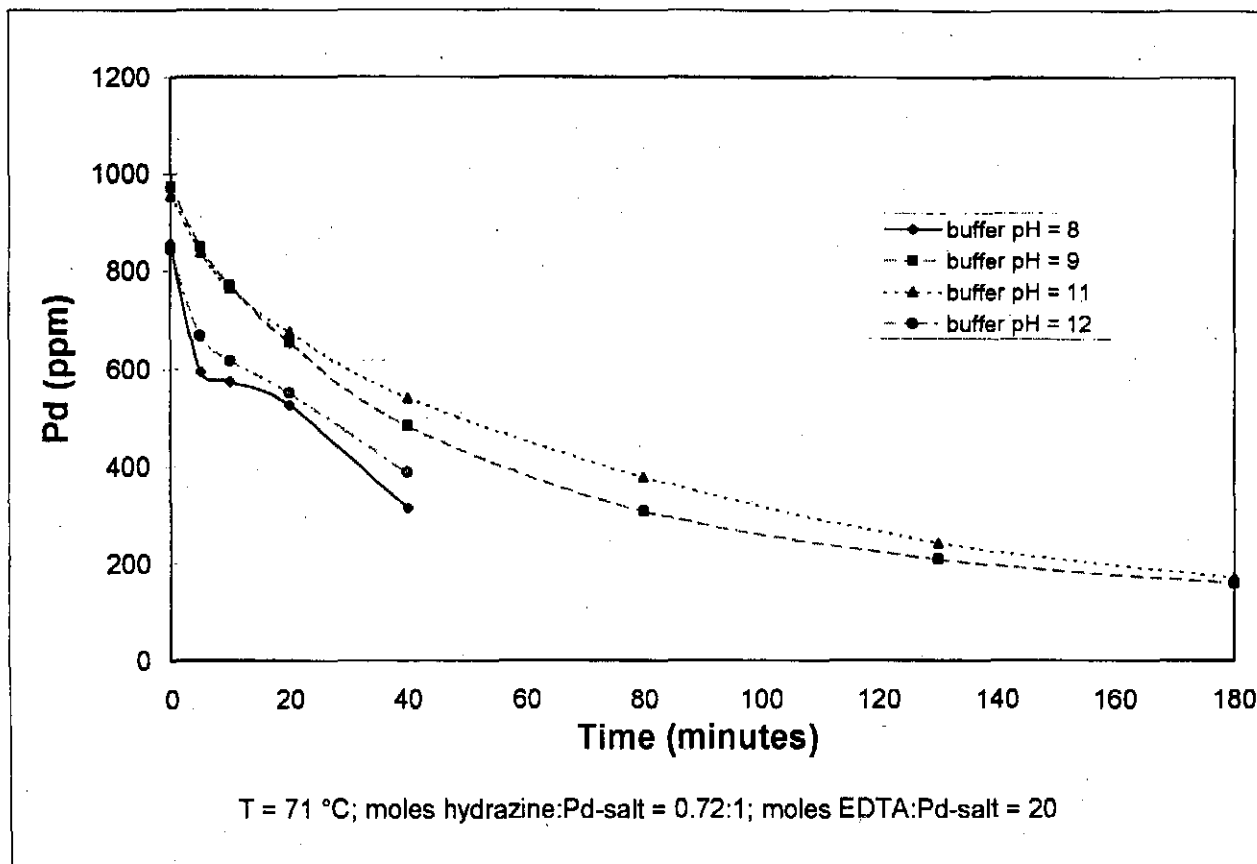


Figure 4.16: The effect of buffer pH on Pd concentration profiles

At buffer pH values of 8 and 12, the bath decomposed after forty minutes and no further analysis could be done. The metal was no longer in ionic form, but in the form of finely dispersed Pd particles. The solution stability was insufficient at these buffer pH values, yielding a very fast reaction rate. The mass transport resistance for deposition on the membrane surface can not be overcome in such a small reaction time, with the result that deposition no longer occurs on the membrane surface.

The Pd conversions for buffer pH values of 9 and 11 are very close to one another after three hours of plating. The conversion is about 80% after three hours and according to Figure 4.16, very close to the maximum value at those conditions.

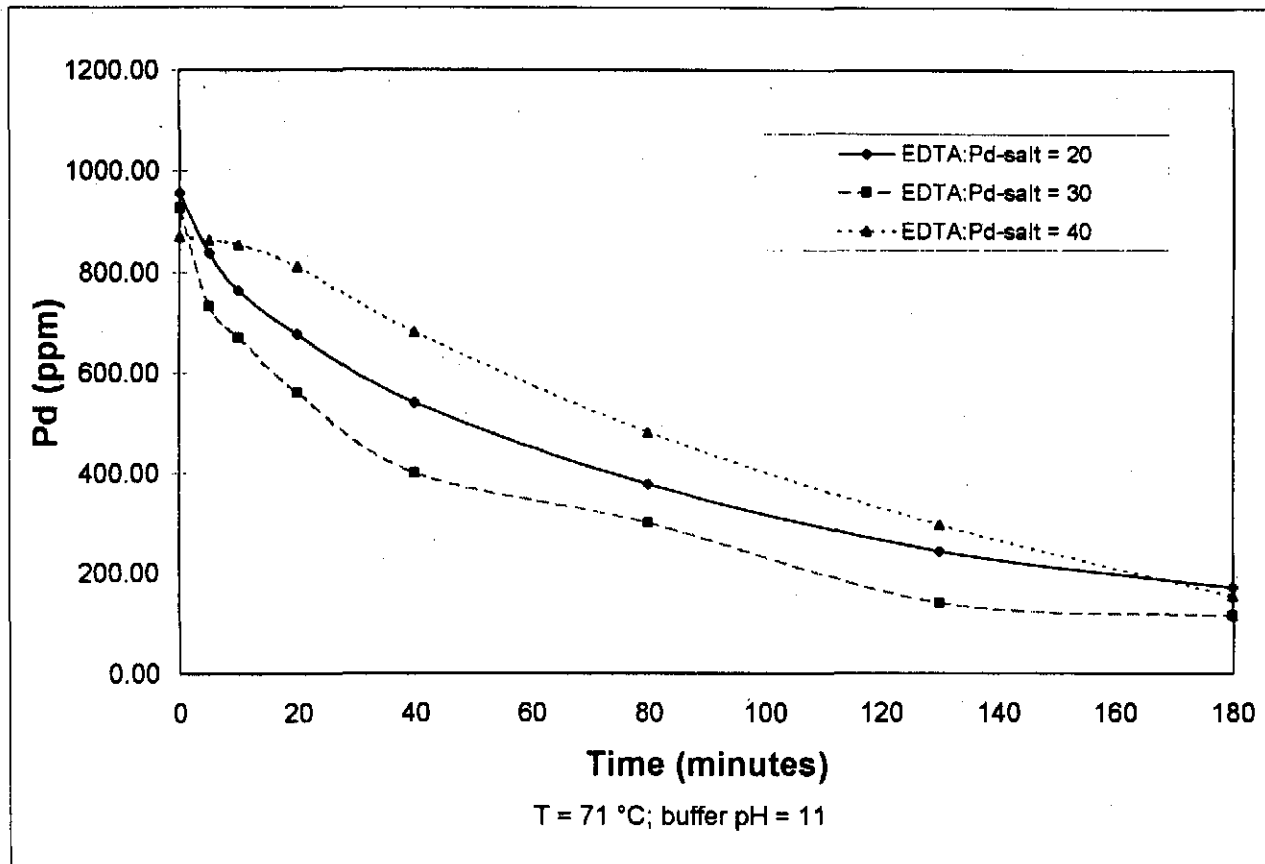


Figure 4.17: The effect of EDTA concentration on Pd concentration profiles

The EDTA concentration has a definite effect on the plating rate (Figure 4.17). The higher the EDTA: Pd-salt molar ratio, the slower the initial reaction. The higher Pd conversion for an EDTA: Pd-salt molar ratio of 30:1 (compared to 20:1) suggests an optimum EDTA concentration for maximum conversion. For EDTA: Pd-salt molar ratios of 20:1 and 30:1, the maximum conversion seems to have been reached after three hours according to the shape of the curves. For an EDTA: Pd-salt molar ratio of 40:1, the maximum had not been reached after three hours and the reaction was still in progress. This was confirmed by a physical observation where tiny bubbles were still forming on the membrane surface after three hours.

The curves in **Figure 4.18** are similar to those in **Figures 4.16** and **4.17**. The reaction rate increases with temperature, resulting in an increased Pd conversion. For 65 °C, the reaction is not fully completed after three hours.

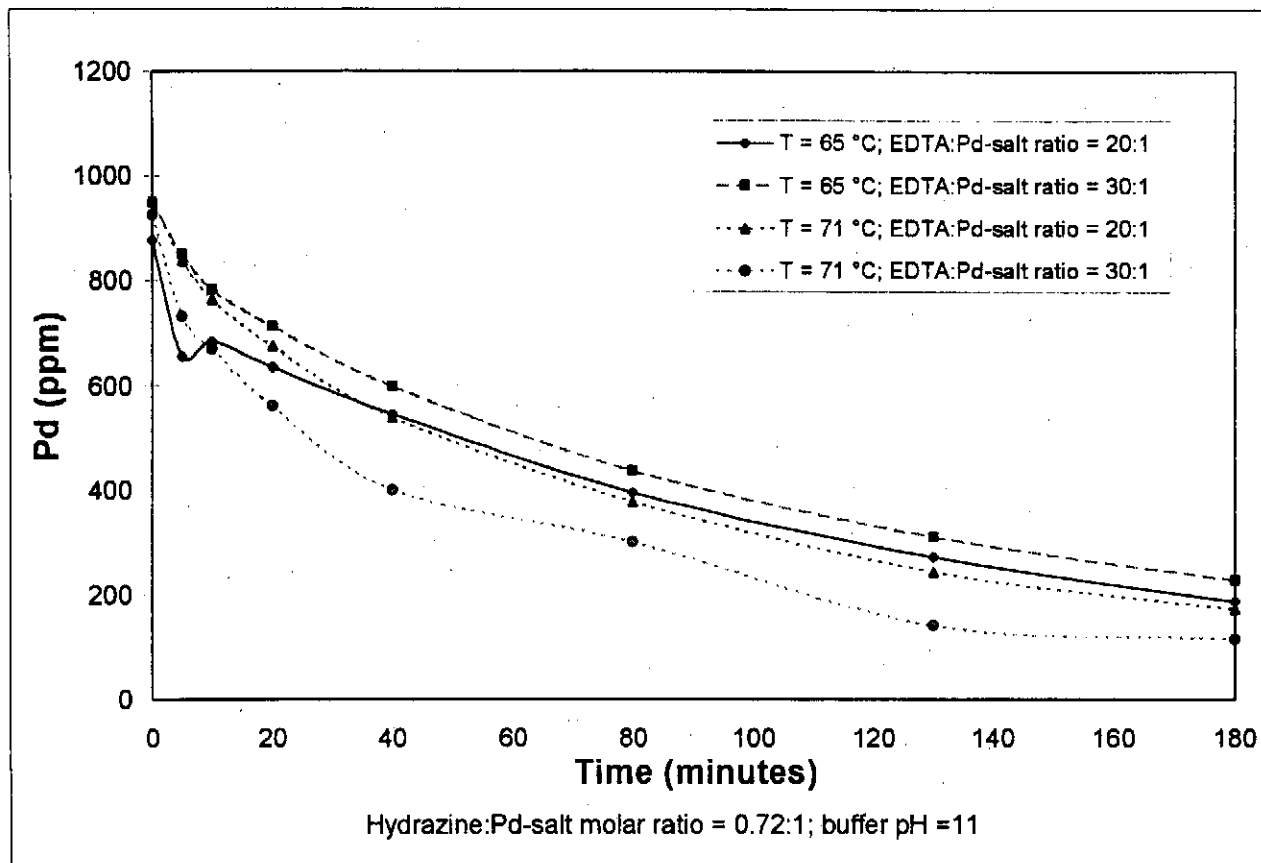


Figure 4.18: The effect of temperature on Pd concentration profiles at various EDTA concentrations

Three hours were found to be a sufficient plating time for comparing Pd conversion and plating rate. The optimum Pd conversion for three hours will represent a sufficiently high plating rate and good plating kinetics.

4.6. EFFECT OF BUFFER pH ON PALLADIUM CONVERSION

Plating was done in an alkaline solution, since hydrazine is a better reducing agent in an alkaline medium than in an acidic medium:



Operating in the pH buffer range of 9 to 11 caused little variation in the conversion of the metal ion (See **Table 4.7**). A value of 9 to 11 is necessary to maintain the correct potential difference for the oxidation and reduction reactions. The data in **Table 4.7** is the average values of the data listed in **Table 4.2**.

Table 4.7: Average conversions for buffer pH values of 9 and 11 at a EDTA:Pd-salt molar ratio of 6:1

| buffer pH | T (°C) | hydrazine (molar ratio) | Conversion |
|-----------|--------|-------------------------|------------|
| 9 | 59 | 0.4 | 19.5 |
| 11 | 59 | 0.4 | 19.0 |
| | | | |
| 9 | 59 | 0.72 | 38.7 |
| 11 | 59 | 0.72 | 35.7 |
| | | | |
| 9 | 71 | 0.4 | 43.0 |
| 11 | 71 | 0.4 | 45.5 |

Using higher or lower pH buffers had the tendency to cause decomposition of the plating solution at either high temperatures or high hydrazine concentrations. This phenomenon can clearly be seen in **Figure 4.19**. Moving outside the pH buffer range of 9-11 caused a sudden decrease in Pd conversion. **Figure 4.20** compares the Pd conversion for buffer pH 9 and 11 at various EDTA concentrations. Slightly better results were obtained with a buffer pH of 9. Below an EDTA:Pd-salt molar ratio of 20, decomposition took place. Optimum conversion can be obtained with pH buffers of 9 to 11.

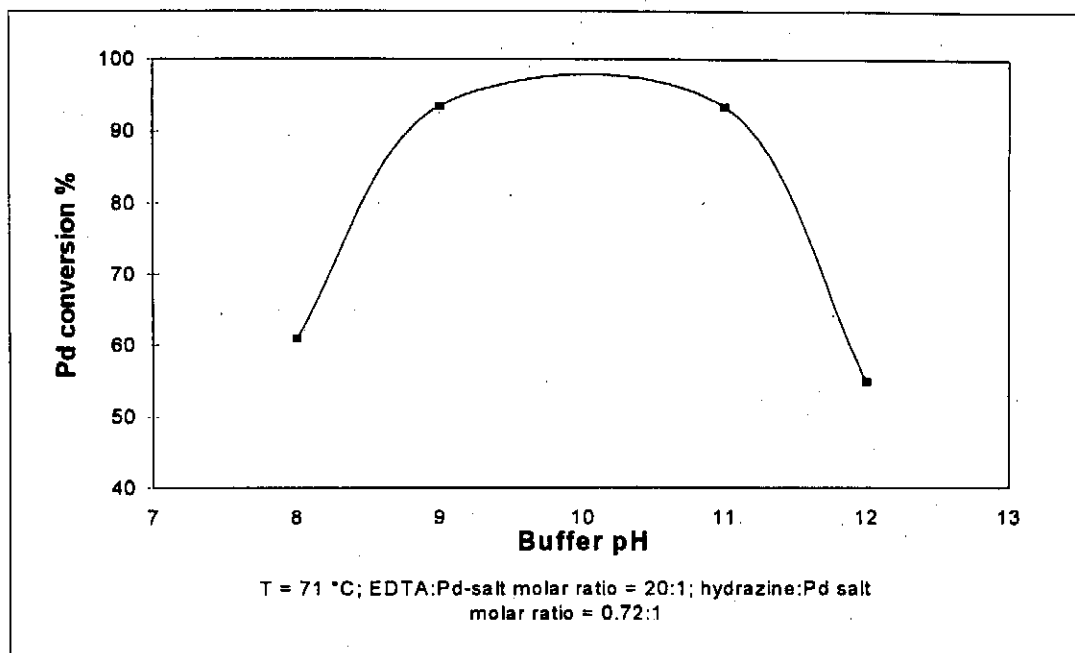


Figure 4.19: Effect of buffer pH on Pd conversion

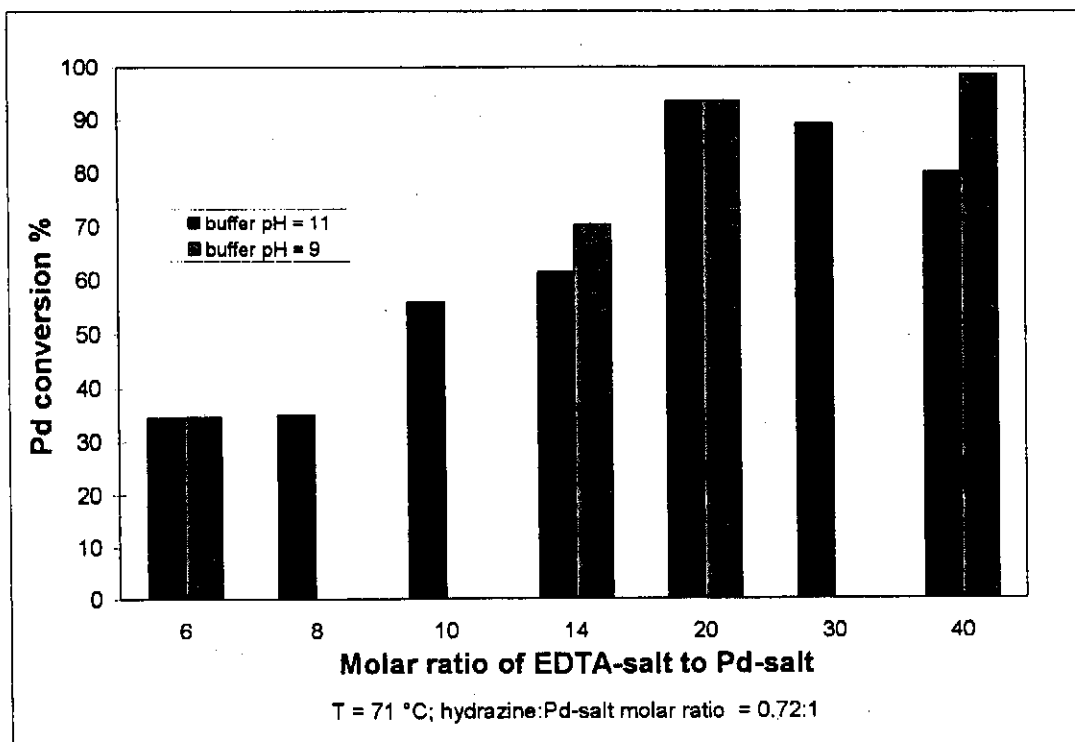
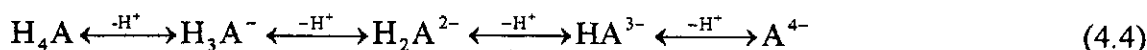


Figure 4.20: The effect of EDTA concentration on Pd conversion

It was previously found that the pH has a large influence on the stability of the Pd complex (Ullmann, 1987b). The pH determines the degree of ionisation of EDTA. There are four stages of dissociation of EDTA as shown in (4.4) with A=EDTA.



The fully ionised chelate anion ($EDTA^{4-}$) forms the strongest metal chelate (Pd-EDTA) complex and the lower the H^+ concentration, the higher the $EDTA^{4-}$ concentration. The amount of uncomplexed metal ions is proportional to the square of the hydrogen concentration (Kirk-Othmer, 1980b).

$$[M^{2+}] = [H^+]^2 \times \frac{[MA^{2-}]}{[H_2A^{2-}]} \times \frac{1}{K_1 K_2 K_3 K_4} \quad (4.5)$$

M = metal ion; K_1 , K_2 , K_3 and K_4 are the equilibrium values of reaction (4.4).

Chelating agents thus require a high alkalinity in order to be very effective (Ullmann, 1987b). In the pH range of 9-11, $EDTA^{3-}$ and $EDTA^{4-}$ dominate (Kirk-Othmer, 1980b) and are capable of strong metal bonding (Figure 4.21).

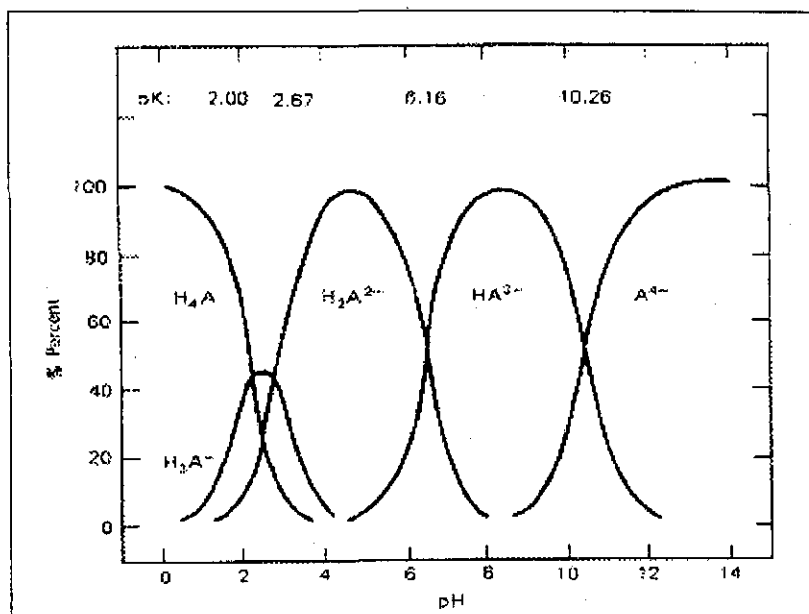


Figure 4.21: Distribution of ionic species of EDTA as a function of pH

4.7. COMBINED EFFECT OF TEMPERATURE AND EDTA CONCENTRATION ON Pd CONVERSION

Temperature and EDTA concentration are interactive parameters. From **Figure 4.22** it can be seen that the temperature and EDTA concentrations must be chosen together to achieve maximum conversion. **Figure 4.22** also shows that low EDTA: Pd-salt molar ratios (6 and 14) cause bath decomposition at high temperatures (above 66 °C) and a decline in Pd conversion. Pd conversions from stable solutions increase as expected (Rhoda, 1959) with increasing temperature, for example the EDTA: Pd-salt molar ratio of 30:1. In general, the Pd conversion is higher for a higher EDTA concentration. This can be seen from **Figure 4.22**.

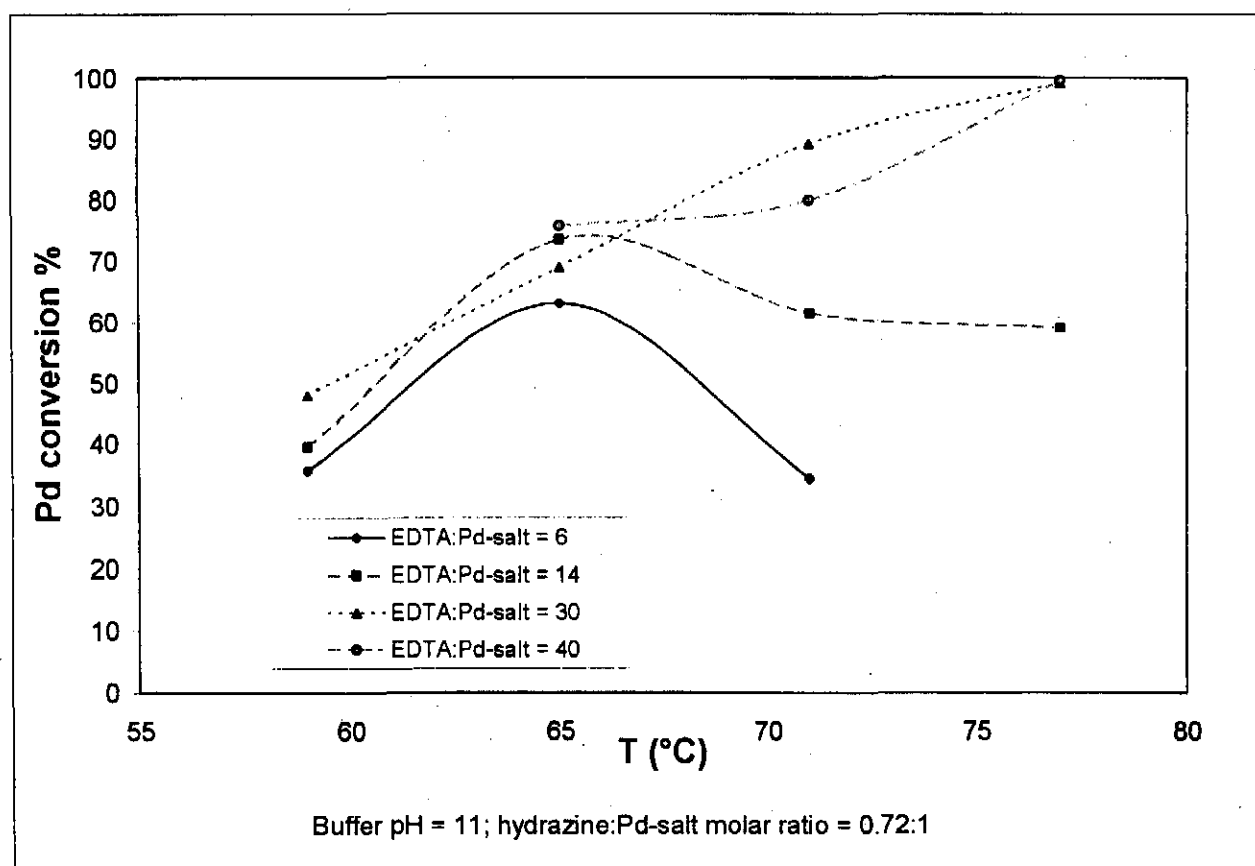


Figure 4.22: The effect of temperature on Pd conversion

According to **Figure 4.23**, the EDTA: Pd salt molar ratio causes one of three effects, which are best illustrated by the T=71 °C and T=77 °C curves. Firstly, at low EDTA: Pd-salt molar ratios (concentrations) the conversion is low due to bath decomposition. Secondly, an

increase in concentration increases stability and conversion. Thirdly, when the EDTA concentration is too high, there is a decline in conversion, presumably due to too high a stability. EDTA: Pd-salt molar ratios of 20:1 to 40:1 and $T \geq 65^\circ\text{C}$ give conversions of greater than 80% (at the given hydrazine and buffer pH values).

At a lower hydrazine concentration (0.56:1), decomposition of the plating solution does not occur easily. For the data plotted in **Figure 4.24**, no decomposition occurred at 71°C , and at 77°C decomposition only took place at an EDTA: Pd-salt molar ratio of 8:1. The trends in **Figure 4.24**, at a lower hydrazine concentration, are not as clear as in **Figure 4.23**, where the hydrazine concentration is 29% higher.

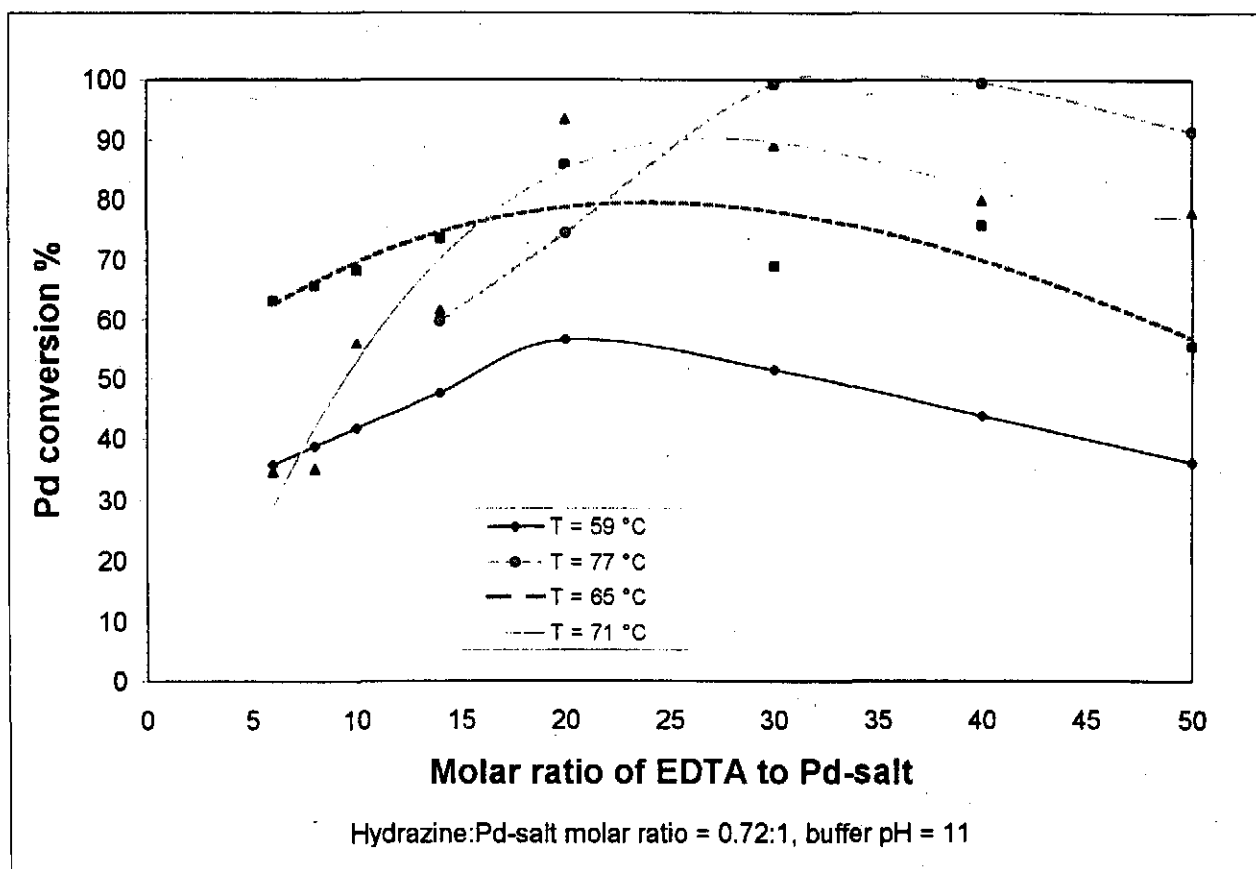


Figure 4.23: The effect of EDTA at various temperatures on Pd conversion

At 71°C (**Figure 4.24**) there is no clear trend for Pd conversion for an increase in EDTA concentration. It appears as if the solution is already stable at an EDTA: Pd-salt molar ratio of 6:1 and that there is a slight decline in conversion for higher EDTA concentrations. The

shape of the curve can be explained by variance around a straight line. At 77 °C the solution becomes unstable at an EDTA: Pd-salt molar ratio of 14:1 and less, thus explaining the sharp drop in conversion for the EDTA: Pd-salt molar ratio of 8:1. In the stable region higher temperatures always result in higher conversions. Maximum conversion for this lower hydrazine concentration (Figure 4.24) is lower when compared to that of Figure 4.23, proving that hydrazine has a definite effect.

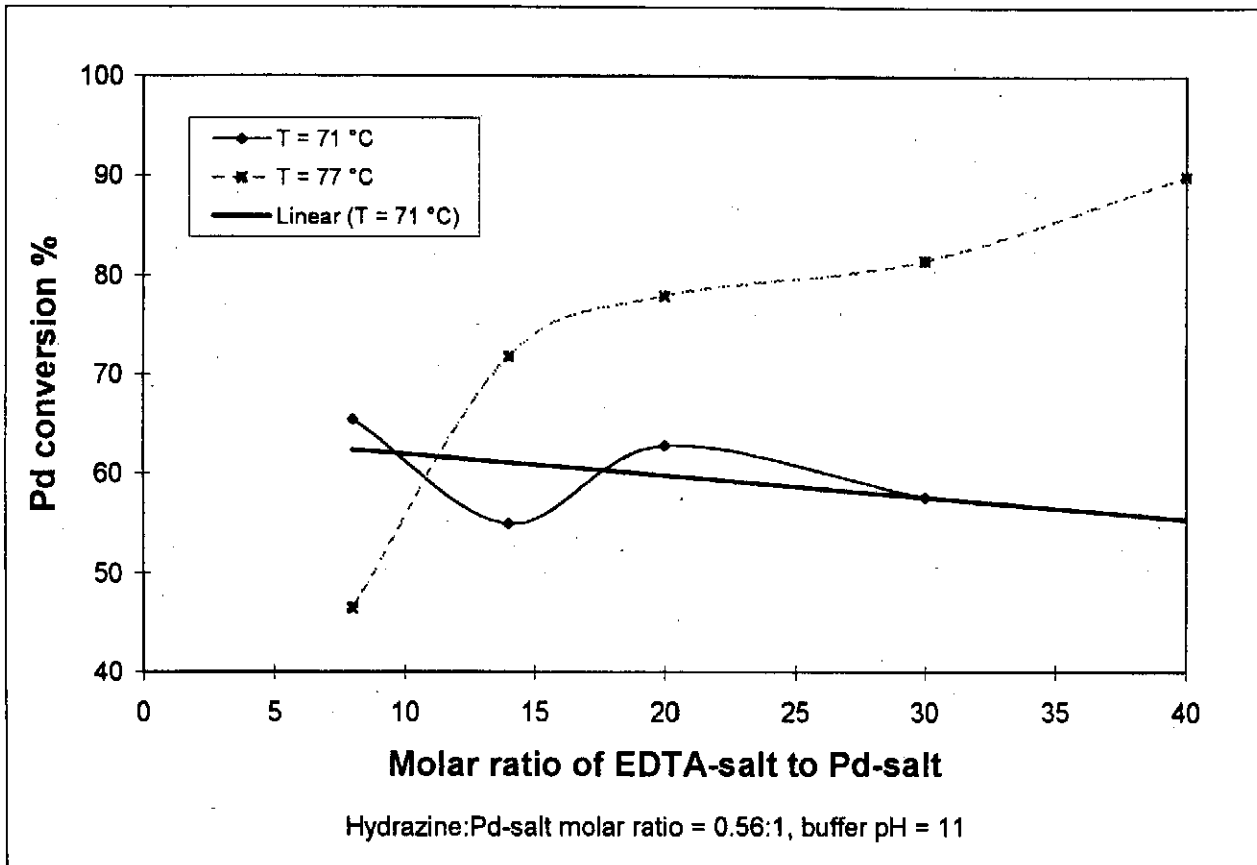


Figure 4.24: The effect of EDTA at various temperatures on Pd conversion

Both temperature and EDTA concentration have an effect on potential difference. Increasing the temperature increases $E_{\text{Pd}^{2+}/\text{Pd}}$ according to the Nernst equation, while increasing EDTA concentration reduces the potential (Shu et al., 1993). It can be concluded that large potential differences will cause decomposition of the plating solution. This was observed at the lower EDTA: Pd-salt molar ratio (value of 6) of Figure 4.22 for $T > 65$ °C where decomposition took place. EDTA is a very good stabilising agent for Pd with a stability constant of $\log K_{\text{PdEDTA}}$ equal to 18.5 (Sillen et al., 1964). EDTA effectively reduces the Pd potential

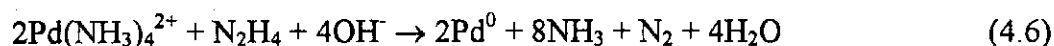
Pd potential (Table 4.8) and stabilises the ion to cause a slower reaction rate, high stability and high Pd conversion. This extra stability caused by the higher EDTA concentration shifts the decomposition of the plating solution to higher temperatures (Figure 4.22).

Table 4.8: $E_{\text{Pd}^{2+}/\text{Pd}}$ for various EDTA to Pd-salt molar ratios at 25 °C

| EDTA: Pd-salt molar ratio | 0 | 6 | 20 | 40 |
|------------------------------------|------|--------|--------|--------|
| $E_{\text{Pd}^{2+}/\text{Pd}}$ (V) | 0.83 | 0.2601 | 0.2446 | 0.2357 |

4.8. COMBINED EFFECT OF HYDRAZINE AND EDTA ON Pd CONVERSION

The complete autocatalytic reaction is :



Stoichiometry predicts that a hydrazine: Pd-salt molar ratio of 0.5:1 is required for complete reaction. However, in practice this was not found. From Figure 4.25 it can be seen that the conversion increased with increasing hydrazine concentration beyond the expected stoichiometric value. This is unlike the results obtained by Rhoda (1959), where the expected stoichiometric value was obtained. The abnormal stoichiometry is due to the higher operating temperatures which results in increased hydrazine decomposition.

The exception on this figure (EDTA: Pd-salt molar ratio of 8:1), where conversion declines, is due to bath decomposition. No instability was encountered with hydrazine: Pd-salt molar ratios of 0.56 and 0.4, respectively. Higher values did cause decomposition below an EDTA: Pd-salt molar ratio of 14:1. Above this value there is an increase in conversion with an increase in hydrazine concentration (Figure 4.26). Figure 4.27 confirms this phenomenon.

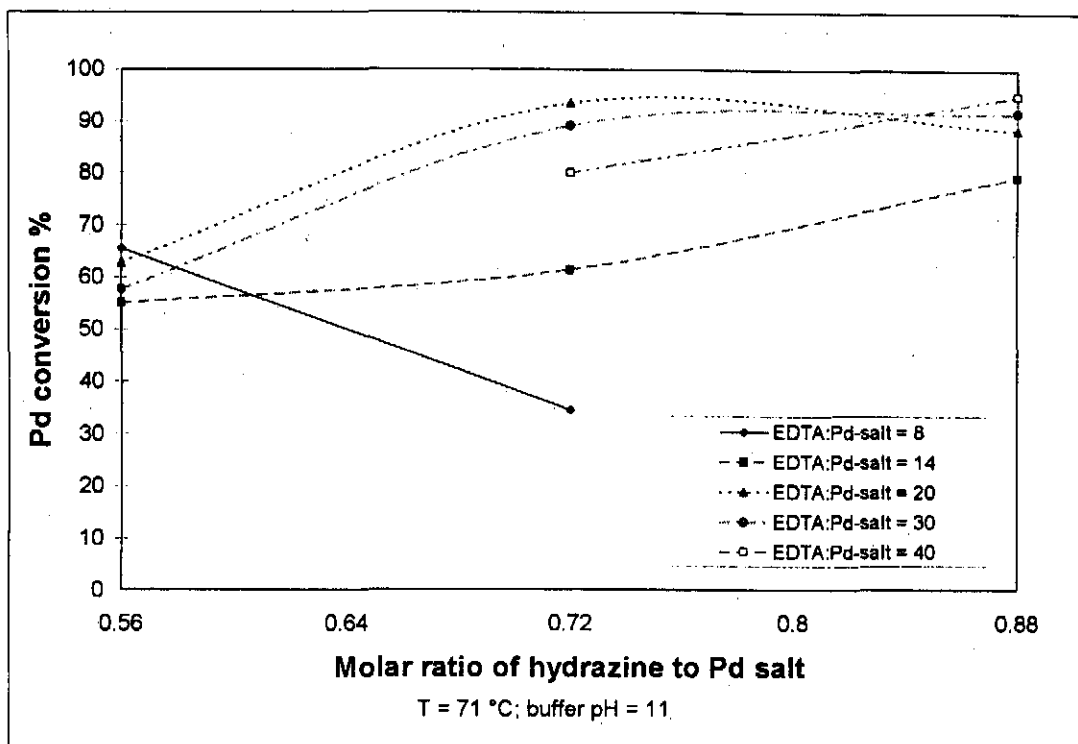


Figure 4.25: The effect of hydrazine on Pd conversion at different EDTA concentrations

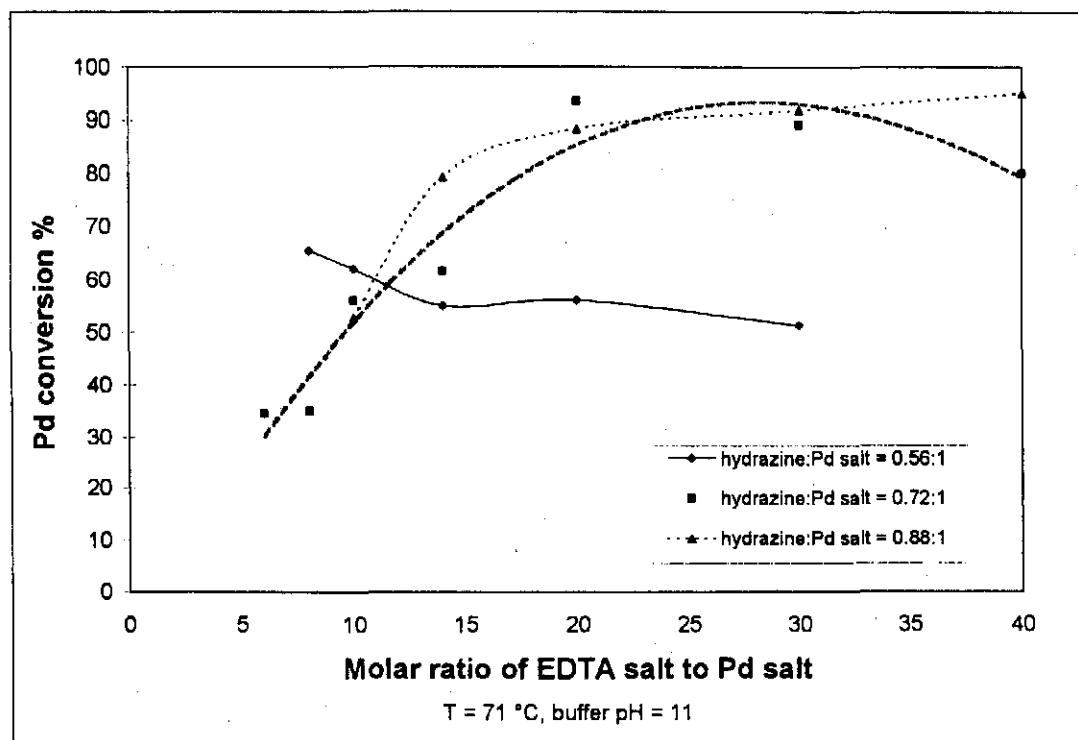


Figure 4.26: The effect of EDTA at various hydrazine concentrations on Pd conversion

The curves in **Figure 4.27** have similar shapes, but the higher hydrazine concentration causes a shift to higher EDTA concentrations required for stability. Stability is reached at an EDTA: Pd-salt molar ratio 14:1 for a hydrazine: Pd-salt molar ratio of 0.56:1, compared to a value of 30:1 for a hydrazine: Pd-salt molar ratio of 0.72:1. The increase in Pd conversion for the hydrazine: Pd-salt molar ratio of 0.56:1 above an EDTA: Pd-salt molar ratio of 30:1 is not clear. This might be due to an experimental error, since all other data indicates that a decline in Pd conversion should have taken place.

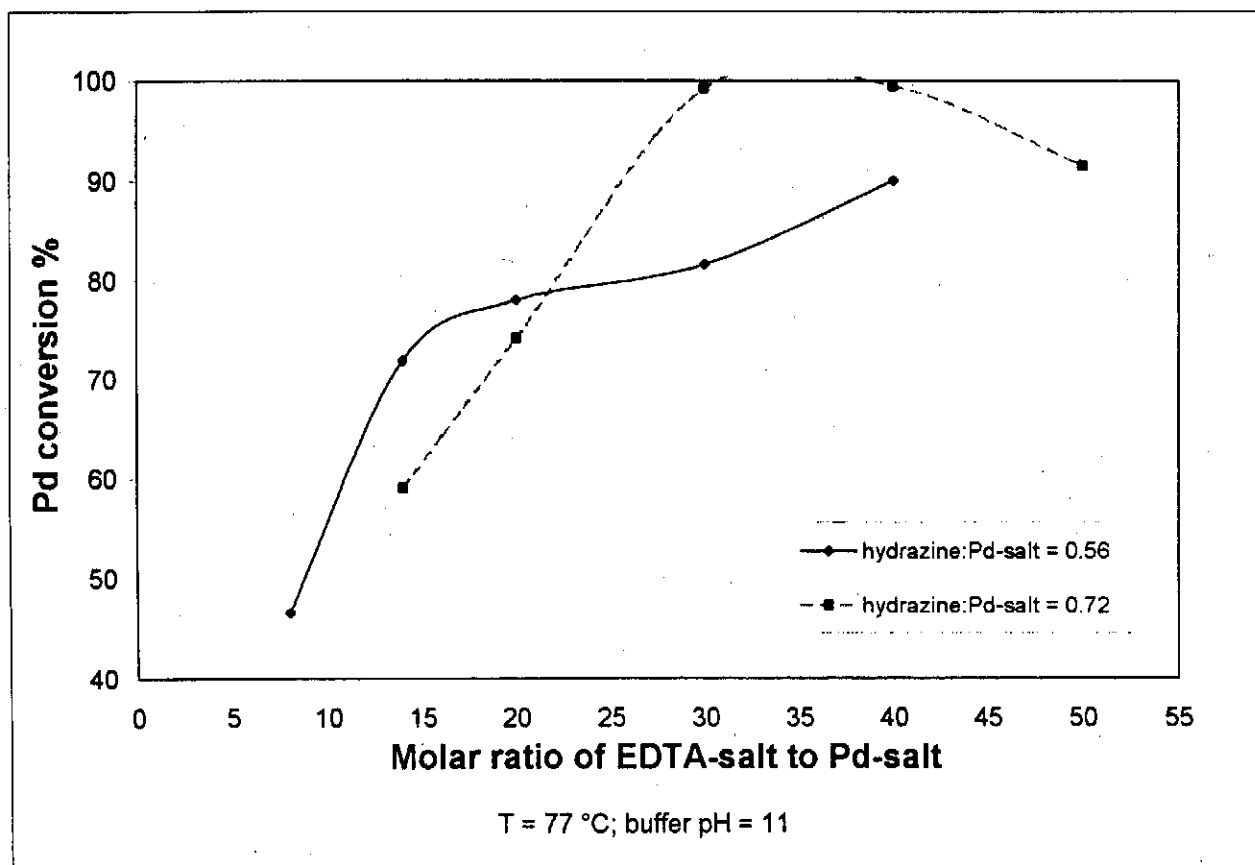
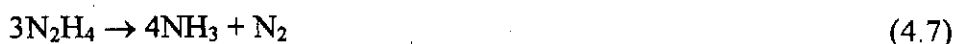


Figure 4.27: The effect of EDTA and hydrazine concentrations on Pd conversion

Figure 4.27 again confirms that an excess amount of hydrazine is required for optimum conversion, since hydrazine catalytically decomposes in the solution. This subject is covered extensively in the literature (Audrieth, Chapter 6, 1951; Schmidt, Chapter 5, 1984). Thermal decomposition increases with increasing temperature and the presence of a metal catalyst. Decomposition proceeds mainly through the following reaction:



Small amounts of hydrogen is also formed according to:



The last reaction increases with increasing pH (Audrieth, Chapter 6, 1951). Forty to sixty percent excess hydrazine is best for obtaining maximum conversion and sufficiently high stability.

4.9. SOLUTION STABILITY AND OPTIMUM PLATING CONDITIONS

A graph was constructed to indicate solution stability as a function of EDTA concentration, hydrazine concentration and temperature. EDTA: Pd-salt molar ratios on and above the response surface in **Figure 4.28** indicate stable solutions at the corresponding hydrazine concentrations and temperatures. Lower EDTA: Pd-salt molar ratios (below the response surface) exhibit unstable solutions and cause bath decomposition.

STATISTICA was used to construct smooth spline surfaces of the plating data at 71 °C with varying hydrazine and EDTA concentrations (**Figure 4.29**) and at a hydrazine: Pd-salt molar ratio of 0.72:1 with varying EDTA concentration and temperature (**Figure 4.30**). From **Figure 4.30** it is clear that an excess of 40-50% hydrazine is essential for high Pd conversions. A temperature above 70 °C (**Figure 4.30**) is necessary to obtain a fast plating rate and high Pd conversion. The EDTA concentration must be chosen in such a way to ensure bath stability. For the temperatures and hydrazine concentrations mentioned, a proper EDTA: Pd-salt molar ratio varies between 30:1 and 40:1.

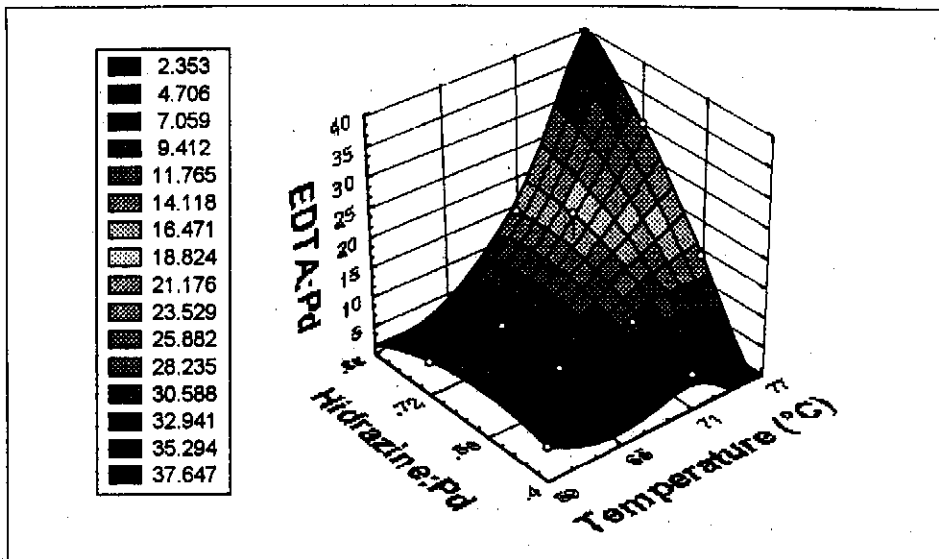


Figure 4.28: EDTA:Pd molar ratio required for stable plating solution

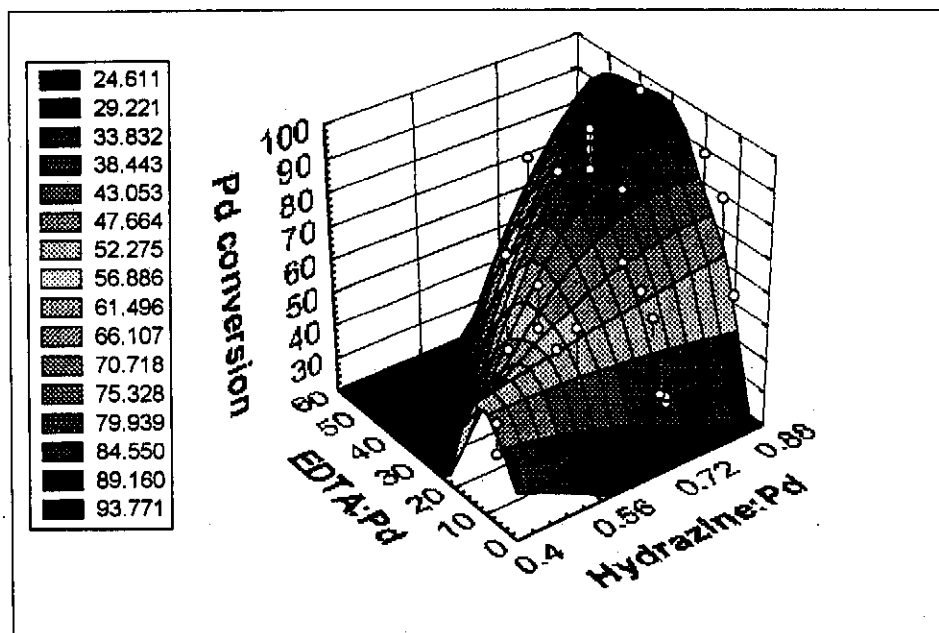


Figure 4.29: Effect of hydrazine, EDTA concentrations on Pd conversion at 71 °C

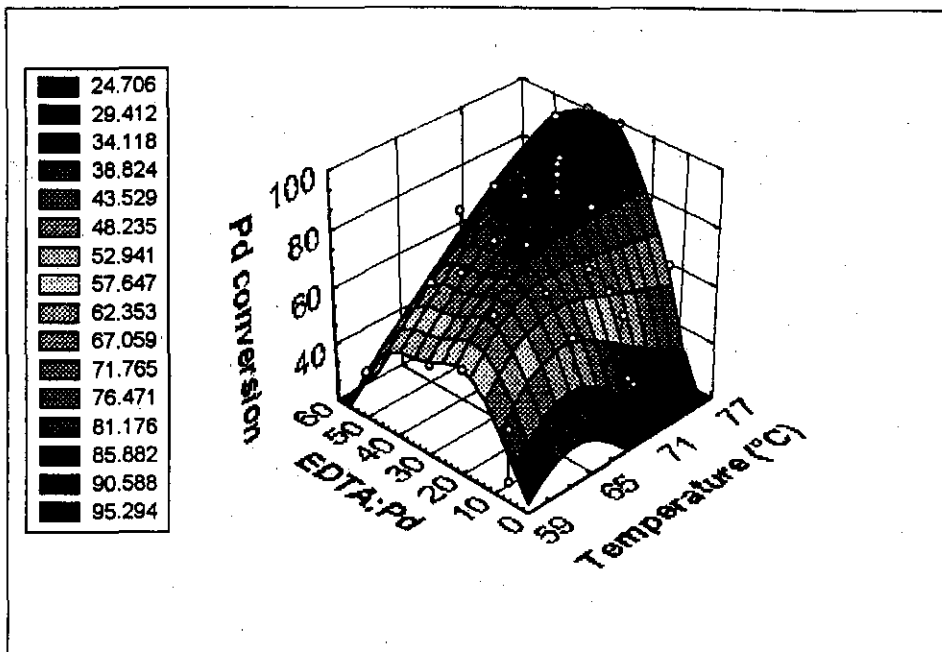


Figure 4.30: Pd conversion at hydrazine: Pd molar ratio of 0.72:1

4.10. MODELLING ELECTROLESS PALLADIUM PLATING

The statistical package, NCSS version 6.0, was used to conduct response surface regression analyses on the electroless palladium plating data. Two empirical models were constructed. The first model used temperature, buffer pH, hydrazine concentration and EDTA concentration as variables. It allowed for quadratic terms of the variables and all possible interactions. In Tables 4.9 and 4.11, A = hydrazine: Pd-salt molar ratio, B = buffer pH, C = temperature (°C) and D = EDTA: Pd-salt molar ratio.

The probability level is the probability that an effect has no influence, in other words, a value close to zero indicates a significant contribution towards the variance, while a value close to one indicates that the effect is insignificant. In Table 4.9 the lack of fit term has a high probability level, in other words the lack of fit is not significant. This indicates that the model is very accurate. From Table 4.10 it can be seen that B (buffer pH) is the least sensitive variable, since it has the smallest R^2 value. The high R^2 values for the EDTA: Pd-salt molar ratio (D) and the temperature (C) indicate that these two variables have the largest influence on the response (palladium conversion).

Table 4.9: Sequential analysis of variance (model 1)

| Source | DF | Sequential Sum-Squares | Mean Square | F-Ratio | Prob. Level | Incremental -Squared |
|--------------------|----|------------------------|-------------|---------|-------------|----------------------|
| Regression | 14 | 21833.2 | 1559.51 | 17.54 | 0.000000 | 0.825219 |
| Linear | 4 | 16033.9 | 4008.47 | 45.08 | 0.000000 | 0.606025 |
| Quadratic | 4 | 2539.7 | 634.93 | 7.14 | 0.000117 | 0.095993 |
| Lin x Lin | 6 | 3259.6 | 543.26 | 6.11 | 0.000068 | 0.123201 |
| Total Error | 52 | 4624.2 | 88.93 | | | 0.174781 |
| Lack of Fit | 33 | 2586.9 | 78.39 | 0.73 | 0.790365 | 0.097775 |
| Pure Error | 19 | 2037.4 | 107.23 | | | 0.077006 |

Table 4.10: Analysis of variance (model 1)

| Factor | DF | Last Sum-Squares | Mean Square | F-Ratio | Prob Level | Term R-Squared |
|--------------------|----|------------------|-------------|---------|------------|----------------|
| A | 5 | 2315.0 | 462.99 | 5.21 | 0.000600 | 0.087498 |
| B | 5 | 1501.0 | 300.20 | 3.38 | 0.010258 | 0.056732 |
| C | 5 | 5216.8 | 1043.36 | 11.73 | 0.000000 | 0.197177 |
| D | 5 | 9884.9 | 1976.97 | 22.23 | 0.000000 | 0.373614 |
| Total Error | 52 | 4624.2 | 88.93 | | | 0.174781 |
| Lack of Fit | 33 | 2586.9 | 78.39 | 0.73 | 0.790365 | 0.097775 |
| Pure Error | 19 | 2037.4 | 107.23 | | | 0.077006 |

From Table 4.10 it can be seen that the parameters D^2 and $C \cdot D$ have the highest R^2 values, which means that they contribute the most to the model.

The R^2 value is a statistical parameter used to indicate the correlation between a regression model and the original data. A value of one indicates a perfect fit, while a value of zero means a complete lack of fit. The R^2 value of model 1 is 0.825, thus 82.5 % of the variability in the data is accounted for by the model.

Table 4.11: Parameter estimation (model 1)

| Parameter | DF | Regression Coefficient | Standard Error | T-Ratio | Prob Level | Last R-Squared |
|----------------|----|------------------------|----------------|---------|------------|----------------|
| Intercept | 1 | -1246.714 | | | | |
| A | 1 | 489.331 | 173.2618 | 2.82 | 0.006704 | 0.026810 |
| B | 1 | 141.268 | 48.9908 | 2.88 | 0.005707 | 0.027948 |
| C | 1 | 12.632 | 5.8168 | 2.17 | 0.034469 | 0.015851 |
| D | 1 | -2.442 | 2.5485 | -0.96 | 0.342366 | 0.003086 |
| A ² | 1 | -113.584 | 83.6706 | -1.36 | 0.180483 | 0.006194 |
| B ² | 1 | -7.504 | 2.1318 | -3.52 | 0.000907 | 0.041642 |
| C ² | 1 | -0.072 | 0.0417 | -1.73 | 0.090386 | 0.010007 |
| D ² | 1 | -0.035 | 0.0079 | -4.41 | 0.000052 | 0.065413 |
| A*B | 1 | 8.615 | 12.9865 | 0.66 | 0.510013 | 0.001479 |
| A*C | 1 | -6.902 | 2.0906 | -3.3 | 0.001743 | 0.036637 |
| A*D | 1 | 4.789 | 1.3892 | 3.45 | 0.001131 | 0.039936 |
| B*C | 1 | 0.110 | 0.3307 | 0.33 | 0.741542 | 0.000370 |
| B*D | 1 | -0.382 | 0.1729 | -2.21 | 0.031380 | 0.016447 |
| C*D | 1 | 0.084 | 0.0180 | 4.63 | 0.000025 | 0.071980 |

Model 1 is very complex and has fourteen terms. Many of the terms can be removed to simplify the model, while maintaining the high accuracy. A second regression model was constructed keeping the buffer pH constant at a pH of 11, reducing the number of variables to three and the number of model terms to seven. The response surface regression results are listed in Tables 4.12 to 4.14. In these tables A = hydrazine: Pd-salt molar ratio, B = temperature (°C) and C = EDTA: Pd-salt molar ratio.

Table 4.12: Sequential analysis of variance (model 2)

| Source | DF | Sequential Sum-Squares | Mean Square | F-Ratio | Prob Level | Incremental R-Squared |
|--------------------|----|------------------------|-------------|---------|------------|-----------------------|
| Regression | 7 | 13774.5 | 1967.79 | 19.15 | 0.000000 | 0.765776 |
| Linear | 3 | 10704.3 | 3568.11 | 34.72 | 0.000000 | 0.595091 |
| Quadratic | 1 | 1111.4 | 1111.36 | 10.82 | 0.002072 | 0.061784 |
| Lin x Lin | 3 | 1958.9 | 652.96 | 6.35 | 0.001224 | 0.108900 |
| Total Error | 41 | 4213.2 | 102.76 | | | 0.234224 |
| Lack of Fit | 29 | 2504.2 | 86.35 | 0.61 | 0.867810 | 0.139215 |
| Pure Error | 12 | 1709.0 | 142.42 | | | 0.095009 |

Table 4.13: Analysis of variance (model 2)

| Factor | DF | Last Sum-Squares | Mean Square | F-Ratio | Prob Level | Term R-Squared |
|--------------------|----|------------------|-------------|---------|------------|----------------|
| A | 3 | 1988.7 | 662.91 | 6.45 | 0.001114 | 0.110560 |
| B | 3 | 4396.7 | 1465.57 | 14.26 | 0.000002 | 0.244429 |
| C | 4 | 6743.2 | 1685.80 | 16.41 | 0.000000 | 0.374877 |
| Total Error | 41 | 4213.2 | 102.76 | | | 0.234224 |
| Lack of Fit | 29 | 2504.2 | 86.35 | 0.61 | 0.867810 | 0.139215 |
| Pure Error | 12 | 1709.0 | 142.42 | | | 0.095009 |

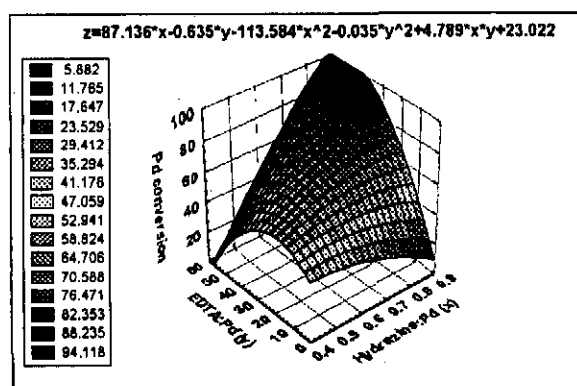
The R^2 value of model 2 is 0.766.

As in model 1, the EDTA concentration and the EDTA-temperature interaction are the most significant parameters for model 2. The R^2 value of model 2 is lower than for model 1, but the model is greatly simplified.

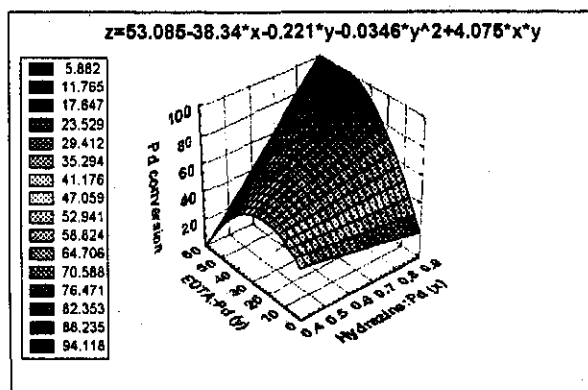
Table 4.14: Parameter estimation (model 2)

| Parameter | DF | Regression Coefficient | Standard Error | T-Ratio | Prob Level | Last R-Squared |
|----------------|----|------------------------|----------------|---------|------------|----------------|
| Intercept | 1 | -290.839 | | | | |
| A | 1 | 515.886 | 182.041 | 2.83 | 0.007104 | 0.045879 |
| B | 1 | 4.844 | 1.666 | 2.91 | 0.005866 | 0.048271 |
| C | 1 | -5.574 | 1.821 | -3.06 | 0.003881 | 0.053531 |
| C ² | 1 | -0.035 | 0.009 | -3.93 | 0.000316 | 0.088413 |
| A*B | 1 | -7.806 | 2.747 | -2.84 | 0.006964 | 0.046125 |
| A*C | 1 | 4.075 | 1.384 | 2.94 | 0.005304 | 0.049540 |
| B*C | 1 | 0.075 | 0.020 | 3.85 | 0.000403 | 0.084806 |

Figures 4.31 to 4.36 show surface plots for models 1 and 2. The plots for the two models are very similar.



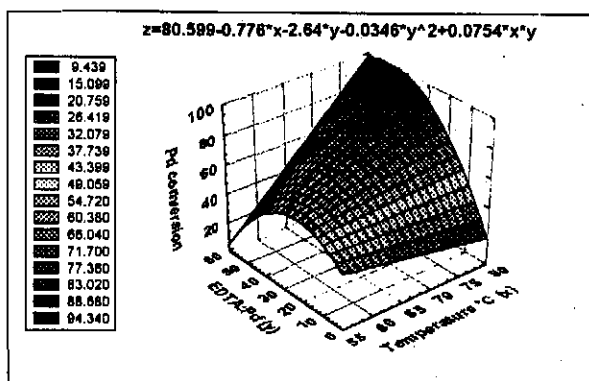
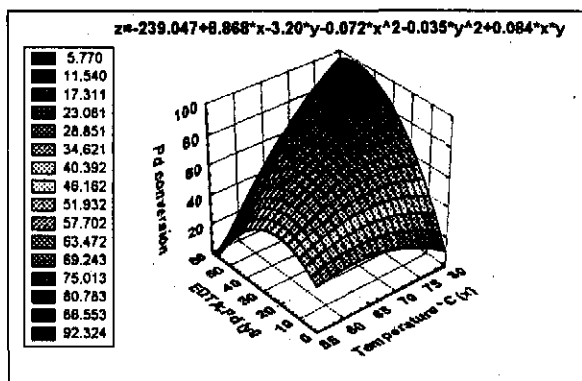
T = 71 °C and buffer pH = 11



T = 71 °C and buffer pH = 11

Figure 4.31: Surface plot of hydrazine and EDTA (model 1)

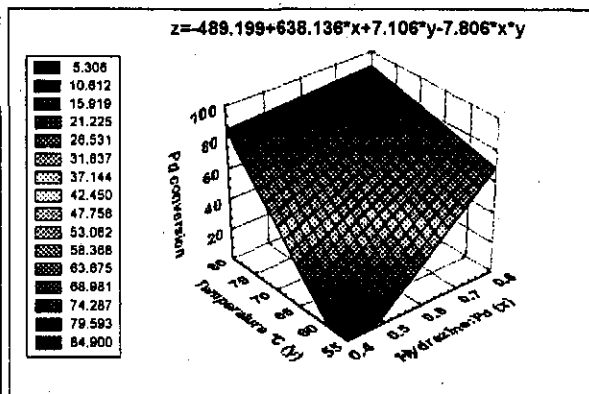
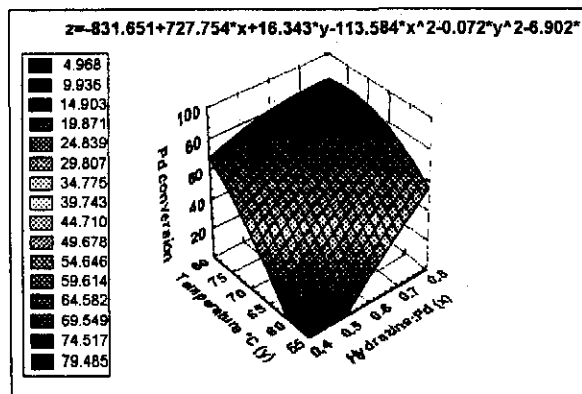
Figure 4.32: Surface plot of hydrazine and EDTA (model 2)



hydrazine: Pd-salt = 0.72:1; buffer pH = 11 hydrazine: Pd-salt = 0.72:1; buffer pH = 11

Figure 4.33: Surface plot of temperature and EDTA (model 1)

Figure 4.33: Surface plot of temperature and EDTA (model 2)



EDTA: Pd-salt = 30:1; buffer pH = 11

EDTA: Pd-salt = 30:1; buffer pH = 11

Figure 4.35: Surface plot of hydrazine and temperature (model 1)

Figure 4.36: Surface plot of hydrazine and temperature (model 2)

The accuracy of a model can be determined by examining the residuals (predicted value by model – actual value). Residuals that have a normal distribution indicate an accurate model. **Figures 4.37 and 4.38** show the residual distribution. A straight line on these figures represents a normal distribution. For both models 1 and 2 the majority of the residuals lie on a straight line confirming the accuracy of the models.

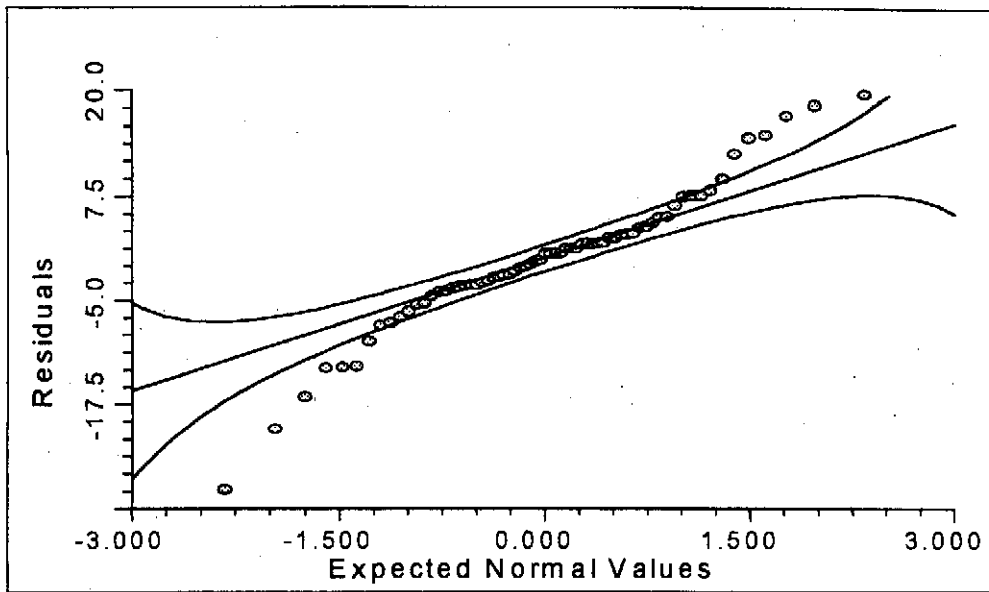


Figure 4.37: Probability plot of residuals (Model 1)

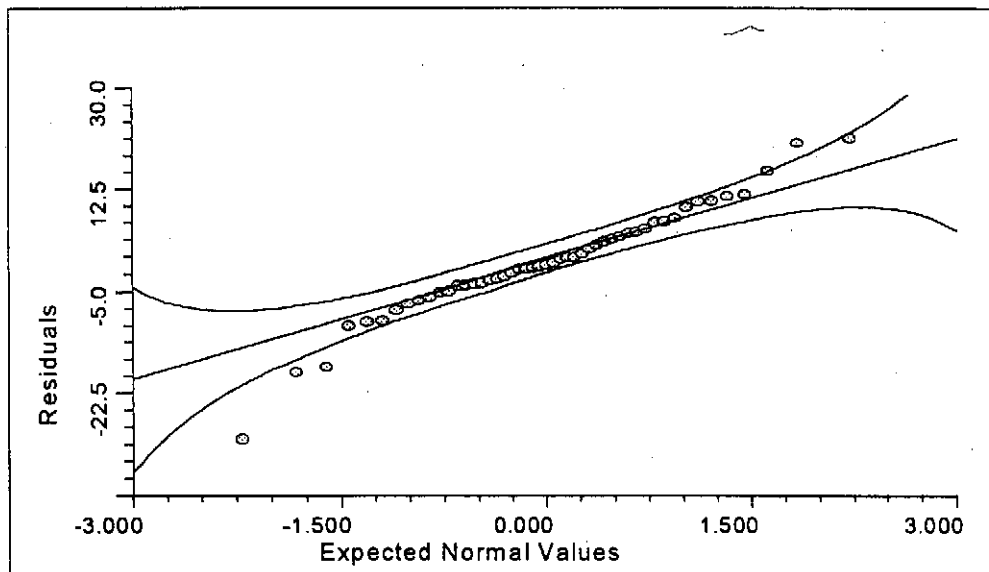


Figure 4.38: Probability plot of residuals (Model 2)

4.11. SUMMARY

The following conclusions can be drawn from work done on electroless palladium plating.

- Tetra-ammine palladium nitrate was found to be the best Pd salt to achieve high Pd conversions. Using hydrazine as the reducing agent produces the purest Pd films.
- Plating requires an alkaline solution with a pH buffer of 9 to 11. In this range, the stabiliser (EDTA) and reducing agent perform best, while higher and lower pH buffers tend to cause bath instability and rapid conversion decline.
- Excess hydrazine (40-60 %) above stoichiometry is required to compensate for thermal decomposition of the hydrazine and to ensure high conversions.
- Decomposition of plating solution occurs more readily when hydrazine concentration and temperature increase. At those conditions, high EDTA concentrations are required to yield a stable solution.
- The effect of EDTA concentration is highly non-linear: too high a value results in too stable a complex, while too low a value shows insufficient stability. Both cause a reduction in conversion.
- Pd conversions in the excess of 90 % were obtained within three hours using tetra-ammine palladium nitrate as Pd salt for the following conditions: $T = 77\text{ }^{\circ}\text{C}$, hydrazine to Pd molar ratio = 0.72:1, EDTA to Pd molar ratio = 30 to 40:1 and buffer pH = 11.

CHAPTER 5

ELECTROLESS SILVER AND NICKEL PLATING

5.1. INTRODUCTION

In this chapter electroless silver, electroless nickel and palladium-silver co-deposition is discussed. The preparation of palladium-silver, palladium-nickel and palladium-silver-nickel composites is also discussed. The palladium-silver co-deposition process is very complex and not widely studied or understood. Chapter 5 gives kinetic insight into this process and a mechanism will be proposed to explain the deposition process. The deposition of silver on palladium and silver on an activated substrate will be compared. A proper choice of operating variables is important to achieve high silver plating rates for two hours plating ($>1.5 \text{ mg/cm}^2$). Such conditions are determined as well as conditions to deposit small amounts of nickel (0.4 mg/cm^2) on palladium.

5.2. PALLADIUM-SILVER CO-DEPOSITION

When performing palladium-silver co-deposition, the concentration of both the silver and the palladium is very low. The palladium concentration is 5 g ($\approx 5 \text{ ml}$) per litre of 10 wt% Pd-salt solution compared to the 27.5 g per litre of 10 wt% Pd-salt solution used for pure palladium plating. The main reason for this is that the silver concentration needed for electroless silver plating is very low, due to difficulty experienced with silver stabilisation. Higher palladium concentrations will need higher silver concentrations and this will result in bath instability.

The silver content has a significant effect on the palladium and silver plating rates. The concentrations investigated varied from 0.02 g/litre to 0.1 g AgNO_3 /litre of plating solution (7% to 27% relative to Pd). **Figure 5.1** shows the palladium concentration profiles in baths with various silver concentrations.

As the silver concentration in the initial solution increases, the palladium deposition rate decreases. Moving from 0.02 to 0.1 g AgNO_3 /litre, the graph shift upwards after thirty

minutes. For $\text{AgNO}_3 = 0.1 \text{ g/litre}$ there is severe inhibition of palladium plating. It can clearly be seen from **Figure 5.1** how a high silver content inhibits palladium plating.

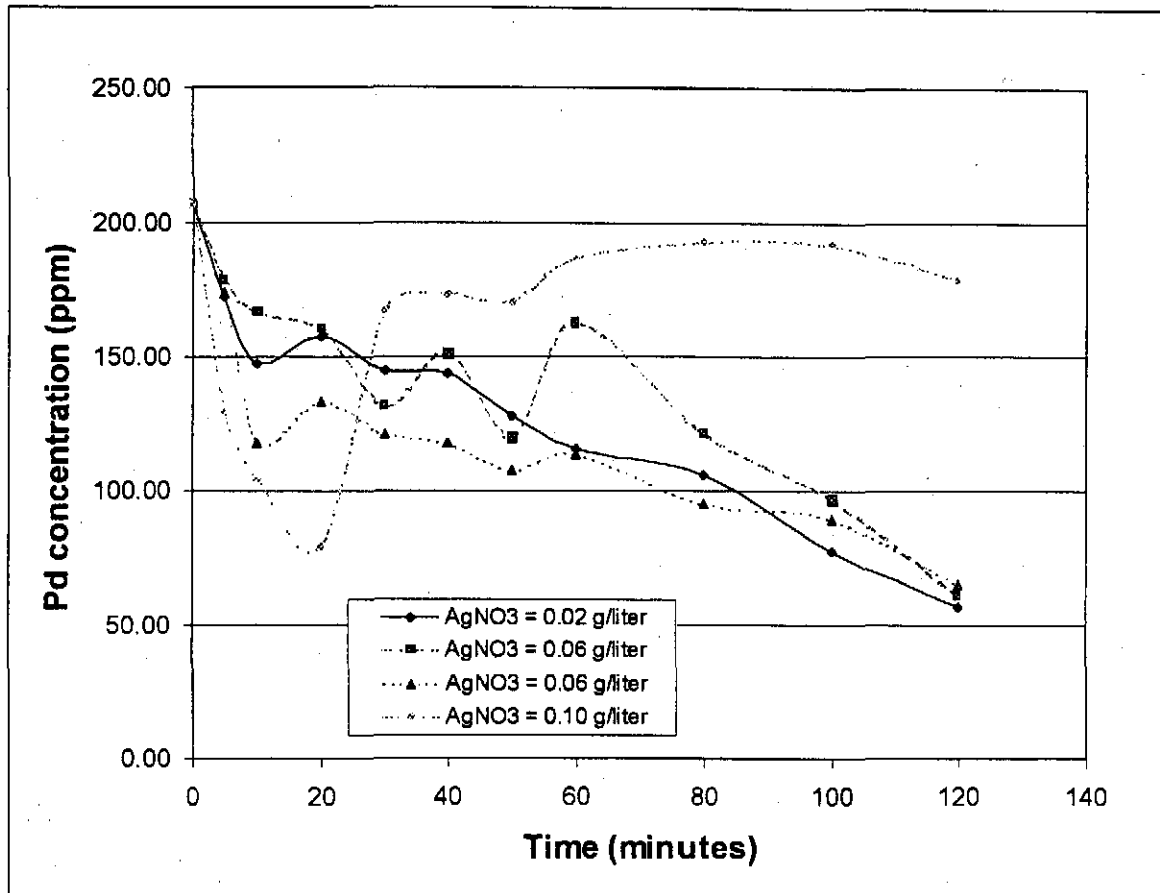


Figure 5.1: Concentration profiles for Pd in solution at various Ag concentrations

Initially the palladium concentration in the solution drops sharply, but then increases again. After two hours of palladium-silver co-deposition (with 0.1 g AgNO_3 , there is little difference between the initial palladium concentration and the final value. The increase in palladium concentration suggests that a second anodic oxidation reaction occurs simultaneously with reaction (2.14) i.e. $\text{Pd}^0 \rightarrow \text{Pd}^{2+} + 2\text{e}^-$. The reason for this reaction is not fully clear, but it is possibly due to the effect of hydrogen overpotentials and the strong coordination effect between EDTA and palladium. At lower silver concentrations (0.06 and $0.02 \text{ g AgNO}_3/\text{litre}$) this phenomenon did not occur to such a great extent. The palladium concentration declined with time as the reaction continued and the metal ions were reduced. Slight local increases occurred due to plating inhibition.

5.2.1. DYNAMICS OF CO-DEPOSITION

APPENDIX C, Figures C1-C4 give the concentration profiles for silver and palladium during two consecutive electroless plating sessions. From **Figure C1** it can be seen that both the silver and the palladium concentrations decrease linearly during both plating sessions. During the second session (2-4 hours) plating rates for both silver and palladium are lower, indicating that the surface on which deposition occurs has a decreased catalytic activity.

For the second plating session a slightly higher hydrazine concentration was used to increase the oxidation potential and maintain sufficient co-deposition rates. The increased hydrazine concentration did not cause any noticeable change. The anodic oxidation of hydrazine is dependent on the composition of the deposit. The potential drops from about -1.04 V for palladium to about -0.70 V for silver (Ohno et al., 1985), indicating that the reaction should slow down as more silver is deposited.

Figures C2 and **C3** show similar trends to that of **C1** for both silver and palladium concentration profiles during the first two hours. During the next two hours (2-4 hours) it seems as if total Pd passivation was reached after about 40 minutes where there was no further decline in the palladium concentration. The silver concentration should keep on decreasing with time. This can not be clearly seen in **Figure C2**, but indeed in **Figures C3** and **C4**. With the higher silver concentration in **Figure C4**, total Pd passivation is reached much sooner (after about 40 minutes in the first plating session) than in **C1-C3**. From **Figures C1** to **C3** it is also evident that in the first plating session most of the silver is deposited, while a much higher percentage of palladium ions remains in solution. The silver plating percentage is higher, but it must be remembered that the silver ions are almost ten times more diluted than the palladium ions and much fewer ions thus need to be reduced.

5.2.2. NON-IDEAL CO-DEPOSITION BEHAVIOUR

Figure 5.2 indicates the relationship between the amount of palladium initially in the solution and that deposited on the activated substrate. The deposition behaviour becomes more non-ideal as the silver content in the initial solution increases. The palladium to silver ratio deposited on the membrane changes from the ratio in the solution as the silver content in the bath increases, favouring silver deposition. When there is 73 % Pd in solution only about 40 % Pd is deposited on the membrane compared to 60 % Ag deposited.

There is not much change in the membrane composition after two and four hours respectively. **Table 5.1** summarises the compositions. For low silver concentration there is little difference between the solution and membrane composition, but the silver content on the membrane increases sharply when the silver solution concentration is increased. These results are in full agreement with what was observed by Shu et al., 1993.

Table 5.1: Percent Pd initially in solution and percent Pd deposited on membrane

| Solution Initial % | On membrane | |
|-----------------------|-------------|----------|
| | after 2h | after 4h |
| 93.1 | 90.8 | 91.5 |
| 81.9 | 72.8 | 68.8 |
| 81.9 | 73.6 | 65.6 |
| 73.1 | 42.7 | 36.2 |

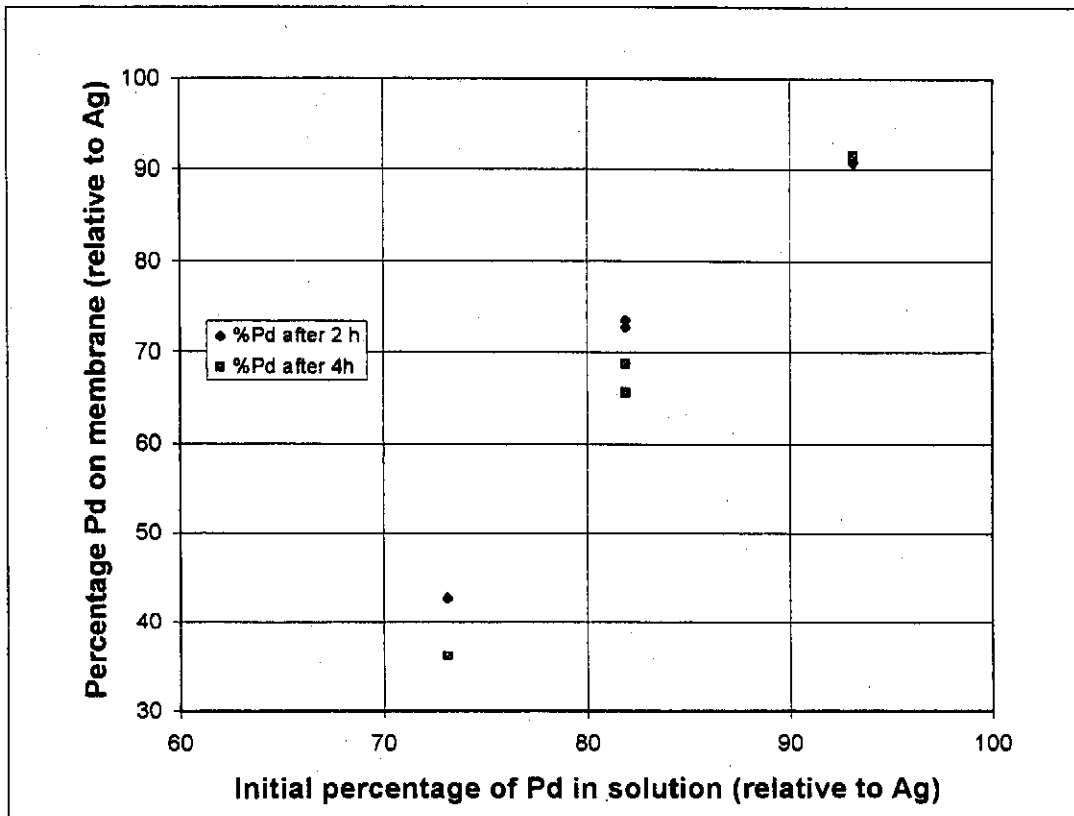


Figure 5.2: Relationship between Pd in solution and Pd deposited on membrane

Reduction favours the higher reduction potential and from **Table 5.2** (taken from Shu et al., 1993) it can be seen that a palladium rich bath must be used before palladium starts to deposits. Values were calculated using equations (2.32-2.39).

Table 5.2: Calculated electrode potentials

| Electrode reaction | 25Pd-75Ag | 50Pd-50Ag | 75Pd-25Ag | 83.4Pd-16.6Ag |
|--|-----------|-----------|-----------|---------------|
| $\text{Pd}^{2+} + 2\text{e}^- \rightarrow \text{Pd}^0$ | 0.213 | 0.222 | 0.227 | 0.228 |
| $\text{Ag}^+ + \text{e}^- \rightarrow \text{Ag}^0$ | 0.256 | 0.245 | 0.228 | 0.217 |

5.2.3. SUGGESTED PALLADIUM-SILVER CO-DEPOSITION MECHANISM

The mechanism proposed in this study is similar to that proposed by Shu and co-workers (1993). **Figures C5-C8** indicate membrane composition with time which were constructed to determine the effects of surface activity and electrode potentials. Many factors influence the co-deposition process of which the above two are the most important. The oxidation reduction reactions which occur in the solution are also dependent on hydrogen overpotentials and EDTA-metal ion complex forming abilities. The process is dynamic and since the palladium and silver concentrations are very low, the reduction potentials of the metal ions vary considerably with time.

At the start of the co-deposition process there are two distinct plating rates; one for palladium and one for silver. The higher the silver content, the higher the silver plating rate compared to palladium. This is very clear when comparing **Figures C5, C6 and C8**. For low silver concentrations (0.02 and 0.06 g AgNO₃/litre) the palladium-silver ratio after 240 minutes remains within 10% of the value after 5 minutes. This is significant, since it indicates that there is an equilibrium between the palladium and silver deposition rates. Both silver and palladium deposition are inhibited (see **Figures C1-C3**) to a small extent. The structure and composition of the plated membrane are suitable for further reaction to occur. The deposited silver cannot agglomerate, because the deposited amount is too small. The palladium is able to cover the silver seeds and prevent them from forming a pure silver layer, because the palladium reaction rate exceeds the mass transfer resistance imposed by the silver nuclei. This maintains an equilibrium between the two deposition rates.

At high silver concentrations (**Figure C7**) there is no longer an equilibrium between palladium and silver deposition rates. The decrease in palladium content of the deposited film is more than 25% from 5 to 240 minutes. Deposited silver nuclei are more catalytic towards further silver deposition than towards palladium deposition. The silver thus inhibits further palladium plating and the palladium deposition rate strives towards zero. A high silver concentration appears to have little effect on further silver plating (**Figure C4**). It continues at a constant rate. For lower initial silver concentrations (**Figures C1-C3**), the silver concentration in the solution is higher after four hours than after two hours.

5.2.4. PROBLEMS OF PALLADIUM-SILVER CO-DEPOSITION

Co-deposition is not a suitable method for preparing palladium-silver composite membranes. The main reasons include the following:

- Obtaining a specific palladium-silver ratio on the membrane is very difficult.
- The results are not very reproducible.
- The silver and palladium concentrations in the initial solution are low and as a result the amount of palladium and silver deposited is also low. The deposited films were non-homogeneous and irregular. Dense, even thickness films (>5 micron) could not successfully be prepared even after 8 consecutive one hour plating sessions.
- The palladium conversion in this reaction is low.

Depositing separate layers of palladium and silver is much easier and pose fewer problems than co-deposition. After the layers are deposited, the film is heat treated to ensure proper diffusion of silver into palladium.

5.3. ELECTROLESS SILVER PLATING

The stability constants for silver complexes are low, because silver has a single positive charge in the ionic form. The silver-EDTA complex has the following stability constant: $\log K_{AgEDTA} = 7.3$ (Sillen et al., 1964). Compared to the stability constant for palladium ($\log K_{PdEDTA} = 18.5$), this value is very low. With this in mind, lower temperatures and higher EDTA concentrations were investigated than those used for optimum palladium conversion. The $AgNO_3$ concentration (0.65 g/litre) is also much lower than the palladium salt concentration (2.75 g/litre) used for electroless palladium plating.

Hydrazine was the only reducing agent investigated and the value was constant at 30% molar excess.

5.3.1. PLATING ON AN ACTIVATED SUBSTRATE

Figures 5.3 and 5.4 represent the silver deposition rate and conversion for plating on an activated substrate.

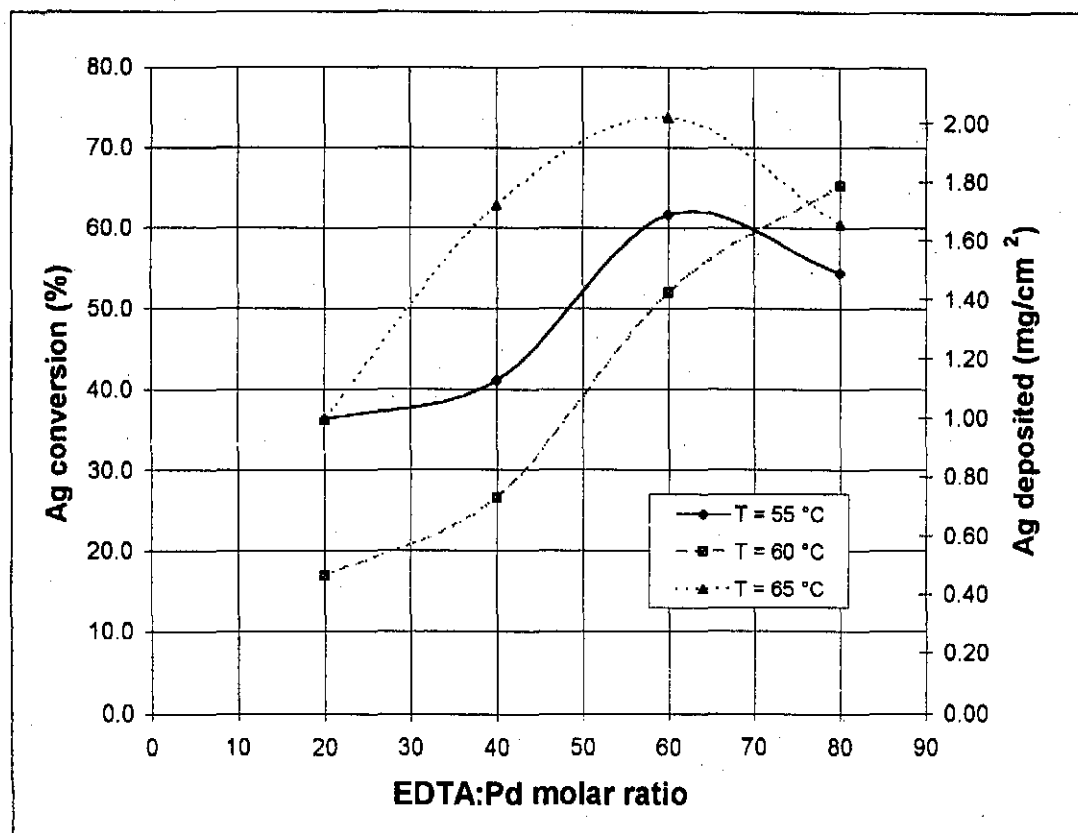


Figure 5.3: Electroless Ag plating on an activated substrate

The maximum conversion obtained for electroless silver plating was 74%. The electroless silver behaviour is similar to that of palladium. The rate increases slightly with temperature (as would be expected), provided that the solution is stable. The effect of temperature is, however, not as significant as in the case of palladium plating. From Figure 5.4 it can be seen that a temperature increase does not result in a very sharp increase in plating rate.

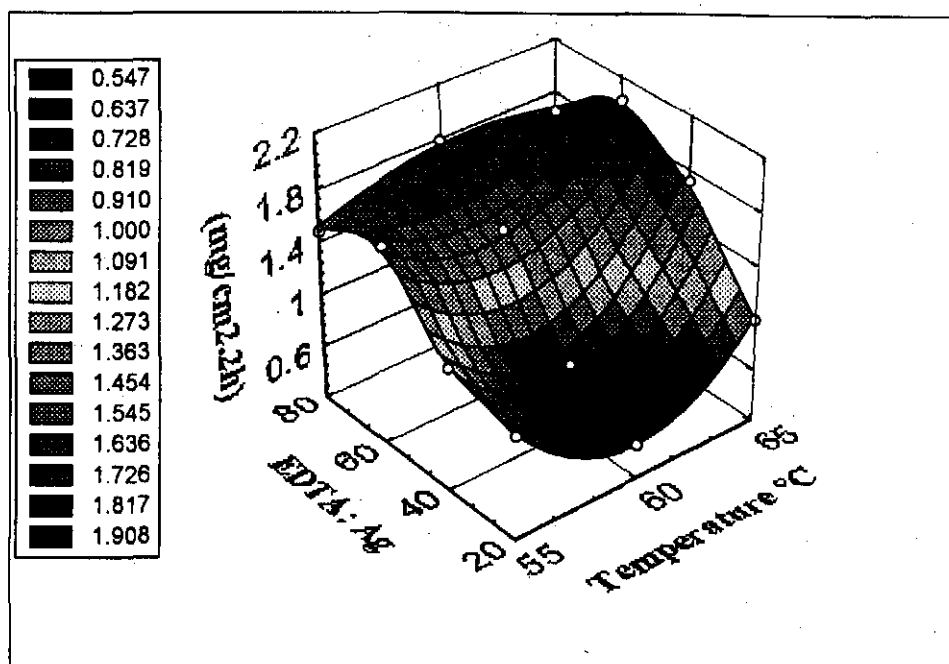


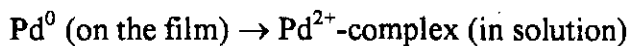
Figure 5.4: Surface plot of Ag plating on an activated substrate

Figures 5.3 and 5.4 indicate that a high EDTA concentration is necessary for an optimum plating rate. As in the case with palladium, there is an optimum EDTA concentration for a maximum plating rate. The optimum EDTA:Ag-salt molar ratio is about 60:1 (depending on the temperature) which is much higher than the value for palladium (30:1 to 40:1). This proves the lower stability of the silver-EDTA complex compared to the palladium-EDTA complex.

The plating mechanism follows reaction (2.14) to (2.16). An excess of hydrazine was necessary to compensate for the catalytic decomposition of hydrazine at high temperatures. A lower excess, compared to electroless palladium plating, was used to prevent bath instability and because plating was performed at a temperature of about 10 °C lower than that used for palladium plating.

5.3.1. PLATING ON A PREDEPOSITED PALLADIUM FILM

Experiments were performed at similar conditions to those used for deposition on an activated substrate. This method has also been used by other researchers (Kikuchi, 1995; Shu et al., 1995; Uemiya et al., 1991b) and they did not report any problems. In this study, problems were encountered with an unwanted side reaction.



(5.1)

The mass loss of the substrate can clearly be seen in **Figures 5.5** and **5.6**. The mass loss was independent of the amount of predeposited palladium and only dependent on the reaction conditions. Small deposits of silver were visible on the palladium film. The silver reduction reaction can not be responsible for palladium oxidation, since this will result in a substrate mass increase. Two moles of silver are reduced for one mole of palladium oxidised. An alternative reaction must be responsible for the palladium mass loss.

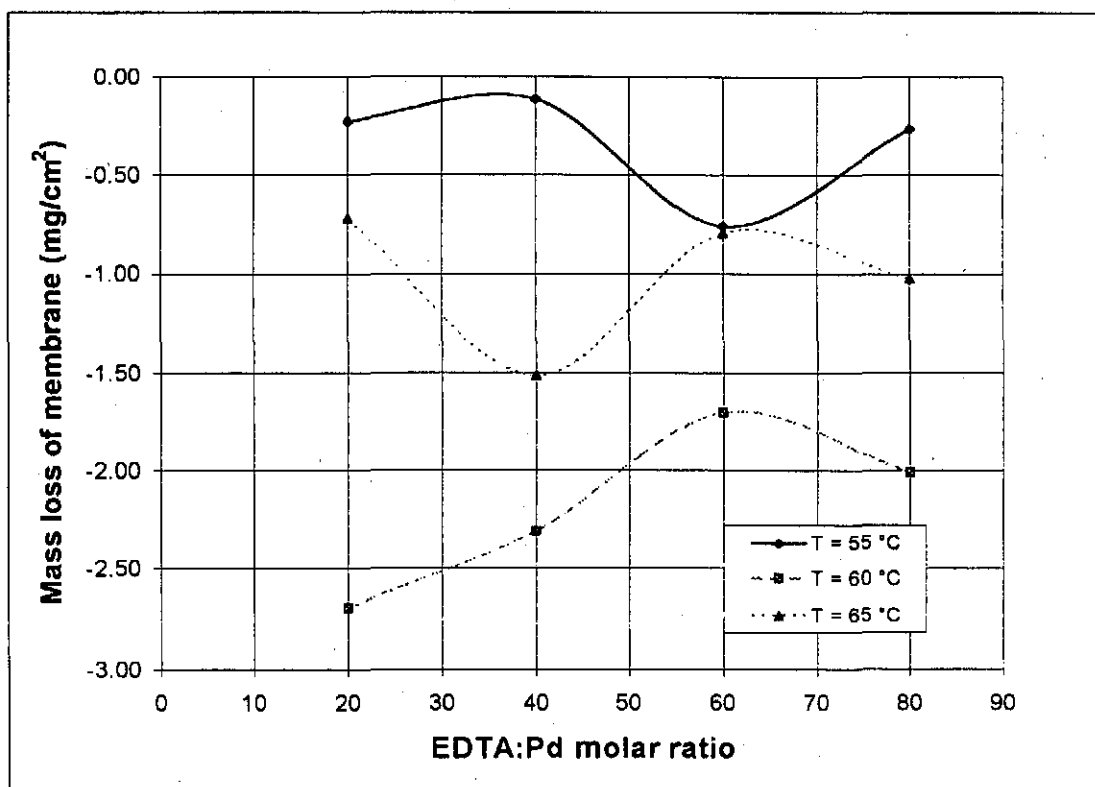


Figure 5.5: Electroless Ag plating on a Pd film

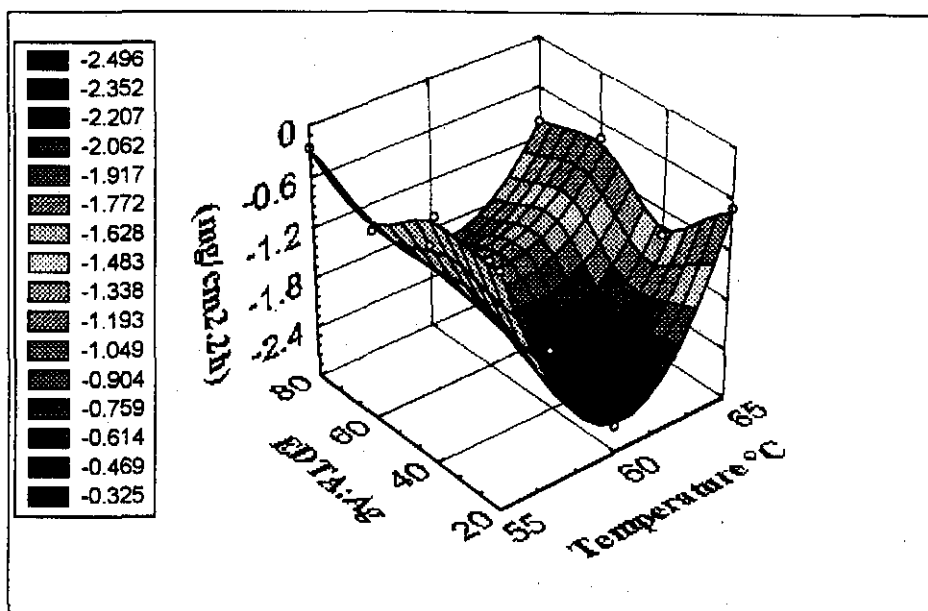
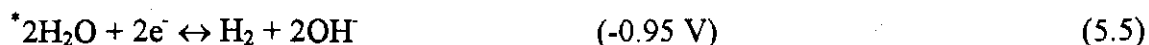


Figure 5.6: Surface plot of Ag plating on a Pd plated surface

All the possible reduction and oxidation reactions are listed below. Values are given at 25 °C, with an EDTA:Ag-salt molar ratio of 60:1 for determining the Ag potential and excluding hydrogen overpotential for Ag.

Reduction reactions:



Oxidation reactions:



* Over potentials included

^a Potential for a silver catalytic surface

Hydrazine acts as a reducing agent, but in some cases also as an oxidising agent (Schmidt, 1984). Although thermodynamics suggests the occurrence of reactions (5.2) and (5.8), experimental observations in this study indicated that reaction (5.3) and (5.7) were also taking place. Combining reaction (5.3) and (5.8) yields the decomposition reaction for hydrazine, which takes place at high temperatures and in the presence of a noble metal catalyst.

5.4. ELECTROLESS NICKEL PLATING

Electroless nickel plating has been used extensively and the literature on the process is abundant (Riedel, 1991). Most electroless nickel plating baths operate at temperatures exceeding 80 °C, which makes the deposition rate very fast. Sodium hypophosphite is mainly used as the reducing agent, since it deposits a nickel-phosphorous compound, which is much harder than pure nickel. The phosphor content is higher in an acidic bath, thus being the preferred one for applications to enhance corrosion resistance.

The alkaline bath has a few characteristics which makes it suitable for preparing palladium composite membranes:

- The plating temperature is low (below 50 °C for certain compositions), and thus the deposition rates slower.
- The percentage phosphor deposited can be below 1% compared to 10% or more for acidic baths.
- The solutions are very stable and the bath formulas very simple.

Two things are of importance when preparing thin film (less than 5 micron thickness) palladium composite membranes:

1. The nickel deposit must be pure, which can be achieved to a great extent by using an alkaline sodium hypophosphite bath. A hydrazine bath can also be used ensuring a completely pure deposit, but since not much work has been done on nickel deposition with hydrazine, the sodium hypophosphite option was taken.
2. The deposition rate must be slow and controllable so that about 0.4 mg/cm² nickel can be deposited with good reliability and reproducibility.

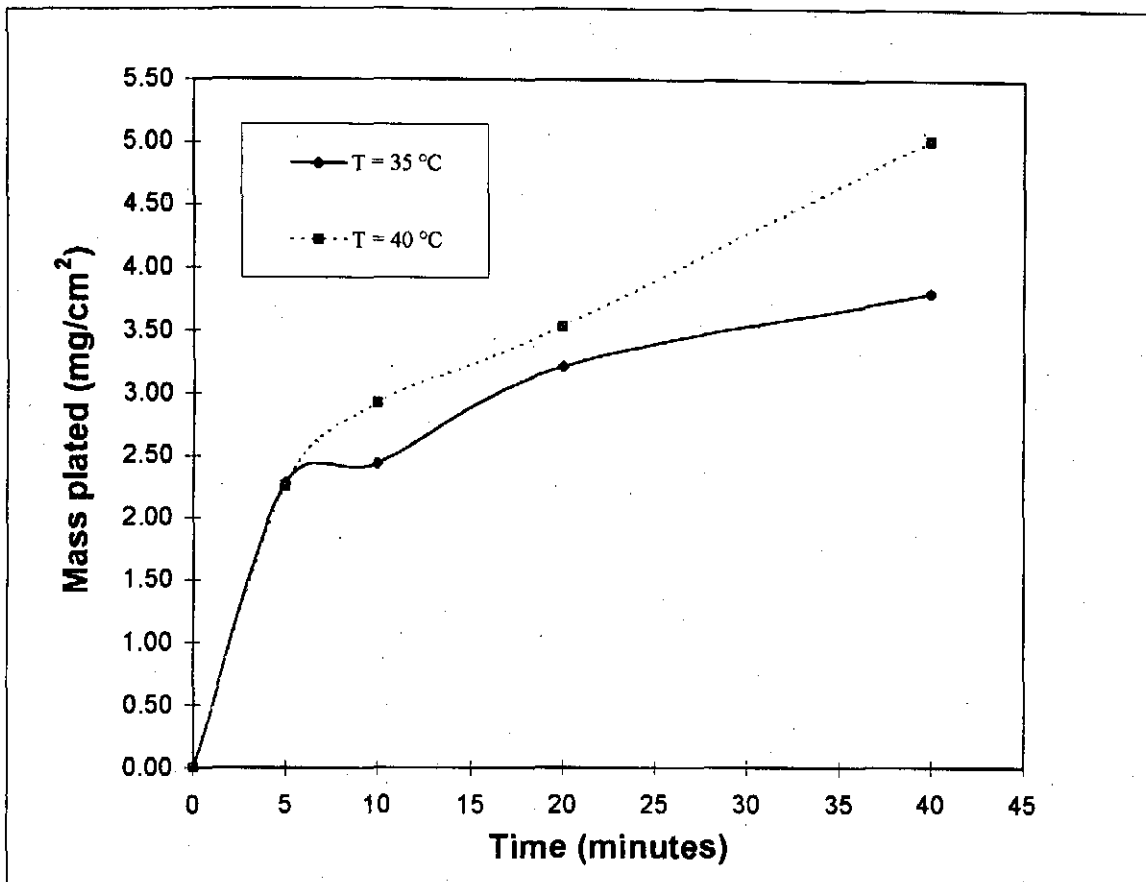


Figure 5.7: Ni plating rates on an activated substrate

With this in mind, the baths listed in Table 3.6 were investigated. Initial experiments used 45 °C, but the deposition rate was too high and peeling occurred after 40 minutes of plating. Peeling (when the metal film does not adhere properly to the activated membrane support) is irrelevant, since it occurred only after about 2.5-3 mg/cm² nickel had been deposited. Further experiments were performed at 40 and 35 °C. In this case no peeling was observed and the adherence of metal to ceramic was very good. Figure 5.7 shows the nickel plating rates at 35 and 40 °C.

When preparing palladium-nickel and palladium-silver-nickel composites, 0.4 mg nickel/cm² had to be deposited for a 5 micron thickness film with 7% nickel. This is very close to the origin in Figure 5.7. The palladium-coated supports were dipped in the 40 °C nickel solution for 30 seconds at a time, until the correct amount of nickel had been deposited.

5.5. PALLADIUM PLATING ON SILVER DEPOSITS

Electroless palladium plating on silver coated substrates was investigated to determine how much silver inhibits palladium plating and if it is possible to prepare palladium-silver composite membranes by first depositing silver. The plating volume was 22 ml, the plating time 3 hours and the membrane length 8 mm. Two possibilities were investigated: (a) Pd deposited directly on Ag and (b) Pd deposited on Ag after the Ag coated membrane was pretreated for a second time.

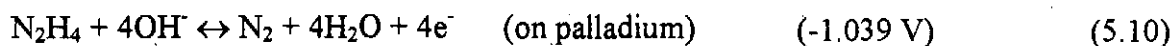
Table 5.3: Conversions for palladium deposited on silver

| EDTA: Pd-salt molar ratio | Conversion for Pd deposited on Ag (a) | Conversion for Pd on Ag (b) | Conversion for Pd on activated substrate |
|------------------------------|--|--------------------------------|---|
| 20 | 67.4 | 66.0 | 87.1 |
| 30 | 58.1 | 80.9 | 89.2 |
| 40 | 45.6 | 83.3 | 80.0 |

All experiments were performed at 71 °C, hydrazine: Pd-salt molar ratio = 0.72:1, buffer pH = 11 and T = 71 °C.

Table 5.3 indicates favourable results especially for (b) where the conversions are similar to the values obtained for palladium deposited on an activated substrate. For (a) the palladium conversion and plating rate are lower due to initial inhibition by silver. Once the silver layer is covered, deposition will occur at the same rate as that for palladium deposited on an activated substrate. In all six experiments, where palladium was deposited on silver, a homogeneous palladium layer was formed which covered the entire silver surface.

The hydrazine oxidation potential is dependent on the composition of the surface in contact with it. The hydrazine oxidation potential for a palladium surface is more negative. This surface, from an electrochemical point of view, is then more favourable for electroless plating using hydrazine. This explains why electroless palladium plating on silver is slower than on palladium (Table 5.3). Hydrazine oxidation potentials were taken from Ohno et al. (1985), with E (standard calomel electrode (SCE)) = 0.242 V.



5.6. SUMMARY

The following conclusions can be drawn from the results presented in this chapter:

- Palladium-silver co-deposition is a very complex process, mainly governed by electrode potential differences and surface catalytic effects. At low silver concentrations (0.02-0.06 g AgNO₃/litre) there is an equilibrium between silver and palladium plating rates. Both are inhibited to some extent by deposited silver. The membrane composition remains constant with time. At high silver concentrations (0.1 g AgNO₃/litre), the palladium plating rate quickly drops to almost zero, while the silver plating rate is not reduced.
- A silver deposition rate of 2 mg/cm² for two hours plating on an activated substrate was obtained at 65 °C, 30% molar excess hydrazine, buffer pH = 11 and EDTA: Pd-salt molar ratio of 60:1. The conversion exceeded 70%. The high EDTA concentration required is an indication of the low silver stability constant.
- Silver deposition on palladium resulted in an unwanted side reaction where palladium was reduced and removed from the substrate.
- A low temperature, alkaline nickel plating bath operating at 40 °C, gave slow deposition rates suitable for preparing low percentage nickel composites.
- Palladium can be deposited on a pure silver coating or on a silver coating which has been pretreated in tin chloride and tetra amine palladium nitrate solutions.

CHAPTER 6

SURFACE CHARACTERISATION USING SEM AND PIXE

6.1. INTRODUCTION

Scanning electron micrographs of pure palladium, silver and nickel membranes were taken using a Cambridge Stereoscan 440 (SEM). Composite Pd-Ni, Ag-Pd, Pd-Ag and Ag-Pd-Ni membranes were prepared and alloyed at 650 °C. Both top views and side views of the membranes were studied to investigate the surface structure and the thickness of the metal layers. PIXE (with a Van de Graaff generator) was used to determine the composition of the metal matrix and to detect any compositional changes after heat treatment.

The silver deposits were non-homogeneous, the palladium deposits dense but columnlike and the nickel deposits very smooth and non-porous. High zinc concentrations (>10 wt%) were oddly found in three of the ten samples after heating, resulting in an unique high density structure with sub-micron pores. The addition of 3-5% nickel to palladium and silver-palladium films, resulted in smooth, defect free top-layers.

6.2. REPRESENTATIVE SAMPLES

Characteristic samples were prepared for analysis with SEM, XRD, EDX and PIXE. They are listed in **Table 6.1**. An alumina-zirconia (stabilised with yttria) membrane was used as support. The membrane outer diameter was 12 mm.

In all experiments with Pd and Ag coatings, Ag was deposited first, followed by Pd, except with (e) where Ag was deposited on a Pd film. In (d), Ni was deposited on the Pd film and in (g) the deposition order was Ag, Pd and then Ni. The adhesion of all layers was excellent prior to heat treatment. With samples (i) and (j) part of the metal layer started to peel away from the support after heat treatment. The mass of nickel plated could not be measured very accurately, because of the small amounts deposited. Uncertainty exists in the final digit of the measured mass and this may result in a percentage fault of up to two percent in nickel content, thus for (d) the nickel content might be 3 to 8%.

Table 6.1: Membranes used for analysis

| Sample | Length mm | Pd plated mg | Ag plated mg | Ni plated mg | Pd:Ag:Ni | Thickness micron |
|----------|--------------|-----------------|-----------------|-----------------|---------------|---------------------|
| a | 10.6 | 33.1 | | | 100:0:0 | 6.9 |
| a + heat | 10.6 | 33.1 | | | 100:0:0 | 6.9 |
| b | 10.6 | | 19.4 | | 0:100:0 | 4.6 |
| b + heat | 10.6 | | 19.4 | | 0:100:0 | 4.6 |
| c | 9.6 | | | 14.3 | 0:0:100 | 4.4 |
| c + heat | 9.6 | | | 14.3 | 0:0:100 | 4.4 |
| d | 9.3 | 17.5 | | 1.0 | 94.6:0:5.4 | 4.5 |
| d + heat | 9.3 | 17.5 | | 1.0 | 94.6:0:5.4 | 4.5 |
| e | 10.2 | 16.8 | 4.8 | | 78:22 | 4.8 |
| e + heat | 10.2 | 16.8 | 4.8 | | 78:22 | 4.8 |
| f | 10.6 | 13.6 | 4.4 | | 76:24:0 | 3.9 |
| f + heat | 10.6 | 13.6 | 4.4 | | 76:24:0 | 3.9 |
| g | 7.5 | 13.1 | 5.1 | 1.1 | 67.9:26.4:5.7 | 6.1 |
| g + heat | 7.5 | 13.1 | 5.1 | 1.1 | 67.9:26.4:5.7 | 6.1 |
| h | 8.0 | 14.5 | 3.0 | | 83:17 | 4.9 |
| h + heat | 8.0 | 14.5 | 3.0 | | 83:17 | 4.9 |
| i | 7.9 | 17.9 | 2.0 | | 90:10:0 | 5.6 |
| i + heat | 7.9 | 17.9 | 2.0 | | 90:10:0 | 5.6 |
| j | 7.8 | 14.2 | 3.1 | | 82:18:0 | 5.0 |
| j + heat | 7.8 | 14.2 | 3.1 | | 82:18:0 | 5.0 |

6.3. MEMBRANE SUPPORT

An aluminum filter was used, and thus the aluminum could not be detected and was calculated using 29 wt% Zr as a reference. The main impurities in the support are hafnium, iron and a bit of calcium. The structure of the support is shown in **Figure 6.1**.

The composition of the membrane support is presented in **Table 6.2**.

Table 6.2: Membrane composition in percentages, with 10 ppm = 0.001 %

| Al | Zr | Y | Hf | Ca | K | Fe | Ti | Ni | Fe |
|--------|--------|-------|-------|-------|-------|-------|-------|-------|-------|
| 68.077 | 29.000 | 2.484 | 0.329 | 0.012 | 0.007 | 0.082 | 0.004 | 0.002 | 0.003 |

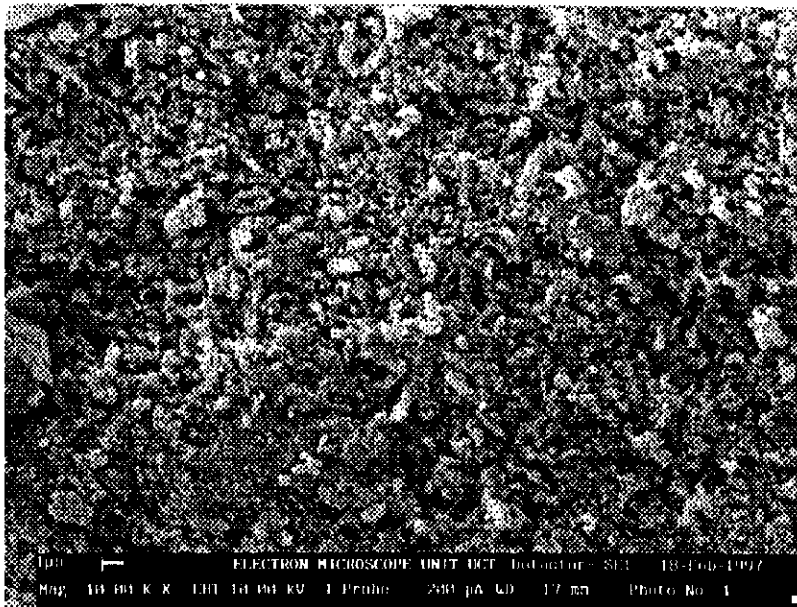


Figure 6.1: SEM image of membrane support

6.4. PURE PALLADIUM (a)

PIXE was used to determine the surface composition of the palladium coating after heat treatment. The results are listed in **Table 6.3**:

Table 6.3: Surface composition of palladium film in percentages

| Pd | Ag | Zr | Y | Sn | Zn | Hf | Pb | Hg |
|--------|-------|-------|-------|-------|-------|-------|-------|-------|
| 90.375 | 0.070 | 8.717 | 0.673 | 0.136 | 0.005 | 0.004 | 0.010 | 0.010 |

The high percentage of zirconium and yttrium is due to the penetration of protons through the palladium layer into the support. Surface impurities (Sn, Ag, Pb and Hg) account for about 0.25% of the mass. Aluminium was not detected, since an aluminium filter was used and aluminium values must necessarily be excluded from all samples. **Figures 6.2-6.5** show the

top and cross section views of (a) and (a + heat), while Figures 6.6 and 6.7 show a film that was prepared under similar conditions. All images were taken at 10 000 magnification.

Before heat treatment, the palladium film appears flaky (Figure 6.2). During heat treatment, palladium nuclei agglomerated to form vertical clusters. The deposit is columnlike and follows the contours of the substrate. From Figure 6.3 it appears as if the palladium film might be very porous, but in fact it is dense when looking at Figures 6.4 and 6.5. The holes in Figure 6.3 are not areas where there is no palladium, but areas where there are irregularities in the substrate and the palladium is deposited in valleys on the surface. Some deposits were fingerlike (Figures 6.6 and 6.7) and allow for a high surface area, which ought to be advantageous from a catalytic point of view. All films were dense and defect free.

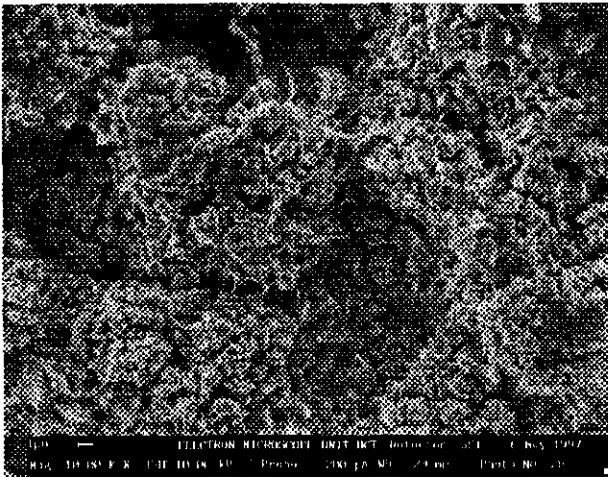


Figure 6.2: Top view of (a)

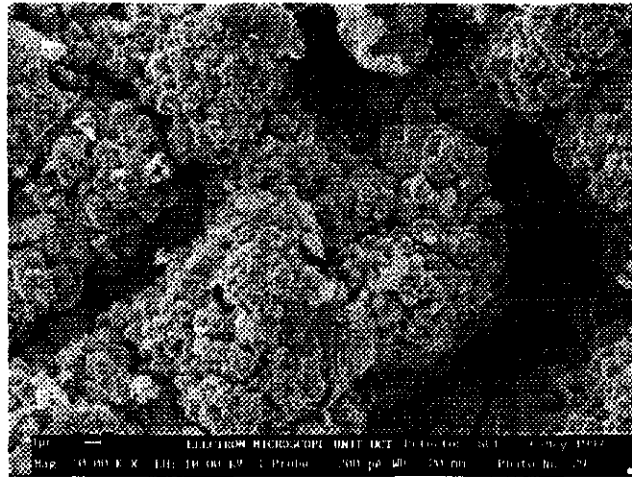


Figure 6.3: Top view of (a + heat)

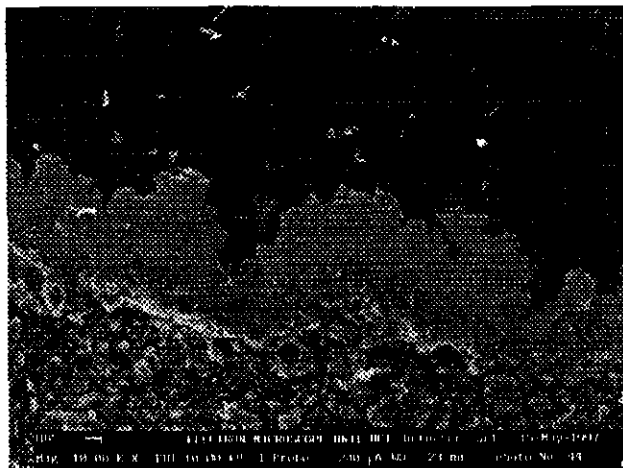


Figure 6.4: Side view of (a)

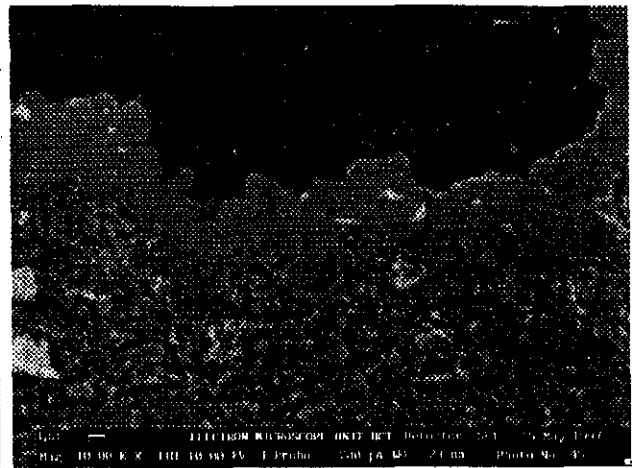


Figure 6.5: Side view of (a + heat)

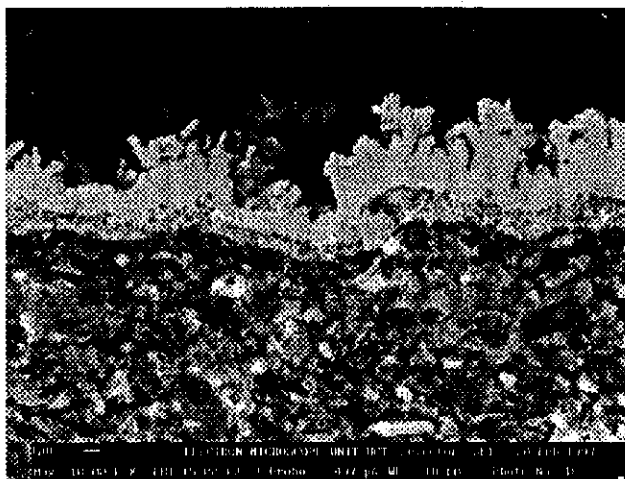


Figure 6.6: Side view of a palladium film before heating with the pre-treatment layer at the bottom of the film

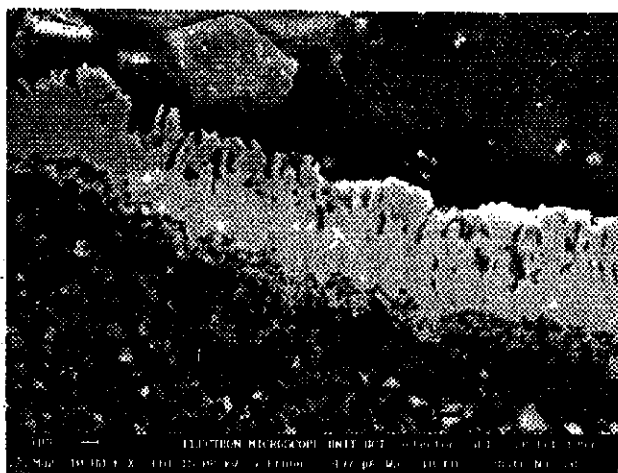


Figure 6.7: Side view of a palladium film after heating

6.5. PURE SILVER (b)

PIXE was used to determine the surface composition of the silver coating after heat treatment. The results are listed in **Table 6.4**:

Table 6.4: Surface composition of the silver film in percentages

| Pd | Ag | Zr | Y | Sn | Ca | Hf | Pb | Fe |
|-------|--------|--------|-------|-------|-------|-------|-------|-------|
| 0.098 | 82.141 | 15.793 | 1.236 | 0.494 | 0.015 | 0.114 | 0.080 | 0.025 |

The concentrations of zirconium and yttrium are higher when compared to the concentrations in **Table 6.3**, indicating that the deposited silver film was not as dense as the palladium film. The hafnium, iron and calcium are impurities in the membrane support, while the tin was deposited in the pretreatment step. The purity of the film was about 99.5%. SEM images confirmed irregular and non-homogeneous silver plating (**Figures 6.8-6.11**). Before heating (**Figure 6.8**), the silver clusters were small and deposited only on certain areas. During heating, the silver nuclei agglomerated and grew to form larger clusters (**Figure 6.9**). The non-homogeneity is clear from **Figures 6.10** and **6.11**. The cross section views show layers which are much thinner than those calculated theoretically. This implies that some areas have thick layers while others have little or no layer. All images were taken at 10000 magnification.

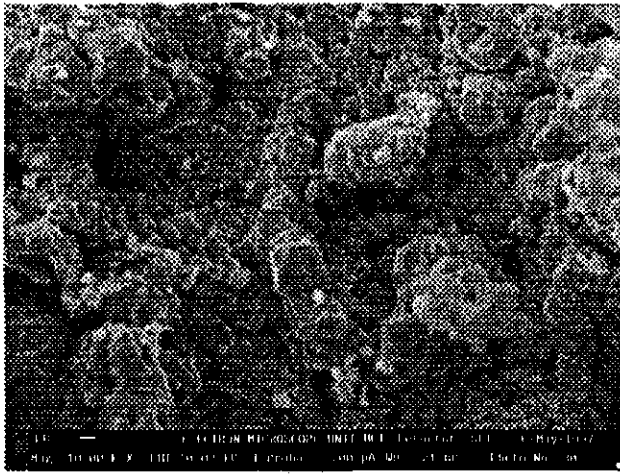


Figure 6.8: Top view of (b)

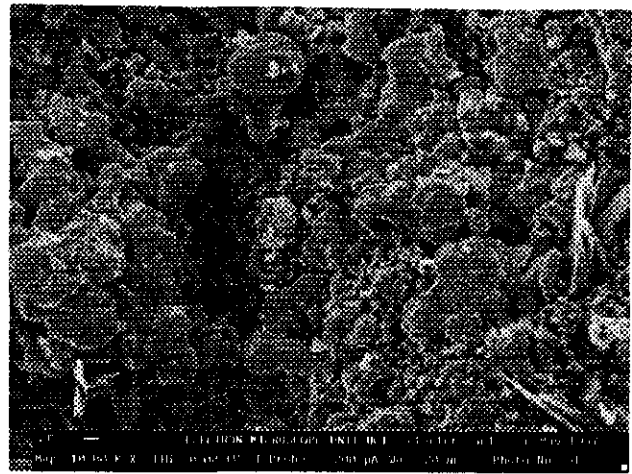


Figure 6.9: Top view of (b + heat)

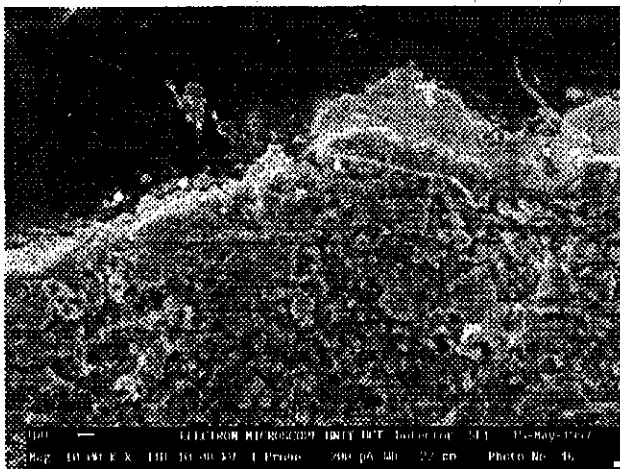


Figure 6.10: Side view of (b)

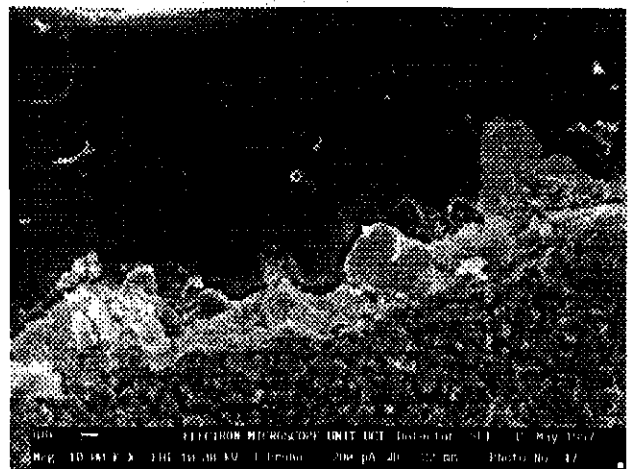


Figure 6.11: Side view of (b+ heat)

6.6. PURE NICKEL (c)

The surface composition of the nickel film is indicated in Table 6.5 and it was constructed using PIXE data. The nickel coating was not as pure as the silver or palladium coatings. The main impurities were cobalt, copper, iron and zinc. The high tin concentration could not be due to pretreatment alone and tin had to be present as an impurity in the nickel salt. The low zirconium and yttrium concentrations indicate weak proton penetration through the nickel layer and thus a dense film. SEM images taken at 10 000 magnification confirm a dense nickel layer.

Table 6.5: Surface composition of the nickel film in percentages

| Ni | Pd | Zr | Y | Sn | Ca | Hf | Pb | Cu | Fe | Co | Zn |
|-------|-------|-------|-------|-------|-------|-------|-------|-------|-------|-------|-------|
| 91.41 | 0.218 | 4.788 | 0.348 | 1.599 | 0.049 | 0.121 | 0.065 | 0.179 | 0.319 | 0.868 | 0.204 |

The nickel deposit was very dense and defect free even before heat treatment. There are no visible defects in **Figures 6.12** and **6.13** and the surface is smooth and non-porous. On the side view images (**Figures 6.14** and **6.15**) there are not a very clear distinction between the membrane support and the nickel layer. The nickel penetrates into the membrane pores forming a very strong and adhering layer.



Figure 6.12: Top view of (c)

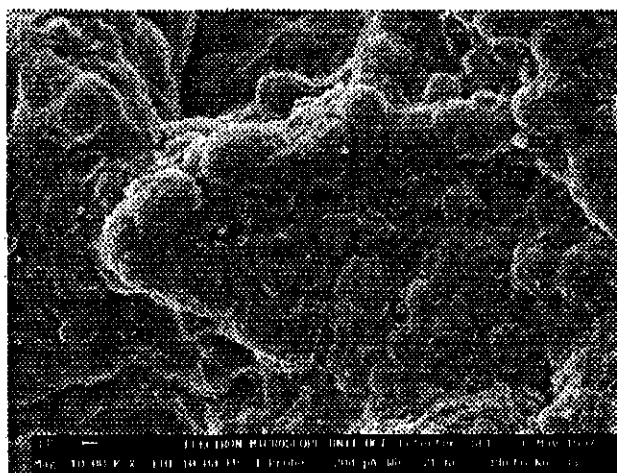


Figure 6.13: Top view of (c + heat)

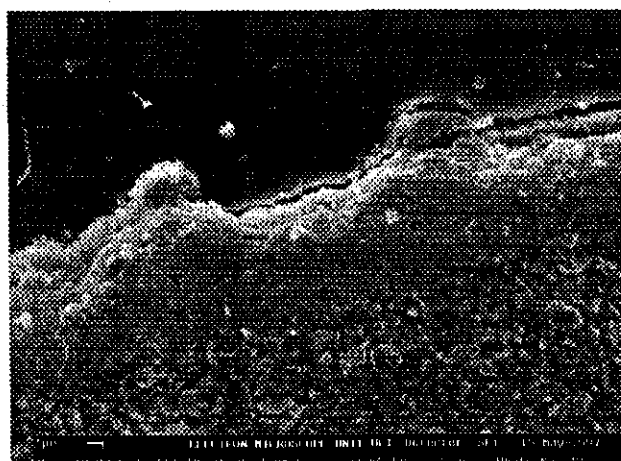


Figure 6.14: Side view of (c)

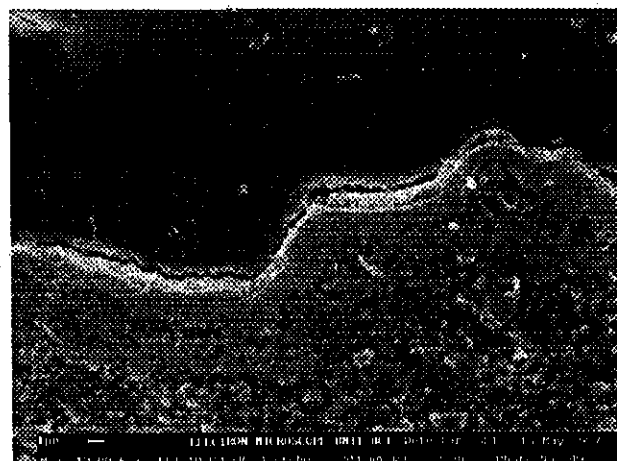


Figure 6.15: Side view of (c+ heat)

6.7. Pd-Ni COMPOSITE MEMBRANE (94.6:5.4) (d)

The film composition before and after heat treatment was determined and compared. The results are shown in Table 6.6:

Table 6.6: Pd-Ni film composition before and after heating

| | Pd | Ni | Ag | Zr | Y | Sn | Fe | Zn | Hf | Pb | Hg | Cu |
|-------------|-------|-------|-------|-------|-------|-------|-------|-------|-------|-------|-------|-------|
| d | 87.12 | 0.987 | 0.151 | 10.15 | 0.857 | 0.488 | 0.017 | 0.007 | 0.065 | 0.007 | 0.133 | 0.027 |
| d + heat | 87.04 | 0.931 | 0.123 | 10.27 | 0.868 | 0.196 | 0.014 | 0.418 | 0.056 | 0.061 | 0.005 | 0.024 |

The amount of nickel deposited was much less than what was measured by weighing the membrane before and after the nickel deposition. Mass measurement is a problem when working with small samples and small deposited amounts (<1 mg). The composition of major elements before and after heating remains fairly constant except for a few elements. The zinc content increased almost 60 times and the lead content increased about 10 times. The mercury content decreased sharply, which is understandable, since mercury is vaporised at 650 °C. SEM images of the Pd-Ni composite at 10 000 magnification are depicted in Figures 6.16-6.19. Nickel was deposited on the Pd film. When comparing Figure 6.16 with Figure 6.2, the nickel nuclei on the palladium surface can be seen clearly. The surface is more granular and the crystals smaller.

The nickel fills voids that might be present in the palladium film, creating a smoother surface. This can be explained by comparing ionic and atomic radii for palladium and nickel. Nickel has a Goldschmidt ionic radius of 0.78 Å and an atomic radius of 1.25 Å (Smithells, 1992). Palladium has an atomic radius of 1.37 Å, and in the plating process nickel ions can easily enter into voids of the deposited palladium structure and then be oxidised to form nickel atoms. After heating, a smooth even surface formed (Figure 6.17). Tiny defects in the top layer is present, but this is understandable if it is taken into account that only 1% Ni was deposited, which represents a top layer of about 60 nm before heating. The side view after heating (Figure 6.19) confirms a very dense and defect free film. The resin, in which the sample was set, pulled away from the metal film upon setting, trapping an air bubble. This is visible at the top of the film.

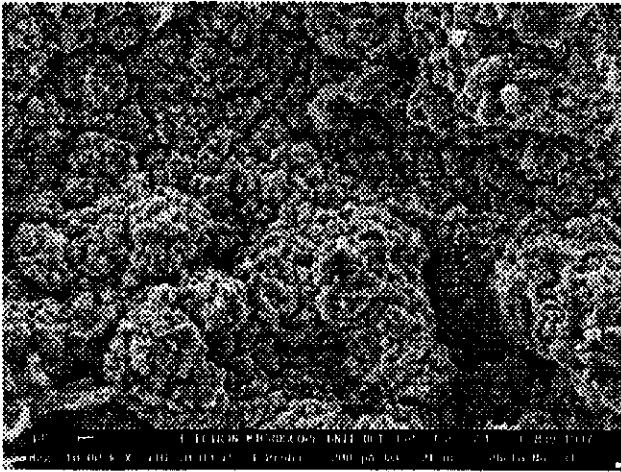


Figure 6.16: Top view of (d)

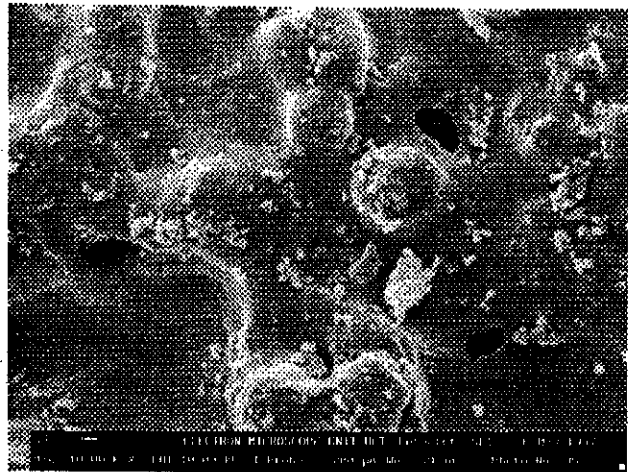


Figure 6.17: Top view of (d + heat)

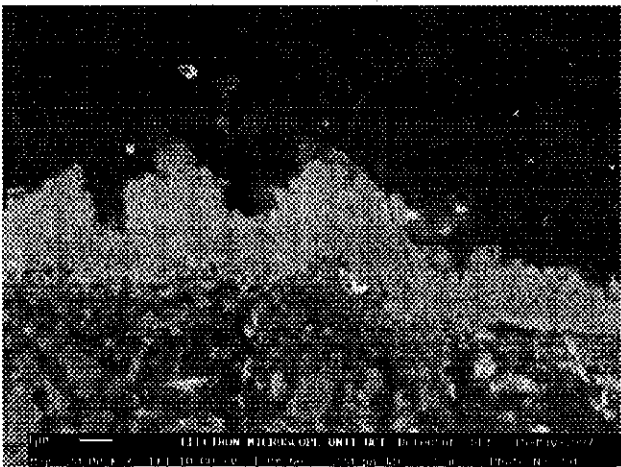


Figure 6.18: Side view of (d)

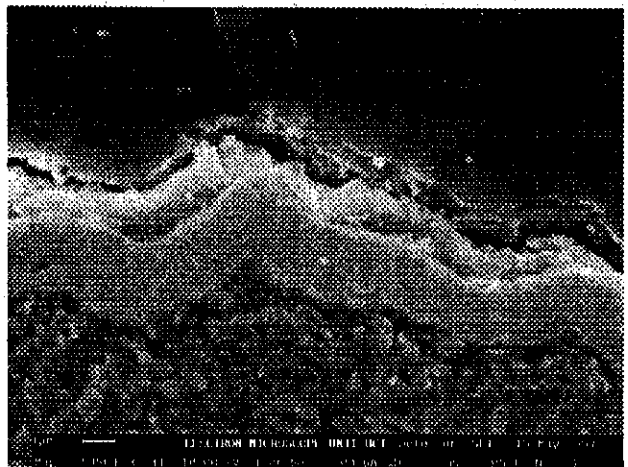


Figure 6.19: Side view of (d + heat)

6.8. Ag ON Pd COMPOSITE MEMBRANE (78:22) (e)

The composition of silver deposited on a palladium film before and after heat treatment was determined and compared. The results are shown in **Table 6.7:**

Table 6.7: Pd-Ag film composition before and after heating

| | Pd | Ag | Zr | Y | Sn | Zn | Hf | Pb | Hg |
|---------------|--------|--------|-------|-------|-------|-------|-------|-------|-------|
| e | 68.932 | 21.205 | 8.871 | 0.741 | 0.167 | 0.000 | 0.040 | 0.007 | 0.031 |
| e+heat | 71.588 | 16.555 | 9.148 | 0.808 | 0.326 | 1.350 | 0.039 | 0.172 | 0.002 |

There was a decrease in silver concentration, which indicates the diffusion of silver into the palladium matrix. The palladium concentration did not change noticeably, but the mercury concentration decreased after heating, while the zinc and lead concentrations increased.

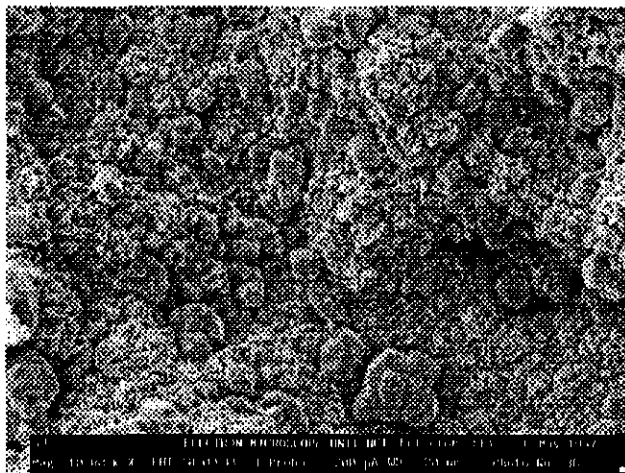


Figure 6.20: Top view of (e)

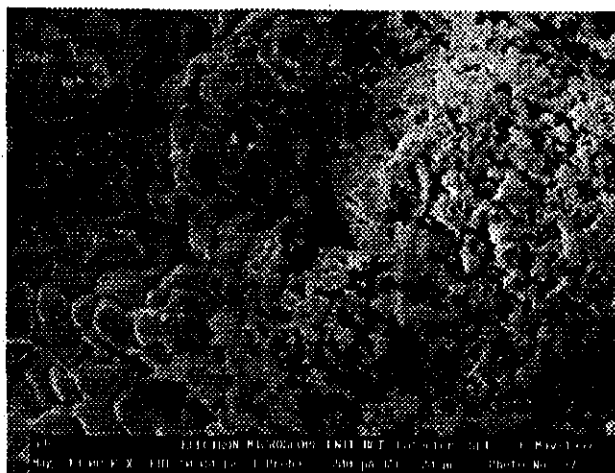


Figure 6.21: Top view of (e + heat)

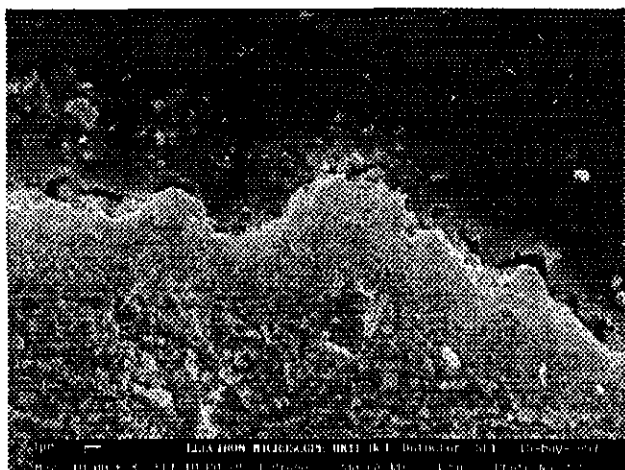


Figure 6.22: Side view of (e)

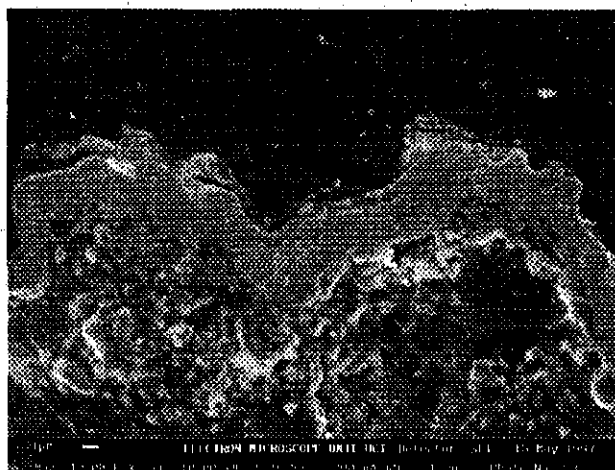


Figure 6.23: Side view of (e + heat)

Before heating, silver clusters can clearly be identified on the predeposited palladium film (Figure 6.20). They are round and much larger than deposited palladium nuclei. Silver crystals tend to grow on other silver crystals, while the palladium crystals do not only grow on other palladium crystals, but over the entire surface. After heating, two unique crystal structures were formed; one being very flaky with tiny crystals (Figure 6.21, right), while the other one is solid with tortuous channels (Figure 6.21, left). From the side view (Figures 6.22 and 6.23) the film appears dense at the top and slightly porous at the base before heating. There is no clear transition from support to metal film, indicating that the film is anchored

inside the membrane pores. After heating, only a single dense layer can be distinguished (Figure 6.23).

6.9. Pd ON Ag COMPOSITE MEMBRANE (24:76) (f)

Element concentrations for a 24 wt% Ag, 76 wt% Pd film are given in Table 6.8.

Table 6.8: Ag-Pd (24:76) film composition before and after heating

| | Pd | Ag | Zr | Y | Sn | Zn | Hf | Pb | Hg |
|---------------|--------|--------|--------|-------|-------|-------|-------|-------|-------|
| f | 77.759 | 10.871 | 10.026 | 0.829 | 0.454 | 0.000 | 0.026 | 0.006 | 0.026 |
| f+heat | 62.820 | 25.960 | 9.507 | 0.791 | 0.645 | 0.019 | 0.044 | 0.030 | 0.001 |

Palladium was deposited on a silver layer. The measured palladium concentration decreased after heating, while the measured silver concentration increased. This means that the silver diffused from the ceramic support outwards into the palladium film. Initially the measured silver concentration was about 11%, but it increased to almost 26% after heating. The decrease in palladium concentration was equal to the increase in silver concentration. Concentrations for other elements remained constant except for mercury, which decreased due to evaporation, and zinc, which increased slightly. The zinc concentration remained very low after heating.

SEM images at 10 000 magnification for top views and 20 000 magnification for side views were taken. Before heating (Figure 6.24), the surface structure is similar to that of pure palladium, since only the top palladium layer can be seen. After heating (Figure 6.25), the structure is similar to that of Figure 6.21 (right). The surface is not columnlike or clusterly, but even. It does not appear completely dense and tiny crystals were formed over the entire surface area. On the side view (Figure 6.26) the bottom silver layer is porous and the top palladium layer dense prior to heating. A single dense layer was formed after heating (Figure 6.27).

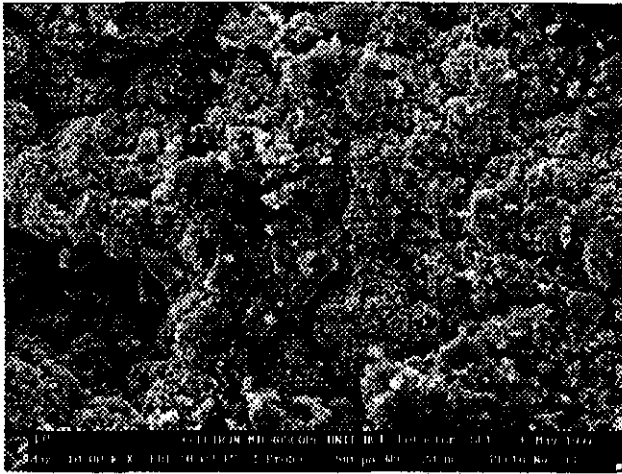


Figure 6.24: Top view of (f)

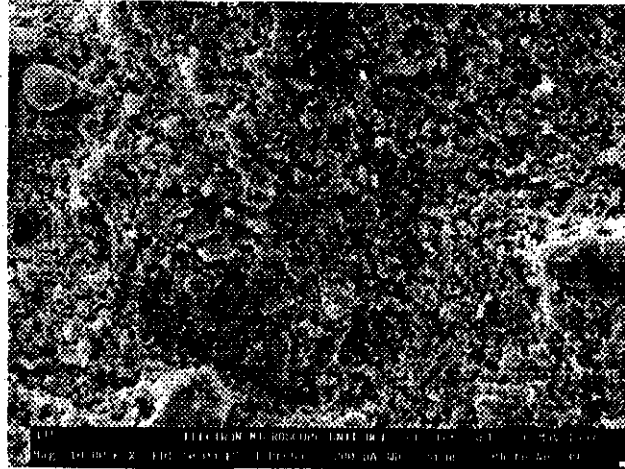


Figure 6.25: Top view of (f + heat)



Figure 6.26: Side view of (f)

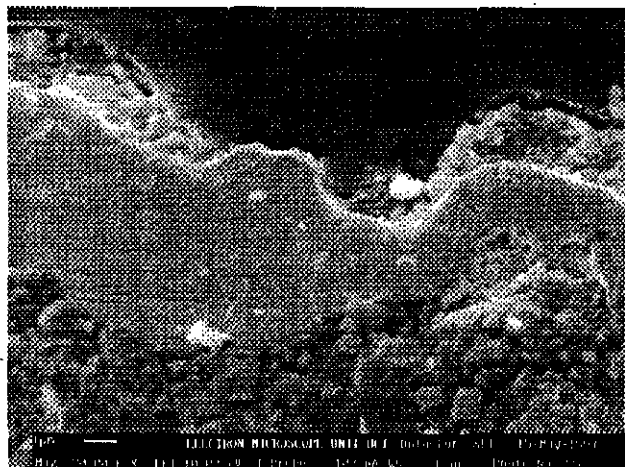


Figure 6.27: Side view of (f + heat)

6.10. Pd ON Ag COMPOSITE MEMBRANE (18:82) (j)

Element concentrations for a 18 wt% Ag, 82 wt% Pd film are given in Table 6.9:

Table 6.9: Ag-Pd (18:82) film composition before and after heating

| | Pd | Ag | Zr | Y | Sn | Zn | Hf | Pb | Hg |
|---------------|--------|--------|-------|-------|-------|--------|-------|-------|-------|
| j | 83.658 | 9.731 | 5.432 | 0.372 | 0.772 | 0.000 | 0.014 | 0.002 | 0.016 |
| j+heat | 66.531 | 12.293 | 6.008 | 0.409 | 0.942 | 13.578 | 0.034 | 0.179 | 0.000 |

The film was more than 99% pure prior to heat treatment. There was a remarkable increase in zinc content after heating. The reason for this phenomenon is not clear, since the alloying was done in a stainless steel 316 reactor, which is supposed to contain no zinc. The composition of stainless steel 316 is: 0.03 wt% C, 17 wt% Cr, 12 wt% Ni, 2 wt% Mn, 2.5 wt% Mo and the balance is iron (Callister, 1994). Furthermore, zinc melts at 420 °C, but vaporises at 907 °C. The maximum heating temperature used was 650 °C, which is considerably lower than the vaporising temperature. The use of a sweep gas would also prevent the deposition of possible zinc atoms by sweeping them away.

Top view SEM images were taken at 10 000 magnification and side view images at 20 000 magnification. After heating (**Figure 6.29**), a compact structure was formed with 1 micron pores in it. This compact structure is due to the presence of zinc, which formed an alloy with palladium. The Ag-Pd layer prior to heating (**Figure 6.30**) was dense with only a few nanometer size holes present in the cross section. After heating (**Figure 6.31**), the layer was even more dense, with no visible defects. The thickness increased due to the extra mass (zinc) deposited. It appears as if the film started to pull away from the substrate after temperature cycling. An air gap of a few nanometer is visible between the metal film and the ceramic substrate (**Figure 6.31**). This only happened with samples (j + heat) and (i + heat), which both had high zinc concentrations. Peeling can be explained by considering the thermal expansion coefficients in **Table 6.10**.

Pure palladium, pure nickel and palladium nickel composites have thermal expansion coefficients which do not differ much from alumina. When heating and cooling palladium or nickel coated ceramic membranes, the thermal stress is not very high and no film cracking was observed. By adding silver to the palladium matrix, the resultant thermal expansion coefficient is still sufficiently low to prevent cracking or peeling during temperature cycling, provided that the palladium concentration is higher than that of the silver. Zinc has a very high thermal expansion coefficient (**Table 6.10**) and by introducing it into the palladium matrix, the resultant coefficient is significantly increased. The difference in expansion coefficients for coatings containing zinc and the alumina based substrate exceeds a critical limit above which peeling starts occurring. Upon cooling, the metal coating with high zinc content, contracts faster than the support and the film is pulled away from the substrate.

Table 6.10: Thermal expansion coefficients

| Material | Thermal expansion coefficient (10^{-6} K^{-1}) |
|-----------|--|
| Palladium | 11.0 |
| Silver | 19.1 |
| Zinc | 31.0 |
| Nickel | 13.3 |
| Alumina | 8.8 |

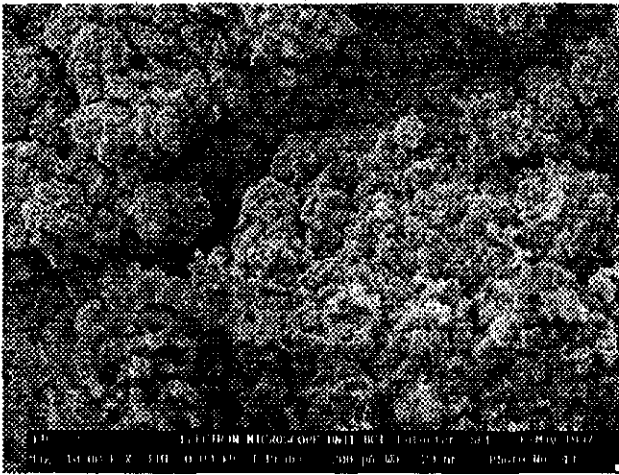


Figure 6.28: Top view of (j)

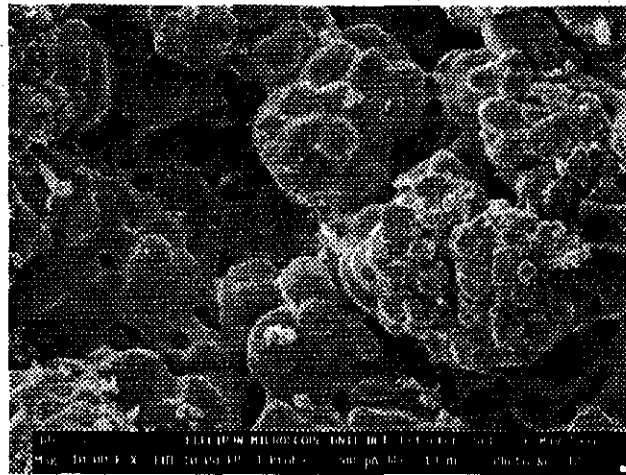


Figure 6.29: Top view of (j+ heat)

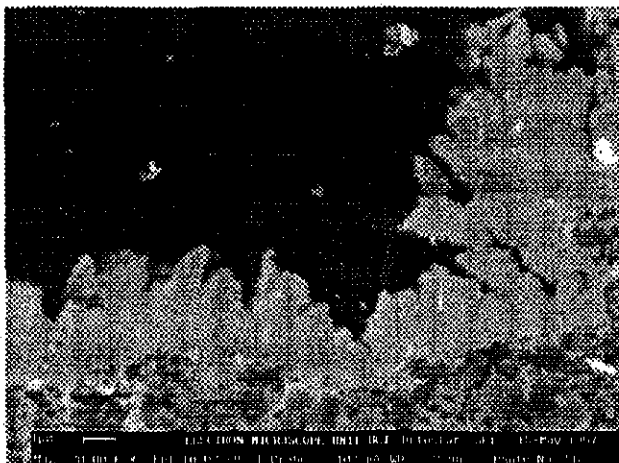


Figure 6.30: Side view of (j)

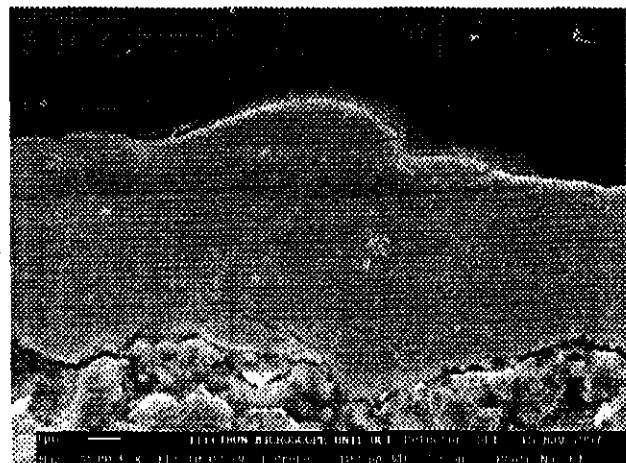


Figure 6.31: Side view of (j + heat)

6.11. Pd ON Ag COMPOSITE MEMBRANE (10:90) (i)

The composition of a 10 wt% Ag, 90 wt% Pd film is presented in Table 6.11:

Table 6.11: Ag-Pd (10:90) film composition before and after heating

| | Pd | Ag | Zr | Y | Sn | Zn | Hf | Pb | Hg |
|---------------|--------|-------|--------|-------|-------|--------|-------|-------|-------|
| i | 63.316 | 20.30 | 14.018 | 1.048 | 1.217 | 0.000 | 0.070 | 0.009 | 0.017 |
| i+heat | 72.508 | 8.822 | 4.191 | 0.292 | 1.026 | 13.031 | 0.017 | 0.096 | 0.000 |

The initial measured silver concentration in (i) is very high. This is unexpected, since theoretically only 10% silver (compared to palladium) was deposited and because silver formed the bottom layer with palladium the top layer. The zirconium concentration in (i) is also very high. After heating, both the measured silver and the zirconium concentrations dropped by more than 10%. The zinc concentration increased by 13%, similar to (j). The palladium concentration increased as well. Concentration profiles across the thickness of the film were determined with PIXE to investigate the metal diffusion processes properly.

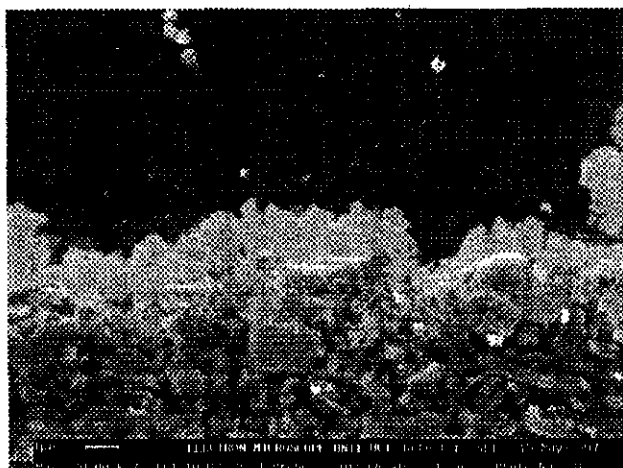


Figure 6.32: Side view of (i)

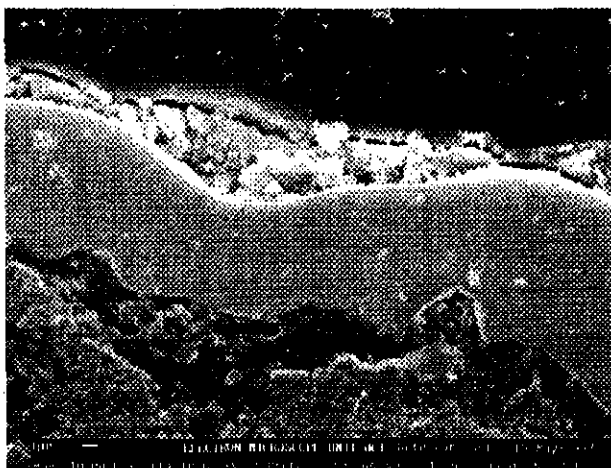


Figure 6.33: Side view of (i + heat)

SEM images of (i) are similar to (j) and are shown in Figures 6.32-6.33. The film thickness from the cross section view (Figure 6.32) before heating seems to be very thin compared to the theoretical value. The silver nuclei deposited on the membrane support cannot be distinguished, making a thickness estimate from the image difficult. As with (j + heat - Figure 6.31), the film is very dense after heating (Figure 6.33). At the top of the film an air

bubble formed during sample preparation and it was filled with sub-micron alumina particles used for polishing the resin disk in which the samples were set.

6.12. Ag-Pd-Ni COMPOSITE MEMBRANE (26.4:67.9:5.7) (g)

The surface composition of the Ag-Pd-Ni film is given in Table 6.12:

Table 6.12: Ag-Pd-Ni film composition before and after heating

| | Pd | Ag | Ni | Zr | Y | Sn | Zn | Hf | Pb | Hg |
|---------------|--------|--------|-------|-------|------|-------|-------|------|------|------|
| g | 65.663 | 19.218 | 3.289 | 10.42 | 0.77 | 0.499 | 0.02 | 0.01 | 0.01 | 0.02 |
| g+heat | 71.312 | 11.583 | 1.641 | 1.38 | 0.06 | 0.310 | 12.62 | 0.00 | 1.09 | 0.00 |

There is no apparent reason for the zinc presence after heating. This phenomenon should be investigated further, since most work with catalytic membranes is performed in stainless steel reactors at high temperatures. All samples discussed in this chapter were placed in the centre of the reactor and were heated at the same time. Five samples have less than 0.5% Zn, one has 1.35% Zn and three have more than 10% Zn. There is no logical explanation why zinc was deposited to such an extent in the three samples.

SEM images of the Ag-Pd-Ni composite are shown in Figures 6.34-6.37. There is a remarkable difference between the top views before and after heat treatment (Figures 6.34 and 6.35). By enlarging Figure 6.34 (more than 10 times), two crystal sizes can be distinguished. The much smaller nickel crystals are deposited on the larger palladium nuclei. During heat treatment, the nickel nuclei agglomerate with surrounding palladium crystals to form a smooth, dense top layer consisting of palladium, silver and nickel. The resulting film shows no defects as was the case with (d+heat). The composite appears completely non-porous and allows for thinner defect free membranes to be made. Not only is this much cheaper, but higher hydrogen fluxes ought to be obtained.

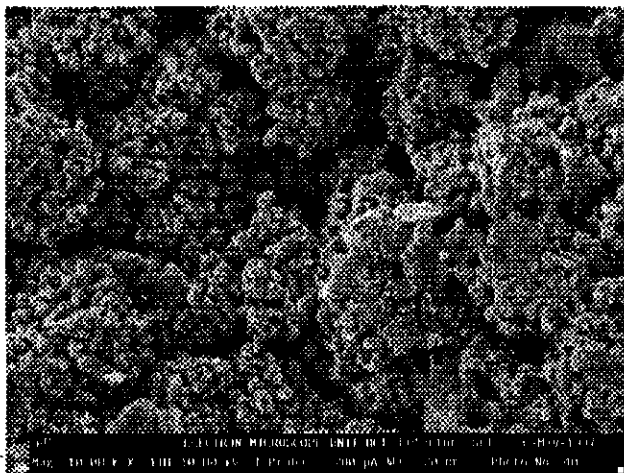


Figure 6.34: Top view of (g)

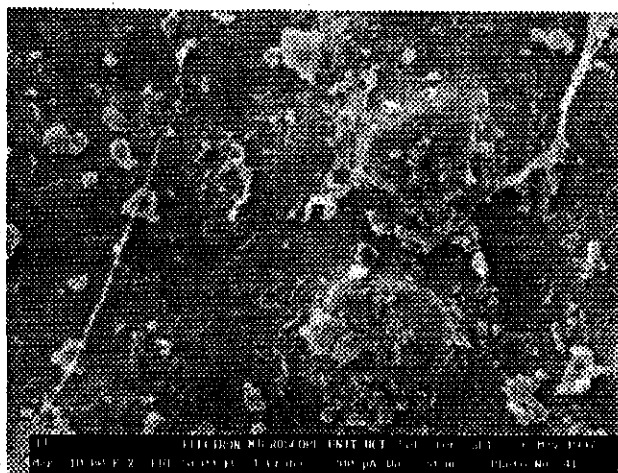


Figure 6.35: Top view of (g + heat)

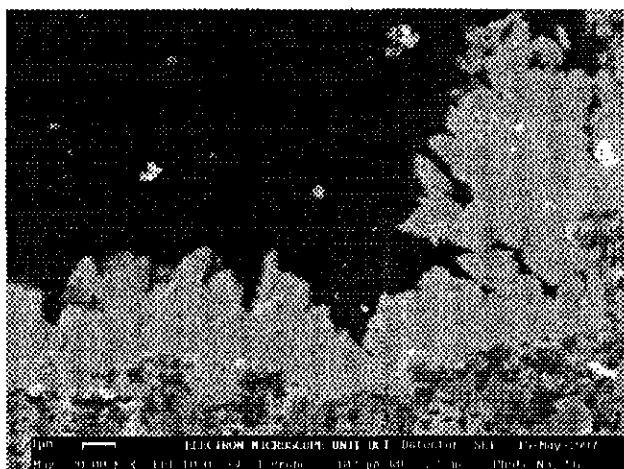


Figure 6.36: Side view of (g)

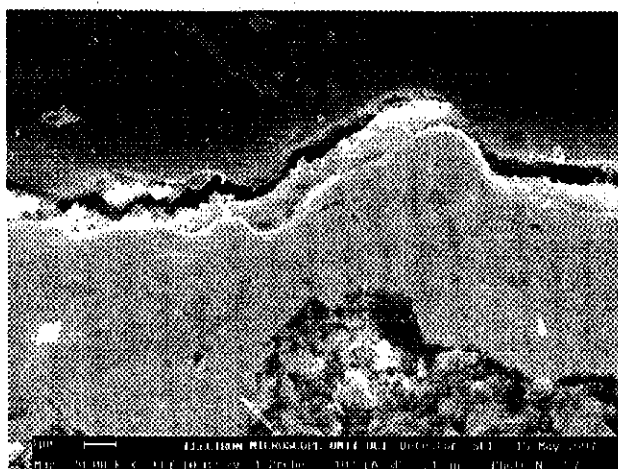


Figure 6.37: Side view of (g + heat)

6.13. SUMMARY

A number of conclusions can be drawn from the SEM and PIXE analyses done on the metal films:

- The palladium deposit was about 99.75% pure with main impurities being tin deposited in the pretreatment step, 700 ppm silver and 100 ppm mercury and 100 ppm lead.
- The silver film was about 99.5% pure with tin (0.49%) and 250 ppm iron the main impurities.
- The nickel deposit was 97% pure. High tin (1.6%), cobalt (0.9%) and iron (0.3%) concentrations were found in the nickel film. There was also about 0.18% copper found.
- The palladium deposit was columnlike, but formed a continuous dense layer covering the entire substrate surface. The silver deposit was non-homogeneous and clusters were

deposited randomly over the palladium film or the activated substrate. No even thickness layer was formed. The nickel deposit was very dense and the plated surface smooth. The layer had an even thickness according to the side view and appeared defect free.

- High zinc concentrations were found in three of the silver-palladium composite membranes after heating. There is no logical explanation for this, since the heating was done well below the vaporising temperature of zinc and in a stainless steel 316 reactor which contains no zinc. The presence of zinc resulted in a high density, compact film with an unique topography and crystal structure.
- The addition of low nickel percentages (3-5%) allows for a novel way to prepare thinner electroless plated palladium membranes. A dense top layer is formed after alloying, when a thin nickel layer is deposited on the palladium film.

CHAPTER 7

STRUCTURAL CHARACTERISATION USING XRD

7.1. INTRODUCTION

In **CHAPTER 6** unique morphologies were obtained by heat treating silver-palladium and silver-palladium-nickel membranes. To gain more insight into this smoothing of membranes, which offer the possibility of ultrathin defect free layers, XRD is to be used in this chapter. The tubular shape of the coated membranes reduced the effectiveness of the X-ray scan, since scanning could only be done on a line instead of a flat rectangular plane. The number of counts was generally low, but still sufficient to make positive identifications of each sample analysed with XRD. The purity of the palladium, silver and nickel coatings were determined by comparing XRD patterns of coatings with that of pure metals. The structure of the palladium, silver and nickel composites were also determined.

7.2. PALLADIUM COATED MEMBRANE (a)

The 1996 X-ray Powder Diffraction File (PDF) published by the Joint Committee on Powder Diffraction Standards (JCPDS) was used for crystal structure identification. PDF is a database containing over 60 000 materials and is updated annually. All the data in this chapter were analysed with the computer package DIFFTECH. K- α stripping was done as well as background smoothing for noisy data.

Palladium has a face centred cubic structure (fcc) and the XRD pattern obtained for the palladium coated membrane is shown in **Figure 7.1**. In **Table 7.1** the crystal structure parameters of pure palladium (PDF_46-1043) are compared to experimentally obtained data. It is clear that the palladium deposit is very pure, which correlates well with PIXE data.

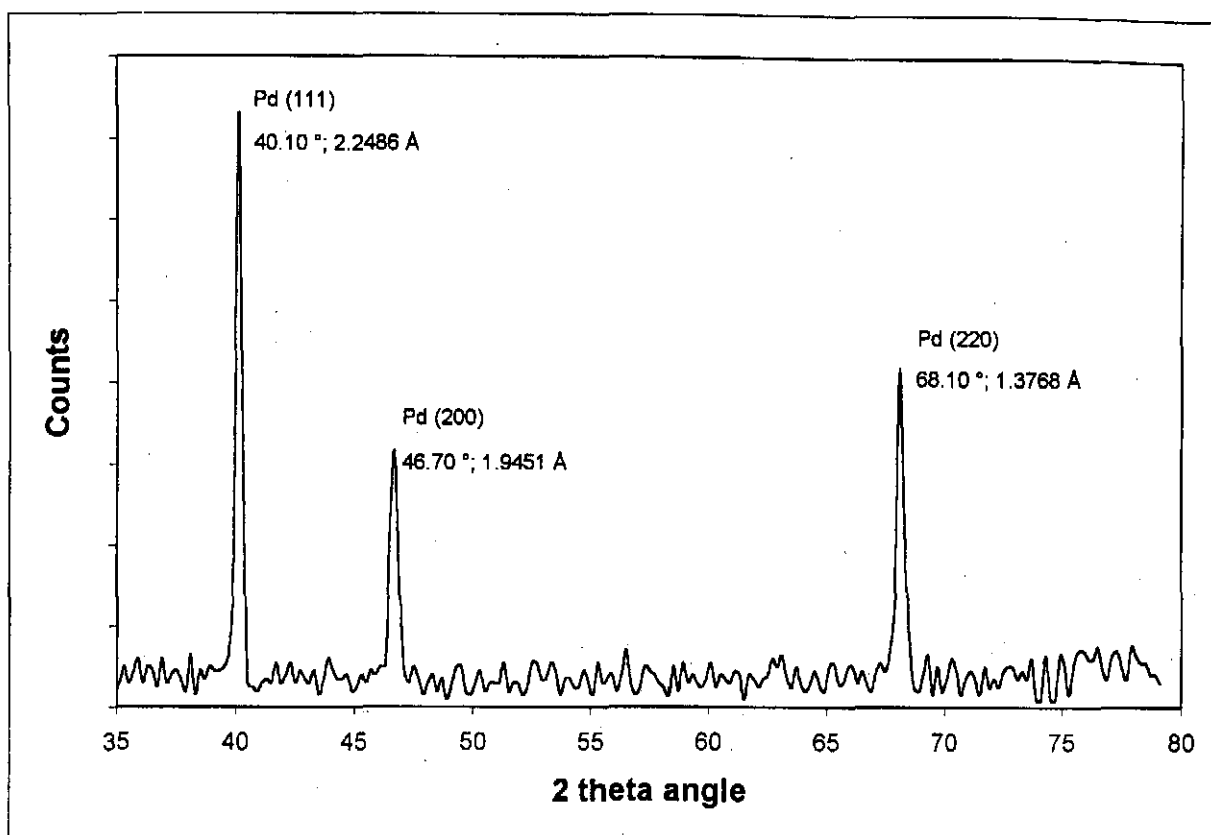


Figure 7.1: XRD pattern for a pure palladium film (a)

Table 7.1: Structural data for the palladium deposit

| | | | | PDF data | | Experimental data | |
|-----------|---|---|---|------------|--------|-------------------|--------|
| Intensity | h | k | l | 2 θ | d Å | 2 θ | d Å |
| 100 | 1 | 1 | 1 | 40.119 | 2.2458 | 40.10 | 2.2486 |
| 60 | 2 | 0 | 0 | 46.659 | 1.9451 | 46.70 | 1.9451 |
| 42 | 2 | 2 | 0 | 68.121 | 1.3754 | 68.10 | 1.3768 |
| 55 | 3 | 1 | 1 | 82.100 | 1.1730 | - | - |

The intensity is a relative measure of the amount of X-rays diffracted for a certain hkl configuration. Only the first four of a possible eight configurations are shown in **Table 7.1**. The others have peaks above 82°. The sensitivity of the diffractometer was 0.1 degrees and the palladium spectrum was taken from 35° to 80°, with the result that the final peak in **Table 7.1** was not experimentally detected.

7.3. SILVER COATED MEMBRANE (b)

X-ray diffraction is used for surface analysis only, and unlike with PIXE, there is very little penetration into the metal film. Although PIXE detected high concentrations of zirconium for a top view point analysis, no zirconium oxide or aluminum oxide peaks are visible on **Figure 7.2**. A high purity, deposited silver film is conferred by PDF data in **Table 7.2**.

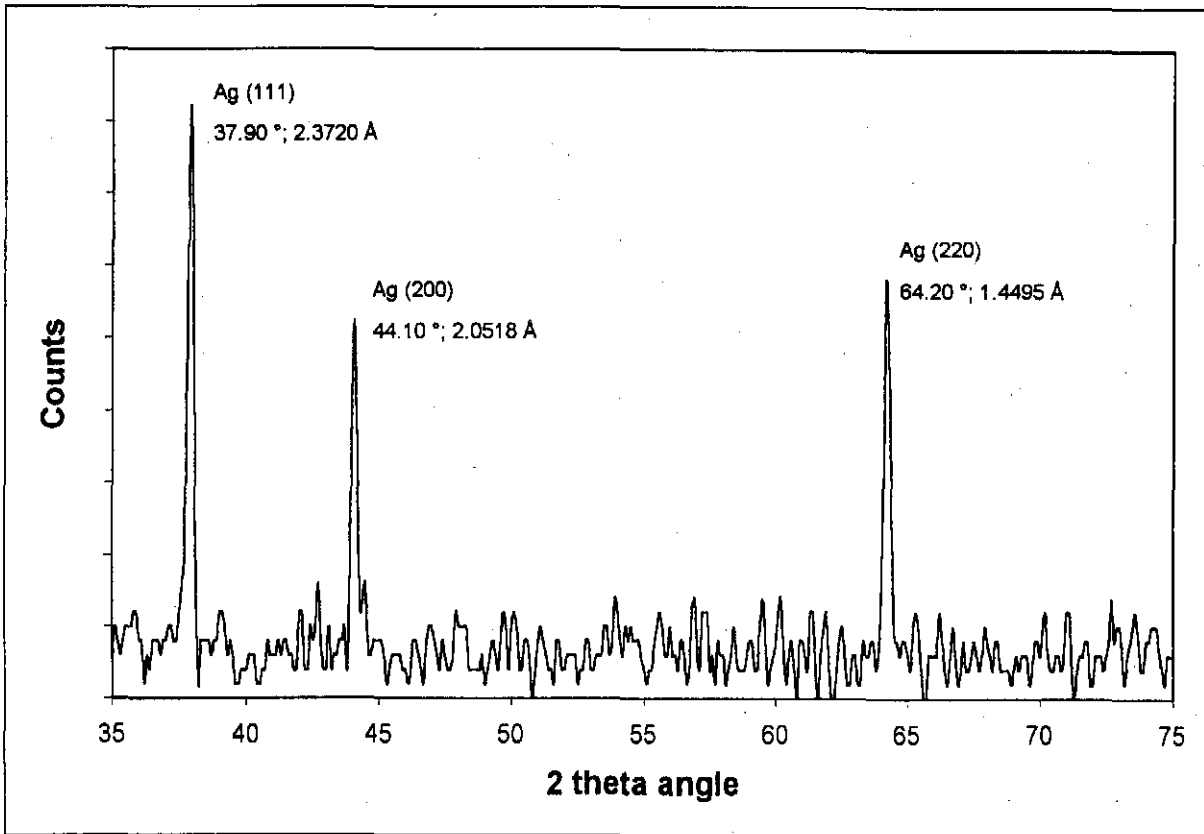


Figure 7.2: XRD pattern for a pure silver film (b)

Table 7.2: Structural data for the silver deposit

| | | | | PDF data | | Experimental data | |
|-----------|---|---|---|----------|--------|-------------------|--------|
| Intensity | h | k | l | 2 θ | d Å | 2 θ | d Å |
| 100 | 1 | 1 | 1 | 38.116 | 2.3590 | 37.90 | 2.3720 |
| 40 | 2 | 0 | 0 | 44.277 | 2.0440 | 44.10 | 2.0518 |
| 25 | 2 | 2 | 0 | 64.426 | 1.4450 | 64.20 | 1.4495 |
| 26 | 3 | 1 | 1 | 77.472 | 1.2310 | - | - |

Silver is deposited in the fcc structural form (PDF_04-0783) and the crystal structure is identical to that of palladium. Palladium and silver have eight similar hkl crystal plane configurations. Silver has slightly larger atoms than palladium (1.44 Å Goldschmidt atomic radius compared to 1.37 Å for palladium) and thus larger d-spacings between atoms or peaks at lower 2θ angles.

There was a shift of about 0.2° in the 2θ angle between pure silver (PDF data) and the electroless plated silver film. The percentage deviation is very small and can be contributed to instrument insensitivity rather than layer impurity.

7.4. NICKEL COATED MEMBRANE (c)

Nickel has more than one possible crystal structure. The deposited nickel has a cubic (fcc) structure (PDF_04-0850) and not the hexagonal structure. The eight hkl planar configurations of nickel and palladium are identical. Unlike with silver, nickel has smaller atoms than palladium (1.25 Å Goldschmidt atomic radius compared to 1.37 Å for palladium) and thus smaller d-spacings between atoms or peaks at higher 2θ angles.

Table 7.3: Structural data for the nickel deposit

| | | | | PDF data | | Experimental data | |
|-----------|---|---|---|-----------|--------|-------------------|--------|
| Intensity | h | k | l | 2θ | d Å | 2θ | d Å |
| 100 | 1 | 1 | 1 | 44.505 | 2.0340 | 44.20 | 2.0474 |
| 42 | 2 | 0 | 0 | 51.644 | 1.7620 | 51.60 | 1.7698 |
| 21 | 2 | 2 | 0 | 76.366 | 1.2460 | 76.10 | 1.2497 |

Experimental data suggests that there are some impurities in the crystal structure of nickel, since there is no systematic drift in the data, which might be contributed to the apparatus. The centre peak corresponds well with PDF data, but the peaks on the left and right hand side of **Figure 7.3** deviate by about 0.3° from pure nickel.

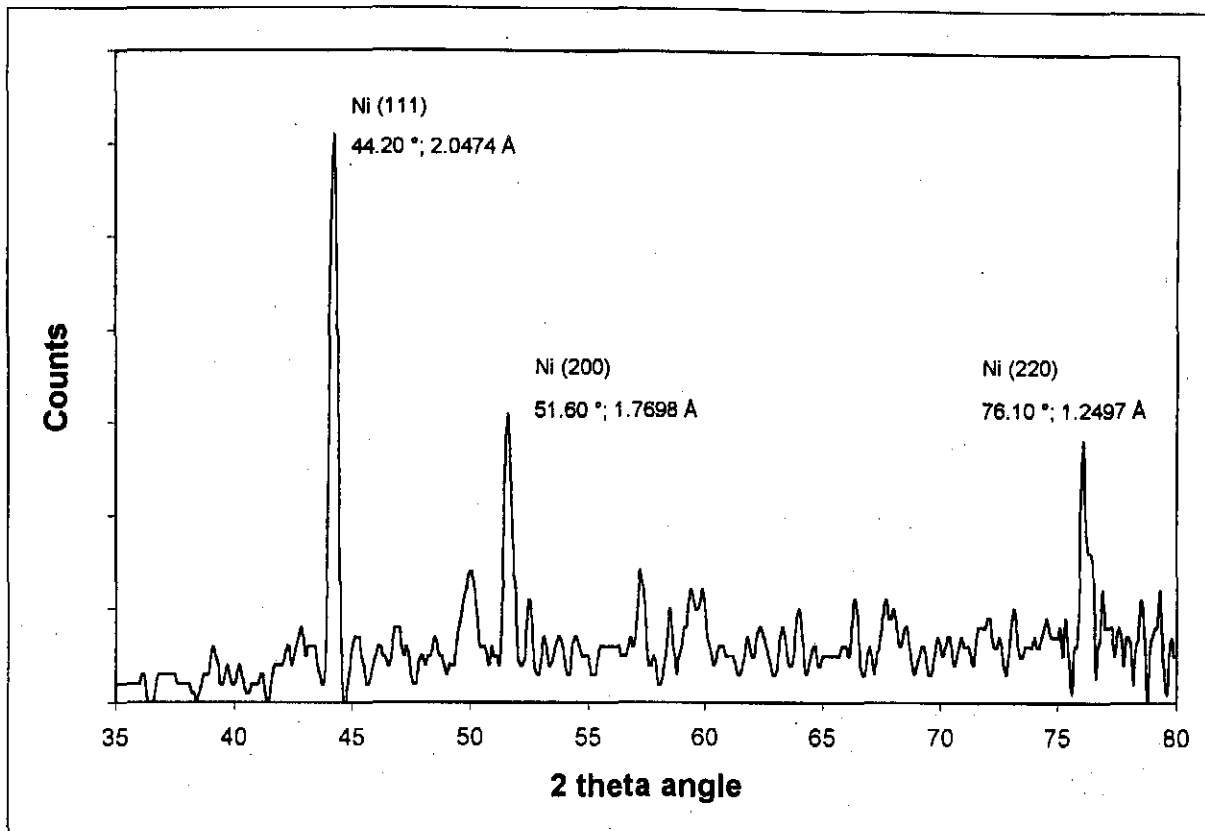
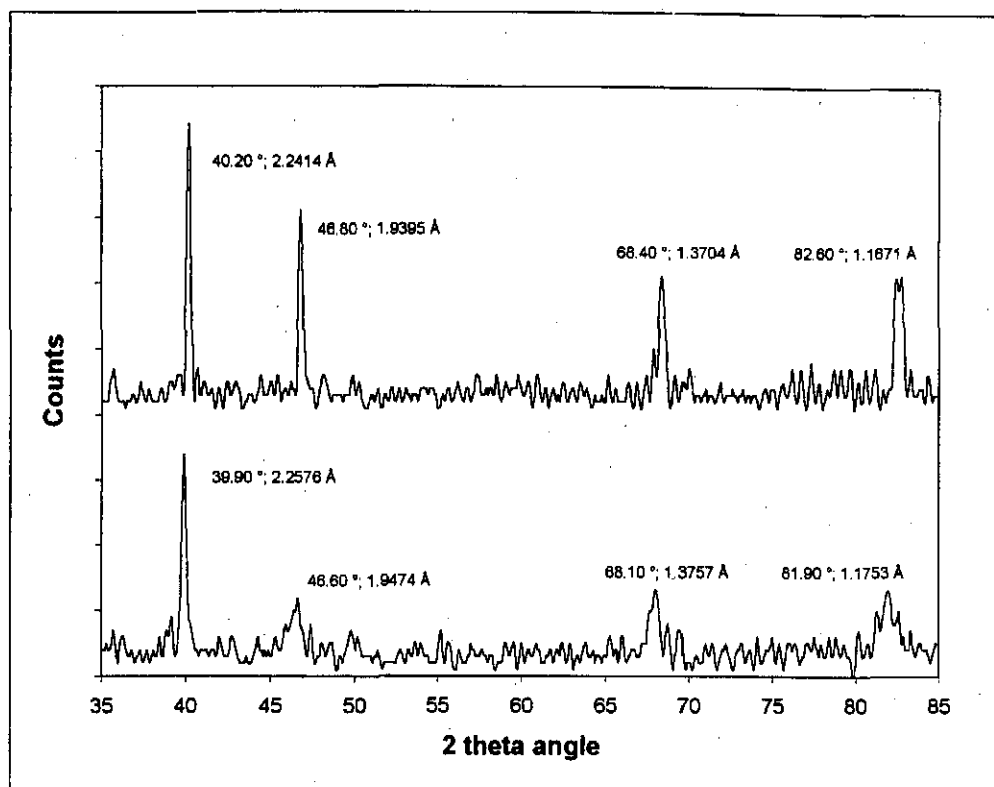


Figure 7.3: XRD pattern for a pure nickel film (c)

7.5. PALLADIUM-NICKEL COATED MEMBRANE (d)

XRD patterns before and after heat treatment are compared to detect changes in the crystal structure. Before heat treatment (bottom graph on **Figure 7.4**), the peaks are broad with peak values similar to that of pure palladium. Separate nickel peaks are not detected due to the small amount of nickel deposited on the palladium. Peak broadening occurs as a result of the nickel deposit. After heat treatment, the peaks (top graph) shifted to slightly higher 2θ values, showing nickel alloying with palladium. The values are still close to that of pure palladium, indicating that the palladium concentration is significantly higher than that of nickel. A new crystal structure is not formed, but a solid solution of nickel atoms dispersed in the palladium matrix. This is in agreement with the equilibrium diagram of the binary Ni-Pd system (Smithells, 1992).

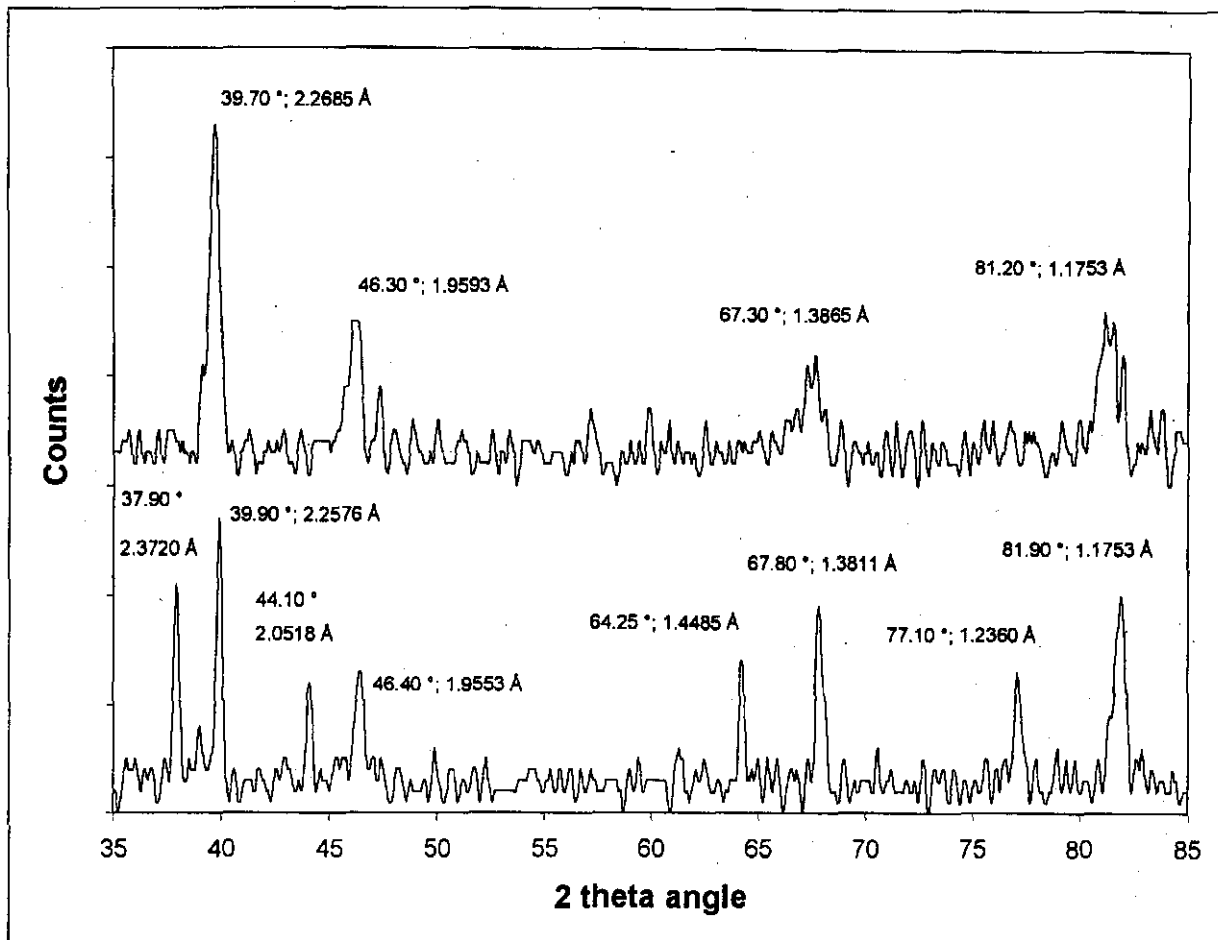


top = after heating; bottom = before heating

Figure 7.4: XRD patterns for a Pd-Ni film (d)

7.6. PALLADIUM-SILVER COATED MEMBRANE (e)

Separate peaks for palladium and silver were detected before heating (Figure 7.5). This confirms that the silver deposit on the palladium was non-continuous so that it did not cover the entire area scanned by the X-rays. During heating, the structure changed to one resembling palladium. A solid solution was formed (Smithells, 1992; Ag-Pd equilibrium diagram). The crystal structure remained similar to that of pure palladium. The (111), (200), (220) and (311) peaks of the fcc matrix of silver and palladium atoms are shown from left to right in Figure 7.5 (top graph). Palladium constituted the highest surface concentration. Peak broadening resulted from a variation in the surface concentrations of palladium and silver.



top = after heating; bottom = before heating

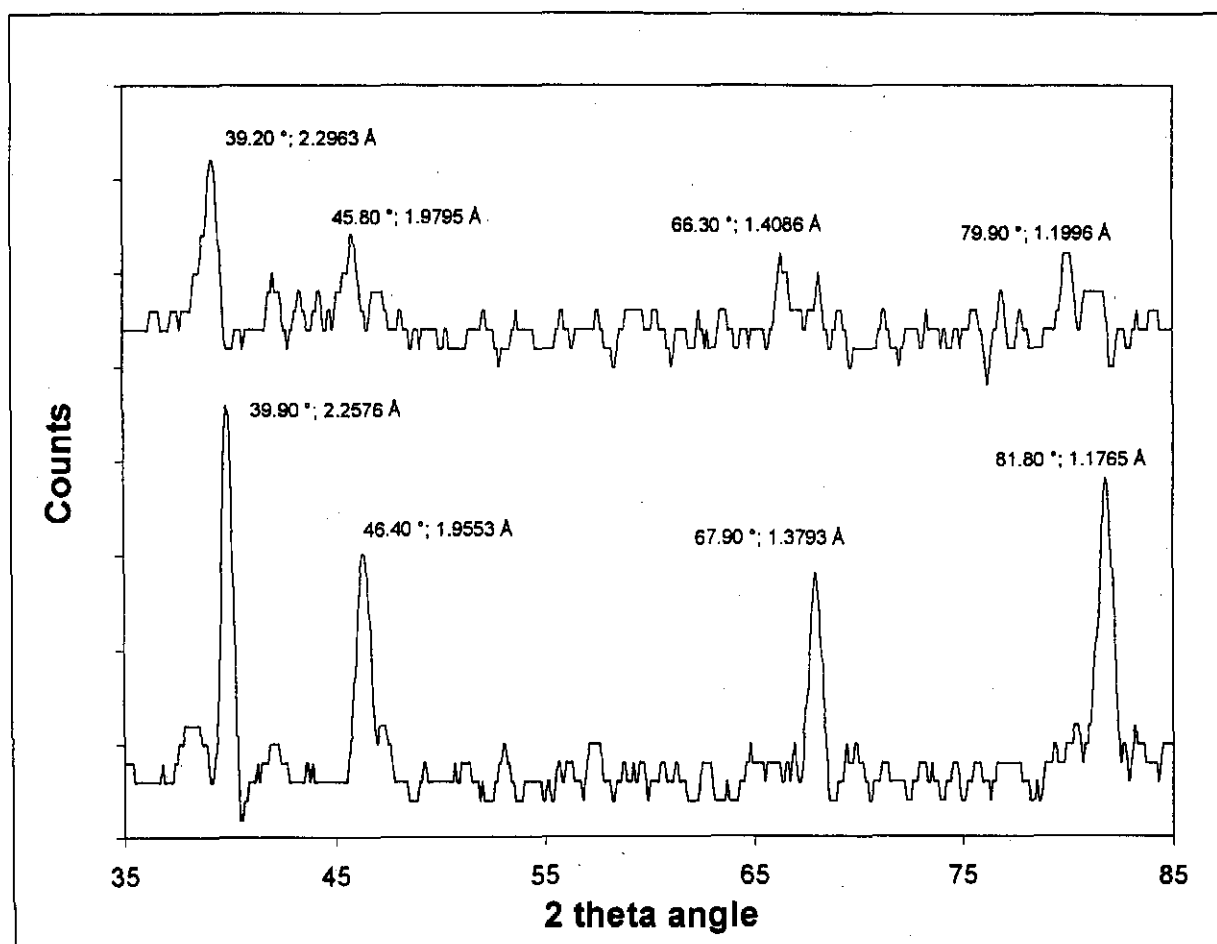
Figure 7.5: XRD patterns for a Ag on Pd film (e)

7.7. SILVER-PALLADIUM (24:76) COATED MEMBRANE (f)

The X-rays in a diffractometer scans over a flat plane, with the result that the scanning area available for a tubular membrane is small (only on a line). Less counts are detected and poor statistics obtained. The number of counts for sample (f) was not very high, but some conclusions can still be drawn. Before heating, only the palladium was detected (Figure 7.6; bottom), since palladium formed a dense continuous top layer. During heating, silver diffused into the palladium layer, with the result that the alloy peaks shifted towards the lower 2θ angles of silver. The crystal structure parameter changes are listed in Table 7.4.

Table 7.4: XRD data before and after heating Ag-Pd (24:76)

| Planes | | | Before heating | | After heating | |
|--------|---|---|----------------|--------|---------------|--------|
| h | k | l | 2θ | d Å | 2θ | d Å |
| 1 | 1 | 1 | 39.90 | 2.2576 | 39.20 | 2.2963 |
| 2 | 0 | 0 | 46.40 | 1.9553 | 45.80 | 1.9795 |
| 2 | 2 | 0 | 67.90 | 1.3793 | 66.30 | 1.4086 |
| 3 | 1 | 1 | 81.80 | 1.1765 | 79.90 | 1.1996 |

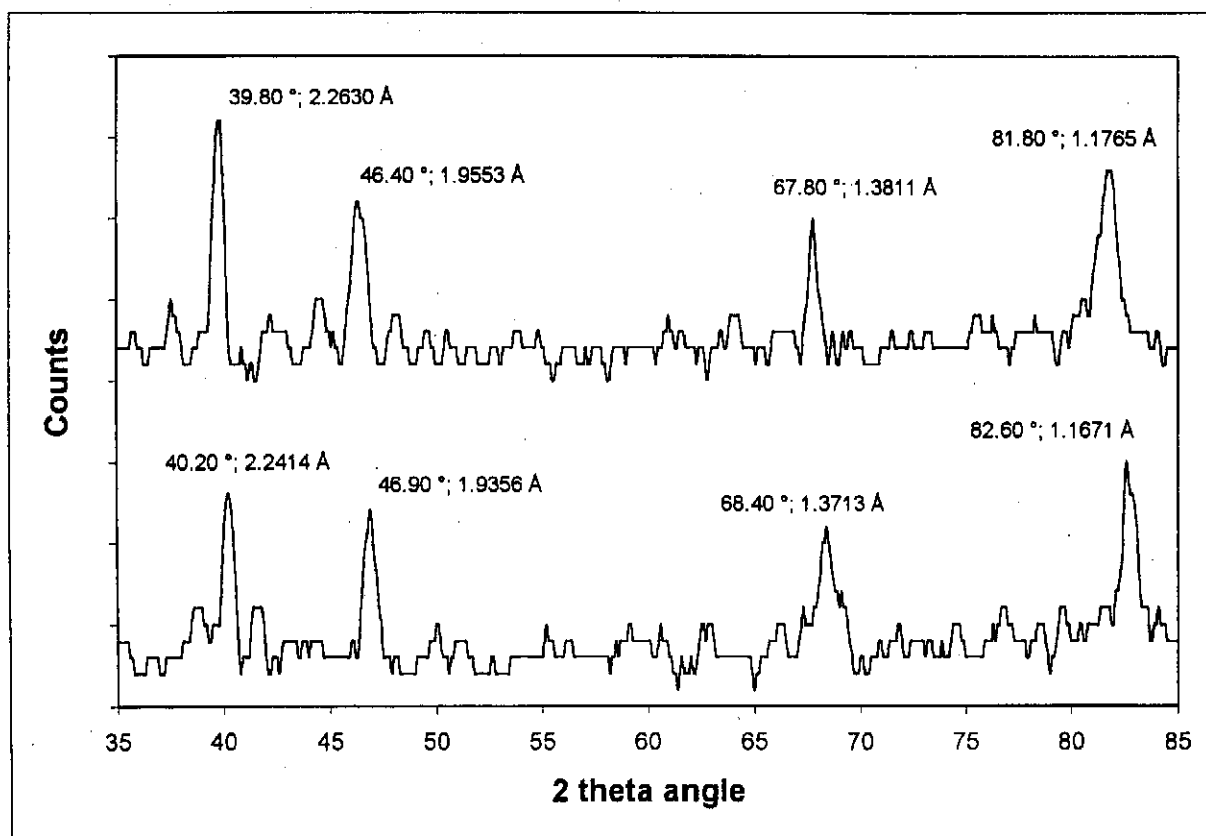


top = after heating; bottom = before heating

Figure 7.6: XRD patterns for a Ag-Pd (24:76) film (f)

7.8. SILVER-PALLADIUM-NICKEL COATED MEMBRANE (g)

PIXE data showed that this sample had a high zinc concentration after heating. No significant changes in the crystal structure were detected after heating (Figure 7.7). The structural changes after heating were similar to those discussed in Section 7.7, where alloy peaks were formed. The structure is that of a solid solution. Palladium, silver and nickel atoms are randomly distributed in the alloy matrix. The alloy has a face centred cubic structure.



top = after heating; bottom = before heating

Figure 7.7: XRD patterns for a Ag-Pd-Ni film (g)

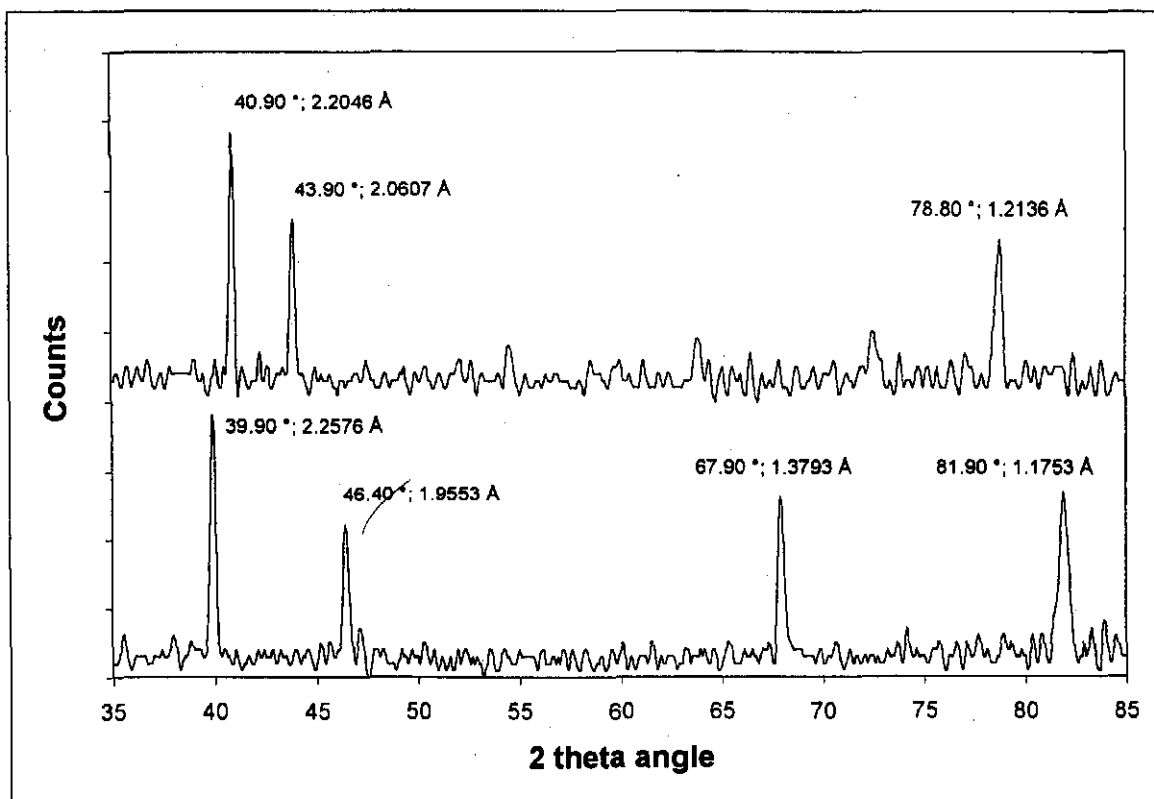
7.9. SILVER-PALLADIUM COATED MEMBRANES

PIXE detected high zinc concentrations in these two samples (Tables 6.9 and 6.11) after heating. Pure zinc has a closed pack hexagonal structure and palladium has a face centred cubic structure. Only the palladium structure was observed before heating (Figures 7.8 and

7.9 bottom). After heating, a completely new structure was formed (Figures 7.8 and 7.9 top; see also Figure 6.29).

Table 7.5: XRD data for Ag-Pd coated membranes (samples i and j) after heating

| Intensit y | h | k | l | PDF data | | i + heat | | j + heat | |
|---------------|---|---|---|----------|--------|----------|--------|----------|--------|
| | | | | 2θ | d Å | 2θ | d Å | 2θ | d Å |
| 100 | 1 | 1 | 1 | 41.222 | 2.1900 | 40.90 | 2.2046 | 41.00 | 2.1995 |
| 100 | 2 | 0 | 0 | 44.180 | 2.0500 | 43.90 | 2.0607 | 43.95 | 2.0582 |
| 30 | 0 | 0 | 2 | 54.454 | 1.6850 | | | 54.60 | 1.6795 |
| 50 | 1 | 1 | 2 | 64.286 | 1.4490 | | | | |
| 50 | 3 | 1 | 0 | 72.743 | 1.3000 | | | 72.70 | 1.2996 |
| 80 | 3 | 1 | 1 | 79.319 | 1.2080 | 78.80 | 1.2136 | 78.95 | 1.2116 |

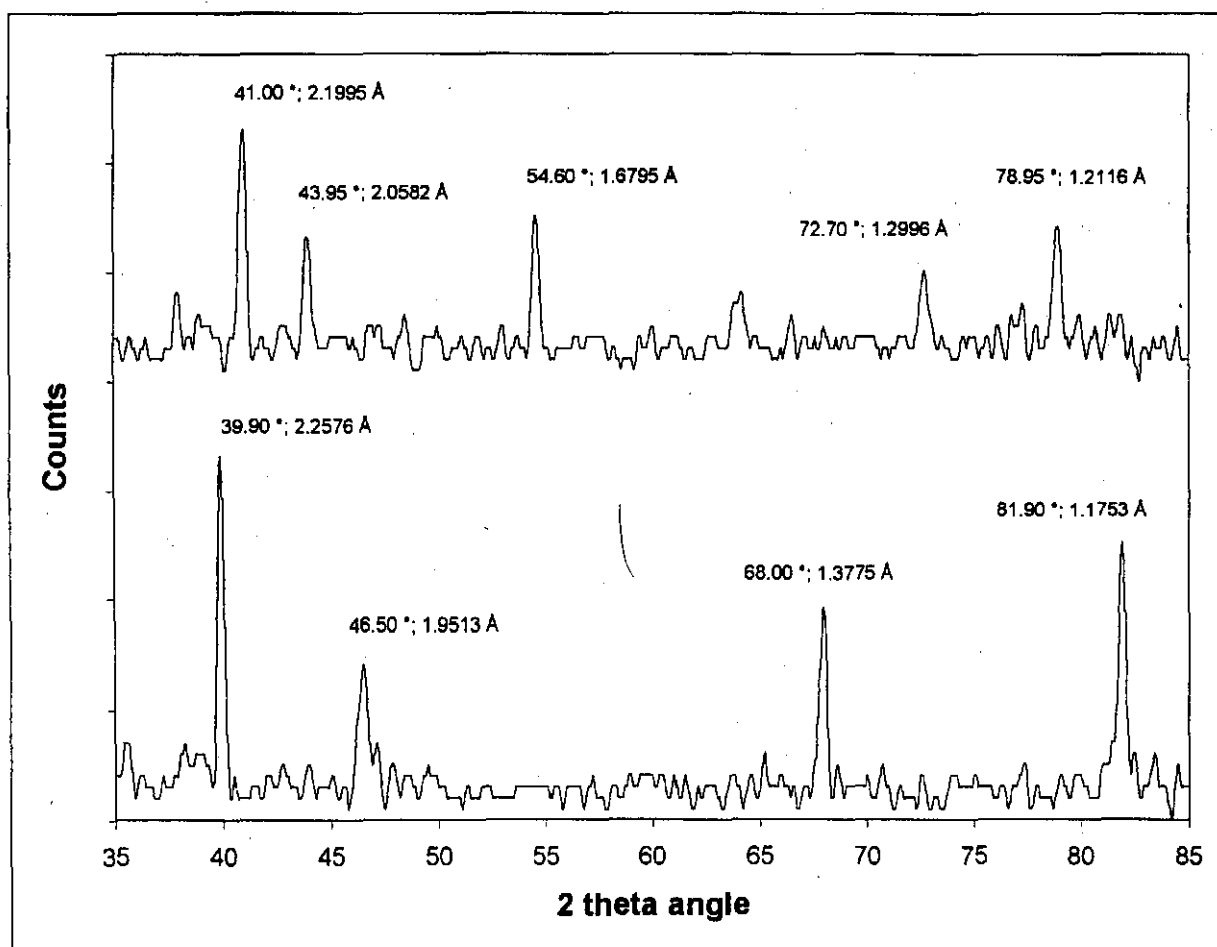


top = after heating; bottom = before heating

Figure 7.8: XRD patterns for a Ag-Pd (10:90) film (i)

PDF confirmed the formation of a tetragonal PdZn crystal structure. Crystal structure parameters for pure PdZn (PDF_06-0620) and values obtained from the X-ray analyses of samples (j) and (i) are compared in Table 7.5. There is a good correlation, especially for the lower 2θ angles. The binary phase diagram for Pd-Zn can be found in Smithells, 1992.

Empty spaces in Table 7.5 are due to insufficient statistics (low counts). From Figures 7.8 and 7.9 it can be seen that small peaks are present where empty spaces occur in Table 7.5.



top = after heating; bottom = before heating

Figure 7.9: XRD patterns for a Ag-Pd (18:82) film (j)

7.10. SUMMARY

The following conclusions can be drawn from XRD analysis:

- The XRD patterns for palladium and silver deposits were similar to those of pure palladium and pure silver. The deposits were very pure which correlate well with PIXE data. With the nickel deposit, peak shifts of about 0.3° (2θ angle) were observed which indicate a low percentage of impurities.
- For a palladium-nickel deposit, the XRD pattern after heating was similar to that of pure palladium, indicating that a solid solution formed with very little nickel (in the order of 1 or 2 percent). Peaks were shifted slightly away from those of pure palladium towards those of pure nickel.
- For silver-palladium deposits, a new set of alloy peaks, with a face centred cubic structure, formed after heating. This structure was similar to both palladium and silver structures, but the 2θ angles were between the values of palladium and silver. The palladium:silver ratio determines the position of the peaks. If the palladium concentration is higher than the silver concentration, the peaks will be closer to the values of pure palladium. The palladium-silver alloy formed a solid solution.
- A new crystal structure was formed for samples (i+heat and j+heat). The structure was identified (with the PDF database) as tetragonal PdZn.
- The two very different structures (**Figures 6.25** and **6.29**) which formed after heating silver-palladium deposits, were positively identified with XRD. **Figure 6.25** is a solid solution (fcc) of palladium and silver, while **Figure 6.29** is tetragonal PdZn.

CHAPTER 8

METAL DIFFUSION

8.1. INTRODUCTION

PIXE was used to construct concentration profiles across the thickness of the film. The degree of silver and nickel diffusion into the palladium layer was investigated as well as the effect of deposition order on concentration profiles. Line scans with point analyses at 0.5 micron intervals were used to obtain the profiles. For most samples, the total scan depth was 8 microns. This allowed for an analysis of 3-4 microns into the support. The depth to which the electroless plated coatings penetrated into the pores of the support membrane was determined. PIXE and EDX were used to create cross section maps of the coatings. The diffusion process was visually examined by taking maps of the main matrix elements before and after heat treatment.

8.2. DATA PROCESSING

The computer program, Gupix96, was used for data processing. This program was developed by Dr. Maxwell and co-workers at the Physics Department of the University of Guelph in Canada.

A line scan across the thickness of each film after heating was performed to determine the degree of metal diffusion and the concentration profiles of the main matrix elements across the film. The line scan consisted of point analyses at 0.5 micron intervals with a sub-micron proton beam. The PIXE spectra were first examined to determine the elements present in a sample. An energy calibration was done for each line scan. The energies of palladium (21.123 keV) and yttrium (14.933 keV) at their corresponding channel positions were used as a standard. Once the elements were identified and energies calibrated, matrix calculations could be done. The settings used for matrix calculation in Gupix96 are as follows:

Main parameters:

| | |
|---|----------------|
| α beam target: | 90 ° |
| θ target detector: | 45 ° |
| incident proton energy: | 2000; 3000 keV |
| maximum number of layers: | 5 |
| depth fraction, density, thickness, exit proton energy: | 0 |
| target: | thick |

Matrix elements (initial values):

| | |
|-----|-------|
| A1: | -2 |
| A2: | 27.81 |
| A3: | 0 |
| A4: | 0.01 |
| A5: | 0.356 |

Detector and peak shape parameters:

| | |
|---|---------------------------|
| Detector: | 4 (New link uncollimated) |
| Be: | 0.0008 cm |
| Au: | 0.000001 cm |
| detector crystal: | 0.48 cm |
| target to detector crystal: | 4.8 cm |
| detector resolution: | 165 eV |
| window: | 47914 |
| default values were used for all other parameters | |

Filters:

| | |
|----------|------------|
| 13,40,0 | (Aluminum) |
| 100,25,0 | (Mylar) |

No layer thickness iteration; No invisible elements and no background edge were used.

The charge varied from sample to sample and the value of H was taken as 0.025. The element concentrations determined at each point were normalised.

8.3. HEAT TREATMENT

The melting points for palladium, silver and nickel are 1554 °C, 962 °C and 1455 °C, respectively. This corresponds to Tamman temperatures of 777 °C, 481 °C and 728 °C. Above their Tamman temperatures, the atoms of silver and nickel will have sufficient energy to vibrate and migrate into the palladium lattice.

Heat treatment was performed at 650 °C for 5 hours (Shu et al., 1996, used 500, 600 and 650 °C). This allowed both nickel and silver atoms to diffuse into the palladium matrix, even though the temperature was lower than the Tamman temperature of nickel. The nickel atoms had enough vibration energy to diffuse into the palladium structure. Heat treatment was done in a hydrogen atmosphere to prevent oxidation.

8.4. CONCENTRATION PROFILES FOR Pd-Ni (d + heat)

The processed data is listed in APPENDIX E. Figures 8.1 and 8.2 show the concentration profiles of palladium and nickel.

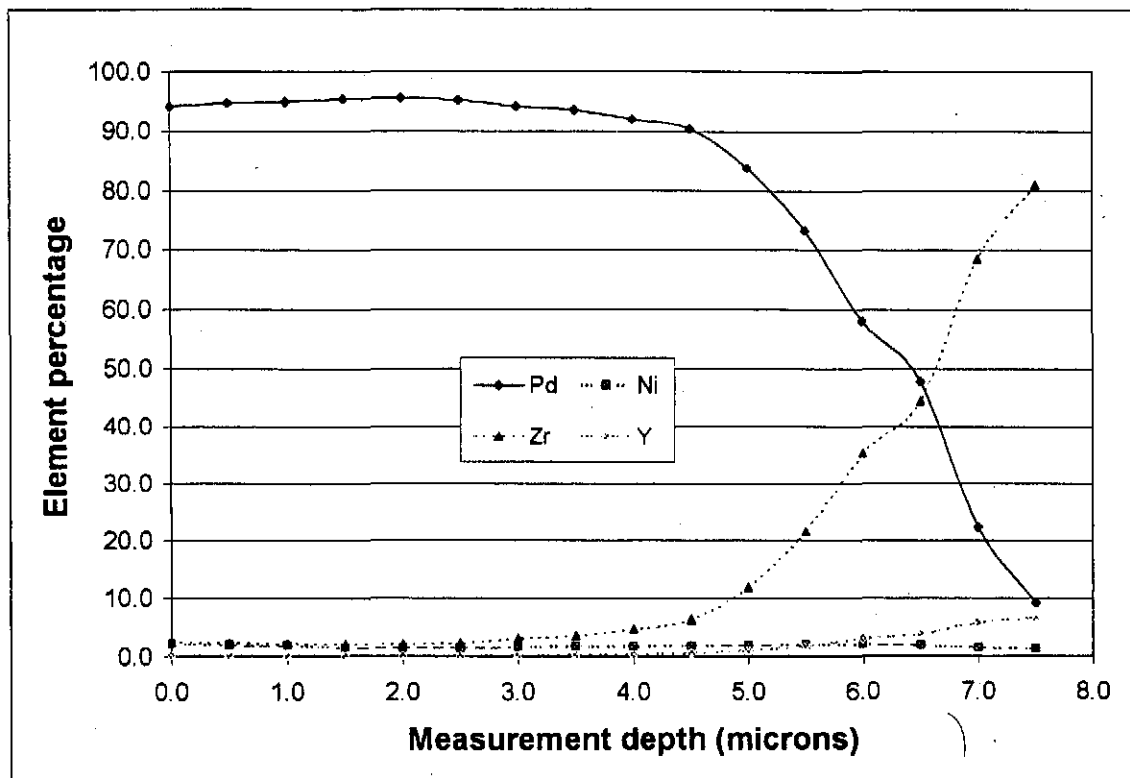


Figure 8.1: Concentration profiles for Pd+Ni (98:2) after heating

Figure 8.1 can be used to determine the film thickness and to see whether there was penetration into the substrate pores. The gradual decline in palladium concentration, after a 4.5 micron depth, confirms the penetration of palladium nuclei into the alumina-zirconia support. The palladium concentration drops to below 10% once it has entered more than 3 microns into the support. Palladium nuclei are strongly anchored inside the membrane pores, which explains the extremely good adhesion between the palladium-nickel film and the ceramic substrate.

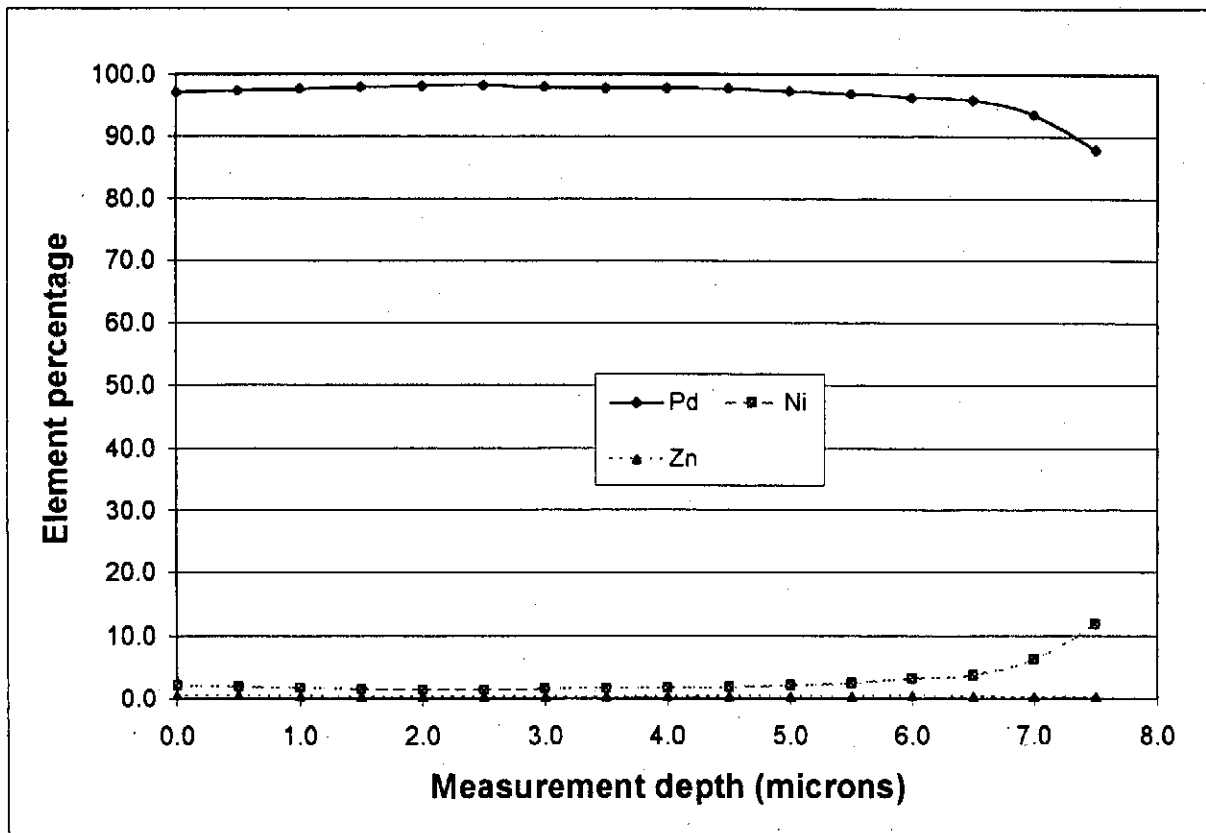


Figure 8.2: Ratio between Pd and Ni (98:2) across the film after heating

The film thickness, according to Figure 8.1, correlates well with the theoretically calculated thickness of 4.5 micron. The theoretical value assumed no penetration and a constant density across the film. Figure 8.2 indicates the ratio between palladium, nickel and zinc. The zinc concentration remained very low for the thickness of the film. For the entire thickness of the film (4.5 microns) the palladium-nickel ratio remained constant, which indicates good nickel diffusion into the palladium matrix and a proper nickel distribution. The nickel did not only

form a dense top layer after heating (**Figure 6.17**), but it also penetrated into pores and defects inside the palladium structure. The palladium to nickel ratio declines after a depth of 6 microns (inside membrane pores). The nickel, with its smaller atoms (1.25 Å atomic radius compared to palladium with an atomic radius of 1.37 Å; Smithells, 1992) can enter membrane pores more easily and therefore nickel becomes more concentrated deeper in the support.

On average, the nickel content across the film, according to the line scan, was about 2% relative to 98% palladium. Mass measurements reported 5.4% nickel and a top view point analysis with PIXE just more than one percent (relative to palladium). The most accurate composition can be obtained with a line scan, since it gives an average value. A single point analysis is not very reliable and neither are mass measurements when measuring masses in the order of 1 mg.

8.5. CONCENTRATION PROFILES FOR Pd-Ag (e + heat)

Silver was deposited on the palladium film. The zinc content remained low after heating. The theoretical thickness of the film was 4.8 microns. According to the concentration profiles (**Figure 8.3**) the measured thickness is closer to 6.5 microns, which implies one of two things: either the film was not completely uniform in thickness, or the film was slightly porous. The theoretical thickness was calculated by dividing the mass plated by the plated area and the densities of the deposited metals. The theoretical value assumed a completely dense and totally uniform film. From **Figures 6.22** and **6.23** it can be seen that the bottom part of the film is not completely dense. The top, however, is dense. As was the case with (d+heat) where palladium formed the bottom layer, there is penetration of palladium into the support membrane pores from 6 microns and deeper (**Figure 8.3**).

Figure 8.4 shows asymmetric Pd-Ag concentration profiles. At the outer edge of the film (0 microns) the silver concentration is high (34%) and it gradually decreases to about 2% at a depth of 7 microns. The composition is not constant at the preferred ratio (Pd:Ag = 76:24) throughout the film. Shu et al. (1996) reported that an asymmetric Pd-Ag film actually achieved higher hydrogen permeability and better conversion for methane steam reforming than conventional Pd-Ag (75:25) films.

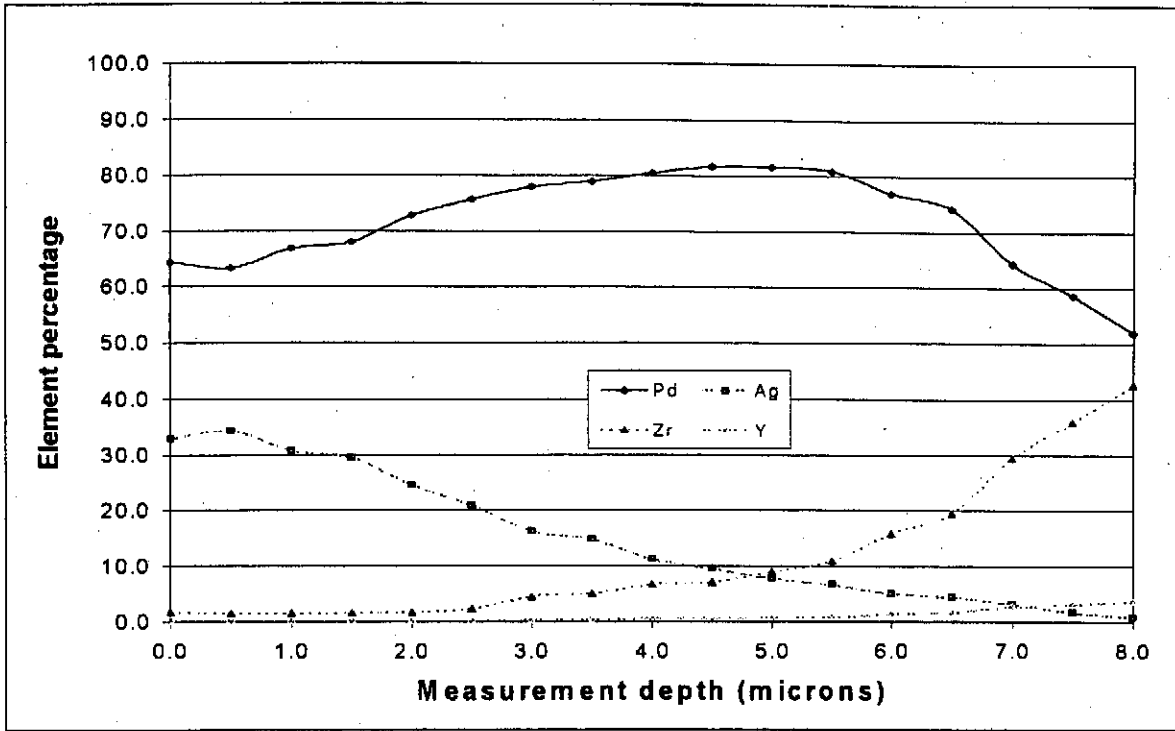


Figure 8.3: Concentration profiles for Pd+Ag (78:22) after heating

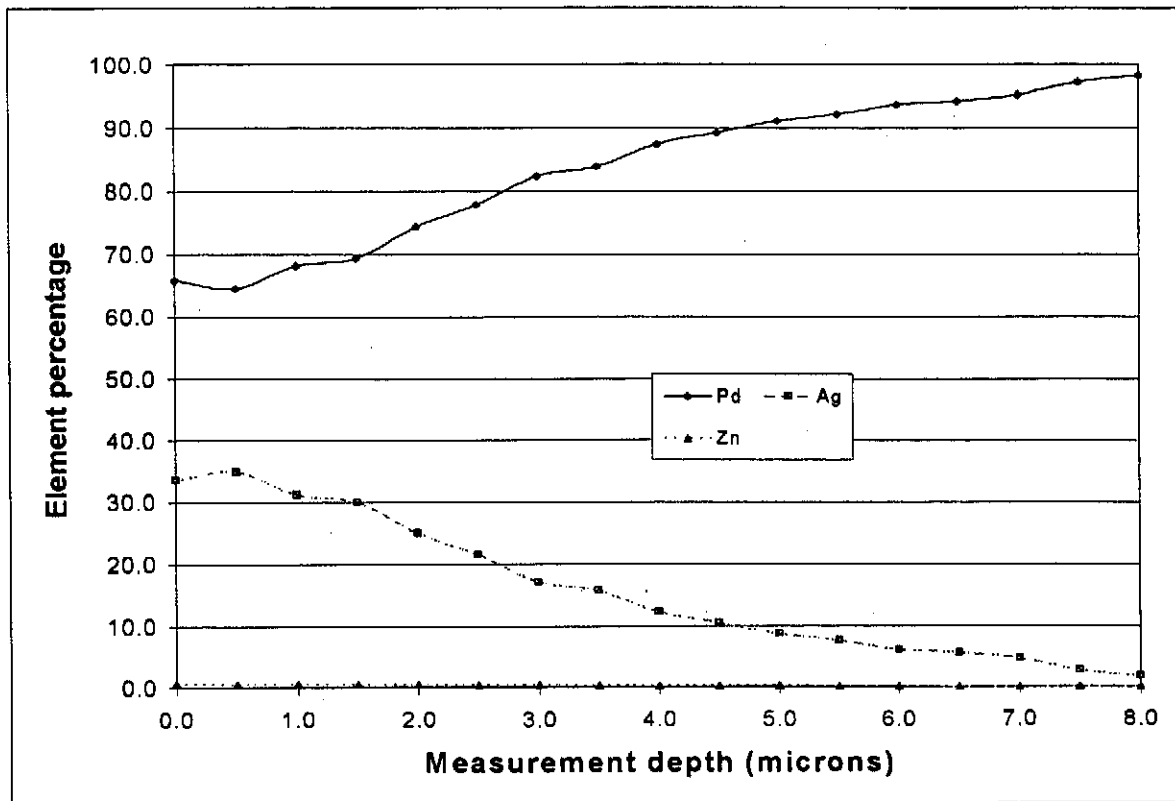


Figure 8.4: Ratio between Pd and Ag (78:22) across the film after heating

8.6. CONCENTRATION PROFILES FOR Ag-Pd (24:76) (f + heat)

The profiles are given in Figures 8.5 and 8.6. From Figure 8.5 it can be seen that the thickness of the metal film is between 4 and 5 microns, which is in good agreement with the theoretically calculated value of 4 microns. The silver was first deposited on the membrane support. The sharp decrease in both silver and palladium concentrations and the increase in zirconium concentration after a 4 micron depth, indicate very little penetration into the support. The difference between samples (e+heat), with good coating penetration into the support, and (f+heat), is the deposition order. When silver is deposited first, the coating after heating shows weaker penetration and reduced adhesion. The larger atoms of silver (1.44 Å atom radius compared to 1.37 Å for palladium) result in weak penetration into membrane pores during electroless plating.

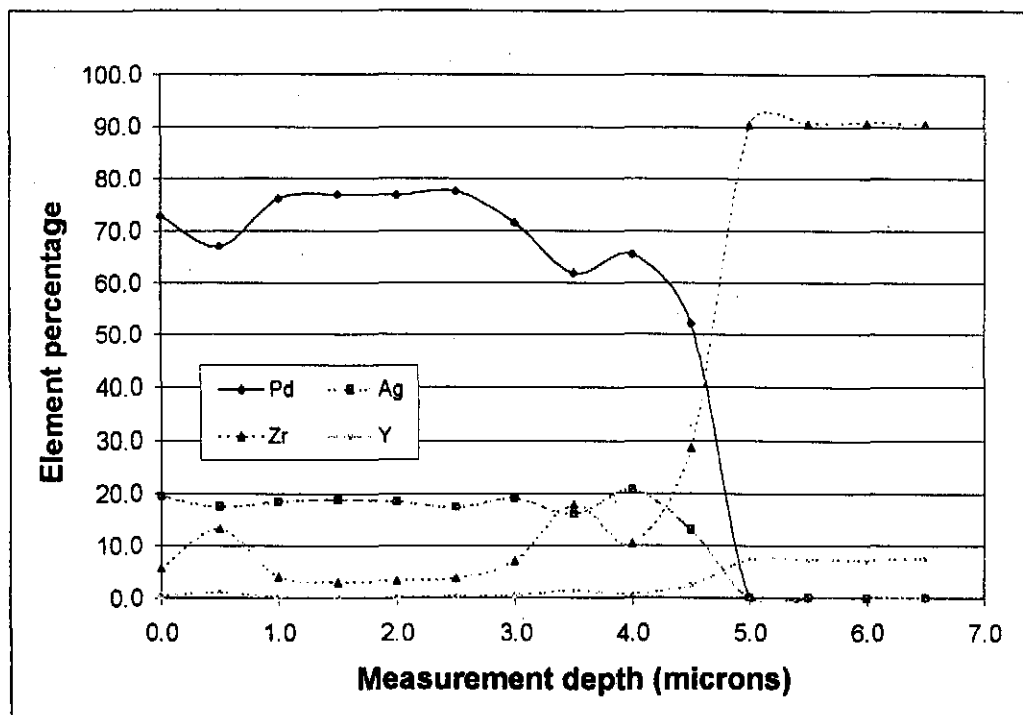


Figure 8.5: Concentration profiles for Ag+Pd (24:76) after heating

The palladium-silver ratio (Figure 8.6) remained constant at 80:20 down to 4.5 microns. Inside the pores the silver concentration increased to above 50 % compared to palladium, since the silver was deposited first and was thus more concentrated at the substrate surface.

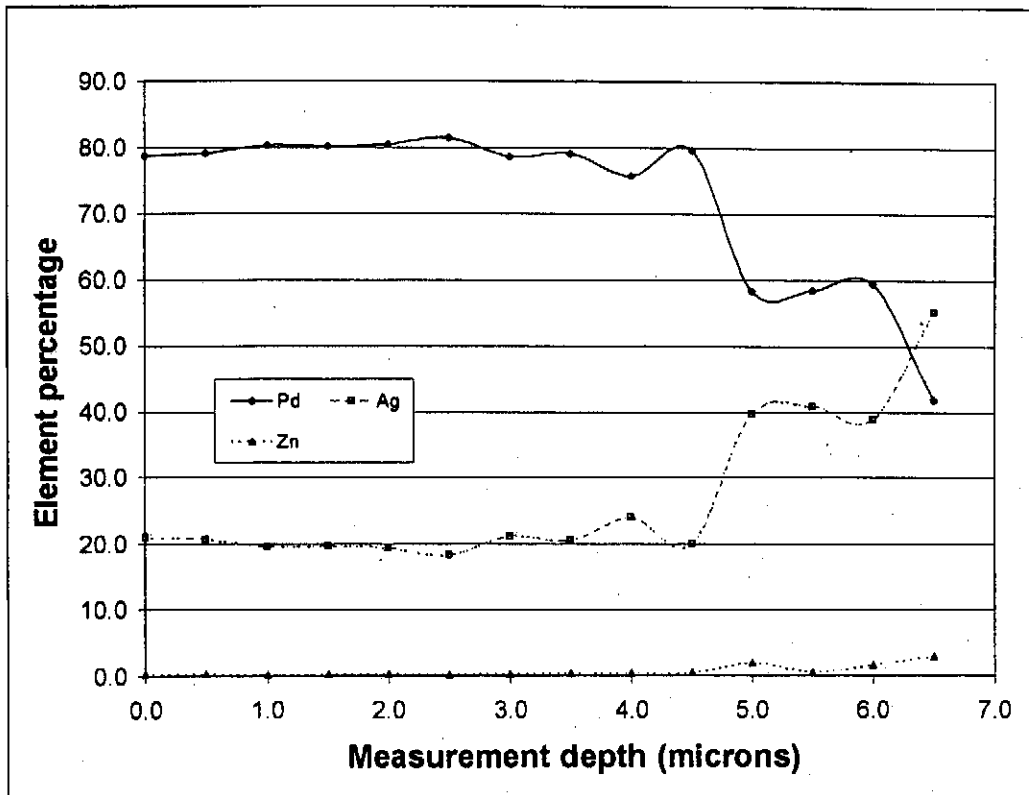


Figure 8.6: Ratio between Ag and Pd (24:76) across the film after heating

8.7. CONCENTRATION PROFILES FOR Ag-Pd (18:82) (j + heat)

A high zinc concentration was observed for this sample (Table 6.9) and the concentration profiles confirmed a high zinc concentration after heating. The theoretically calculated film thickness was 5 microns. Figure 8.7 shows no sharp decline in the sum of palladium and silver concentrations at a specific depth from 0-8 microns. The palladium concentration does, however, start to decline after a 3 micron measurement depth. Figure 6.31 also shows a film thickness in the order of 8 microns rather than 5 microns. This higher than expected value is due to the high concentration of zinc deposited in the heating process. The zinc concentration at the outer film edge is in the order of 20 % (APPENDIX E). The silver increases and the palladium decreases in concentration (Figure 8.8) when moving from the outer film edge towards the substrate. The zinc concentration declines steadily from the outer edge of the film towards the substrate.

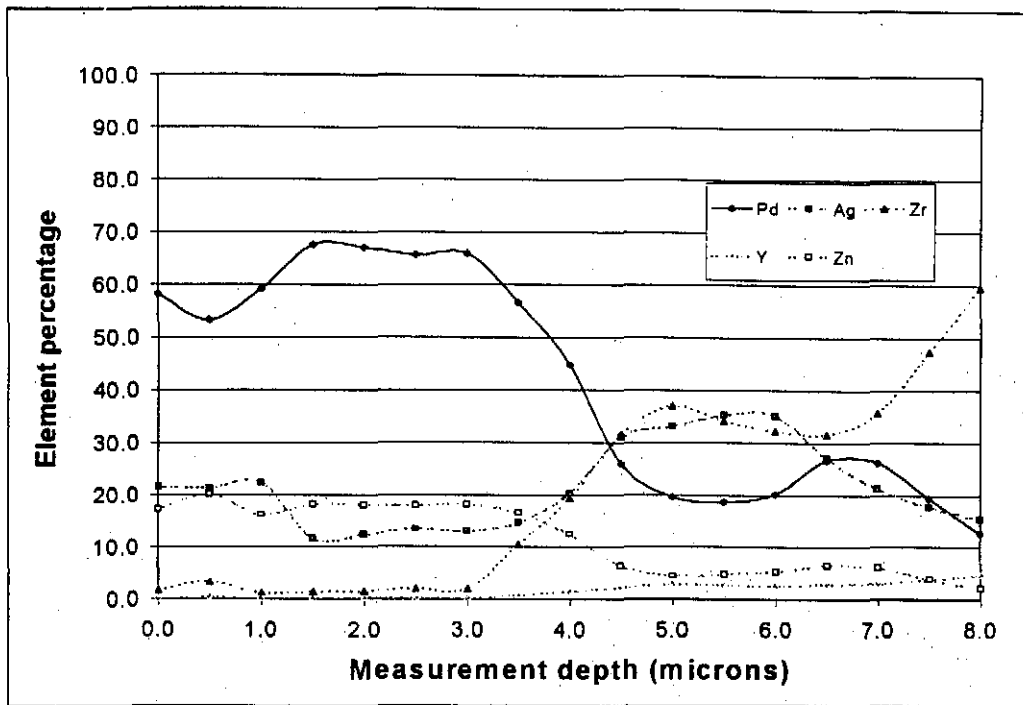


Figure 8.7: Concentration profiles for Ag+Pd (18:82) after heating

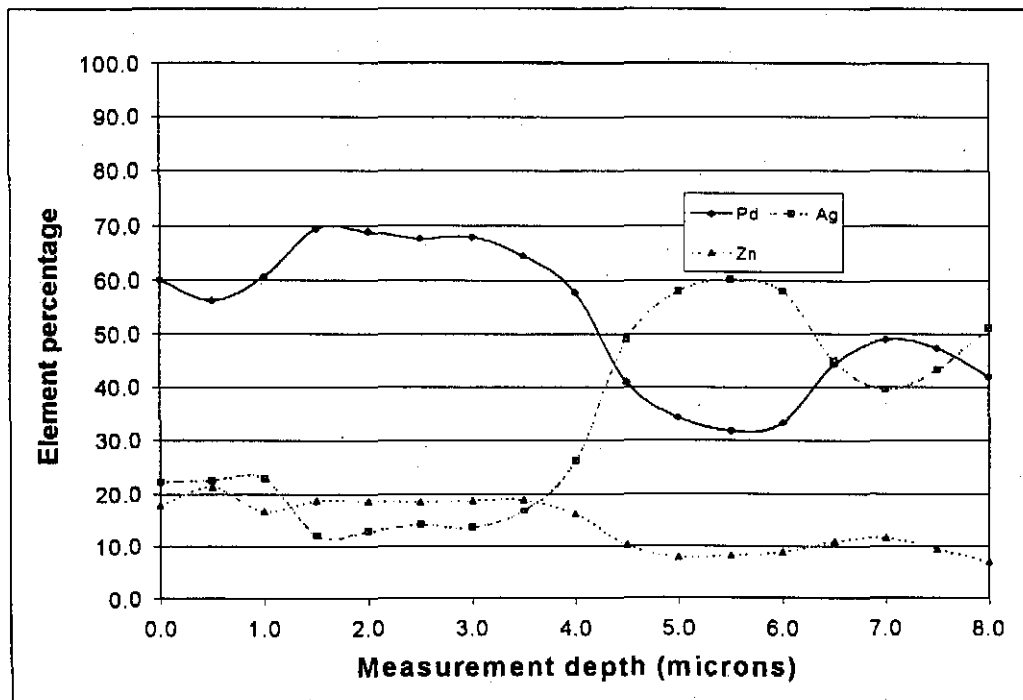


Figure 8.8: Ratio between Ag and Pd (18:82) across the film after heating

Maps (Figures 8.9 to 8.13) were constructed with PIXE to visualise the distribution of elements in the cross section of the metal film after heating. White areas indicate high concentrations and the closer to black the lower the concentration. High concentrations of

palladium and zinc were situated at the top of the metal film and declined downwards in the maps. The silver is evenly distributed at the top of the film, indicating a proper diffusion of silver into the palladium matrix. Zirconium and yttrium are situated at the bottom of the maps (Figures 8.12 and 8.13), indicating the start of the membrane support. Their concentrations increase downwards.

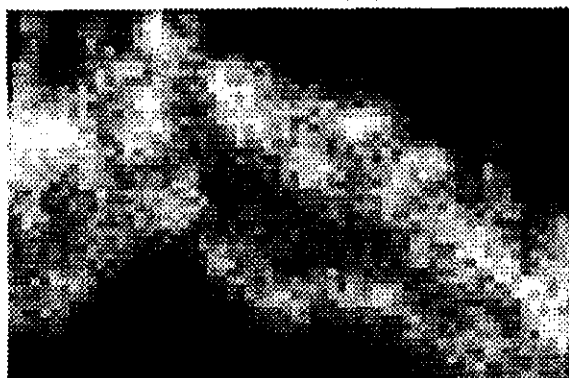


Figure 8.9: Silver layer

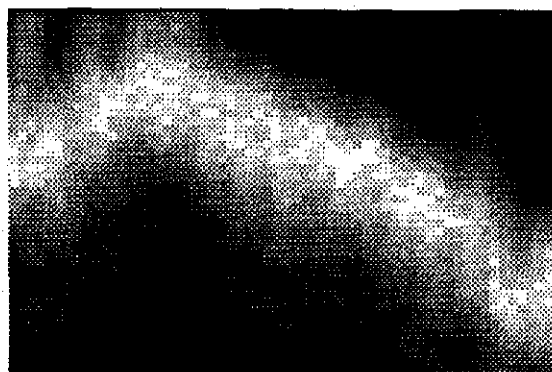


Figure 8.10: Palladium layer

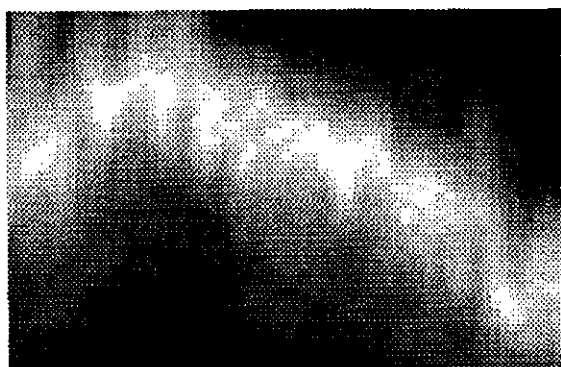


Figure 8.11: Zinc layer

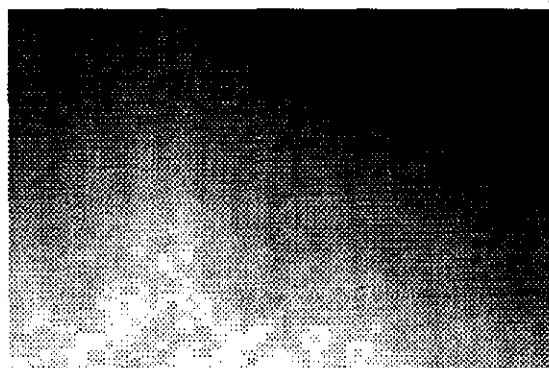


Figure 8.12: Zirconium layer

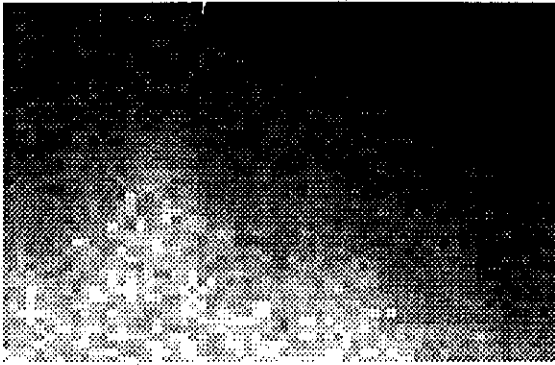


Figure 8.13: Yttrium layer

8.8. CONCENTRATION PROFILES FOR Ag-Pd-Ni (g + heat)

The concentration profiles for the silver-palladium-nickel composite are presented in **Figures 8.14 and 8.15**.

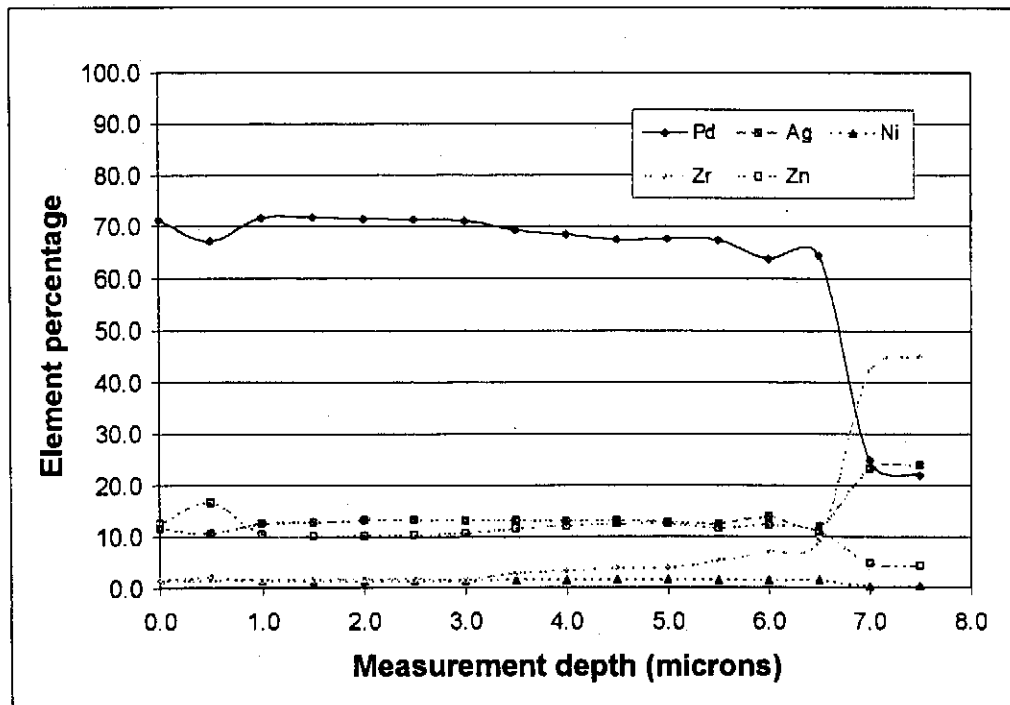


Figure 8.14: Concentration profiles for Ag+Pd+Ni (16:82:2) after heating

The theoretically calculated film thickness of 6.1 microns is in good agreement with the data of **Figure 8.14**, which indicates a thickness of 6.5 microns. The amount in the pores is not clearly defined as in the case of (f+heat). The coating was too thick to get a clear answer.

The concentrations of all deposited elements remain close to constant from 0-6.5 micron depth (Figure 8.15). From the line scan, the average nickel content is about 1.8%. The silver concentration is about 13.4% on average and the zinc concentration 12.4%.

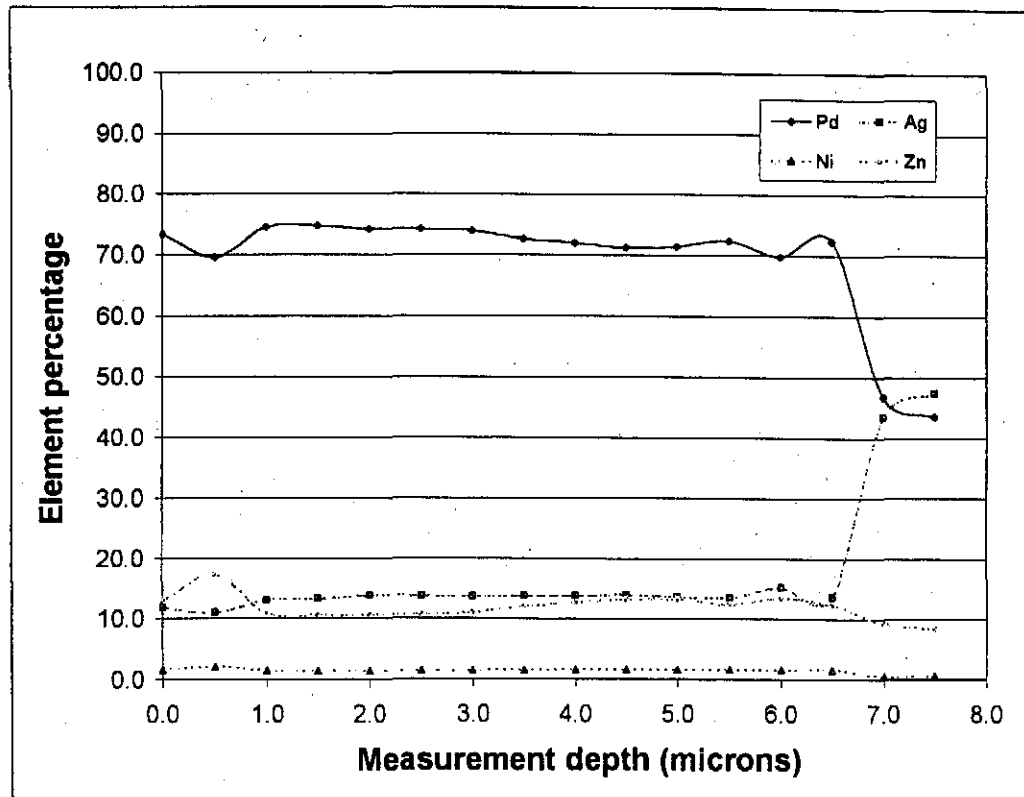


Figure 8.15: Concentration profiles for Ag+Pd+Ni (16:82:2) after heating

EDX was used to construct Figures 8.16 to 8.21. Figures 8.16-8.18 were compiled before heating and it shows how the metal layers were deposited. Starting from *right to left* (Figure 8.18 to 8.16) the silver was deposited first, followed by palladium and finally nickel.

Figures 8.19-8.21 show the metal film after heating. Both nickel and silver diffused into the palladium layer through a counter diffusion process. Nickel diffused from left to right and silver from right to left into the palladium, resulting in a homogeneous distribution. The nickel penetrated into pores and defects that might have been present in the palladium-silver alloy, creating a dense, smooth structure (Figure 6.35). It appears as if there were small localised areas with increased silver and nickel concentrations (Figures 8.19-8.20).



Figure 8.16: Ni

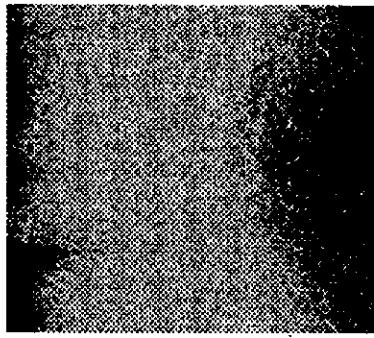


Figure 8.17: Pd

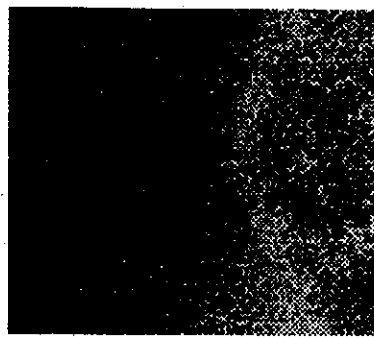


Figure 8.18: Ag

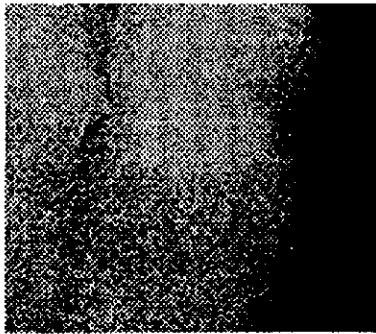


Figure 8.19: Ni

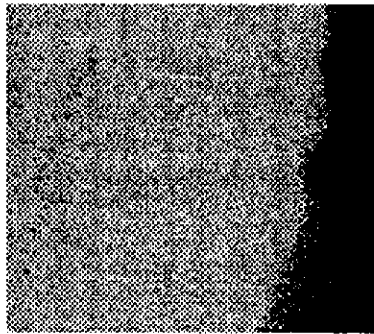


Figure 8.20: Pd

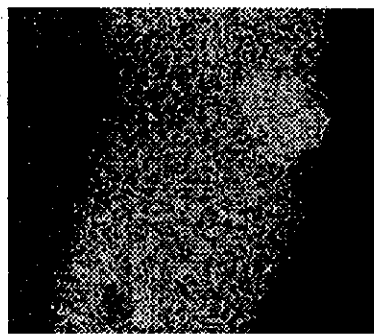


Figure 8.21: Ag

8.9. SUMMARY

Several important conclusions can be drawn from the work conducted in this chapter. They are:

- Palladium penetrates deeper into membrane pores than silver. By first depositing palladium and then silver, the composite coating penetrated into the membrane pores for at least three to four microns. Coatings, where silver was deposited first, showed very little pore penetration (in the order of one micron) and weaker metal to ceramic adhesion can be expected.
- By first depositing palladium and then silver, asymmetric palladium and silver concentrations profiles can be obtained after heating. The silver concentration is high at the edge of the film and then declines towards the support.
- If palladium is deposited on silver, the palladium to silver ratio remains constant across the thickness of the film after heating.
- A composite metal film can be prepared by first depositing silver, then palladium and finally nickel. After heat treating the coating, a dense, defect free structure can be

obtained. A counter diffusion process takes place and nickel penetrates into pores and defects that might be present in the palladium-silver structure. The nickel content required is in the order of 2-5%.

CHAPTER 9

CONCLUSIONS

The aim of this study was to investigate the preparation of palladium composite membranes. Palladium conversion in the electroless palladium plating reaction was optimised. Palladium-silver, palladium-nickel and silver-palladium-nickel composite coatings were prepared and fully characterised with SEM, XRD, PIXE and EDS. The most important findings in this work can be summarised as follows:

- Proper cleaning and pretreatment of the substrate is essential to obtain a uniform coating.
- Electroless palladium plating requires an alkaline solution with a pH of between 9 and 11 for hydrazine to act as proper reducing agent and for EDTA to be in the correct ionic form to best stabilise the palladium ions. A forty to sixty percent molar excess hydrazine is required for optimum palladium conversion, since hydrazine decomposes at high temperatures and in the presence of a metal catalyst. The most important variable in the electroless plating process is the EDTA concentration. If the EDTA concentration is too low, the plating bath becomes unstable and the palladium conversion drops sharply. If the EDTA concentration is too high, the bath tends to become over stable and the metal ions cannot be sufficiently released, reducing the palladium conversion. For optimum palladium conversion (> 90%) the following operating conditions are suggested per litre of plating solution:

| | |
|--|---|
| $(\text{NH}_3)_4\text{Pd}(\text{NO}_3)_2$ (10 % solution) | 27.5 g |
| NH_4OH (25 %) | 200 ml |
| Disodium EDTA | EDTA: Pd-salt molar ratio of between 30 and 40 |
| Hydrazine | Hydrazine: Pd-salt molar ratio of between 0.7 and 0.8 |
| pH buffer | between 9 and 11 |
| Temperature ($^{\circ}\text{C}$) | between 70 and 75 $^{\circ}\text{C}$ |

- Electroless palladium-silver co-deposition is a complex process, which is difficult to control. Electrode potential differences and surface catalytic effects influence the

composition of the deposit and the deposition rate. At low silver concentrations (< 0.06 g AgNO_3 /liter) there is an equilibrium between silver and palladium plating rates, but at high silver concentrations (0.1 g AgNO_3 /liter) palladium deposition is completely inhibited. The palladium plating rate quickly drops to almost zero, while the silver plating rate is not reduced.

- Silver deposition on an activated substrate resulted in higher plating rates and more homogeneous coatings than deposition on a palladium film. When preparing palladium-silver composite membranes, the suggested deposition order is first silver and then palladium.
- Palladium-nickel composite membranes can be prepared by depositing nickel on palladium. A low temperature nickel bath (40 °C) must be used, since only a very small amount of nickel needs to be deposited and a slow reaction is thus required.
- According to PIXE data the purity of the deposits were 99.75% for palladium, 99.5% for silver and about 97% for nickel. The palladium deposit was columnlike, dense and formed a continuous defect free layer for coatings exceeding 7 micron thickness. The silver deposit was non-homogeneous and not of even thickness across the entire substrate. The nickel deposit was very dense, smooth and totally defect free.
- The coatings were heat treated at 650 °C for 5 hours in a hydrogen atmosphere to allow for inter-metal diffusion and proper alloying. X-ray diffraction patterns confirmed the formation of a solid solution for both the palladium-nickel and palladium-silver composites. The composite structures were similar to that of the pure metals, but the alloy peaks shifted to angles between those of the pure metals.
- PIXE data indicated high zinc concentrations for three of the samples after heating. This was confirmed by XRD patterns, which matched the tetragonal PdZn structure.
- Palladium penetrated 3-4 microns into the support membrane, while silver did not penetrate by more than 1 micron.
- By first depositing palladium and then silver, asymmetric concentration profiles across the thickness of the film were obtained after heating. If silver was deposited first, the palladium to silver ratio remained constant for the entire thickness of the film after heating.
- Silver-palladium-nickel composites can be prepared by depositing silver, then palladium and finally nickel. By depositing as little as 2-5% nickel, a defect free structure can be obtained, which is very dense and non-porous. The characteristics of the silver-palladium

alloy, which allows for very high hydrogen permeation rates, are retained. Silver and nickel diffuse into the palladium matrix from opposite sides and by doing so the smaller nickel atoms penetrate into pores and defects that might be present in the palladium-silver structure. This is a novel way of preparing thinner (<5 micron) defect free palladium-silver coatings. Thinner, dense coatings reduce cost and increase the hydrogen permeation rate.

A new range of well-defined membranes can now be made. These membranes will be used for studying dehydrogenation reactions. Both liquid reactants, with dehydrogenation temperatures in the region of 200 °C to 300 °C, and gas reactants (propane, butane, etc.), with dehydrogenation temperatures above 400 °C, will be investigated.

REFERENCES

- Ali JK and Rippin DWT, 1994, Effect of reaction and permeation rates on the performance of a catalytic membrane reactor for methylcyclohexane dehydrogenation, *Separation Science and Technology*, Vol. 29, No. 18, pp. 2475-2492
- Armor JN, 1995, Membrane catalysis: where it is now, what needs to be done?, *Catalysis Today*, Vol. 25, pp. 199-207
- Athavale SN and Totlani MK, 1989, Electroless plating of palladium, *Metal finishing*, Vol. 87, No. 1, pp. 23-27
- Audrieth LF, 1951, The Chemistry of Hydrazine, 244 pages, *John Wiley and Sons, New York*
- Barrer RM, 1951, Diffusion in and through solids, *Cambridge University Press, London*
- Baudrand DW, 1984, Cleaning and preparation of ceramic and metallized ceramic materials for plating, *Plating and Surface Finishing*, Vol. 71, No. 10, pp. 72-75
- Brinker CJ and Scherer GW, 1990, Sol-gel Science, *Academic Press, New York*
- Bulenkova LF, Shimanskaya MV, et al., 1978, Reaction and adsorption of furan compounds on a membrane catalyst made from a palladium-nickel alloy, *Chemical Abstracts* 92:180393m
- Buxbaum RE and Marker TL, 1993, Hydrogen transport in nonporous membranes of palladium-coated niobium, tantalum and vanadium, *Journal of Membrane Science*, Vol. 89, pp. 29-38
- Buxbaum RE and Kinney AB, 1996, Hydrogen transport through tubular membranes of palladium-coated tantalum and niobium, *Industrial Engineering Chem. Research*, Vol. 35, pp. 530-537
- Cachet H, Froment M, et al., 1992, Selective metal deposition on silicon substrates, *Journal of Electrochemical Society*, Vol. 139, No. 10, pp. 2920-2925
- Callister WD, 1994, Material Science and Engineering: An introduction, Third Edition, 811 pages, *John Wiley & Sons Inc., New York*
- Cannon KC and Hacskaylo JJ, 1992, Evaluation of palladium-impregnation on the performance of a Vycor glass catalytic membrane reactor, *Journal of Membrane Science*, Vol. 65, pp. 259-268
- Casanave D, Giroir-Fendler A, et al., 1995, Control of transport properties with a microporous membrane reactor to enhance yields in dehydrogenation reactions, *Catalysis Today*, Vol. 25, pp. 309-314

- Champagnie AM, Tsotsis TT, et al., 1992, The study of ethane dehydrogenation in a catalytic membrane reactor, *Journal of Catalysis*, Vol. 134, pp. 713-730
- Cheng S and Shuai X, 1995, Simulation of a catalytic membrane reactor for oxidative coupling of methane, *AIChE Journal*, Vol. 41, No. 6, pp. 1598-1601
- Christian GD and O'Reilly JE, 1986, Instrumental analysis, Second Edition, p. 61, *Prentice Hall, New Jersey, USA*
- Clayson DM and Howard P, 1987, Improved synthesis of aromatics from alkanes, *UK patent*, GB 2 190 397 A
- Cohen RL, D'Amico JF, et al., 1971, *Journal of Electrochemical Society: Electrochemical Science and Technology*, Vol. 118, p. 2042
- Cohen RL and West KW, 1973, *Journal of Electrochemical Society: Electrochemical Science and Technology*, Vol. 120, p. 502
- Cohen RL and Meek RL, 1976, *Plating*, Vol. 63, p. 47
- Collins JP, 1993, Catalytic decomposition of ammonia in a membrane reactor, *PhD thesis*, 196 pages, *Oregon State University, USA*
- Collins JP and Way JD, 1993b, Preparation and characterisation of a composite palladium-ceramic membrane, *Industrial Engineering Chem. Research*, Vol. 32, pp. 3006-3013
- Compagnie des Métaux Précieux, 1976, Hydrogen from water, *French Patent* 2,302,273
- Cullity BD, 1978, Elements of X-ray diffraction, Second Edition, 555 pages, *Addison-Wesley Publishing Company Inc., Massachusetts, USA*
- Davies OL, 1978, The design and analysis of industrial experiments, 636 pages, *Longman Group Limited, London*
- Deuis RL, Subramanian C, et al., 1995, Study of electroless nickel plating of ceramic particles, *Scripta Metallurgia et Materialia*, Vol. 33, No. 8, pp. 1217-1224
- Dressick WJ, Dulcey CS, et al., 1994, Covalent binding of Pd catalysts to ligating self-assembled monolayer films for selective electroless metal deposition, *Journal of Electrochemical Society*, Vol. 141, No. 1, pp. 210-220
- Edlund DJ and Pledger WA, 1993, Thermolysis of hydrogen sulfide in a metal-membrane reactor, *Journal of Membrane Science*, Vol. 77, No. 2-3, p. 255
- Fan S, Li C, et al., 1994, Preparation and characterization of zeolitic membranes, *Third International conference on inorganic membranes*, Worcester, *Massachusetts, USA*
- Farris TS and Armor JN, 1993, Liquid-phase catalytic hydrogenation using palladium alloy membranes, *Applied Catalysis A: General*, Vol. 96, pp. 25-32

Feldstein N, 1974, Electron microscope investigation of mixed stannous chloride/palladium chloride catalysts for plating dielectric substrates, *Journal of Electrochemical Society: Electrochemical Science and Technology*, Vol. 121, No. 6, pp. 738-744

Fritsch D and Peinemann KV, 1995, Catalysis with homogeneous membranes loaded with nanoscale metallic clusters and their preparation, *Catalysis Today*, Vol. 25, pp. 277-283

Gallaher GR, Gerdes TE, et al., 1993, Experimental evaluation of dehydrogenations using catalytic membrane processes, *Separation Science and Technology*, Vol. 28, No. 1-3, pp. 309-326

Gobina E, Hou K, et al., 1995a, Ethane dehydrogenation in a catalytic membrane reactor coupled with a reactive sweep gas, *Chemical Engineering Science*, Vol. 50, No. 14, pp. 2311-2319

Gobina E, Hou K, et al., 1995b, Equilibrium-shift in alkane dehydrogenation using a high-temperature catalytic membrane reactor, *Catalysis Today*, Vol. 25, pp. 365-370

Gobina E and Hughes R, 1996a, Reaction assisted hydrogen transport during catalytic dehydrogenation in a membrane reactor, *Applied Catalysis A: General*, Vol. 137, pp. 119-127

Gobina E, Oklany JS, et al., 1996b, An integrated composite membrane reactor for the purification of coal gasification streams, *The 1996 ICHIME research event/second European conference for young researchers*

Goodhew PJ, 1975, Electron microscopy and analysis, 191 pages, *Wykeham Publications Ltd.*, London, Great Britain

Gopalan R, Chang CH, et al., 1994, Nanopore yttria doped zirconia membranes prepared by sol-gel method, *Third International conference on inorganic membranes*, Worcester, Massachusetts, USA

Graham AK, 1971, Electroplating Engineering Handbook, Third Edition, 845 pages, *Van Nostrand Reinold*, New York

Gryaznov VM and Smirnov VS, 1974, The reactions of hydrogenations on membrane catalysts, *Russ. Chem Rev.*, Vol. 43, pp. 821-834

Gryaznov VM, 1986a, *Platinum Metals Revue*, Vol. 30, p. 78

Gryaznov VM, Mishchenko AP, et al., 1986b, Alloy membrane catalysts for cyclization of 1,3-pentadiene to cyclopentane and cyclopentene, *French Patent 2,595,092*

Gryaznov VM, Serebryannikova OS, et al., 1993, Preparation and catalysis over palladium composite membranes, *Applied Catalysis A: General*, Vol. 96, pp. 15-23

- Guizard C, Julbe A, et al., 1994, Sol-gel processing of zirconia and titania microporous membranes, *Third International conference on inorganic membranes*, Worcester, Massachusetts, USA
- Han J and Lin YS, 1994, Oxygen permeation through electrochemical vapor deposited solid oxide membranes, *Third International conference on inorganic membranes*, Worcester, Massachusetts, USA
- Hearle JWS, Sparrow JT, et al., 1974, The use of the scanning electron microscope, 278 pages, *Pergamon Press, Oxford*, Great Britain
- Holleck GL, 1970, Diffusion and solubility of hydrogen in Pd and Pd-Ag alloys, *Journal of Physical Chemistry*, Vol. 74, No. 3, pp. 503-511
- Hongbin Z, Guoxing X, et al., 1995, Preparation and characterization of novel porous metal/ceramic catalytic membrane materials, *Catalysis Today*, Vol. 25, pp. 237-240
- Honma H, Koshio T, et al., 1995, Fabrication of nickel film on a glass disk by electroless nickel plating, *Plating and Surface Finishing*, pp. 60-62
- Horkans J, 1983, A cyclic voltammetric study of Pd-Sn colloidal catalysts for electroless deposition, *Journal of Electrochemical Society: Electrochemical Science and Technology*, Vol. 130, No. 2, pp.311-317
- Hough WV, Little JL, et al., 1981, *US Patent 4,255,194*
- Hsieh HP, 1989, Inorganic membrane reactors - A review, *AIChE Symposium Series*, Vol. 85, No. 268, pp. 53-67
- Huang SM and He BL, 1994, *Reactive Polymers*, Vol. 23, pp. 1-9
- Illias S and Govind R, 1989, Development of high temperature membranes for membrane reactor: An overview, *AIChE Symposium Series*, Vol. 85, No. 268, pp. 53-67
- Itoh N, 1987, A membrane reactor using palladium, *AIChE Journal*, Vol. 33, No. 9, pp. 1576-1578
- Itoh N and Govind R, 1989a, Combined oxidation and dehydrogenation in a palladium membrane, *Ind. Eng. Chem. Res.*, Vol. 28, pp. 1554-1557
- Itoh N, Haratania K, et al., 1989b, Ceramic membranes for the separation of hydrogen from gas mixtures, *Japanese Patent 89,04,216*
- Itoh N, Machida T, et al., 1995, Amorphous Pd-Si alloys for hydrogen-permeable and catalytically active membranes, *Catalysis Today*, Vol. 25, pp. 241-247
- Jayaraman V and Lin YS, 1995a, Synthesis and hydrogen permeation properties of ultrathin palladium-silver alloy membranes, *Journal of Membrane Science*, Vol. 104, pp. 251-262

Jayaraman V, Lin YS, et al., 1995b, Fabrication of ultrathin metallic membranes on ceramic supports by sputter deposition, *Journal of Membrane Science*, Vol. 99, pp. 89-100

Johansson SAE and Campbell JL, 1988, PIXE: A novel technique for elemental analysis *John Wiley & Sons, Great Britain*

Julbe A, Guizard C, et al., 1993, The sol-gel approach to prepare candidate microporous inorganic membranes for membrane reactors, *Journal of Membrane Science*, Vol. 77, pp. 137-153

Kikuchi E, 1988, Alloy-plated membranes for hydrogen separation and their manufacture *Japanese Patent 88,294,925*

Kikuchi E, Uemiya S, et al., 1989, Membrane reactor using microporous glass-supported thin film of palladium. Application to the water gas shift reaction, *Chemical Letters*, Vol. 3, pp. 489-492

Kikuchi E, 1995, Palladium/ceramic membranes for selective hydrogen permeation and their application to membrane reactor, *Catalysis Today*, Vol. 25, pp. 333-337

Kirk-Othmer, 1980a, Encyclopaedia of chemical technology, Vol. 8, pp. 738-750, Third Edition, *John Wiley and Sons, New York*

Kirk-Othmer, 1980b, Encyclopaedia of chemical technology, Vol. 5, p. 353, Third Edition, *John Wiley and Sons, New York*

Laaziz I, Larbot A, et al., 1992, Hydrolysis of mixed titanium and zirconium alkoxides by an esterification reaction, *Journal of Solid State Chemistry*, Vol. 98, pp. 393-403

Li A, Xiong G, et al., 1996, Preparation of Pd/ceramic composite membrane 1. Improvement of the conventional preparation technique, *Journal of Membrane Science*, Vol. 110, pp. 257-260

Li Y, Zheng L, et al., 1994, Synthesis of SO₂ membrane by modified chemical vapor deposition, *Third International conference on inorganic membranes*, Worcester, Massachusetts, USA

Lin K and Jong C, 1993, The deposition behaviour of electroless nickel on alumina substrates, *Materials Chemistry and Physics*, Vol. 35, pp. 53-57

Lin YS and Burggraaf AJ, 1991, *Journal of American Ceramic Society*, Vol. 6, p. 219

Linkov VM, 1994, Preparation and application of hollow fibre carbon membranes, *PhD thesis*, 126 pages, University of Stellenbosch, Stellenbosch, SA

Livage J, Henry M, et al., 1988, Sol-gel chemistry of transition metal oxides, *Prog. Solid State Chemistry*, Vol. 18, pp. 259-341

Loweheim FA, 1974, Modern Electroplating, pp. 342-357, 739-747, *John Wiley & Sons, New York*

Makrides AC, 1964, Absorption of hydrogen by silver-palladium alloys, *Journal of Physical Chemistry*, Vol. 68, No. 8, pp. 2160-2169

Montgomery DC, 1991, Design and analysis of experiments, Third Edition, 649 pages, *Johan Wiley & Sons, New York*

Mulder M, 1991, Basic principles of membrane technology, Chap IV, *Kluwer Academic Publishers, The Netherlands*

Nam SW and Gavalas GR, 1989, Stability of H₂-permselective SiO₂ films formed by chemical vapour deposition, *AIChE Symposium Series*, Vol. 85, No. 268, pp. 68-74

Nourbakhsh N, Champagnie A, et al., 1989, Transport and reaction studies using ceramic membranes, *AIChE Symposium Series*, Vol. 85, No. 268, pp. 75-84

Ohno I, Wakabayashi O, et al., 1985, Anodic oxidation of reductants in electroless plating, *Journal of Electrochemical Society: Electrochemical Science and Technology*, Vol. 132, No. 10, pp. 2323-2330

Osaka T and Takematsu H, 1980, A study on activation and acceleration by mixed PdCl₂/SnCl₂ catalysts for electroless metal deposition, *Journal of Electrochemical Society: Electrochemical Science and Technology*, Vol. 127, No. 5, pp. 1021-1029

Pantazidis A, Dalmon JA, et al., 1995, Oxidative dehydrogenation of propane on catalytic membrane reactors, *Catalysis Today*, Vol. 25, pp. 403-408

Parfenova NI, Polyakova VP, et al., 1983, Palladium alloys as hydrogen permeable membranes for improving butane dehydrogenation, *Chemical Abstracts* 100:11269d

Peachey NM, Snow RC, et al., 1996, Composite Pd/Ta membranes for hydrogen separation, *Journal of Membrane Science*, Vol. 111, pp. 123-133

Pearlstein F and Weightman RF, October 1969, Electroless palladium deposition, *Plating*, pp. 1158-1161

Pearlstein F and Weightman RF, 1974, *Plating*, Vol. 61, p. 154

Rao MB and Sircar S, 1994, Novel nanoporous carbon membranes for gas separation, *Third International conference on inorganic membranes*, Worcester, Massachusetts, USA

Rhoda RN, 1959, Electroless palladium plating, *Transactions of the Institute of Metal Finishing*, Vol. 36, pp. 82-85

Rhoda RN and Madison AM, 1959b, *US Patent* 2,915,406

Riedel C and Spohr R, 1980, *Journal of Membrane Science*, Vol. 7, p. 225

- Riedel W, 1991, Electroless nickel plating, *ASM International*, Metals Park, Ohio, USA
- Rodina AA, Gurevich MA, et al., 1971, The interaction of hydrogen with certain palladium-gold and palladium-silver-gold alloys, *Russian Journal of Physical Chemistry*, Vol. 45, pp. 621-623
- Sasaki YT, 1991, A survey of vacuum material cleaning procedures: A subcommittee report of the American Vacuum Society Recommended Practices Committee, *Journal of Vacuum Science and Technology: A*, Vol. 9, No. 3, pp. 2025-2035
- Sathe AM, Itoh N, et al., 1994, Some new considerations about ethylene hydrogenation in a 77 wt% palladium and 23 wt% silver membrane reactor, *Indian Chemical Engineering*, Section A, Vol. 36, No. 3, pp. 131-135
- Schmidt EW, 1984, Hydrazine and its Derivatives: Preparation, properties, application, 1059 pages, *John Wiley and Sons*, New York
- Sheintuch M and Dessau RM, 1996, Observations, modeling and optimization of yield, selectivity and activity during dehydrogenation of isobutane and propane in a Pd membrane reactor, *Chemical Engineering Science*, Vol. 51, No. 4, pp. 535-547
- Shiple CR, 1984, Historical highlights of electroless plating, *Plating and Surface Finishing*, Vol. 71, pp. 92-99
- Shu J, Grandjean BPA, et al., 1991, Catalytic palladium-based membrane reactors: A review, *The Canadian Journal of Chemical Engineering*, Vol. 69, pp. 1036-1060
- Shu J, Grandjean BPA, et al., 1993, Simultaneous deposition of Pd and Ag on porous stainless steel by electroless plating, *Journal of Membrane Science*, Vol. 77, pp. 181-195
- Shu J, Grandjean BPA, et al., 1994, Methane steam reforming in asymmetric Pd- and Pd-Ag/porous SS membrane reactors, *Applied Catalysis A: General*, Vol. 119, pp. 305-325
- Shu J, Grandjean BPA, et al., 1995, Asymmetric Pd-Ag/stainless steel catalytic membranes for methane steam reforming, *Catalysis Today*, Vol. 25, pp. 327-332
- Shu J, Adnot A, et al., 1996, Structurally stable composite Pd-Ag alloy membranes: Introduction of a diffusion barrier, *Thin Solid Films*, Vol. 286, pp. 72-79
- Sillen LG and Martell AE, 1964, Stability constants of metal-ion complexes; Special Publication No. 17, p. 639, *The Chemical Society*, London
- Skakunova EV, Ermilova MM, et al., 1988, Hydrogenolysis of propane on a Pd-Ru alloy membrane catalyst, *Izv. Akad. Nauk SSSR, Ser. Khim.*, Vol. 5, pp. 986-991
- Smirnov VS, Gryaznov VM, et al., 1978, Dehydro- β -ionone, *Soviet Patent* 437,743

- Smith SPJ, 1995, Preparation of hollow-fibre composite carbon-zeolite membranes, *M.Sc.*, 142 pages, University of Stellenbosch, Stellenbosch, SA
- Smithells CJ, 1992, Metals reference book, Seventh Edition, Chapter 11, *Butterworth-Heinemann Ltd.*, Oxford, Great Britain
- Soria R, 1995, Overview on industrial membranes, *Catalysis Today*, Vol. 25, pp. 285-290
- Stremsdoerfer G, Calais C, et al., 1990, Low resistance ohmic contacts onto n-InP by palladium electroless bath deposition, *Journal Electrochemical Society*, Vol. 137, No. 3, pp. 835-838
- Torres M, Sanchez J, et al., 1994, Modelling and simulation of a three phase catalytic membrane reactor for nitrobenzene hydrogenation, *Ind. Eng. Chem. Res.*, Vol. 33, pp. 2421-2425
- Tsotsis TT, Champagnie AM, et al., 1992, Packed bed catalytic membrane reactors, *Chemical Engineering Science*, Vol. 47, No. 9-11, pp. 2903-2908
- Uemiya S, Kude Y, et al., 1988, Palladium/porous glass composite membrane for hydrogen separation, *Chemical Letters*, Vol. 10, pp. 1687-1690
- Uemiya S, Sato N, et al., 1991a, Separation of hydrogen through palladium thin film supported on a porous glass tube, *Journal of Membrane Science*, Vol. 56, pp. 303-313
- Uemiya S, Matsuda T, et al., 1991b, Hydrogen permeable palladium-silver alloy membrane supported on porous ceramics, *Journal of Membrane Science*, Vol. 56, pp. 315-325
- Uemiya S, Koseki M, et al., 1994, Preparation of highly permeable membranes for hydrogen separation using a CVD technique, *Third International conference on inorganic membranes*, Worcester, Massachusetts, USA
- Ullmann, 1987, Ullmann's encyclopaedia of industrial chemistry, Fifth revised edition, Vol. A26, pp. 681-689, *VHC Publishers*, Germany
- Ullmann, 1987b, Ullmann's encyclopaedia of industrial chemistry, Vol A10, p. 96, Fifth revised edition, *VHC Publishers*, Germany
- Van den Meerakker JEAM, 1981, *J. Applied Electrochem.*, Vol. 11, p. 395
- Van der Putten AMT, De Bakker J, et al., 1992, Electrochemistry of colloidal palladium, *Journal of Electrochemical Society*, Vol. 139, No. 12, pp. 3475-3480
- Veldsink JW, Van Damme RMJ, et al., 1992, A catalytically active membrane reactor for fast, exothermic, heterogeneously catalysed reactions, *Chemical Engineering Science*, Vol. 47, No. 9-11, pp. 2939-2944

Veldsink JW, 1993, A catalytically active, non-permselective membrane reactor for kinetically fast, strongly exothermic heterogeneous reactions., *PhD Thesis*, Chapter 1&2, University of Twente, The Netherlands

Vitulli G, Pitzalis E, et al., 1995, Porous Pt/SiO₂ catalytic membranes prepared using mesitylene solvated Pt atoms as a source of Pt particles, *Catalysis Today*, Vol. 25, pp. 249-253

Wachtman JB and Haber RA, 1986, Ceramic films and coatings, *Chem. Eng. Prog.*, Vol. 82, No. 1, pp. 39-46

Willard HH, Merritt LL, et al., 1981, Instrumental methods of analysis, Sixth Edition, p. 268
D. Van Nostrand Company, New York, USA

Yeung KL, Aravind R, et al., 1994, Non-uniform catalyst distribution for inorganic membrane reactors: Theoretical considerations and preparation techniques, *Chemical Engineering Science*, Vol. 49, No. 24A, pp. 4823-4838

Yeung KL, Sebastian JM, et al., 1995a, Novel preparation of Pd/Vycor composite membranes, *Catalysis Today*, Vol. 25, pp. 231-236

Yeung KL, Varma A, et al., 1995b, Novel preparation techniques for thin metal-ceramic composite membranes, *AIChE Journal*, Vol. 41, No. 9, pp. 2131-2139

APPENDIX A

(List of chemicals used in this study)

| <u>Chemical</u> | <u>Company:</u> | <u>Purity (grade)</u> |
|---|------------------------|------------------------------|
| PdCl ₂ | Aldrich | 99.99% |
| (NH ₃) ₄ Pd(NO ₃) ₂ | Aldrich | 99.99% (10 wt% solution) |
| SnCl ₂ | Fluka | > 98% |
| HCl (32%) | Saarchem | univAR |
| Na ₂ EDTA | Saarchem | > 99% (univAR) |
| Buffers (pH=8-12) | Saarchem | (univAR) |
| Hydrazine hydrate | Saarchem | 98% (univAR) |
| NiSO ₄ | Saarchem | (uniLAB) |
| NaH ₂ PO ₄ | Saarchem | (uniLAB) |
| AgNO ₃ | Aldrich | 99.9999% |
| Isopropanol | Saarchem | 99.5% (uniLAB) |
| NaOH | Saarchem | 97% (uniLAB) |
| Ammonia (25%) | Saarchem | (univAR) |

APPENDIX B

(Electroless plating data)

| Electroless palladium plating data | | | | | | | | | | | | |
|---|-------|-----------------|--------------|---------|----------|--------|---------------------|-------------------|--------------------|-----------------|-------------|---------------------|
| Run | Layer | hydrazin: Pd | Buffer pH | Temp °C | EDTA: Pd | Stable | Initial mass (g) | Final mass (g) | Mass difference | Conver- sion | Mass out | ICP con- version |
| 1 | 1 | 0.4 | 9 | 59 | 6 | Y | 0.8264 | 0.8310 | 4.6 | 23.0 | | |
| 2 | 2 | 0.4 | 9 | 59 | 6 | Y | 0.8310 | 0.8343 | 3.3 | 16.5 | | |
| 3 | 1 | 0.4 | 9 | 71 | 6 | Y | 0.7374 | 0.7458 | 8.4 | 42.0 | | |
| 4 | 2 | 0.4 | 9 | 71 | 6 | Y | 0.7458 | 0.7546 | 8.8 | 44.0 | | |
| 5 | 1 | 0.72 | 9 | 71 | 6 | N | 0.8036 | 0.8096 | 6.0 | 30.0 | | |
| 6 | 2 | 0.72 | 9 | 71 | 6 | N | 0.8096 | 0.8174 | 7.8 | 39.0 | | |
| 7 | 1 | 0.72 | 9 | 59 | 6 | Y | 0.7578 | 0.7649 | 7.1 | 35.5 | | |
| 8 | 2 | 0.72 | 9 | 59 | 6 | Y | 0.7649 | 0.7733 | 8.4 | 42.0 | | |
| 9 | 1 | 0.4 | 11 | 59 | 6 | Y | 0.7381 | 0.7423 | 4.2 | 21.0 | | |
| 10 | 2 | 0.4 | 11 | 59 | 6 | Y | 0.7423 | 0.7457 | 3.4 | 17.0 | | |
| 11 | 1 | 0.4 | 11 | 71 | 6 | Y | 0.7116 | 0.7216 | 10.0 | 50.0 | | |
| 12 | 2 | 0.4 | 11 | 71 | 6 | Y | 0.7216 | 0.7298 | 8.2 | 41.0 | | |
| 13 | 1 | 0.72 | 11 | 71 | 6 | N | 0.6826 | 0.6893 | 6.7 | 33.5 | | |
| 14 | 2 | 0.72 | 11 | 71 | 6 | N | 0.6893 | 0.6964 | 7.1 | 35.5 | | |
| 15 | 1 | 0.72 | 11 | 59 | 6 | Y | 0.7260 | 0.7350 | 9.0 | 45.0 | | |
| 16 | 2 | 0.72 | 11 | 59 | 6 | Y | 0.7350 | 0.7403 | 5.3 | 26.5 | | |
| 17 | 1 | 0.56 | 10 | 66 | 6 | Y | 0.7362 | 0.7492 | 13.0 | 65.0 | | |
| 18 | 2 | 0.56 | 10 | 66 | 6 | Y | 0.7492 | 0.7590 | 9.8 | 49.0 | | |
| 19 | 1 | 0.56 | 10 | 66 | 8 | Y | 0.7397 | 0.7519 | 12.2 | 61.0 | | |
| 20 | 2 | 0.56 | 10 | 66 | 8 | Y | 0.7519 | 0.7619 | 10.0 | 50.0 | | |
| 21 | 1 | 0.72 | 11 | 71 | 8 | N | 0.7475 | 0.7545 | 7.0 | 35.0 | | |
| 22 | 1 | 0.72 | 11 | 71 | 10 | N | 0.7883 | 0.7995 | 11.2 | 56.0 | | |
| 23 | 2 | 0.72 | 11 | 71 | 14 | N (30) | 0.8009 | 0.8132 | 12.3 | 61.5 | | |
| 24 | 1 | 0.72 | 11 | 71 | 20 | Y | 0.6130 | 0.6273 | 14.3 | 87.1 | 3.6 | 83.0 |
| 25 | 1 | 0.72 | 11 | 71 | 30 | Y | 0.7135 | 0.7309 | 17.4 | 87.0 | | |
| 26 | 2 | 0.72 | 11 | 71 | 40 | Y | 0.7298 | 0.7435 | 13.7 | 80.0 | 2.9 | 83.6 |
| 27 | 1 | 0.72 | 11 | 71 | 50 | Y | 0.5598 | 0.5754 | 15.6 | 78.0 | | |
| 28 | 2 | 0.56 | 11 | 71 | 14 | Y | 0.7555 | 0.7665 | 11.0 | 55.0 | | |
| 29 | 2 | 0.56 | 11 | 77 | 30 | Y | 0.7623 | 0.7786 | 16.3 | 81.5 | | |
| 30 | 1 | 0.72 | 11 | 71 | 30 | Y | 0.6817 | 0.7014 | 16.5 | 98.3 | 3.2 | 80.7 |
| 31 | 1 | 0.72 | 11 | 77 | 30 | Y | 0.6035 | 0.6205 | 17.0 | 99.2 | 2.9 | 83.4 |
| 32 | 2 | 0.56 | 11 | 71 | 30 | Y | 0.5848 | 0.5965 | 11.7 | 71.8 | 3.7 | 73.9 |

| | | | | | | | | | | | | |
|----|---|------|----|----|----|----------|--------|--------|------|------|-----|------|
| 33 | 2 | 0.56 | 11 | 77 | 14 | Y | 0.5806 | 0.5929 | 12.3 | 71.8 | 2.9 | 83.7 |
| 34 | 1 | 0.72 | 11 | 71 | 30 | Y | 0.5562 | 0.5721 | 15.9 | 96.4 | 3.5 | 82.5 |
| 35 | 1 | 0.72 | 11 | 71 | 30 | Y | 0.5886 | 0.6046 | 16.0 | 92.8 | 2.8 | 89.1 |
| 36 | 1 | 0.72 | 11 | 77 | 14 | N(90) | 0.5735 | 0.5853 | 11.8 | 59.0 | | |
| 37 | 1 | 0.72 | 8 | 71 | 20 | N(40) | 0.7345 | 0.7454 | 10.9 | 61.0 | 2.1 | 66.3 |
| 38 | 1 | 0.72 | 9 | 71 | 20 | Y | 0.7369 | 0.7536 | 16.7 | 98.3 | 3.0 | 85.3 |
| 39 | 1 | 0.72 | 12 | 71 | 20 | N(40) | 0.7422 | 0.7520 | 9.8 | 55.0 | 2.2 | 57.0 |
| 40 | 1 | 0.72 | 9 | 71 | 14 | Y | 0.7269 | 0.7389 | 12.0 | 70.3 | 2.9 | 81.5 |
| 41 | 1 | 0.72 | 9 | 71 | 20 | Y | 0.6379 | 0.6525 | 14.6 | 88.7 | 3.5 | 84.4 |
| 42 | 3 | 0.72 | 9 | 71 | 40 | Y | 0.7623 | 0.7820 | 19.7 | 98.5 | | |
| 43 | 2 | 0.72 | 11 | 77 | 50 | Y | 0.7338 | 0.7521 | 18.3 | 91.5 | | |
| 44 | 2 | 0.56 | 11 | 71 | 20 | Y | 0.7559 | 0.7670 | 11.1 | 69.1 | 3.9 | 70.7 |
| 45 | 2 | 0.88 | 11 | 71 | 20 | Y | 0.7014 | 0.7099 | 8.5 | 52.9 | 3.9 | 57.0 |
| 46 | 1 | 0.88 | 11 | 71 | 14 | Y | 0.5718 | 0.5856 | 13.8 | 79.3 | 2.6 | 90.1 |
| 47 | 1 | 0.88 | 11 | 71 | 10 | N(100) | 0.5699 | 0.5792 | 9.3 | 52.8 | 2.4 | 68.7 |
| 48 | 1 | 0.56 | 11 | 71 | 8 | Y | 0.6170 | 0.6285 | 11.5 | 65.5 | 2.4 | 91.0 |
| 49 | 1 | 0.72 | 11 | 77 | 40 | Y | 0.5822 | 0.5990 | 16.8 | 99.5 | 3.1 | 84.3 |
| 50 | 2 | 0.56 | 11 | 77 | 20 | Y | 0.5876 | 0.6008 | 13.2 | 77.9 | 3.1 | 80.8 |
| 51 | 2 | 0.72 | 11 | 65 | 20 | Y | 0.6296 | 0.6440 | 14.4 | 86.0 | 3.3 | 82.0 |
| 52 | 2 | 0.72 | 11 | 65 | 14 | Y | 0.7409 | 0.7534 | 12.5 | 73.5 | 3.0 | 85.6 |
| 53 | 2 | 0.72 | 11 | 65 | 30 | Y | 0.5764 | 0.5896 | 13.2 | 81.9 | 3.9 | 76.3 |
| 54 | 3 | 0.88 | 11 | 71 | 20 | Y | 0.8173 | 0.8350 | 17.7 | 88.5 | | |
| 55 | 3 | 0.56 | 11 | 77 | 8 | N(60-70) | 0.6966 | 0.7059 | 9.3 | 46.5 | | |
| 56 | 1 | 0.72 | 11 | 65 | 6 | Y | 0.5640 | 0.5766 | 12.6 | 63.0 | | |
| 57 | 1 | 0.72 | 11 | 65 | 40 | Y | 0.5208 | 0.5381 | 17.3 | 86.5 | | |
| 58 | 1 | 0.88 | 11 | 71 | 40 | Y | 0.5501 | 0.5691 | 19.0 | 95.0 | | |
| 59 | 1 | 0.56 | 11 | 77 | 40 | Y | 0.5848 | 0.6028 | 18.0 | 90.0 | | |
| 60 | 1 | 0.72 | 11 | 59 | 20 | Y | 0.4383 | 0.4496 | 11.3 | 56.5 | | |
| 61 | 1 | 0.72 | 11 | 59 | 30 | Y | 0.4573 | 0.4676 | 10.3 | 51.5 | | |
| 62 | 1 | 0.72 | 11 | 59 | 50 | Y | 0.4731 | 0.4803 | 7.2 | 36.0 | | |
| 63 | 1 | 0.72 | 11 | 65 | 30 | Y | 0.4478 | 0.4590 | 11.2 | 56.0 | | |
| 64 | 1 | 0.72 | 11 | 65 | 40 | Y | 0.5044 | 0.5174 | 13.0 | 65.0 | | |
| 65 | 1 | 0.72 | 11 | 65 | 50 | Y | 0.4784 | 0.4895 | 11.1 | 55.5 | | |
| 66 | 1 | 0.56 | 11 | 71 | 20 | Y | 0.5478 | 0.5591 | 11.3 | 56.5 | | |
| 67 | 1 | 0.56 | 11 | 71 | 30 | Y | 0.5794 | 0.5881 | 8.7 | 43.5 | | |

Kinetic data for Pd plating (determined by ICP)

| Kinetic data for Pd plating (determined by ICP) | | | | | | | | | |
|---|-----------|----------|-----------|--------------|-------------|--------|--|--------------|------------|
| run 24 | | | | | | | | | |
| Time min. | Empty (g) | with H2O | with sol. | ICP Pd (ppm) | true ppm Pd | mg out | | mg Pd plated | conversion |
| 0 | 7.5808 | 17.2385 | 18.1607 | 83.30 | 955.66 | 0.88 | | | |
| 5 | 8.0873 | 17.6435 | 18.6835 | 82.19 | 837.41 | 0.87 | | | |
| 10 | 7.6807 | 17.2494 | 18.2412 | 71.73 | 763.77 | 0.76 | | | |
| 20 | 7.6665 | 17.1383 | 18.1747 | 66.62 | 675.47 | 0.70 | | | |
| 40 | 8.1229 | 17.628 | 18.5619 | 48.31 | 540.00 | 0.50 | | | |
| 80 | 7.6949 | 17.2914 | 18.2178 | 33.27 | 377.91 | 0.35 | | | |
| 130 | 7.6688 | 17.1912 | 18.1933 | 23.15 | 243.13 | 0.24 | | | |
| 180 | 8.0351 | 17.515 | 18.4667 | 15.67 | 171.76 | 0.16 | | | |
| | | 121.656 | 128.539 | | | 3.59 | | 13.30 | 83.02 |
| run 26 | | | | | | | | | |
| Time min. | Empty (g) | with H2O | with sol. | ICP Pd (ppm) | true ppm Pd | mg out | | mg Pd plated | conversion |
| 0 | | | 22.5031 | | 870.10 | | | | |
| 5 | 7.9477 | 17.6614 | 18.3045 | 61.09 | 862.19 | 0.63 | | | |
| 10 | 7.5445 | 17.1819 | 17.9004 | 59.27 | 854.27 | 0.61 | | | |
| 20 | 7.5184 | 17.3034 | 18.0035 | 54.11 | 810.38 | 0.57 | | | |
| 40 | 7.4819 | 17.0708 | 17.7347 | 44.02 | 679.81 | 0.45 | | | |
| 80 | 7.5971 | 17.1129 | 17.7224 | 29.01 | 481.93 | 0.29 | | | |
| 130 | 7.5317 | 17.2162 | 17.8724 | 18.78 | 295.94 | 0.19 | | | |
| 180 | 6.5098 | 16.4453 | 17.2316 | 11.32 | 154.36 | 0.12 | | | |
| | | 119.991 | 124.769 | | | 2.87 | | 13.97 | 83.62 |
| run 30 | | | | | | | | | |
| Time min. | Empty (g) | with H2O | with sol. | ICP Pd (ppm) | true ppm Pd | mg out | | mg Pd plated | conversion |
| 0 | | | 23.94 | | 817.88 | | | | |
| 5 | 7.5669 | 17.3144 | 18.3527 | 60.36 | 627.02 | 0.65 | | | |
| 10 | 7.8936 | 17.536 | 18.494 | 62.9 | 696.00 | 0.67 | | | |
| 20 | 7.7991 | 17.2664 | 18.2926 | 58.16 | 594.72 | 0.61 | | | |
| 40 | 7.5831 | 17.3292 | 18.3188 | 47.62 | 516.61 | 0.51 | | | |

| | | | | | | | | | |
|-----------|-----------|----------|-----------|--------------|-------------|--------|--|--------------|------------|
| 80 | 7.8097 | 17.3699 | 18.3033 | 32.71 | 367.74 | 0.34 | | | |
| 130 | 8.1336 | 17.7767 | 18.7791 | 24.19 | 256.90 | 0.26 | | | |
| 180 | 7.7869 | 17.5871 | 18.5209 | 16.09 | 184.95 | 0.17 | | | |
| | | 122.179 | 129.061 | | | 3.21 | | 13.21 | 80.72 |
| run 31 | | | | | | | | | |
| Time min. | Empty (g) | with H2O | with sol. | ICP Pd (ppm) | true ppm Pd | mg out | | mg Pd plated | conversion |
| 0 | | | 23.9483 | | 817.59 | | | | |
| 5 | 8.4669 | 17.7592 | 18.6017 | 54.25 | 652.60 | 0.55 | | | |
| 10 | 7.7187 | 17.1805 | 18.1288 | 56.91 | 624.74 | 0.59 | | | |
| 20 | 8.013 | 17.5217 | 18.4697 | 53.67 | 591.99 | 0.56 | | | |
| 40 | 7.3914 | 16.7936 | 17.7504 | 45.51 | 492.72 | 0.47 | | | |
| 80 | 7.9725 | 17.4837 | 18.421 | 31.45 | 350.59 | 0.33 | | | |
| 130 | 7.4828 | 16.8839 | 17.7835 | 21.41 | 245.15 | 0.22 | | | |
| 180 | 7.9454 | 17.3123 | 18.2185 | 13.96 | 158.26 | 0.14 | | | |
| | | 120.934 | 127.373 | | | 2.87 | | 13.94 | 83.42 |
| run 32 | | | | | | | | | |
| Time min. | Empty (g) | with H2O | with sol. | ICP Pd (ppm) | true ppm Pd | mg out | | mg Pd plated | conversion |
| 0 | 7.646 | 17.1361 | 18.0452 | 83.80 | 958.59 | 0.87 | | | |
| 5 | 7.7409 | 17.3937 | 18.4223 | 80.94 | 840.51 | 0.86 | | | |
| 10 | 7.5473 | 17.3167 | 18.3697 | 73.26 | 752.94 | 0.79 | | | |
| 20 | 7.5636 | 17.2574 | 18.208 | 59.39 | 665.02 | 0.63 | | | |
| 40 | 7.7707 | 17.4849 | 18.4264 | 46.29 | 523.90 | 0.49 | | | |
| 80 | 8.014 | 17.7625 | 18.6727 | 34.6 | 405.18 | 0.37 | | | |
| 130 | 8.2176 | 17.8522 | 18.8643 | 28.78 | 302.75 | 0.31 | | | |
| 180 | 8.1995 | 17.8457 | 18.806 | 23.89 | 263.86 | 0.25 | | | |
| | | 122.913 | 129.769 | | | 3.71 | | 11.57 | 72.81 |
| run 33 | | | | | | | | | |
| Time min. | Empty (g) | with H2O | with sol. | ICP Pd (ppm) | true ppm Pd | mg out | | mg Pd plated | conversion |
| 0 | | | 21.698 | | 902.39 | | | | |
| 5 | 7.6797 | 17.0123 | 18.0126 | 64.35 | 664.72 | 0.66 | | | |

| | | | | | | | | | |
|-----------|-----------|----------|-----------|--------------|-------------|--------|--|--------------|------------|
| 10 | 7.806 | 17.0942 | 19.0149 | 58.68 | 342.45 | 0.66 | | | |
| 20 | 7.7154 | 17.0356 | 17.9636 | 52.04 | 574.69 | 0.53 | | | |
| 40 | 7.9742 | 17.2773 | 18.0695 | 35.06 | 446.78 | 0.35 | | | |
| 80 | 7.7137 | 17.1582 | 18.1125 | 27.95 | 304.57 | 0.29 | | | |
| 130 | 7.7538 | 17.0156 | 17.946 | 19.42 | 212.74 | 0.20 | | | |
| 180 | 7.593 | 16.8286 | 17.7392 | 17.12 | 190.76 | 0.17 | | | |
| | | 119.421 | 126.858 | | | 2.87 | | 13.99 | 83.72 |
| run 34 | | | | | | | | | |
| Time min. | Empty (g) | with H2O | with sol. | ICP Pd (ppm) | true ppm Pd | mg out | | mg Pd plated | conversion |
| 0 | 7.8191 | 17.2738 | 18.2154 | 86.60 | 956.16 | 0.90 | | | |
| 5 | 7.512 | 17.1851 | 18.1461 | 76.91 | 851.06 | 0.82 | | | |
| 10 | 7.9134 | 17.4124 | 18.3441 | 69.43 | 777.29 | 0.72 | | | |
| 20 | 7.7636 | 17.3392 | 18.3431 | 66.53 | 701.12 | 0.70 | | | |
| 40 | 7.5554 | 17.1133 | 18.097 | 51.18 | 548.46 | 0.54 | | | |
| 80 | 8.1879 | 17.8067 | 18.7867 | 32.67 | 353.33 | 0.35 | | | |
| 130 | 8.1767 | 17.7417 | 18.6642 | 20.8 | 236.47 | 0.22 | | | |
| 180 | 7.5704 | 17.142 | 18.0895 | 15.13 | 167.97 | 0.16 | | | |
| | | 121.740 | 128.470 | | | 3.51 | | 13.27 | 82.59 |
| run 35 | | | | | | | | | |
| Time min. | Empty (g) | with H2O | with sol. | ICP Pd (ppm) | true ppm Pd | mg out | | mg Pd plated | conversion |
| 0 | 7.6562 | 17.1413 | 18.0863 | 83.87 | 925.69 | 0.87 | | | |
| 5 | 8.0012 | 17.5724 | 18.5299 | 66.52 | 731.46 | 0.70 | | | |
| 10 | 7.822 | 17.4399 | 18.4034 | 60.92 | 669.01 | 0.64 | | | |
| 20 | 8.0883 | 17.6948 | 18.6837 | 52.38 | 561.22 | 0.55 | | | |
| 40 | 7.8986 | 17.5806 | 18.561 | 36.84 | 400.66 | 0.39 | | | |
| 80 | 7.8037 | 17.3411 | 18.1005 | 22.09 | 299.52 | 0.23 | | | |
| 130 | 8.0669 | 17.7073 | 18.6529 | 12.58 | 140.83 | 0.13 | | | |
| 180 | 8.0874 | 17.6244 | 18.5669 | 10.36 | 115.19 | 0.11 | | | |
| | | 122.960 | 129.498 | | | 2.76 | | 15.52 | 92.29 |
| run 37 | | | | | | | | | |
| Time | Empty | with H2O | with sol. | ICP Pd | true ppm | mg out | | mg Pd | conversion |

| | | | | | | | | | |
|-----------|-----------|----------|-----------|--------------|-------------|--------|--|--------------|------------|
| min. | (g) | | | (ppm) | Pd | | | plated | sion |
| 0 | | | 22.8723 | | 856.06 | | | plated | sion |
| 5 | 7.7324 | 17.596 | 18.5909 | 54.39 | 593.62 | 0.59 | | | |
| 10 | 8.0575 | 17.913 | 18.9395 | 54.2 | 574.58 | 0.59 | | | |
| 20 | 7.8417 | 17.6574 | 18.8867 | 58.46 | 525.25 | 0.65 | | | |
| 40 | 7.5394 | 17.2112 | 18.1434 | 27.6 | 313.96 | 0.29 | | | |
| | | 70.3776 | 97.4328 | | | 2.12 | | 11.59 | 66.40 |
| run 38 | | | | | | | | | |
| Time min. | Empty (g) | with H2O | with sol. | ICP Pd (ppm) | true ppm Pd | mg out | | mg Pd plated | conversion |
| 0 | | | 23.5324 | | 832.04 | | | | |
| 5 | 7.7092 | 17.5061 | 18.4124 | 49.85 | 588.72 | 0.53 | | | |
| 10 | 7.8643 | 17.7122 | 18.6825 | 56.15 | 626.04 | 0.61 | | | |
| 20 | 8.3582 | 18.0375 | 19.0338 | 56.03 | 600.38 | 0.60 | | | |
| 40 | 7.6946 | 17.2939 | 18.5734 | 59.58 | 506.57 | 0.65 | | | |
| 80 | 7.545 | 17.2525 | 18.1688 | 28.19 | 326.84 | 0.30 | | | |
| 130 | 7.7991 | 17.3565 | 18.2589 | 18.67 | 216.41 | 0.20 | | | |
| 180 | 7.7622 | 17.4614 | 18.3559 | 12.33 | 146.03 | 0.13 | | | |
| | | 122.6201 | 129.485 | | | 3.01 | | 14.13 | 85.31 |
| run 39 | | | | | | | | | |
| Time min. | Empty (g) | with H2O | with sol. | ICP Pd (ppm) | true ppm Pd | mg out | | mg Pd plated | conversion |
| 0 | | | 23.1877 | | 844.41 | | | | |
| 5 | 7.657 | 17.4269 | 18.3943 | 60.17 | 667.83 | 0.65 | | | |
| 10 | 7.9805 | 17.5682 | 18.5718 | 58.43 | 616.63 | 0.62 | | | |
| 20 | 8.1617 | 17.8556 | 18.8497 | 51.25 | 551.01 | 0.55 | | | |
| 40 | 7.6654 | 17.2815 | 18.2501 | 35.44 | 387.28 | 0.38 | | | |
| | | 70.1322 | 74.0659 | | | 2.19 | | 9.94 | 57.13 |
| run 40 | | | | | | | | | |
| Time min. | Empty (g) | with H2O | with sol. | ICP Pd (ppm) | true ppm Pd | mg out | | mg Pd plated | conversion |
| 0 | | | 22.5753 | | 867.32 | | | | |
| 5 | 7.8654 | 17.8182 | 18.7892 | 60 | 675.00 | 0.66 | | | |

| | | | | | | | | | |
|-----------|-----------|----------|-----------|--------------|-------------|--------|--|--------------|------------|
| 10 | 7.9644 | 17.8041 | 18.7586 | 55.24 | 624.70 | 0.60 | | | |
| 20 | 9.0913 | 17.91 | 18.8514 | 49.57 | 513.92 | 0.48 | | | |
| 40 | 8.0348 | 17.8462 | 18.7512 | 39.55 | 468.32 | 0.42 | | | |
| 80 | 7.722 | 17.4801 | 18.6601 | 36.57 | 338.99 | 0.40 | | | |
| 130 | 7.8022 | 17.5125 | 18.4466 | 19.44 | 221.53 | 0.21 | | | |
| 180 | 8.1523 | 17.938 | 18.8366 | 16.31 | 193.92 | 0.17 | | | |
| | | 124.309 | 131.093 | | | 2.94 | | 13.58 | 81.60 |
| run 41 | | | | | | | | | |
| Time min. | Empty (g) | with H2O | with sol. | ICP Pd (ppm) | true ppm Pd | mg out | | mg Pd plated | conversion |
| 0 | 7.9166 | 17.5714 | 18.4828 | 83.90 | 972.68 | 0.89 | | | |
| 5 | 8.0576 | 17.5241 | 18.7576 | 97.75 | 847.93 | 1.05 | | | |
| 10 | 7.5012 | 16.8815 | 17.8283 | 70.62 | 770.28 | 0.73 | | | |
| 20 | 7.5576 | 16.862 | 17.8171 | 60.94 | 654.61 | 0.63 | | | |
| 40 | 7.538 | 16.8728 | 17.8445 | 45.44 | 481.97 | 0.47 | | | |
| 80 | 7.7336 | 17.0684 | 18.0592 | 29.48 | 307.23 | 0.30 | | | |
| 130 | 8.0724 | 17.4975 | 18.5262 | 20.59 | 209.24 | 0.22 | | | |
| 180 | 7.7996 | 17.2179 | 18.1692 | 14.72 | 160.45 | 0.15 | | | |
| | | 119.924 | 127.002 | | | 3.54 | | 13.51 | 84.47 |
| run 44 | | | | | | | | | |
| Time min. | Empty (g) | with H2O | with sol. | ICP Pd (ppm) | true ppm Pd | mg out | | mg Pd plated | conversion |
| 0 | | | 23.8757 | | 820.08 | | | | |
| 5 | 8.0354 | 17.8742 | 18.8322 | 59.46 | 670.12 | 0.64 | | | |
| 10 | 7.7717 | 17.5168 | 18.4572 | 55.76 | 633.59 | 0.60 | | | |
| 20 | 7.5663 | 17.0877 | 18.0802 | 63.96 | 677.55 | 0.67 | | | |
| 40 | 7.6152 | 17.2505 | 18.3848 | 72.68 | 690.06 | 0.78 | | | |
| 80 | 7.86 | 17.5977 | 18.6057 | 57.24 | 610.20 | 0.62 | | | |
| 130 | 7.6653 | 17.2559 | 18.1914 | 35.67 | 401.35 | 0.38 | | | |
| 180 | 7.8639 | 17.6933 | 18.668 | 24.29 | 269.24 | 0.26 | | | |
| | | 122.276 | 129.219 | | | 3.95 | | 11.08 | 70.84 |
| run 45 | | | | | | | | | |
| Time | Empty | with H2O | with sol. | ICP Pd | true ppm | mg out | | mg Pd | conver- |

| | | | | | | | | | |
|-----------|-----------|----------|-----------|--------------|-------------|--------|--|--------------|------------|
| min. | (g) | | | (ppm) | Pd | | | plated | sion |
| 0 | | | 22.5167 | | 869.58 | | | | |
| 5 | 7.9157 | 17.7482 | 18.7723 | 60.6 | 642.43 | 0.66 | | | |
| 10 | 7.9011 | 17.7016 | 18.5777 | 55.67 | 678.42 | 0.59 | | | |
| 20 | 7.6675 | 17.4742 | 18.4492 | 62.76 | 694.01 | 0.68 | | | |
| 40 | 7.624 | 17.4276 | 18.338 | 51.14 | 601.84 | 0.55 | | | |
| 80 | 7.7445 | 17.5534 | 18.5438 | 55.07 | 600.48 | 0.59 | | | |
| 130 | 7.5981 | 17.3981 | 18.3243 | 44.55 | 515.93 | 0.48 | | | |
| 180 | 8.1054 | 17.9225 | 18.8164 | 35.17 | 421.42 | 0.38 | | | |
| | | 123.225 | 129.821 | | | 3.93 | | 8.94 | 57.14 |
| run 46 | | | | | | | | | |
| Time min. | Empty (g) | with H2O | with sol. | ICP Pd (ppm) | true ppm Pd | mg out | | mg Pd plated | conversion |
| 0 | | | 22.3444 | | 876.28 | | | | |
| 5 | 7.804 | 17.6515 | 18.5919 | 54.31 | 623.02 | 0.59 | | | |
| 10 | 8.1197 | 17.9579 | 18.9196 | 54.84 | 615.85 | 0.59 | | | |
| 20 | 7.9453 | 17.7794 | 18.721 | 47.52 | 543.82 | 0.51 | | | |
| 40 | 7.7591 | 17.5975 | 18.4797 | 35.92 | 436.50 | 0.39 | | | |
| 80 | 7.5009 | 17.3218 | 18.2695 | 25.39 | 288.50 | 0.27 | | | |
| 130 | 8.054 | 17.8854 | 18.8775 | 15.12 | 164.95 | 0.16 | | | |
| 180 | 7.5319 | 17.2782 | 18.1692 | 7.89 | 94.20 | 0.08 | | | |
| | | 123.4717 | 130.028 | | | 2.60 | | 15.50 | 91.24 |
| run 47 | | | | | | | | | |
| Time min. | Empty (g) | with H2O | with sol. | ICP Pd (ppm) | true ppm Pd | mg out | | mg Pd plated | conversion |
| 0 | | | 22.4075 | | 873.81 | | | | |
| 5 | 7.7833 | 17.5531 | 18.5203 | 55.38 | 614.78 | 0.59 | | | |
| 10 | 8.0724 | 17.707 | 18.66 | 54.29 | 603.15 | 0.57 | | | |
| 20 | 8.077 | 17.9244 | 18.8899 | 48.63 | 544.62 | 0.53 | | | |
| 40 | 8.1551 | 17.9021 | 18.823 | 39.93 | 462.56 | 0.43 | | | |
| 80 | 7.5678 | 17.1303 | 18.0418 | 26.35 | 302.79 | 0.28 | | | |
| | | 88.2169 | 92.935 | | | 2.40 | | 11.83 | 68.83 |
| run 48 | | | | | | | | | |

| Time min. | Empty (g) | with H2O | with sol. | ICP Pd (ppm) | true ppm Pd | mg out | | mg Pd plated | conversion |
|-----------|-----------|----------|-----------|--------------|-------------|--------|--|--------------|------------|
| 0 | | | 22.2395 | | 880.42 | | | | |
| 5 | 7.6286 | 17.3583 | 18.3143 | 52.98 | 592.18 | 0.57 | | | |
| 10 | 7.5082 | 17.3093 | 18.257 | 51.91 | 588.76 | 0.56 | | | |
| 20 | 7.6028 | 17.2036 | 18.1479 | 45.36 | 506.54 | 0.48 | | | |
| 40 | 7.7734 | 17.3481 | 18.27 | 35.94 | 409.21 | 0.38 | | | |
| 80 | 6.5135 | 16.2162 | 17.0168 | 20 | 262.39 | 0.21 | | | |
| 130 | 6.4904 | 16.356 | 17.2612 | 15.13 | 180.03 | 0.16 | | | |
| 180 | 6.5424 | 16.3725 | 17.2821 | 8.25 | 97.41 | 0.09 | | | |
| | | 118.164 | 124.549 | | | 2.44 | | 15.59 | 90.99 |
| run 49 | | | | | | | | | |
| Time min. | Empty (g) | with H2O | with sol. | ICP Pd (ppm) | true ppm Pd | mg out | | mg Pd plated | conversion |
| 0 | | | 23.9032 | | 819.14 | | | | |
| 5 | 8.1184 | 17.3004 | 18.2098 | 76.78 | 852.01 | 0.77 | | | |
| 10 | 7.5243 | 16.9935 | 17.999 | 60.6 | 631.29 | 0.63 | | | |
| 20 | 7.5724 | 17.0868 | 18.1178 | 57.42 | 587.31 | 0.61 | | | |
| 40 | 7.865 | 17.3509 | 18.2664 | 42.75 | 485.70 | 0.44 | | | |
| 80 | 7.5341 | 16.9442 | 17.8962 | 32.42 | 352.88 | 0.34 | | | |
| 130 | 7.5716 | 17.0122 | 17.8372 | 18.04 | 224.47 | 0.19 | | | |
| 180 | 7.5053 | 16.9552 | 17.8817 | 13.24 | 148.28 | 0.14 | | | |
| | | 119.6432 | 126.208 | | | 3.12 | | 13.89 | 84.38 |
| run 50 | | | | | | | | | |
| Time min. | Empty (g) | with H2O | with sol. | ICP Pd (ppm) | true ppm Pd | mg out | | mg Pd plated | conversion |
| 0 | | | 22.0752 | | 886.97 | | | | |
| 5 | 7.9736 | 17.0854 | 18.0831 | 69.69 | 706.16 | 0.70 | | | |
| 10 | 8.133 | 17.2885 | 18.1991 | 55.36 | 611.97 | 0.56 | | | |
| 20 | 7.4695 | 16.8625 | 17.7924 | 53.35 | 592.24 | 0.55 | | | |
| 40 | 7.8856 | 17.1506 | 18.0949 | 46.82 | 506.19 | 0.48 | | | |
| 80 | 7.9535 | 17.2993 | 18.249 | 33.4 | 362.08 | 0.34 | | | |
| 130 | 7.4995 | 16.9224 | 17.8298 | 22.54 | 256.61 | 0.23 | | | |
| 180 | 8.1094 | 17.4255 | 18.3488 | 18.35 | 203.50 | 0.19 | | | |

| | | | | | | | | | |
|-----------|-----------|----------|-----------|--------------|-------------|--------|--|--------------|------------|
| | | 120.0342 | 126.597 | | | 3.06 | | 13.37 | 80.90 |
| run 51 | | | | | | | | | |
| Time min. | Empty (g) | with H2O | with sol. | ICP Pd (ppm) | true ppm Pd | mg out | | mg Pd plated | conversion |
| 0 | | | 22.3223 | | 877.15 | | | | |
| 5 | 8.0959 | 17.4246 | 18.384 | 61.13 | 655.53 | 0.63 | | | |
| 10 | 7.5036 | 16.9177 | 17.8752 | 63.15 | 684.04 | 0.65 | | | |
| 20 | 7.5508 | 16.946 | 17.947 | 61.16 | 635.20 | 0.64 | | | |
| 40 | 7.6732 | 16.9677 | 17.9828 | 53.77 | 546.10 | 0.55 | | | |
| 80 | 7.7334 | 17.3629 | 18.2882 | 34.63 | 395.02 | 0.37 | | | |
| 130 | 8.0116 | 17.5869 | 18.4654 | 22.77 | 270.95 | 0.24 | | | |
| 180 | 7.6885 | 17.3994 | 18.3461 | 16.6 | 186.88 | 0.18 | | | |
| | | 120.6052 | 127.288 | | | 3.25 | | 13.40 | 82.10 |
| run 52 | | | | | | | | | |
| Time min. | Empty (g) | with H2O | with sol. | ICP Pd (ppm) | true ppm Pd | mg out | | mg Pd plated | conversion |
| 0 | | | 22.1778 | | 882.86 | | | | |
| 5 | 7.8197 | 17.3953 | 18.3409 | 60.68 | 675.15 | 0.64 | | | |
| 10 | 7.5554 | 17.0856 | 18.0658 | 62.06 | 665.45 | 0.65 | | | |
| 20 | 7.8148 | 17.272 | 18.2251 | 53.93 | 589.05 | 0.56 | | | |
| 40 | 8.0826 | 17.8936 | 18.8928 | 44.3 | 479.28 | 0.48 | | | |
| 80 | 7.9013 | 17.4899 | 18.4218 | 29.82 | 336.65 | 0.31 | | | |
| 130 | 8.2326 | 17.6021 | 18.513 | 20.33 | 229.44 | 0.21 | | | |
| 180 | 7.8411 | 17.3892 | 18.3223 | 13.68 | 153.66 | 0.14 | | | |
| | | 122.1277 | 128.781 | | | 3.00 | | 14.20 | 85.62 |
| run 53 | | | | | | | | | |
| Time min. | Empty (g) | with H2O | with sol. | ICP Pd (ppm) | true ppm Pd | mg out | | mg Pd plated | conversion |
| 0 | 7.9652 | 17.5584 | 18.467 | 82.10 | 948.93 | 0.86 | | | |
| 5 | 8.1573 | 17.6597 | 18.641 | 79.51 | 849.44 | 0.83 | | | |
| 10 | 7.8154 | 17.2654 | 18.2908 | 76.58 | 782.33 | 0.80 | | | |
| 20 | 7.8697 | 17.4775 | 18.4598 | 66.13 | 712.94 | 0.70 | | | |
| 40 | 8.0919 | 17.4009 | 18.3745 | 56.76 | 599.47 | 0.58 | | | |

| | | | | | | | | | |
|-----|--------|----------|---------|-------|--------|------|--|-------|-------|
| 80 | 8.0193 | 17.5106 | 18.4907 | 40.91 | 437.08 | 0.43 | | | |
| 130 | 7.3944 | 16.9007 | 17.8634 | 28.56 | 310.58 | 0.30 | | | |
| 180 | 7.5756 | 17.269 | 18.2875 | 21.63 | 227.49 | 0.23 | | | |
| | | 121.4838 | 128.407 | | | 3.88 | | 12.21 | 77.44 |

Kinetic data for Pd-Ag co-deposition

MF1BA

hydrazine (0.02M): 250 ml per litre plating solution

Ag salt: 0.02 g per litre

| time (min) | empty bottle (g) | with added water (g) | with solution (g) | measured Ag (ppm) | actual Ag (ppm) | Ag extracted (g) | Ag in solution (g) | Ag (g) on membrane | measured Pd (ppm) | actual Pd (ppm) | Pd extracted (g) | Pd in solution (g) | Pd (g) on membrane |
|------------|------------------|----------------------|-------------------|-------------------|-----------------|------------------|--------------------|--------------------|-------------------|-----------------|------------------|--------------------|--------------------|
| 0 | | | | | 18.00 | | 0.000432 | 0.000000 | | 207.42 | | 0.004978 | 0.000000 |
| 5 | 6.6512 | 9.8808 | 10.9126 | 4.25 | 17.55 | 0.000018 | 0.000421 | 0.000011 | 41.72 | 172.31 | 0.000178 | 0.004135 | 0.000843 |
| 10 | 6.2550 | 9.6917 | 10.6904 | 4.01 | 17.81 | 0.000018 | 0.000410 | 0.000005 | 33.22 | 147.54 | 0.000147 | 0.003393 | 0.001412 |
| 20 | 6.5896 | 9.7342 | 10.7125 | 3.91 | 16.48 | 0.000016 | 0.000363 | 0.000034 | 37.34 | 157.36 | 0.000154 | 0.003462 | 0.001196 |
| 30 | 6.4882 | 9.9231 | 10.9250 | 3.54 | 15.68 | 0.000016 | 0.000329 | 0.000051 | 32.64 | 144.54 | 0.000145 | 0.003035 | 0.001465 |
| 40 | 6.8111 | 10.2211 | 11.2139 | 3.32 | 14.72 | 0.000015 | 0.000294 | 0.000070 | 32.43 | 143.82 | 0.000143 | 0.002876 | 0.001480 |
| 50 | 6.7958 | 10.2273 | 11.2113 | 2.31 | 10.37 | 0.000010 | 0.000197 | 0.000153 | 28.46 | 127.71 | 0.000126 | 0.002426 | 0.001786 |
| 60 | 6.7240 | 10.2107 | 11.2201 | 2.01 | 8.95 | 0.000009 | 0.000170 | 0.000180 | 25.89 | 115.32 | 0.000116 | 0.002191 | 0.002021 |
| 80 | 6.8417 | 10.2671 | 11.3002 | 1.43 | 6.17 | 0.000006 | 0.000105 | 0.000224 | 24.56 | 105.99 | 0.000110 | 0.001802 | 0.002155 |
| 100 | 6.5167 | 9.8978 | 10.9250 | 0.69 | 2.96 | 0.000003 | 0.000047 | 0.000275 | 18.09 | 77.63 | 0.000080 | 0.001242 | 0.002609 |
| 120 | 6.3375 | 9.7777 | 10.7723 | 0.36 | 1.61 | 0.000002 | 0.000024 | 0.000296 | 12.78 | 56.98 | 0.000057 | 0.000855 | 0.002919 |
| Totals: | | | | | | 0.000113 | | 0.000296 | | | 0.001255 | | 0.002919 |

MF1BA

hydrazine (0.02M): 500 ml per litre plating solution

Ag salt: 0.02 g per litre

| time (min) | empty bottle (g) | with added water (g) | with solution (g) | measured Ag (ppm) | actual Ag (ppm) | Ag extracted (g) | Ag in solution (g) | Ag (g) on membrane | measured Pd (ppm) | actual Pd (ppm) | Pd extracted (g) | Pd in solution (g) | Pd (g) on membrane |
|------------|------------------|----------------------|-------------------|-------------------|-----------------|------------------|--------------------|--------------------|-------------------|-----------------|------------------|--------------------|--------------------|
|------------|------------------|----------------------|-------------------|-------------------|-----------------|------------------|--------------------|--------------------|-------------------|-----------------|------------------|--------------------|--------------------|

| | | | | | | | | | | | | | | |
|---------|--------|---------|---------|--|-------|-------|----------|----------|----------|--------|--------|----------|----------|----------|
| 0 | | | | | 18.00 | | 0.000432 | 0.000296 | | 207.42 | | 0.004978 | 0.002919 | |
| 5 | 6.3647 | 9.8045 | 10.9202 | | 4.99 | 20.37 | 0.000023 | 0.000489 | 0.000239 | 36.66 | 149.69 | 0.000167 | 0.003592 | 0.004304 |
| 10 | 6.7705 | 10.3376 | 11.3840 | | 4.24 | 18.69 | 0.000020 | 0.000430 | 0.000279 | 35.74 | 157.58 | 0.000165 | 0.003624 | 0.004115 |
| 20 | 6.9000 | 10.5767 | 11.6180 | | 4.27 | 19.35 | 0.000020 | 0.000426 | 0.000263 | 35.78 | 162.11 | 0.000169 | 0.003567 | 0.004006 |
| 30 | 6.8145 | 10.1868 | 11.2111 | | 4.81 | 20.65 | 0.000021 | 0.000434 | 0.000232 | 41.68 | 178.90 | 0.000183 | 0.003757 | 0.003603 |
| 40 | 6.2860 | 9.5895 | 10.5784 | | 4.25 | 18.45 | 0.000018 | 0.000369 | 0.000285 | 45.87 | 199.10 | 0.000197 | 0.003982 | 0.003118 |
| 50 | 6.6318 | 10.1163 | 11.1206 | | 3.95 | 17.65 | 0.000018 | 0.000335 | 0.000304 | 39.25 | 175.43 | 0.000176 | 0.003333 | 0.003686 |
| 60 | 7.6630 | 11.1383 | 12.1535 | | 3.85 | 17.03 | 0.000017 | 0.000307 | 0.000319 | 37.73 | 166.89 | 0.000169 | 0.003004 | 0.003891 |
| 80 | 7.5922 | 11.1921 | 12.2004 | | 3.34 | 15.26 | 0.000015 | 0.000259 | 0.000361 | 34.36 | 157.03 | 0.000158 | 0.002670 | 0.004128 |
| 100 | 7.9369 | 11.3009 | 12.2810 | | 2.84 | 12.59 | 0.000012 | 0.000201 | 0.000426 | 29.94 | 132.70 | 0.000130 | 0.002123 | 0.004712 |
| 120 | 7.6090 | 10.7349 | 11.7160 | | 2.40 | 10.05 | 0.000010 | 0.000151 | 0.000487 | 26.41 | 110.56 | 0.000108 | 0.001658 | 0.005243 |
| Totals: | | | | | | | 0.000174 | | 0.000487 | | | 0.001623 | | 0.005243 |
| MF1CA | | | | | | | | | | | | | | |

hydrazine (0.02M): 250 ml per litre plating solution

Ag salt: 0.06 g per litre

| time (min) | empty bottle (g) | with added water (g) | with solution (g) | measured Ag (ppm) | actual Ag (ppm) | Ag extracted (g) | Ag in solution (g) | Ag (g) on membrane | measured Pd (ppm) | actual Pd (ppm) | Pd extracted (g) | Pd in solution (g) | Pd (g) on membrane |
|------------|------------------|----------------------|-------------------|-------------------|-----------------|------------------|--------------------|--------------------|-------------------|-----------------|------------------|--------------------|--------------------|
| 0 | | | | | 54.00 | | 0.001296 | 0.000000 | | 207.42 | | 0.004978 | 0.000000 |
| 5 | 6.3618 | 10.7667 | 11.7395 | 7.79 | 43.06 | 0.000042 | 0.001034 | 0.000262 | 31.44 | 173.80 | 0.000169 | 0.004171 | 0.000807 |
| 10 | 6.4254 | 10.7376 | 11.7032 | 5.40 | 29.52 | 0.000029 | 0.000679 | 0.000574 | 21.55 | 117.79 | 0.000114 | 0.002709 | 0.002095 |
| 20 | 6.3170 | 10.5207 | 11.4800 | 5.11 | 27.50 | 0.000026 | 0.000605 | 0.000618 | 24.74 | 133.15 | 0.000128 | 0.002929 | 0.001757 |
| 30 | 6.3545 | 10.5299 | 11.4537 | 4.29 | 23.68 | 0.000022 | 0.000497 | 0.000699 | 21.90 | 120.88 | 0.000112 | 0.002539 | 0.002015 |
| 40 | 6.3336 | 10.5310 | 11.5015 | 4.04 | 21.51 | 0.000021 | 0.000430 | 0.000742 | 22.05 | 117.42 | 0.000114 | 0.002348 | 0.002084 |
| 50 | 6.4130 | 10.4252 | 11.4399 | 3.52 | 17.44 | 0.000018 | 0.000331 | 0.000819 | 21.71 | 107.55 | 0.000109 | 0.002044 | 0.002272 |
| 60 | 6.6550 | 10.8446 | 11.8282 | 2.71 | 14.25 | 0.000014 | 0.000257 | 0.000877 | 21.58 | 113.50 | 0.000112 | 0.002043 | 0.002165 |
| 80 | 6.5144 | 10.4813 | 11.4584 | 1.69 | 8.55 | 0.000008 | 0.000145 | 0.000970 | 18.85 | 95.38 | 0.000093 | 0.001621 | 0.002478 |
| 100 | 6.2935 | 10.4459 | 11.4076 | 1.15 | 6.12 | 0.000006 | 0.000098 | 0.001009 | 16.80 | 89.34 | 0.000086 | 0.001429 | 0.002575 |
| 120 | 6.4639 | 10.7240 | 11.8353 | 0.64 | 3.09 | 0.000003 | 0.000046 | 0.001055 | 13.49 | 65.20 | 0.000072 | 0.000978 | 0.002937 |
| Totals: | | | | | | 0.000189 | | 0.001055 | | | 0.001109 | | 0.002937 |
| MF1CA | | | | | | | | | | | | | |

| hydrazine (0.02M): 500 ml per litre plating solution | | | | | | | | | | | | | | |
|--|------------------|----------------------|-------------------|--|-------------------|-----------------|------------------|--------------------|--------------------|-------------------|-----------------|------------------|--------------------|--------------------|
| Ag salt: 0.06 g per litre | | | | | | | | | | | | | | |
| time (min) | empty bottle (g) | with added water (g) | with solution (g) | | measured Ag (ppm) | actual Ag (ppm) | Ag extracted (g) | Ag in solution (g) | Ag (g) on membrane | measured Pd (ppm) | actual Pd (ppm) | Pd extracted (g) | Pd in solution (g) | Pd (g) on membrane |
| 0 | | | | | | 54.00 | | 0.001296 | 0.001055 | | 207.42 | | 0.004978 | 0.002937 |
| 5 | 6.3418 | 10.7212 | 11.7475 | | 7.59 | 39.98 | 0.000041 | 0.000959 | 0.001391 | 31.89 | 167.97 | 0.000172 | 0.004031 | 0.003884 |
| 10 | 6.6284 | 10.5477 | 11.5743 | | 6.61 | 31.85 | 0.000033 | 0.000732 | 0.001586 | 27.57 | 132.83 | 0.000136 | 0.003055 | 0.004727 |
| 20 | 6.8729 | 11.1446 | 12.0844 | | 7.20 | 39.93 | 0.000038 | 0.000878 | 0.001393 | 30.22 | 167.58 | 0.000157 | 0.003687 | 0.003893 |
| 30 | 6.4855 | 10.7358 | 11.6983 | | 7.03 | 38.07 | 0.000037 | 0.000800 | 0.001437 | 31.08 | 168.33 | 0.000162 | 0.003535 | 0.003875 |
| 40 | 6.3385 | 10.7118 | 11.6796 | | 6.50 | 35.87 | 0.000035 | 0.000717 | 0.001490 | 30.34 | 167.44 | 0.000162 | 0.003349 | 0.003897 |
| 50 | 6.3200 | 10.5578 | 11.7064 | | 6.84 | 32.08 | 0.000037 | 0.000609 | 0.001581 | 36.63 | 171.78 | 0.000197 | 0.003264 | 0.003793 |
| 60 | 7.7410 | 11.8779 | 12.8529 | | 7.30 | 38.27 | 0.000037 | 0.000689 | 0.001432 | 32.76 | 171.76 | 0.000167 | 0.003092 | 0.003793 |
| 80 | 7.5953 | 11.8753 | 12.7916 | | 5.84 | 33.12 | 0.000030 | 0.000563 | 0.001556 | 29.42 | 166.84 | 0.000153 | 0.002836 | 0.003911 |
| 100 | 7.7794 | 12.0181 | 12.9904 | | 4.88 | 26.15 | 0.000025 | 0.000418 | 0.001723 | 32.98 | 176.75 | 0.000172 | 0.002828 | 0.003673 |
| 120 | 7.4787 | 11.6820 | 12.6486 | | 3.36 | 17.97 | 0.000017 | 0.000270 | 0.001919 | 33.16 | 177.36 | 0.000171 | 0.002660 | 0.003659 |
| Totals: | | | | | | | 0.000330 | | 0.0019194 | | | 0.006512 | | 0.003658 |
| MF1CB | | | | | | | | | | | | | | |

| hydrazine (0.02M): 500 ml per litre plating solution | | | | | | | | | | | | | | |
|--|------------------|----------------------|-------------------|--|-------------------|-----------------|------------------|--------------------|--------------------|-------------------|-----------------|------------------|--------------------|--------------------|
| Ag salt: 0.10 g per litre | | | | | | | | | | | | | | |
| time (min) | empty bottle (g) | with added water (g) | with solution (g) | | measured Ag (ppm) | actual Ag (ppm) | Ag extracted (g) | Ag in solution (g) | Ag (g) on membrane | measured Pd (ppm) | actual Pd (ppm) | Pd extracted (g) | Pd in solution (g) | Pd (g) on membrane |
| 0 | | | | | | 90.00 | | 0.002160 | 0.000000 | | 207.42 | | 0.004978 | 0.000000 |
| 5 | 6.8176 | 11.2395 | 12.2330 | | 9.91 | 54.02 | 0.000054 | 0.001296 | 0.000864 | 23.69 | 129.13 | 0.000128 | 0.003099 | 0.001879 |
| 10 | 6.6018 | 10.8595 | 11.8610 | | 6.70 | 35.18 | 0.000035 | 0.000809 | 0.001297 | 19.80 | 103.98 | 0.000104 | 0.002391 | 0.002457 |
| 20 | 6.5203 | 10.7208 | 11.7100 | | 4.21 | 22.09 | 0.000022 | 0.000486 | 0.001585 | 15.24 | 79.95 | 0.000079 | 0.001759 | 0.002986 |
| 30 | 6.6218 | 10.8467 | 11.8340 | | 10.07 | 53.16 | 0.000052 | 0.001116 | 0.000932 | 31.61 | 166.88 | 0.000165 | 0.003504 | 0.001161 |
| 40 | 6.5032 | 10.7238 | 11.7033 | | 9.11 | 48.36 | 0.000047 | 0.000967 | 0.001028 | 32.65 | 173.34 | 0.000170 | 0.003467 | 0.001031 |
| 50 | 7.1122 | 11.1970 | 12.1809 | | 9.59 | 49.40 | 0.000049 | 0.000939 | 0.001009 | 33.16 | 170.83 | 0.000168 | 0.003246 | 0.001079 |
| 60 | 6.5120 | 10.6586 | 11.6174 | | 9.30 | 49.52 | 0.000047 | 0.000891 | 0.001006 | 35.05 | 186.63 | 0.000179 | 0.003359 | 0.000795 |
| 80 | 6.6361 | 10.8643 | 11.8277 | | 8.80 | 47.42 | 0.000046 | 0.000806 | 0.001042 | 35.81 | 192.97 | 0.000186 | 0.003281 | 0.000703 |
| 100 | 6.7650 | 10.9722 | 11.7631 | | 6.60 | 41.71 | 0.000033 | 0.000667 | 0.001134 | 30.36 | 191.86 | 0.000152 | 0.003070 | 0.000720 |

| | | | | | | | | | | | | | | |
|---------|--------|---------|---------|--|------|-------|----------|----------|----------|-------|--------|----------|----------|----------|
| 120 | 6.6046 | 10.7894 | 11.8108 | | 6.94 | 35.37 | 0.000036 | 0.000531 | 0.001229 | 35.09 | 178.86 | 0.000183 | 0.002683 | 0.000915 |
| Totals: | | | | | | | 0.000422 | | 0.001229 | | | 0.001513 | | 0.000915 |
| MF1CB | | | | | | | | | | | | | | |

hydrazine (0.02M): 500 ml per litre plating solution

Ag salt: 0.10 g per litre

| time (min) | empty bottle (g) | with added water (g) | with solution (g) | | measured Ag (ppm) | actual Ag (ppm) | Ag extracted (g) | Ag in solution (g) | Ag (g) on membrane | measured Pd (ppm) | actual Pd (ppm) | Pd extracted (g) | Pd in solution (g) | Pd (g) on membrane |
|------------|------------------|----------------------|-------------------|--|-------------------|-----------------|------------------|--------------------|--------------------|-------------------|-----------------|------------------|--------------------|--------------------|
| 0 | | | | | | 90.00 | | 0.002160 | 0.001229 | | 207.42 | | 0.004978 | 0.000915 |
| 5 | 6.7382 | 11.1484 | 12.1970 | | 9.85 | 51.28 | 0.000054 | 0.001231 | 0.002158 | 32.89 | 171.22 | 0.000180 | 0.004109 | 0.001784 |
| 10 | 6.5364 | 10.9173 | 11.8675 | | 9.94 | 55.77 | 0.000053 | 0.001283 | 0.002050 | 31.57 | 177.12 | 0.000168 | 0.004074 | 0.001643 |
| 20 | 6.5063 | 10.6373 | 11.6571 | | 10.24 | 51.72 | 0.000053 | 0.001138 | 0.002147 | 33.39 | 168.65 | 0.000172 | 0.003710 | 0.001846 |
| 30 | 7.2967 | 11.4279 | 12.3719 | | 7.54 | 40.54 | 0.000038 | 0.000851 | 0.002416 | 36.72 | 197.42 | 0.000186 | 0.004146 | 0.001156 |
| 40 | 6.8405 | 10.7700 | 11.7684 | | 8.79 | 43.39 | 0.000043 | 0.000868 | 0.002347 | 34.78 | 171.67 | 0.000171 | 0.003433 | 0.001774 |
| 50 | 6.4104 | 10.5243 | 11.5123 | | 9.95 | 51.38 | 0.000051 | 0.000976 | 0.002156 | 34.77 | 179.55 | 0.000177 | 0.003411 | 0.001584 |
| 60 | 7.8606 | 11.9675 | 12.9606 | | 7.73 | 39.70 | 0.000039 | 0.000715 | 0.002436 | 32.51 | 166.95 | 0.000166 | 0.003005 | 0.001887 |
| 80 | 7.6206 | 11.7725 | 12.6862 | | 8.47 | 46.96 | 0.000043 | 0.000798 | 0.002262 | 36.09 | 200.08 | 0.000183 | 0.003401 | 0.001091 |
| 100 | 7.5278 | 11.6050 | 12.5866 | | 5.54 | 28.55 | 0.000028 | 0.000457 | 0.002703 | 36.03 | 185.69 | 0.000182 | 0.002971 | 0.001437 |
| 120 | 8.1016 | 12.2006 | 13.1592 | | 5.26 | 27.75 | 0.000027 | 0.000416 | 0.002723 | 34.33 | 181.13 | 0.000174 | 0.002717 | 0.001546 |
| Totals: | | | | | | | 0.000429 | | 0.002723 | | | 0.001759 | | 0.001546 |
| MF1CC | | | | | | | | | | | | | | |

hydrazine (0.02M): 250 ml per litre plating solution

Ag salt: 0.06 g per litre

| time (min) | empty bottle (g) | with added water (g) | with solution (g) | | measured Ag (ppm) | actual Ag (ppm) | Ag extracted (g) | Ag in solution (g) | Ag (g) on membrane | measured Pd (ppm) | actual Pd (ppm) | Pd extracted (g) | Pd in solution (g) | Pd (g) on membrane |
|------------|------------------|----------------------|-------------------|--|-------------------|-----------------|------------------|--------------------|--------------------|-------------------|-----------------|------------------|--------------------|--------------------|
| 0 | | | | | | 54.00 | | 0.001296 | 0.000000 | | 207.42 | | 0.004978 | 0.000000 |
| 5 | 7.5384 | 12.3538 | 13.3166 | | 6.90 | 41.41 | 0.000040 | 0.000994 | 0.000302 | 29.82 | 178.96 | | 0.004295 | 0.000683 |
| 10 | 7.7558 | 12.4522 | 13.4232 | | 5.90 | 34.44 | 0.000033 | 0.000792 | 0.000463 | 28.56 | 166.70 | 0.000162 | 0.003834 | 0.000965 |
| 20 | 7.7922 | 12.2478 | 13.2302 | | 5.82 | 32.22 | 0.000032 | 0.000709 | 0.000511 | 28.91 | 160.03 | 0.000157 | 0.003521 | 0.001112 |
| 30 | 7.7665 | 11.8854 | 12.9038 | | 5.16 | 26.03 | 0.000027 | 0.000547 | 0.000641 | 26.08 | 131.56 | 0.000134 | 0.002763 | 0.001710 |

| | | | | | | | | | | | | | | |
|---------|--------|---------|---------|--|------|-------|----------|----------|----------------|-------|--------|---------------|----------|-----------|
| 40 | 7.5409 | 11.9312 | 12.8877 | | 4.82 | 26.94 | 0.000026 | 0.000539 | 0.000623 | 27.01 | 150.98 | 0.000144 | 0.003020 | 0.001321 |
| 50 | 7.6189 | 11.7562 | 12.7338 | | 3.50 | 18.31 | 0.000018 | 0.000348 | 0.000787 | 22.86 | 119.61 | 0.000117 | 0.002273 | 0.001917 |
| 60 | 7.4966 | 12.2552 | 13.2182 | | 3.95 | 23.47 | 0.000023 | 0.000422 | 0.000694 | 27.39 | 162.74 | 0.000157 | 0.002929 | 0.001141 |
| 80 | 7.5270 | 11.9816 | 12.9753 | | 2.35 | 12.88 | 0.000013 | 0.000219 | 0.000879 | 22.09 | 121.12 | 0.000120 | 0.002059 | 0.001892 |
| 100 | 7.7170 | 12.0366 | 13.0123 | | 0.87 | 4.72 | 0.000005 | 0.000076 | 0.001010 | 17.88 | 97.04 | 0.000095 | 0.001553 | 0.002277 |
| 120 | 7.7967 | 11.8298 | 13.0185 | | 0.49 | 2.15 | 0.000003 | 0.000032 | 0.001048 | 13.98 | 61.41 | 0.000073 | 0.000921 | 0.002811 |
| Totals: | | | | | | | 0.000218 | | 0.0010484 5 | | | 0.001159 1 | | 0.0028113 |
| MF1CC | | | | | | | | | | | | | | |

hydrazine (0.02M): 500 ml per litre plating solution

Ag salt: 0.06 g per litre

| time (min) | empty bottle (g) | with added water (g) | with solution (g) | | measured Ag (ppm) | actual Ag (ppm) | Ag extracted (g) | Ag in solution (g) | Ag (g) on membrane | measured Pd (ppm) | actual Pd (ppm) | Pd extracted (g) | Pd in solution (g) | Pd (g) on membrane |
|------------|------------------|----------------------|-------------------|--|-------------------|-----------------|------------------|--------------------|--------------------|-------------------|-----------------|------------------|--------------------|--------------------|
| 0 | | | | | | 54.00 | 0.000000 | 0.001296 | 0.001048 | | 207.42 | 0.000000 | 0.004978 | 0.002811 |
| 5 | 7.6125 | 11.9004 | 12.9415 | | 7.59 | 38.85 | 0.000040 | 0.000932 | 0.001412 | 31.96 | 163.59 | 0.000170 | 0.003926 | 0.003863 |
| 10 | 7.7674 | 12.0508 | 13.0643 | | 7.39 | 38.62 | 0.000039 | 0.000888 | 0.001418 | 31.71 | 165.73 | 0.000168 | 0.003812 | 0.003812 |
| 20 | 7.5973 | 11.9604 | 12.9950 | | 8.93 | 46.59 | 0.000048 | 0.001025 | 0.001226 | 41.90 | 218.60 | 0.000226 | 0.004809 | 0.002543 |
| 30 | 7.7539 | 12.4915 | 13.4537 | | 8.94 | 52.96 | 0.000051 | 0.001112 | 0.001073 | 39.83 | 235.94 | 0.000227 | 0.004955 | 0.002127 |
| 40 | 8.0460 | 12.5497 | 13.5246 | | 6.95 | 39.06 | 0.000038 | 0.000781 | 0.001407 | 30.55 | 171.68 | 0.000167 | 0.003434 | 0.003669 |
| 50 | 7.9572 | 12.1305 | 13.1482 | | 7.65 | 39.02 | 0.000040 | 0.000741 | 0.001408 | 36.32 | 185.26 | 0.000189 | 0.003520 | 0.003343 |
| 60 | 7.8009 | 12.1517 | 13.1058 | | 7.17 | 39.87 | 0.000038 | 0.000718 | 0.001388 | 33.34 | 185.37 | 0.000177 | 0.003337 | 0.003340 |
| 80 | 8.1222 | 12.3249 | 13.3151 | | 7.52 | 39.44 | 0.000039 | 0.000670 | 0.001398 | 31.49 | 165.14 | 0.000164 | 0.002807 | 0.003826 |
| 100 | 8.0698 | 12.4240 | 13.3953 | | 7.97 | 43.70 | 0.000042 | 0.000699 | 0.001296 | 36.17 | 198.31 | 0.000193 | 0.003173 | 0.003030 |
| 120 | 7.7958 | 12.2353 | 13.2026 | | 7.38 | 41.25 | 0.000040 | 0.000619 | 0.001354 | 35.81 | 200.16 | 0.000194 | 0.003002 | 0.002985 |
| Totals: | | | | | | | 0.000416 | | 0.001354 | | | 0.001874 | | 0.002985 |

Ag plating:

Silver on palladium

Vol = 20 ml; plating time = 2h

Membrane dimensions: outer diameter = 12 mm; length 6 to 8 mm

AgNO₃ = 0.65 g/l; hydrazine:AgNO₃ = 1.3:1 on molar basis

| Run | Pd layer (mg) | Temp. (°C) | EDTA: Pd | Mass before (g) | Mass after (g) | Mass loss (mg) |
|-----|---------------|------------|----------|-----------------|----------------|----------------|
| 1 | 9.3 | 55 | 20 | 0.4476 | 0.4470 | 0.6 |
| 2 | 8.3 | 55 | 40 | 0.4656 | 0.4653 | 0.3 |
| 3 | 5.2 | 55 | 60 | 0.4783 | 0.4763 | 2.0 |
| 4 | 9.2 | 55 | 80 | 0.4570 | 0.4563 | 0.7 |
| 5 | 11 | 60 | 20 | 0.5154 | 0.5083 | 7.1 |
| 6 | 9.1 | 60 | 40 | 0.4875 | 0.4814 | 6.1 |
| 7 | 5.5 | 60 | 60 | 0.5536 | 0.5491 | 4.5 |
| 8 | 9.3 | 60 | 80 | 0.5571 | 0.5518 | 5.3 |
| 9 | 6.7 | 65 | 20 | 0.5861 | 0.5842 | 1.9 |
| 10 | 14.1 | 65 | 40 | 0.5823 | 0.5783 | 4.0 |
| 11 | 14.6 | 65 | 60 | 0.5744 | 0.5723 | 2.1 |
| 12 | 7.5 | 65 | 80 | 0.5284 | 0.5257 | 2.7 |

Silver on activated substrate

Vol = 20 ml; plating time = 2h

Membrane dimensions: outer diameter = 12 mm; length 6 to 8 mm

AgNO₃ = 0.65 g/l; hydrazine:AgNO₃ = 1.3:1 on molar basis

| Run | Temp. (°C) | EDTA: Pd | Before (g) | Mass after (g) | Mass plated (mg) | Thickness microns | Conversion | mg/cm ² ·2h |
|-----|------------|----------|------------|----------------|------------------|-------------------|------------|------------------------|
| 1 | 55 | 20 | 0.5632 | 0.5662 | 3.0 | 1.1 | 36.3 | 0.99 |
| 2 | 55 | 40 | 0.5717 | 0.5751 | 3.4 | 1.2 | 41.1 | 1.13 |
| 3 | 55 | 60 | 0.5261 | 0.5312 | 5.1 | 1.8 | 61.7 | 1.69 |
| 4 | 55 | 80 | 0.5378 | 0.5423 | 4.5 | 1.6 | 54.4 | 1.49 |
| 5 | 60 | 20 | 0.5351 | 0.5365 | 1.4 | 0.5 | 16.9 | 0.46 |
| 6 | 60 | 40 | 0.6181 | 0.6203 | 2.2 | 0.8 | 26.6 | 0.73 |

| | | | | | | | | |
|----|----|----|--------|--------|-----|-----|------|------|
| 7 | 60 | 60 | 0.4879 | 0.4922 | 4.3 | 1.6 | 52.0 | 1.43 |
| 8 | 60 | 80 | 0.5844 | 0.5898 | 5.4 | 1.9 | 65.3 | 1.79 |
| 9 | 65 | 20 | 0.5481 | 0.5511 | 3.0 | 1.1 | 36.3 | 0.99 |
| 10 | 65 | 40 | 0.5754 | 0.5806 | 5.2 | 1.9 | 62.9 | 1.72 |
| 11 | 65 | 60 | 0.5755 | 0.5816 | 6.1 | 2.2 | 73.8 | 2.02 |
| 12 | 65 | 80 | 0.5493 | 0.5543 | 5.0 | 1.8 | 60.5 | 1.66 |

Palladium on silver

Vol = 22 ml; time = 3h

Palladium salt = 27.5 g 10% solution per litre

| Run | Silver layer (mg) | | Temp. (°C) | EDTA: Pd | hydrazine: Pd | Before (g) | Mass after (g) | Plated (mg) | Conversion |
|-----|-------------------|----------------|------------|----------|---------------|------------|----------------|-------------|------------|
| 1 | 3.0 | | 71 | 20 | 0.72 | 0.5662 | 0.5807 | 14.5 | 67.4 |
| 2 | 5.1 | | 71 | 30 | 0.72 | 0.5312 | 0.5437 | 12.5 | 58.1 |
| 3 | 4.5 | | 71 | 40 | 0.72 | 0.5423 | 0.5521 | 9.8 | 45.6 |
| 4 | 4.3 | * pretrea- | 71 | 20 | 0.72 | 0.491 | 0.5052 | 14.2 | 66.0 |
| 5 | 5.4 | * ted twice | 71 | 30 | 0.72 | 0.5872 | 0.6046 | 17.4 | 80.9 |
| 6 | 3.0 | * | 71 | 40 | 0.72 | 0.5501 | 0.5680 | 17.9 | 83.3 |
| | | | | | | | | | |
| | | | | | | | | | |

Nickel on palladium:

Membrane dimensions: outer diameter = 12 mm; length 8 mm

Vol. = 20 ml

30 g/l nickel sulfate (6 mole crystal water); 15 g/l NaHPO₄; 200 ml/l ammonia

T = 45 °C

| Run | Temp. (°C) | Time (min.) | Before (g) | Mass after (g) | Mass plated (mg) | |
|-----|------------|-------------|------------|----------------|------------------|---------|
| 1 | 45 | 5 | 0.5951 | 0.5971 | 2.0 | |
| 2 | 45 | 15 | 0.5347 | 0.5408 | 6.1 | |
| 3 | 45 | 35 | 0.7418 | 0.7544 | 12.6 | peeling |
| 4 | 45 | 60 | 0.5213 | 0.5334 | 12.1 | peeling |

20 g/l nickel sulfate (6 mole crystal water); 10 g/l NaHPO₄; 200 ml/l ammonia

Vol = 20 ml

Membrane dimensions: outer diameter = 12 mm; length 10 mm

| Run | Temp. (°C) | Time (min.) | Before (g) | Mass after (g) | Mass plated (mg) | Thickness microns | mg/cm ² |
|-----|------------|-------------|------------|----------------|------------------|-------------------|--------------------|
| 1 | 35 | 5 | 0.5899 | 0.5985 | 8.6 | 2.6 | 2.28 |
| 2 | 35 | 10 | 0.571 | 0.5802 | 9.2 | 2.7 | 2.44 |
| 3 | 35 | 20 | 0.5911 | 0.6032 | 12.1 | 3.6 | 3.21 |
| 4 | 35 | 40 | 0.5848 | 0.5991 | 14.3 | 4.3 | 3.79 |
| 5 | 40 | 5 | 0.6076 | 0.6161 | 8.5 | 2.5 | 2.25 |
| 6 | 40 | 10 | 0.5899 | 0.6009 | 11.0 | 3.3 | 2.92 |
| 7 | 40 | 20 | 0.6088 | 0.6221 | 13.3 | 4.0 | 3.53 |
| 8 | 40 | 40 | 0.6164 | 0.6353 | 18.9 | 5.6 | 5.01 |

APPENDIX C

(Concentration profiles for simultaneous Ag and Pd deposition)

Figure C1:

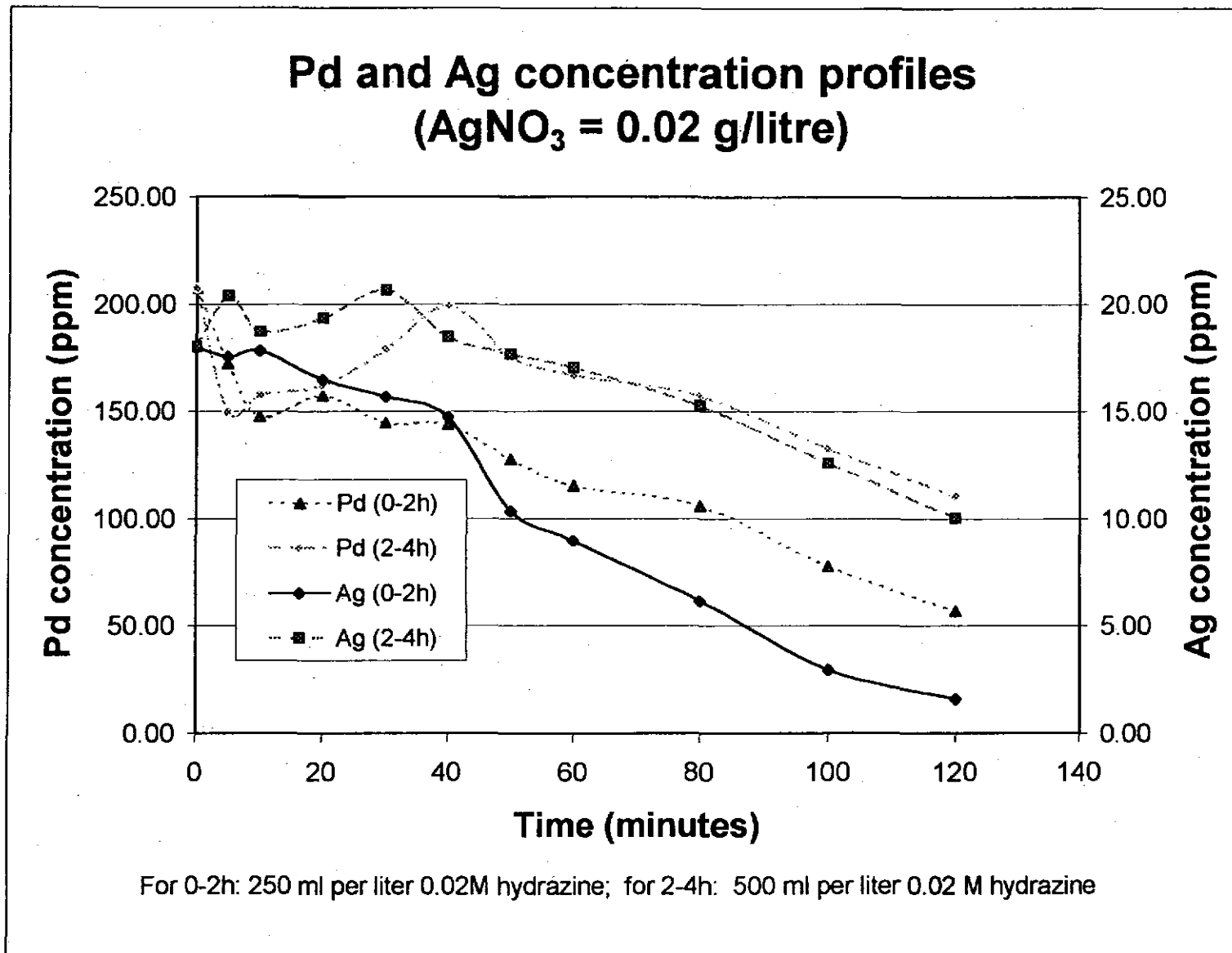


Figure C2:

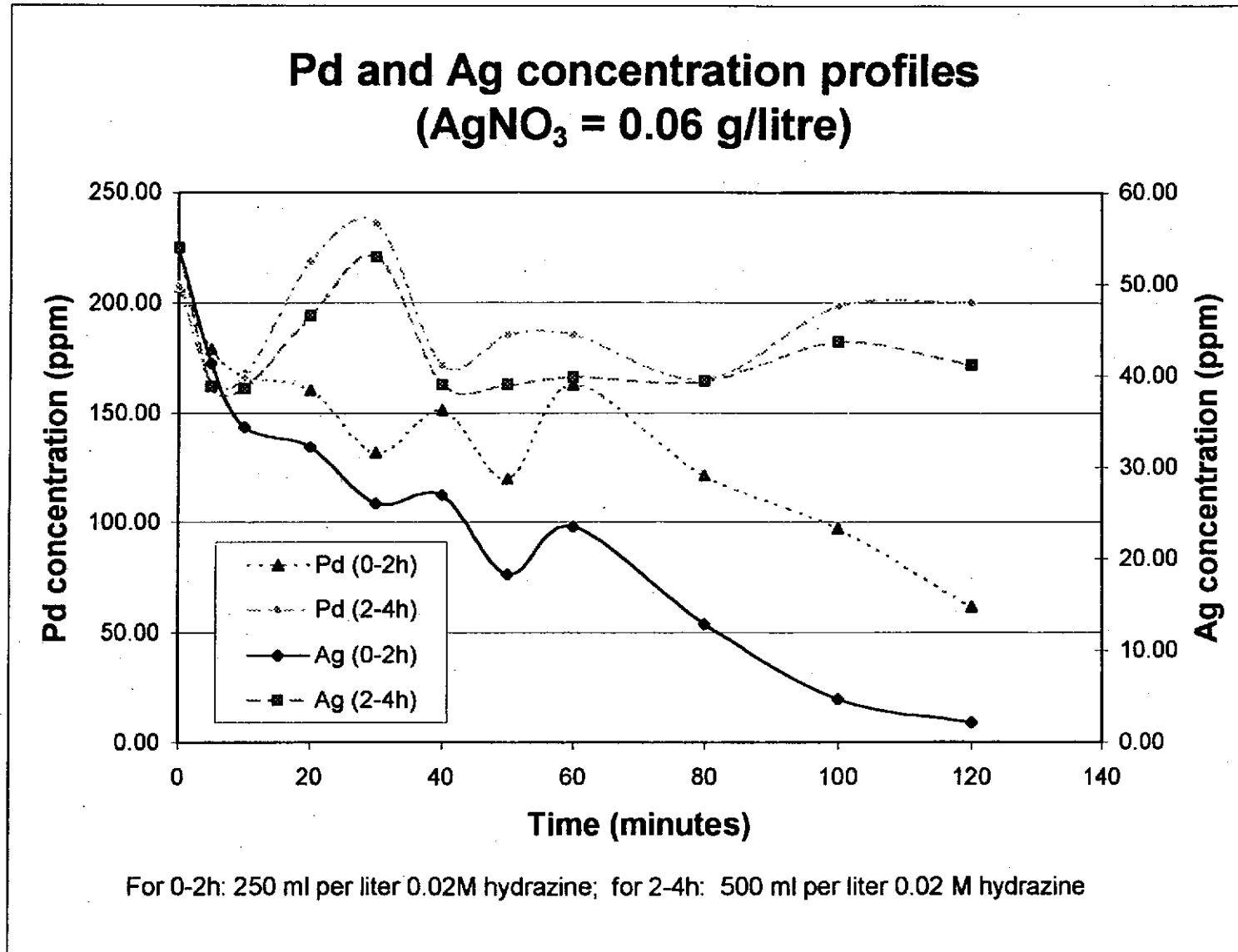


Figure C3:

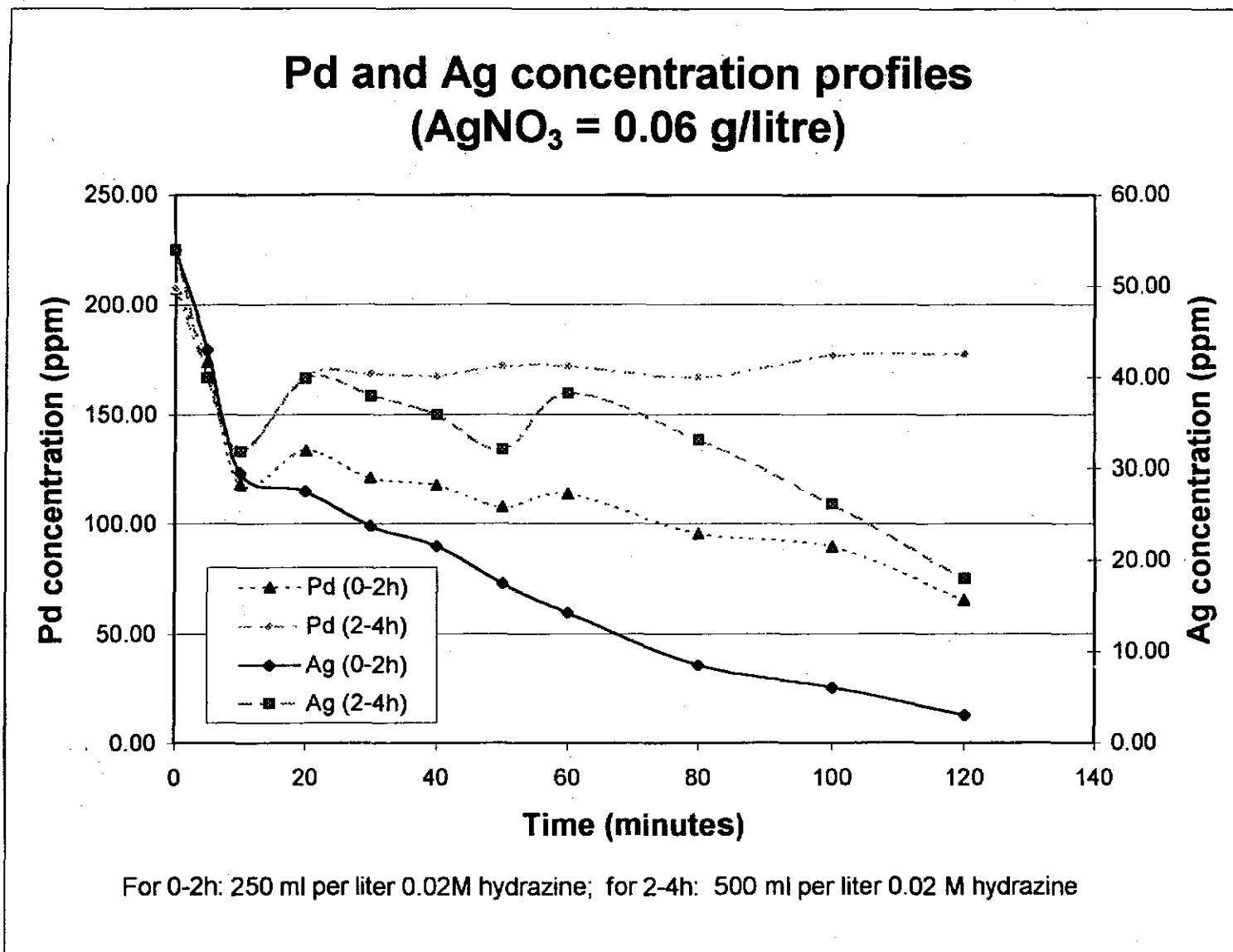


Figure C4:

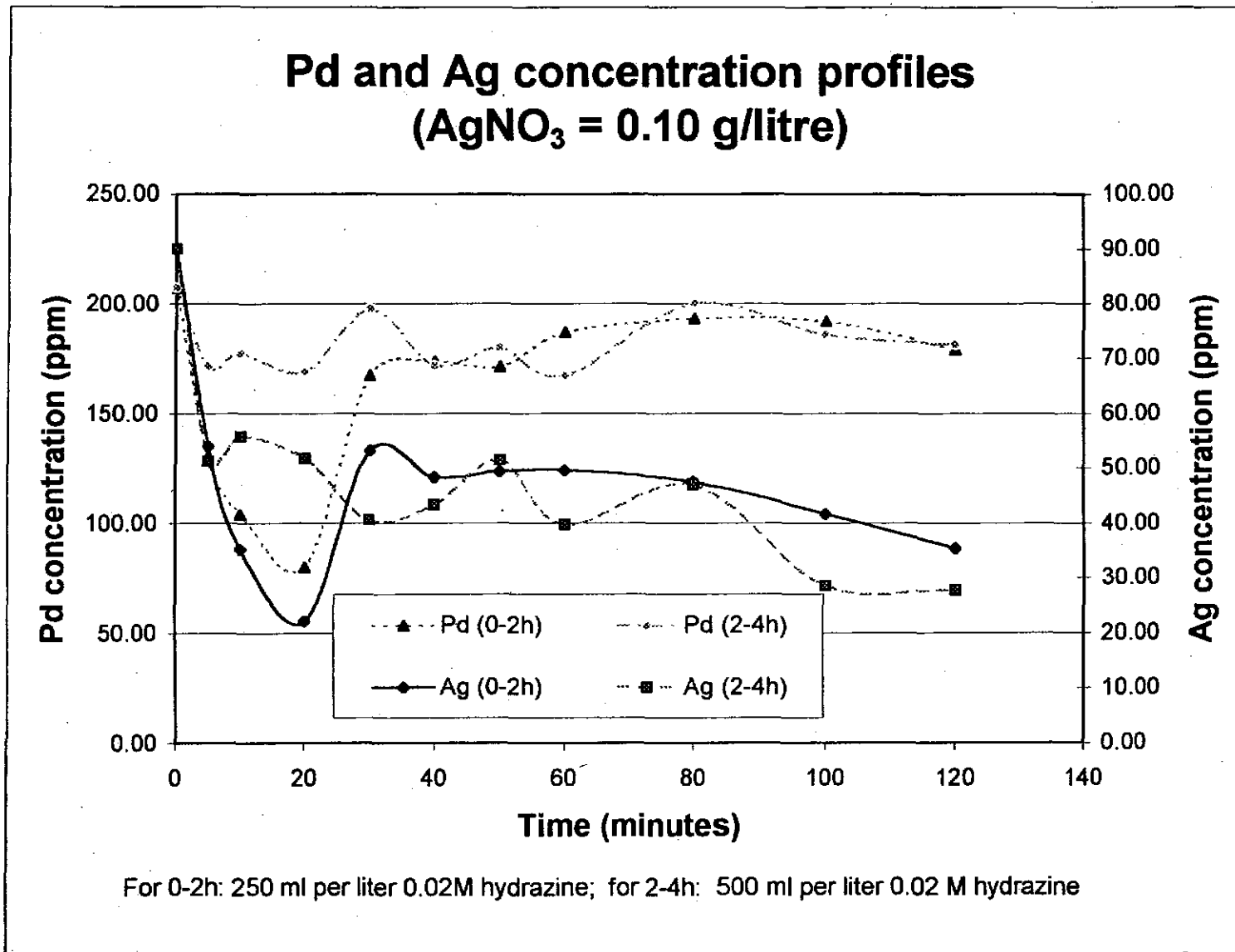


Figure C5:

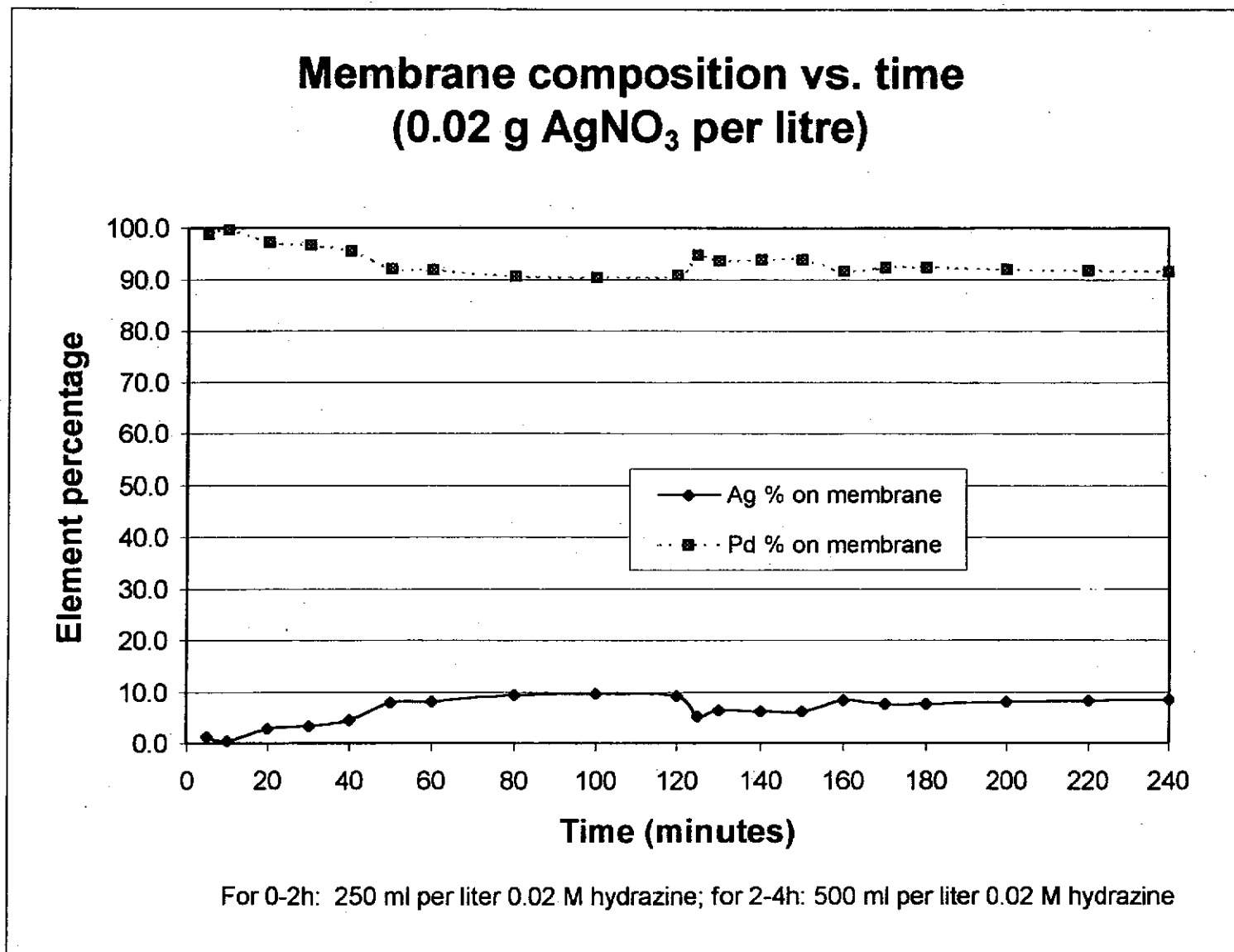


Figure C6:

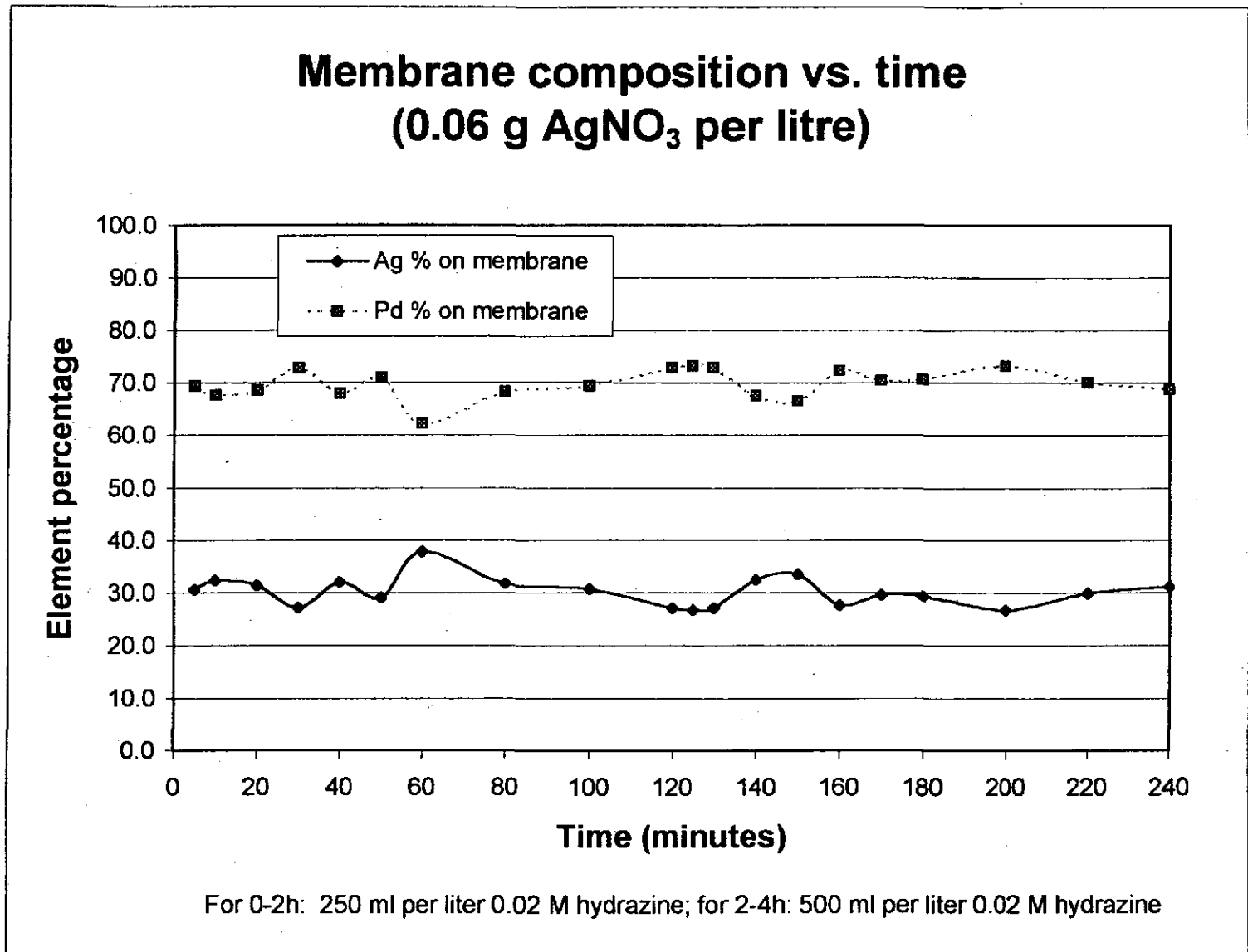


Figure C7:

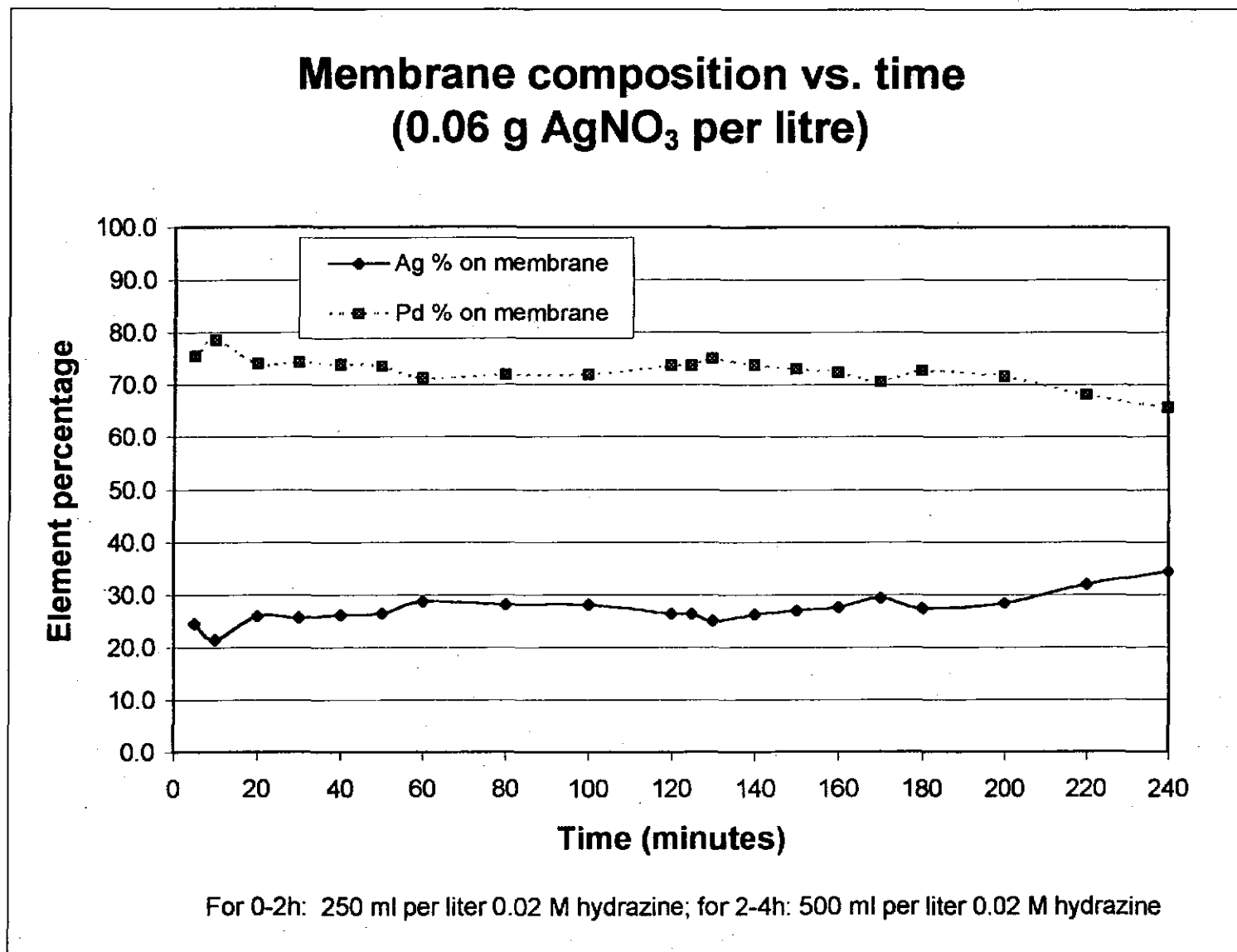
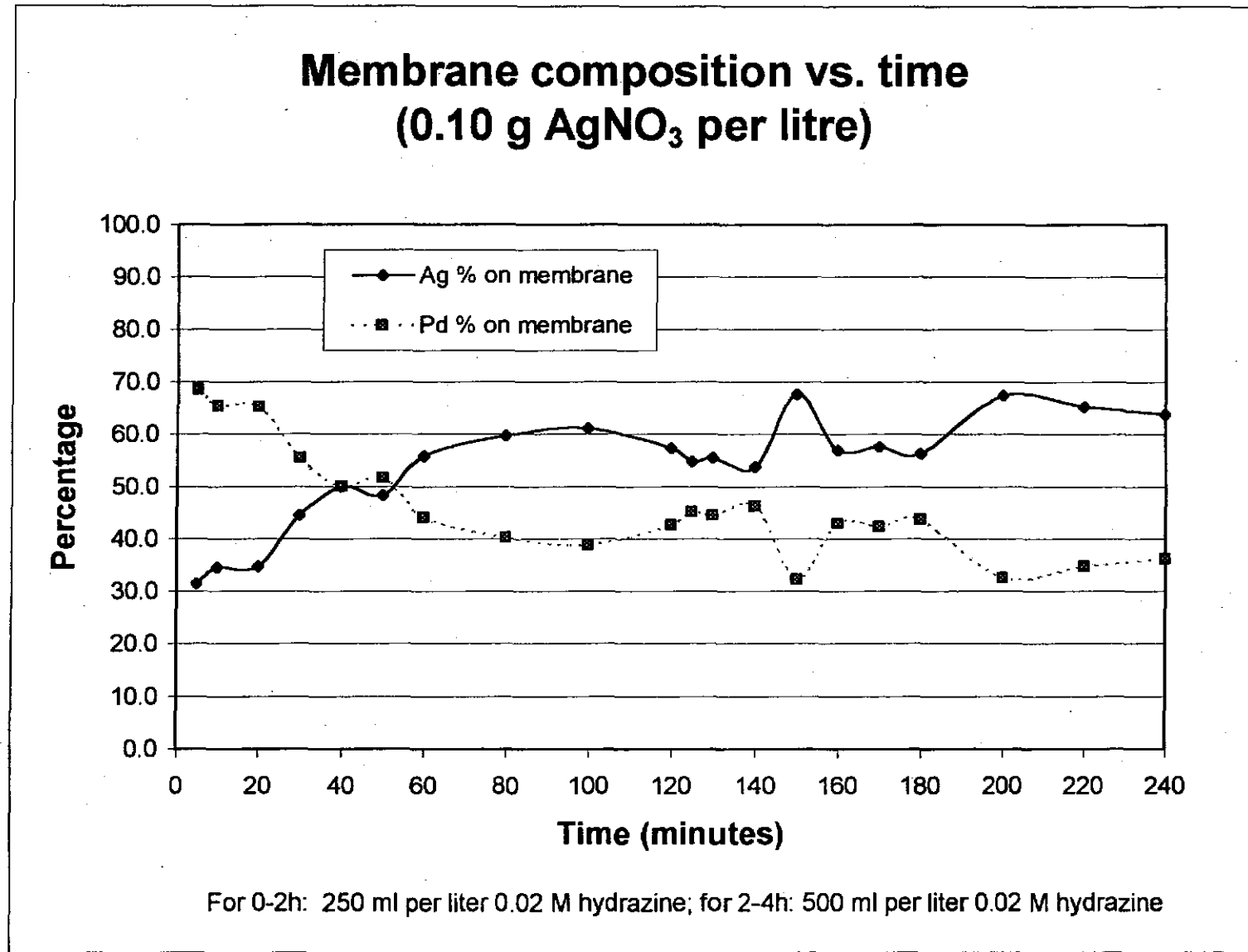


Figure C8:



APPENDIX D

(PIXE spectra for various metal films)

Figure D1:

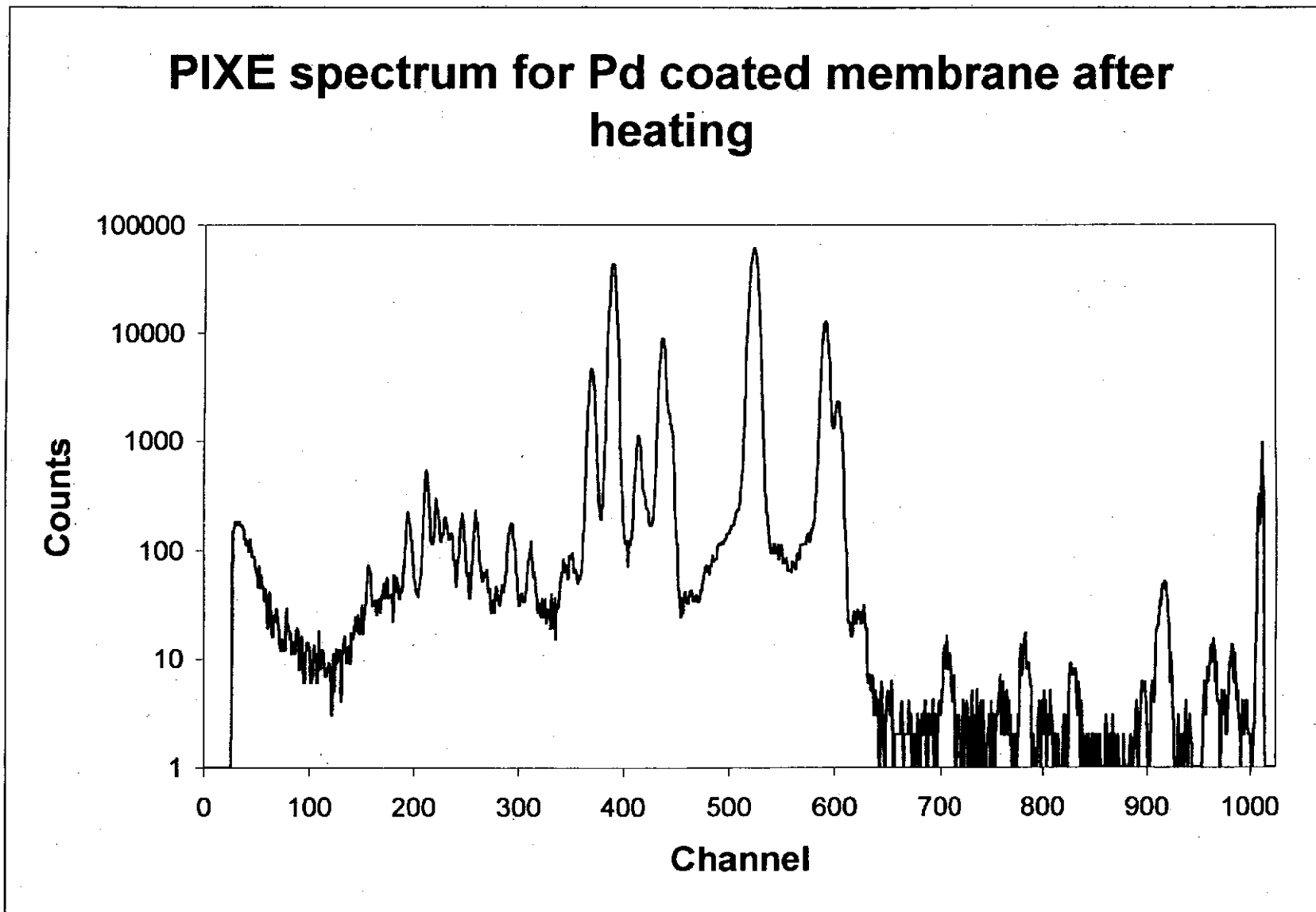


Figure D2:

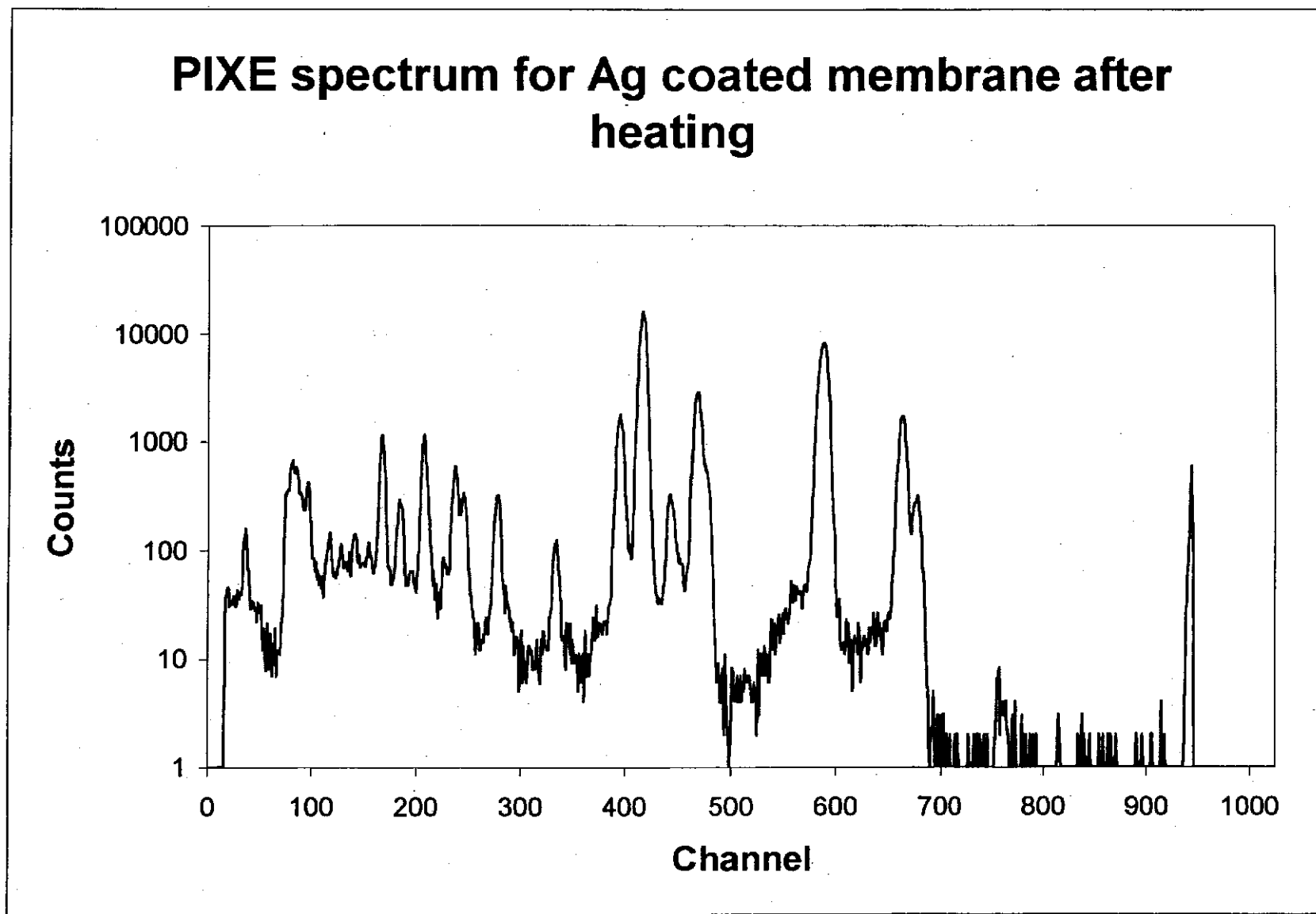


Figure D3:

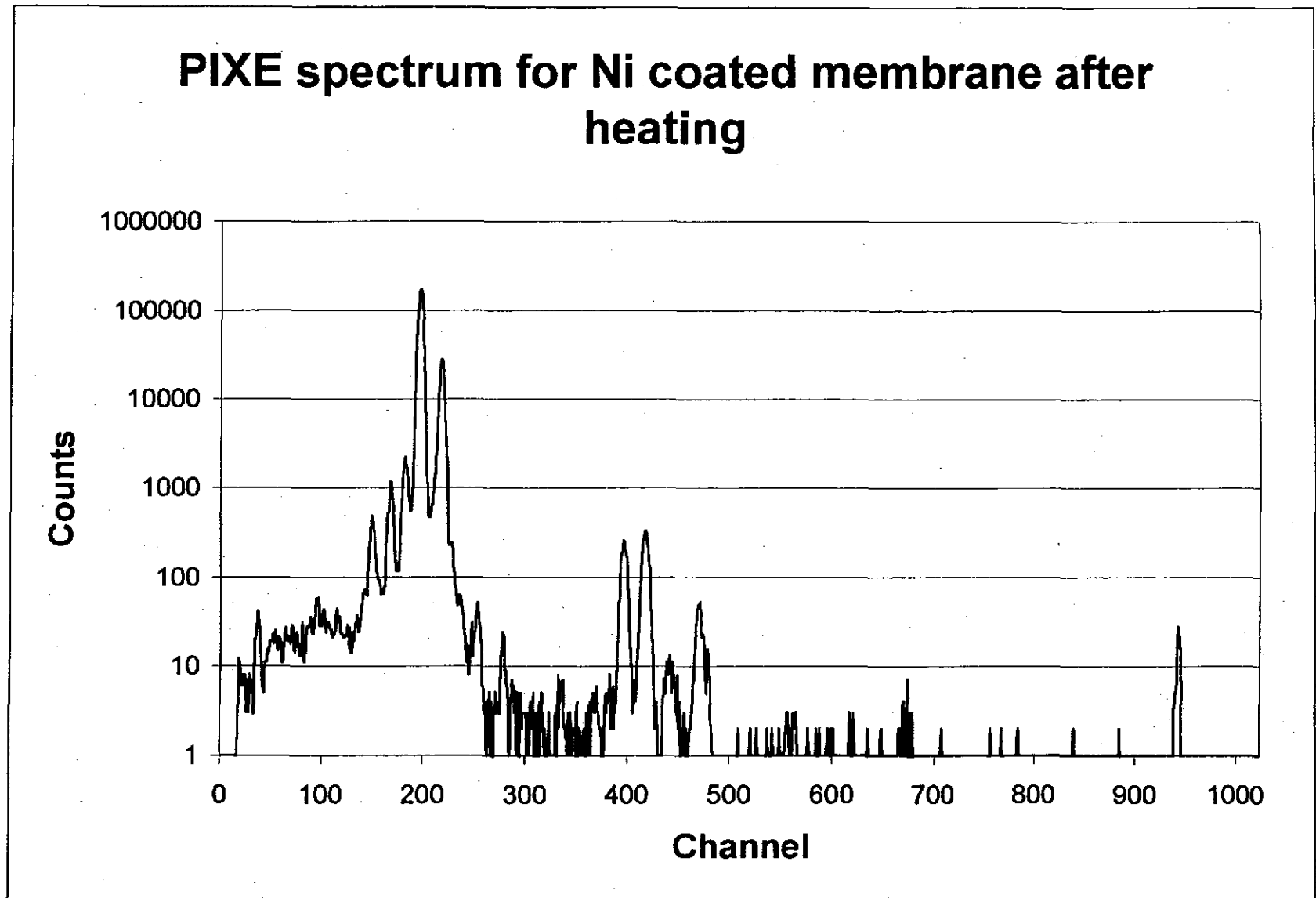


Figure D4:

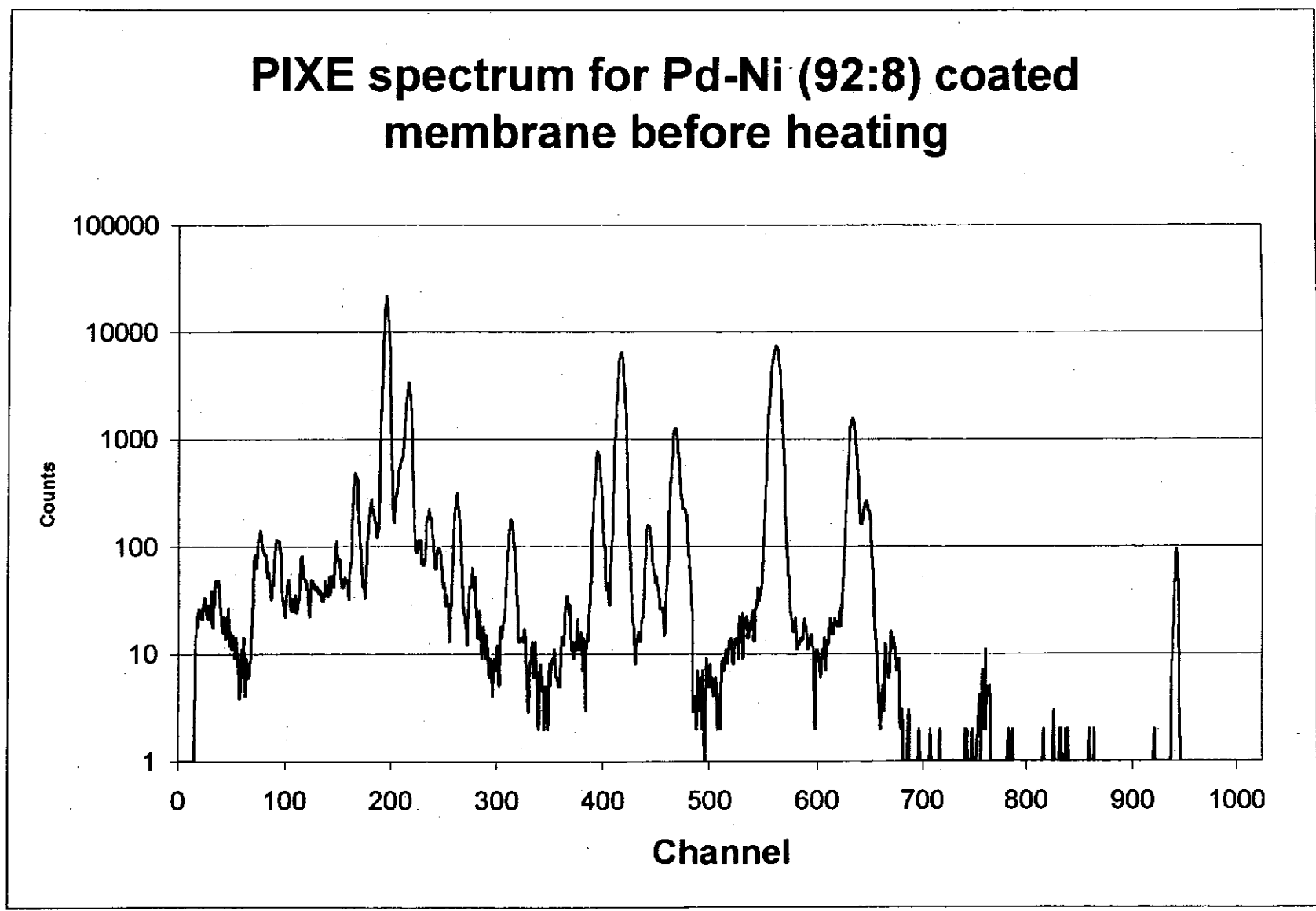


Figure D5:

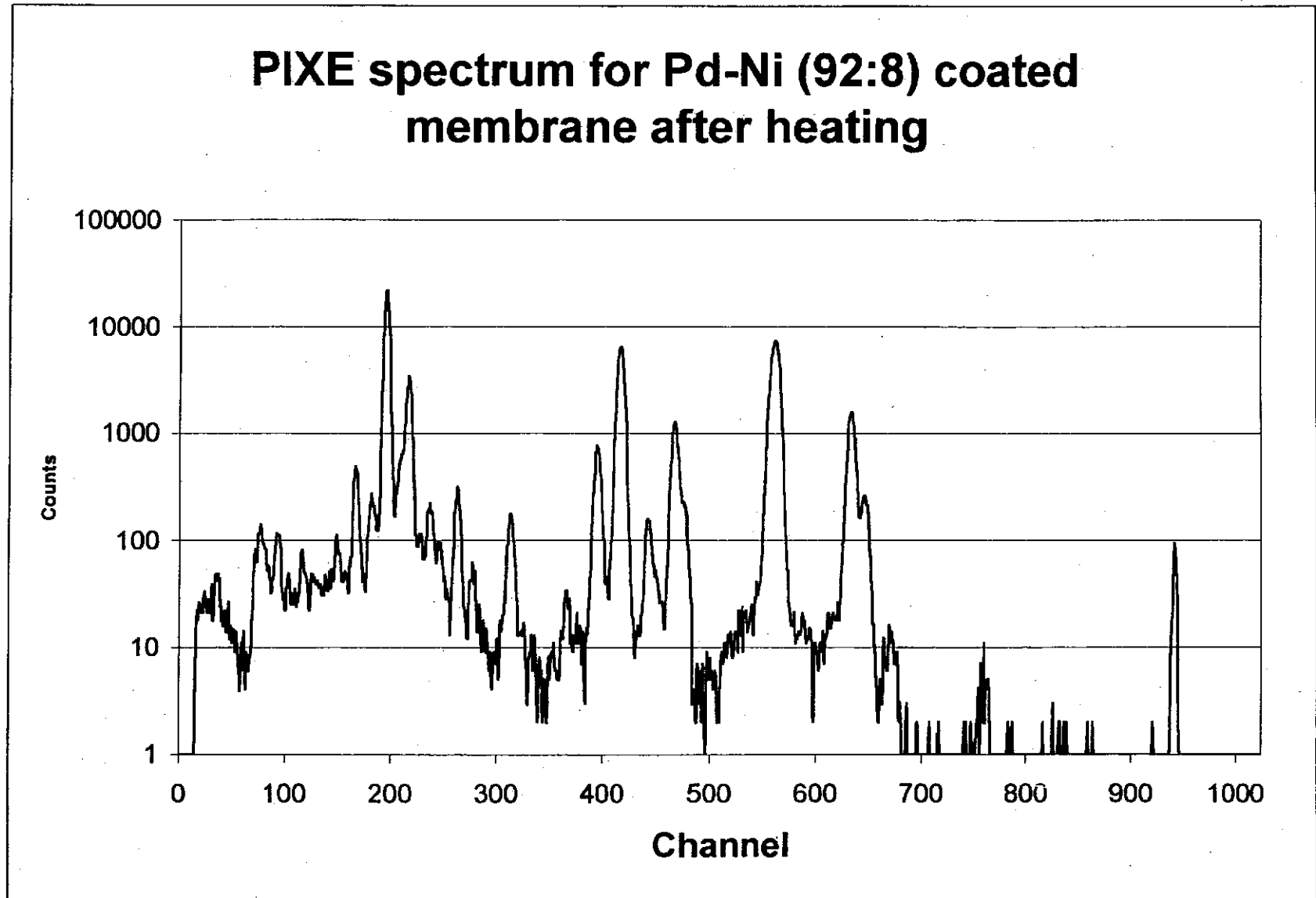


Figure D6:

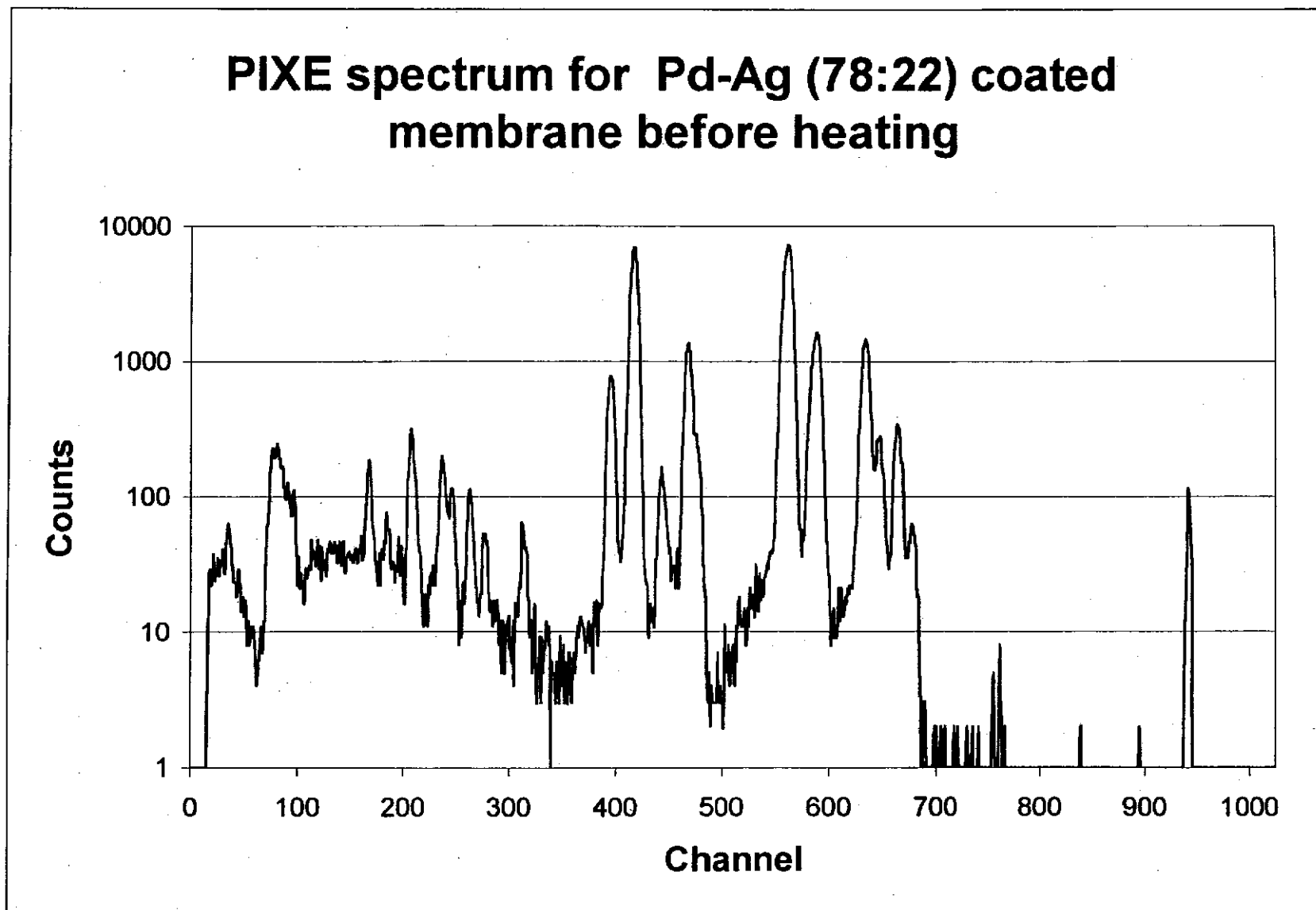


Figure D7:

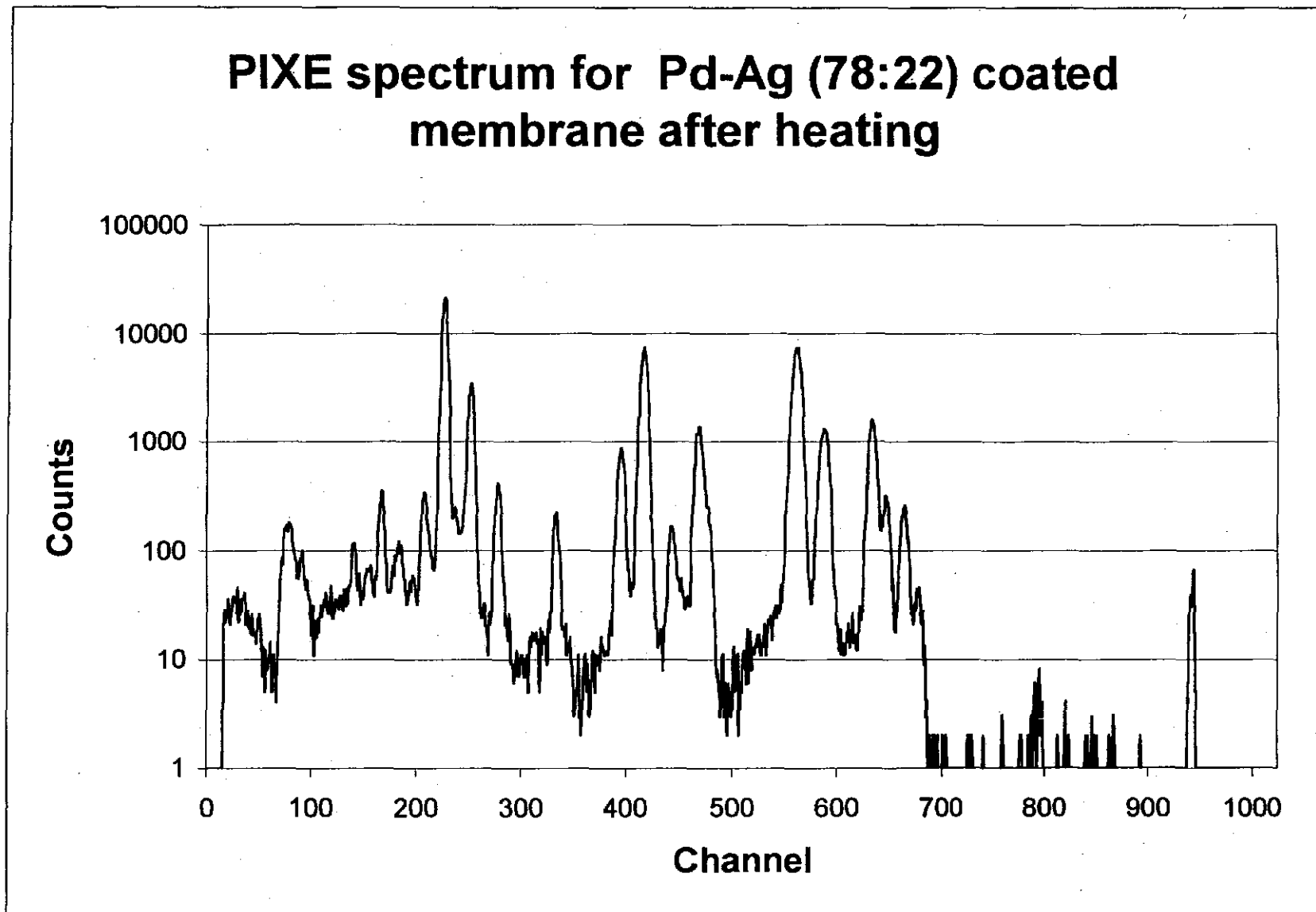


Figure D8:

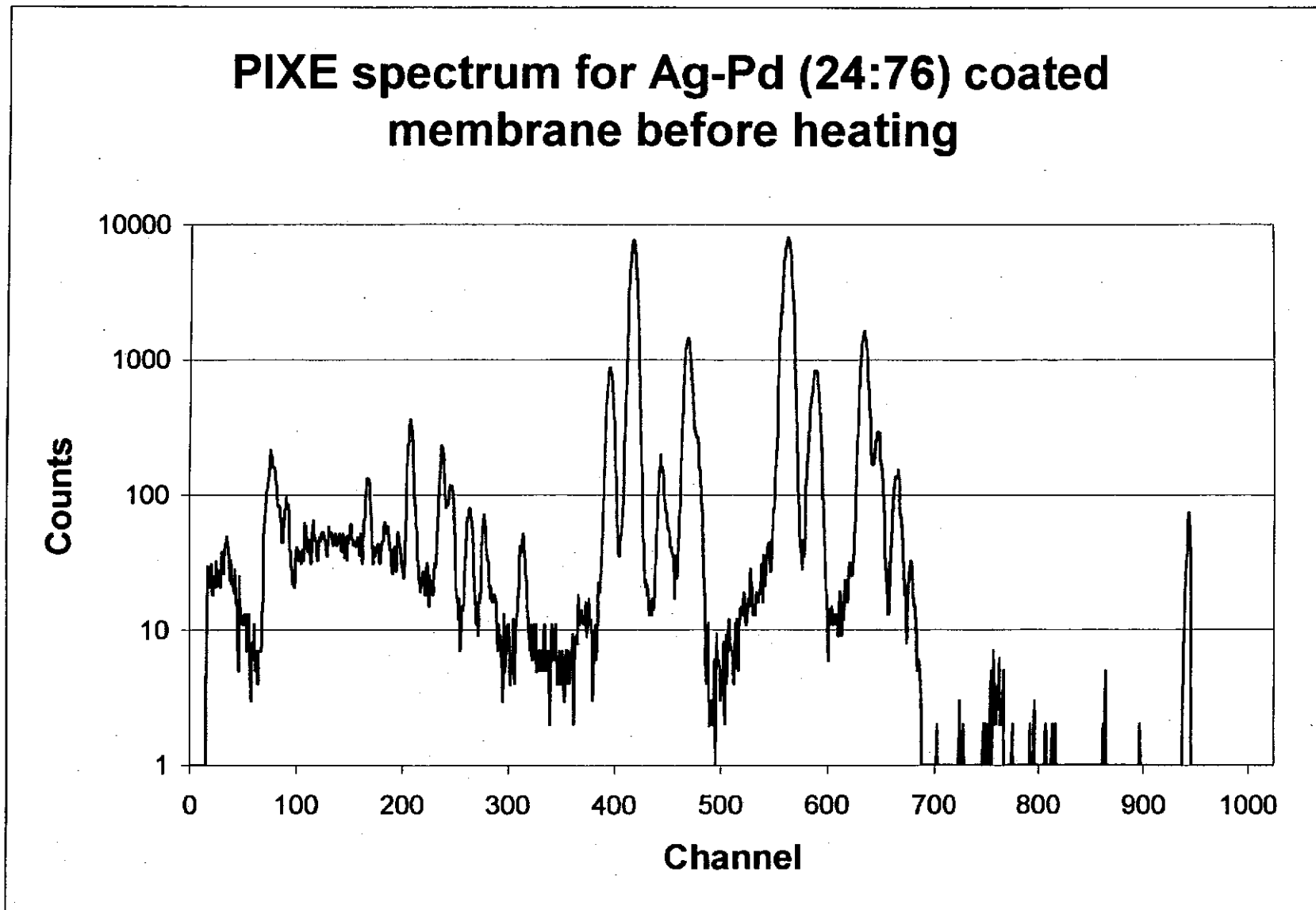


Figure D9:

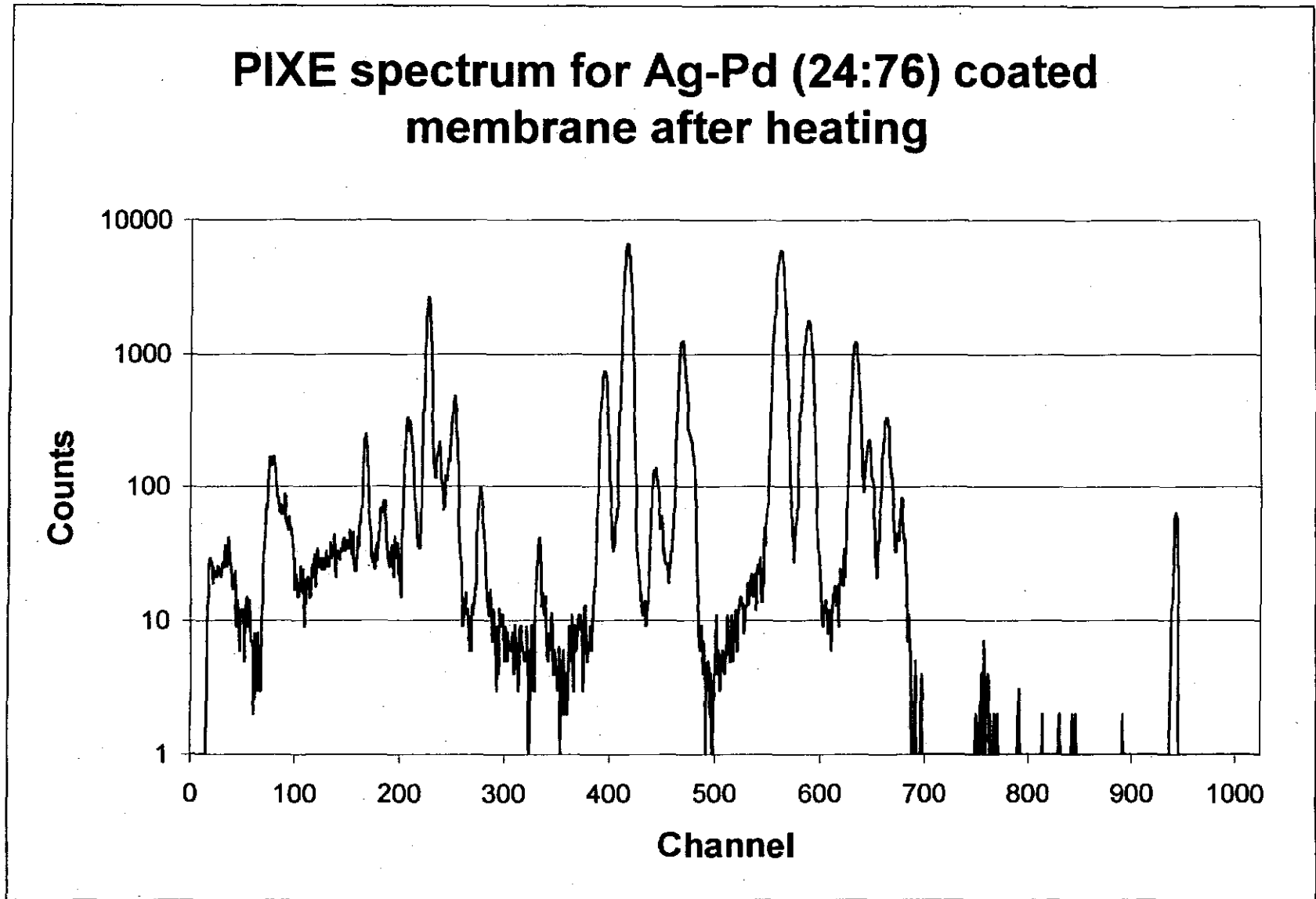
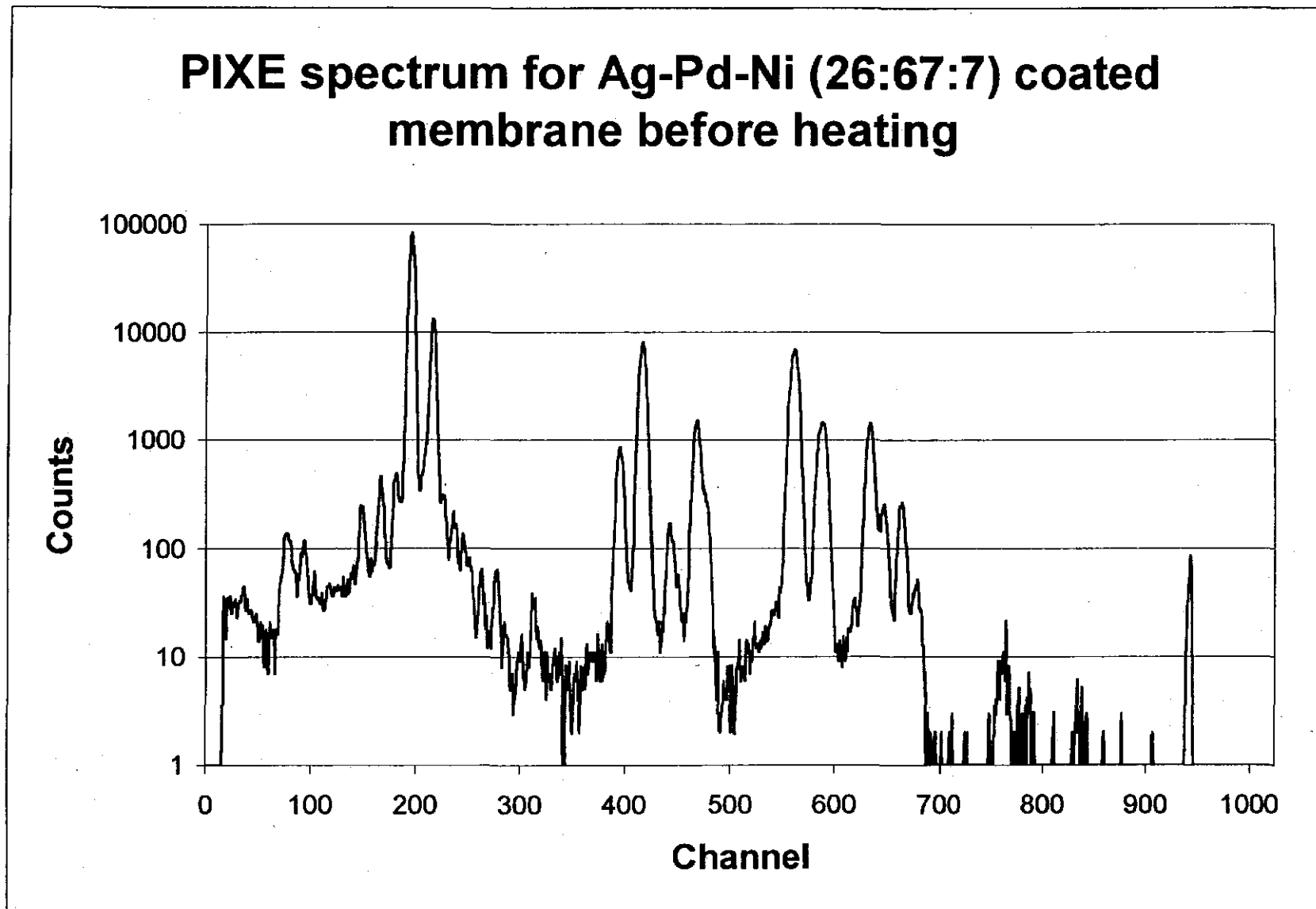


Figure D10:



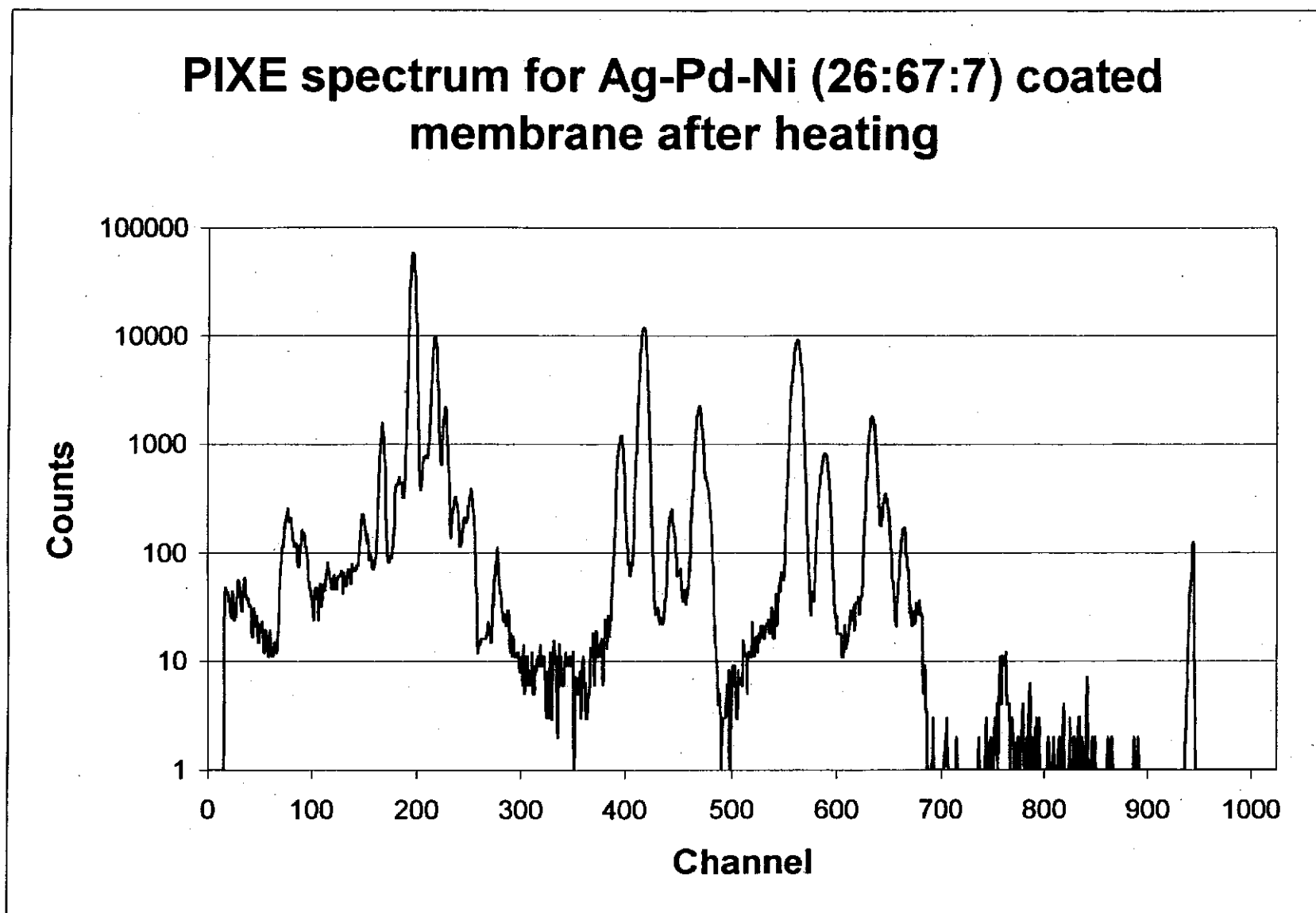


Figure D11:

Figure D12:

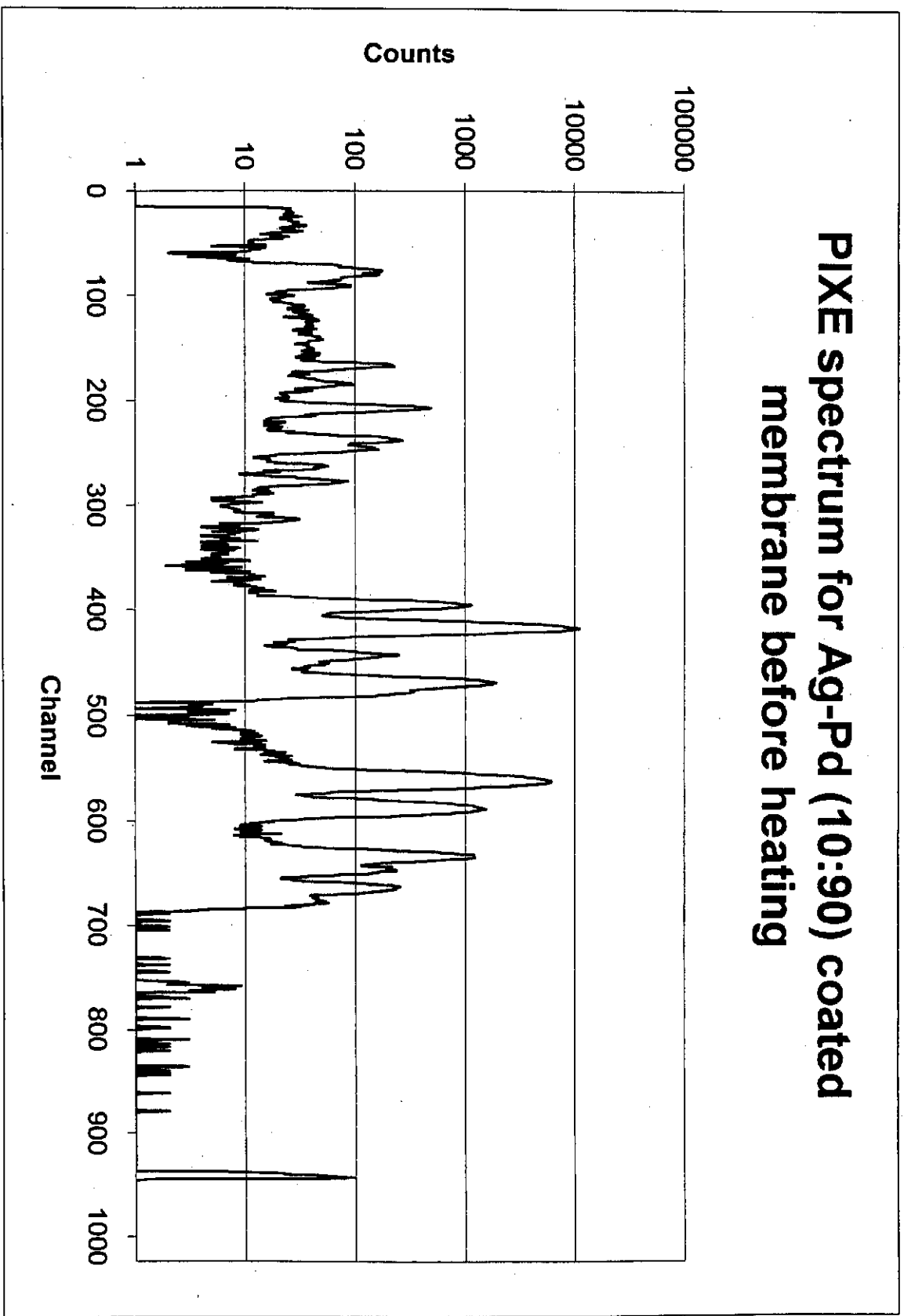


Figure D13:

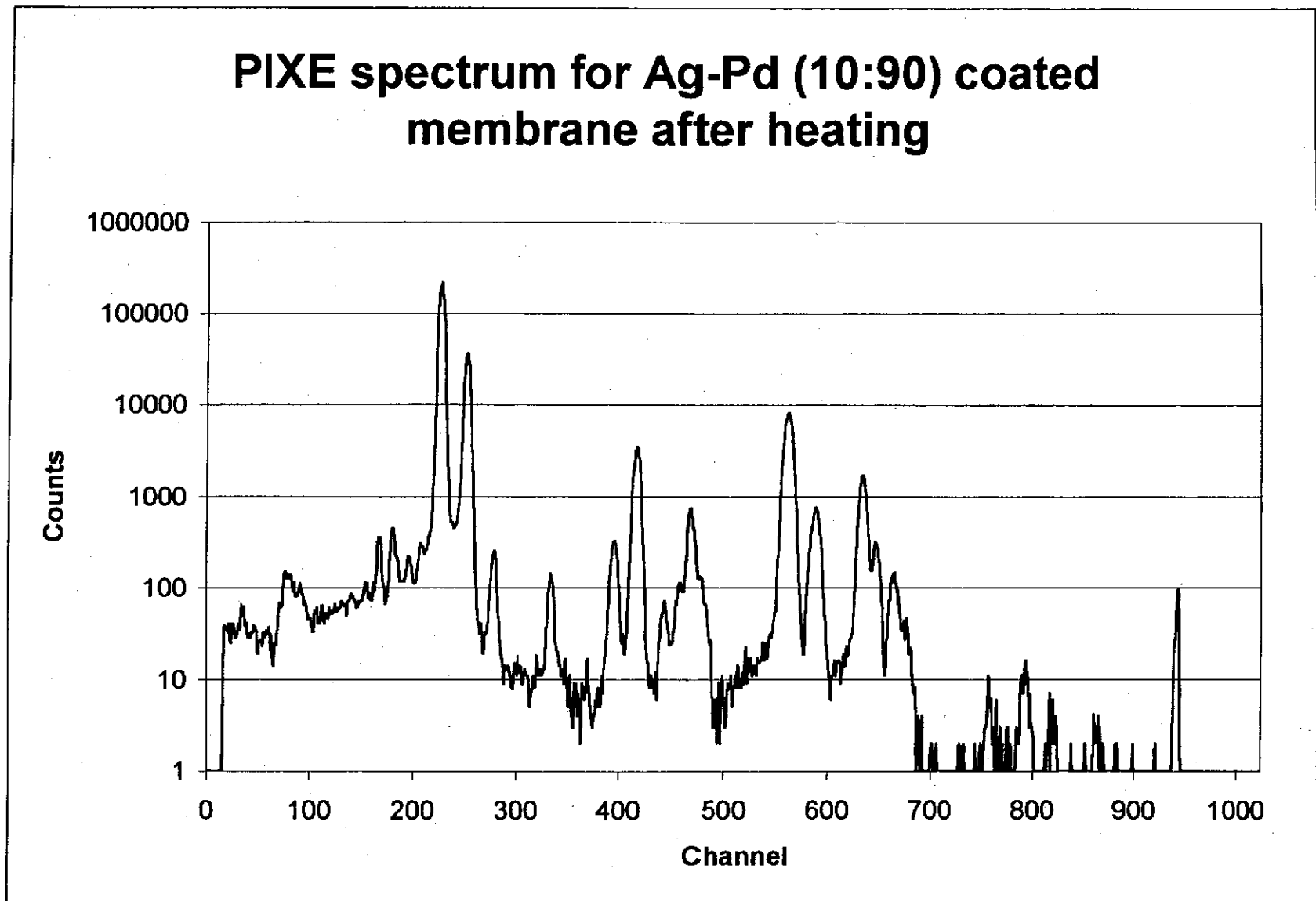


Figure D14:

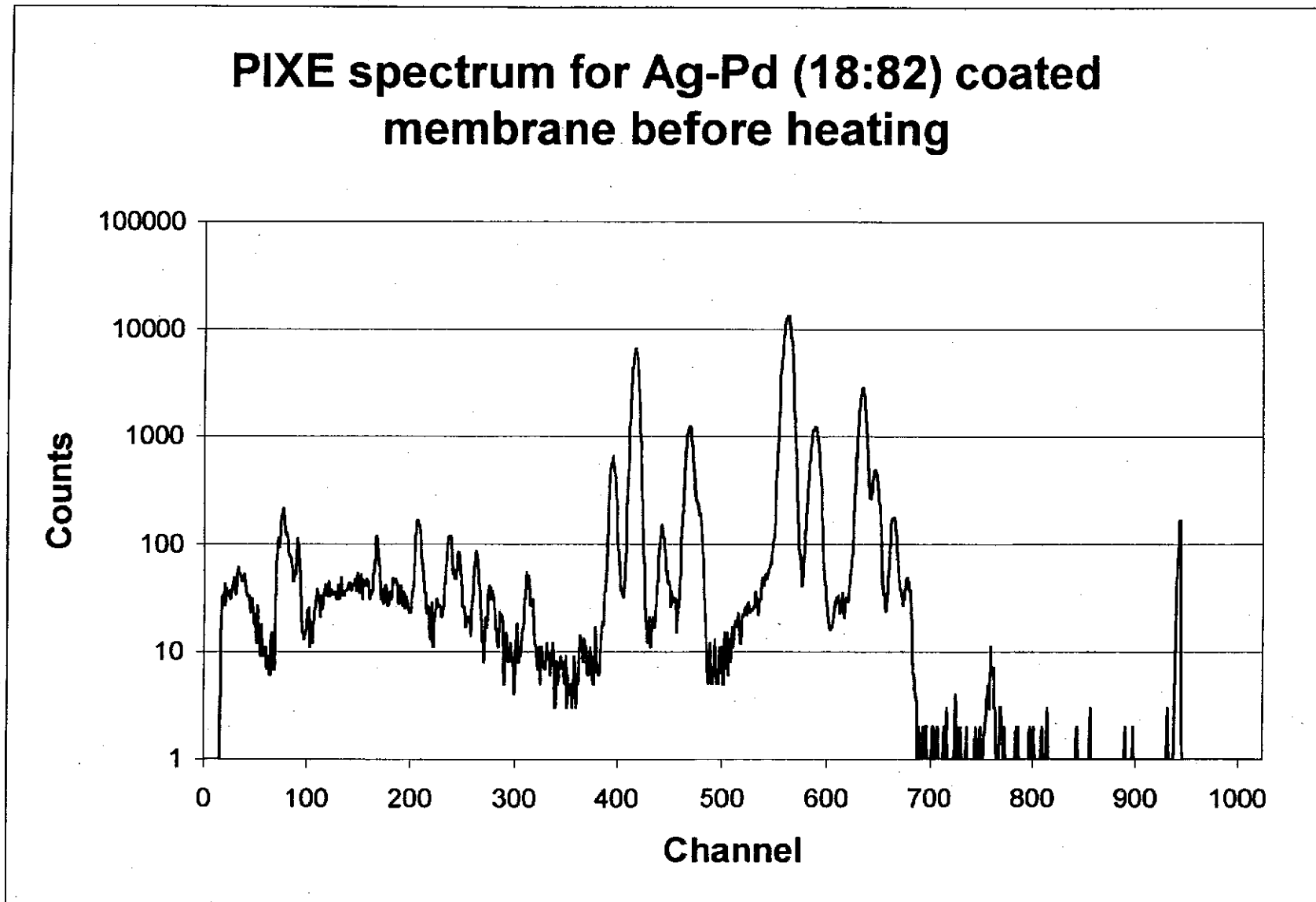
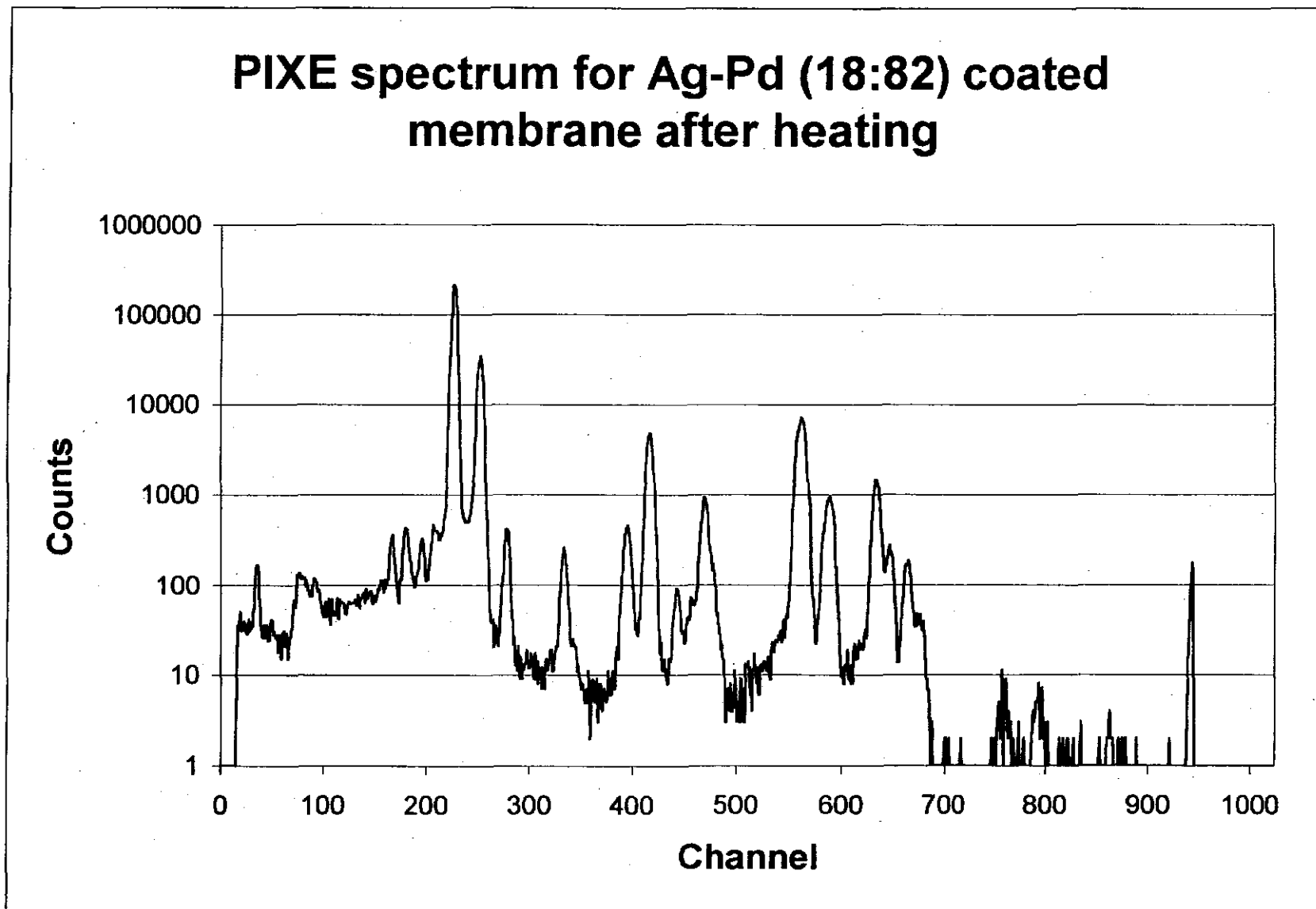


Figure D15:



APPENDIX E

(PIXE data from line scans after heating)

d + heat:

| Depth | Ch ² | Pd | Ag | Ni | Zr | Y | Sn | Zn | Pb | Hf | Fe |
|-------|-----------------|---------|--------|--------|---------|--------|--------|--------|--------|--------|--------|
| 7.5 | 10.1 | 9.1565 | 0.0485 | 1.2240 | 80.9303 | 6.4820 | 0.5543 | 0.0259 | 0.0130 | 1.3903 | 0.1752 |
| 7.0 | 9.1 | 22.3578 | 0.0000 | 1.4577 | 68.4472 | 5.7648 | 0.6063 | 0.0693 | 0.0196 | 1.1395 | 0.1378 |
| 6.5 | 8.3 | 47.8307 | 0.1323 | 1.8504 | 44.5289 | 3.7933 | 0.8766 | 0.1769 | 0.0325 | 0.6867 | 0.0916 |
| 6.0 | 8.4 | 58.0920 | 0.0645 | 1.9548 | 35.1931 | 2.9802 | 0.7846 | 0.2686 | 0.0334 | 0.5500 | 0.0788 |
| 5.5 | 8.6 | 73.2029 | 0.0492 | 1.9689 | 21.6185 | 1.8493 | 0.5579 | 0.3319 | 0.0505 | 0.3218 | 0.0491 |
| 5.0 | 8.4 | 83.8257 | 0.0188 | 1.9244 | 11.9956 | 1.0287 | 0.6432 | 0.3351 | 0.0559 | 0.1466 | 0.0260 |
| 4.5 | 8.1 | 90.4053 | 0.0824 | 1.7554 | 6.2824 | 0.5243 | 0.4772 | 0.3202 | 0.0686 | 0.0696 | 0.0147 |
| 4.0 | 7.9 | 92.0965 | 0.0747 | 1.7371 | 4.6559 | 0.3661 | 0.6256 | 0.3204 | 0.0713 | 0.0430 | 0.0095 |
| 3.5 | 8.7 | 93.6494 | 0.0478 | 1.7219 | 3.5364 | 0.2646 | 0.3437 | 0.3363 | 0.0653 | 0.0274 | 0.0072 |
| 3.0 | 8.7 | 94.2012 | 0.0581 | 1.6436 | 3.0600 | 0.2230 | 0.3949 | 0.3346 | 0.0655 | 0.0133 | 0.0059 |
| 2.5 | 7.9 | 95.2417 | 0.0620 | 1.4337 | 2.3374 | 0.1512 | 0.3877 | 0.3147 | 0.0638 | 0.0032 | 0.0045 |
| 2.0 | 9.1 | 95.5428 | 0.0711 | 1.4502 | 2.1453 | 0.1439 | 0.2642 | 0.3151 | 0.0575 | 0.0050 | 0.0050 |
| 1.5 | 10.5 | 95.4524 | 0.0549 | 1.6025 | 2.1127 | 0.1434 | 0.1947 | 0.3627 | 0.0682 | 0.0017 | 0.0068 |
| 1.0 | 10.0 | 94.9681 | 0.1170 | 1.8123 | 2.1648 | 0.1543 | 0.2492 | 0.4523 | 0.0724 | 0.0000 | 0.0095 |
| 0.5 | 10.5 | 94.7510 | 0.0000 | 2.0005 | 2.3424 | 0.1584 | 0.1378 | 0.5137 | 0.0815 | 0.0000 | 0.0146 |
| 0.0 | 12.6 | 94.1990 | 0.0646 | 2.1923 | 2.5517 | 0.1853 | 0.1557 | 0.5449 | 0.0834 | 0.0000 | 0.0230 |
| | | | | | | | | | | | |
| | | | | | | | | | | | |

e + heat:

| Depth | Ch ² | Pd | Ag | Zr | Y | Sn | Zn | Pb | Hf | Fe |
|-------|-----------------|---------|---------|---------|--------|--------|--------|--------|--------|--------|
| 0.0 | 3.3 | 64.3684 | 32.8456 | 1.6438 | 0.1135 | 0.2345 | 0.6326 | 0.1581 | 0.0019 | 0.0016 |
| 0.5 | 3.6 | 63.3543 | 34.2997 | 1.4467 | 0.0948 | 0.0901 | 0.5739 | 0.1395 | 0.0000 | 0.0011 |
| 1.0 | 3.3 | 66.8998 | 30.6869 | 1.4880 | 0.1031 | 0.1199 | 0.5724 | 0.1290 | 0.0000 | 0.0009 |
| 1.5 | 4.0 | 68.0705 | 29.4544 | 1.5684 | 0.1040 | 0.1283 | 0.5535 | 0.1199 | 0.0000 | 0.0009 |
| 2.0 | 5.2 | 72.8460 | 24.5736 | 1.7327 | 0.1222 | 0.1059 | 0.5143 | 0.1043 | 0.0000 | 0.0009 |
| 2.5 | 2.2 | 75.6939 | 20.9286 | 2.2967 | 0.1744 | 0.3279 | 0.4801 | 0.0934 | 0.0042 | 0.0007 |
| 3.0 | 2.3 | 77.9421 | 16.2873 | 4.4814 | 0.3474 | 0.4625 | 0.3807 | 0.0720 | 0.0254 | 0.0012 |
| 3.5 | 2.0 | 78.9489 | 14.8458 | 5.0916 | 0.3699 | 0.3222 | 0.3290 | 0.0622 | 0.0287 | 0.0018 |
| 4.0 | 2.0 | 80.4599 | 11.2314 | 6.6975 | 0.5489 | 0.7084 | 0.2617 | 0.0518 | 0.0384 | 0.0020 |
| 4.5 | 1.6 | 81.6027 | 9.5532 | 7.1051 | 0.5465 | 0.8610 | 0.2436 | 0.0496 | 0.0348 | 0.0035 |
| 5.0 | 1.7 | 81.5403 | 7.7539 | 9.0010 | 0.6977 | 0.7335 | 0.1839 | 0.0349 | 0.0457 | 0.0091 |
| 5.5 | 1.5 | 80.8525 | 6.6450 | 10.9051 | 0.8629 | 0.5006 | 0.1383 | 0.0293 | 0.0510 | 0.0153 |
| 6.0 | 1.4 | 76.9206 | 5.0019 | 15.8337 | 1.3195 | 0.7060 | 0.0869 | 0.0238 | 0.0955 | 0.0122 |
| 6.5 | 1.5 | 74.1845 | 4.3979 | 19.3917 | 1.5908 | 0.2141 | 0.0597 | 0.0217 | 0.1295 | 0.0102 |
| 7.0 | 1.7 | 64.3559 | 3.1674 | 29.3880 | 2.6731 | 0.1307 | 0.0378 | 0.0212 | 0.2341 | 0.0117 |
| 7.5 | 1.5 | 58.5923 | 1.6595 | 35.9699 | 3.1111 | 0.3132 | 0.0198 | 0.0193 | 0.3009 | 0.0141 |
| 8.0 | 1.5 | 51.8633 | 0.9159 | 42.5755 | 3.6911 | 0.5256 | 0.0088 | 0.0163 | 0.3833 | 0.0201 |
| | | | | | | | | | | |
| | | | | | | | | | | |

f + heat:

| Depth | Ch ² | Pd | Ag | Zr | Y | Sn | Zn | Pb | Hf | Fe |
|-------|-----------------|---------|---------|---------|--------|--------|--------|--------|--------|--------|
| 0.0 | 3.2 | 72.7700 | 19.3818 | 5.7626 | 0.4940 | 1.1699 | 0.2883 | 0.0490 | 0.0570 | 0.0275 |
| 0.5 | 3.9 | 66.9799 | 17.4638 | 13.2423 | 1.1023 | 0.7370 | 0.2069 | 0.0287 | 0.2101 | 0.0291 |
| 1.0 | 3.0 | 76.0297 | 18.4702 | 4.1843 | 0.3068 | 0.7358 | 0.2057 | 0.0269 | 0.0291 | 0.0117 |
| 1.5 | 2.6 | 76.9085 | 18.7774 | 3.1154 | 0.2147 | 0.6836 | 0.2417 | 0.0368 | 0.0104 | 0.0116 |
| 2.0 | 2.6 | 76.7539 | 18.4114 | 3.4075 | 0.2592 | 0.8834 | 0.2211 | 0.0326 | 0.0194 | 0.0114 |
| 2.5 | 3.0 | 77.5081 | 17.3925 | 3.8736 | 0.3212 | 0.6227 | 0.1978 | 0.0304 | 0.0269 | 0.0269 |
| 3.0 | | 71.5069 | 19.0461 | 7.1859 | 0.5991 | 1.2827 | 0.2484 | 0.0338 | 0.0702 | 0.0269 |
| 3.5 | | 61.8349 | 16.0589 | 17.9552 | 1.5350 | 2.0077 | 0.2697 | 0.0351 | 0.2551 | 0.0484 |

| | | | | | | | | | | | |
|-----|-----|---------|---------|---------|--------|--------|--------|--------|--------|--------|--|
| 4.0 | 3.2 | 65.5058 | 20.6998 | 10.4983 | 0.8770 | 1.9426 | 0.2989 | 0.0372 | 0.1136 | 0.0269 | |
| 4.5 | 3.9 | 52.1629 | 13.0718 | 28.7245 | 2.4708 | 2.7327 | 0.2911 | 0.0363 | 0.4401 | 0.0699 | |
| 5.0 | 6.1 | 0.2084 | 0.1420 | 90.4312 | 7.3981 | 0.0000 | 0.0069 | 0.0166 | 1.6090 | 0.1877 | |
| 5.5 | 5.2 | 0.1467 | 0.1028 | 90.5672 | 7.3843 | 0.0000 | 0.0015 | 0.0138 | 1.6043 | 0.1794 | |
| 6.0 | 5.9 | 0.1344 | 0.0880 | 90.7162 | 7.3202 | 0.0000 | 0.0037 | 0.0080 | 1.5907 | 0.1387 | |
| 6.5 | 6.2 | 0.0557 | 0.0735 | 90.4401 | 7.6475 | 0.0000 | 0.0039 | 0.0370 | 1.5780 | 0.1642 | |
| | | | | | | | | | | | |
| | | | | | | | | | | | |

g + heat:

| Depth | Ch ² | Pd | Ag | Ni | Zr | Y | Sn | Zn | Pb | Hf | Fe |
|-------|-----------------|---------|---------|--------|---------|--------|--------|---------|--------|--------|--------|
| 0.0 | 2.6 | 71.3125 | 11.5828 | 1.6410 | 1.3798 | 0.0619 | 0.3101 | 12.6186 | 1.0886 | 0.0000 | 0.0047 |
| 0.5 | 1.5 | 67.1671 | 10.5970 | 2.0585 | 1.4831 | 0.0477 | 0.8258 | 16.6604 | 1.1453 | 0.0000 | 0.0151 |
| 1.0 | 3.9 | 71.7237 | 12.5797 | 1.4533 | 1.5264 | 0.0661 | 0.5554 | 10.5153 | 1.5755 | 0.0000 | 0.0046 |
| 1.5 | 4.2 | 71.8074 | 12.7569 | 1.3473 | 1.5928 | 0.0528 | 0.5381 | 10.1263 | 1.7736 | 0.0000 | 0.0046 |
| 2.0 | 4.3 | 71.4548 | 13.3121 | 1.3349 | 1.7319 | 0.0693 | 0.2540 | 10.1889 | 1.6500 | 0.0000 | 0.0041 |
| 2.5 | 3.8 | 71.3531 | 13.2094 | 1.3385 | 1.7542 | 0.0724 | 0.3740 | 10.2750 | 1.6191 | 0.0000 | 0.0043 |
| 3.0 | 3.9 | 71.1625 | 13.1047 | 1.4103 | 1.6292 | 0.0825 | 0.4049 | 10.5889 | 1.6118 | 0.0000 | 0.0053 |
| 3.5 | | 69.3069 | 13.1286 | 1.5065 | 2.7624 | 0.1594 | 0.2380 | 11.5256 | 1.3628 | 0.0000 | 0.0097 |
| 4.0 | | 68.4787 | 13.0045 | 1.5577 | 3.3398 | 0.2035 | 0.1390 | 12.0277 | 1.2372 | 0.0000 | 0.0119 |
| 4.5 | 2.4 | 67.4513 | 13.1526 | 1.6028 | 3.8957 | 0.2363 | 0.0710 | 12.4624 | 1.1137 | 0.0000 | 0.0141 |
| 5.0 | 3.3 | 67.6505 | 12.8804 | 1.6088 | 3.9172 | 0.2475 | 0.0401 | 12.5298 | 1.1116 | 0.0000 | 0.0141 |
| 5.5 | 3.3 | 67.3477 | 12.5394 | 1.5558 | 5.3365 | 0.3534 | 0.0463 | 11.6026 | 1.2092 | 0.0000 | 0.0090 |
| 6.0 | 3.3 | 63.6517 | 13.8551 | 1.4774 | 7.1500 | 0.5089 | 0.0356 | 12.2296 | 1.0138 | 0.0512 | 0.0267 |
| 6.5 | 3.0 | 64.2961 | 12.0533 | 1.4819 | 9.2271 | 0.6716 | 0.0448 | 10.9690 | 1.2490 | 0.0000 | 0.0071 |
| 7.0 | 4.3 | 24.8862 | 23.1123 | 0.2923 | 42.1276 | 3.2196 | 0.0379 | 4.9250 | 0.6458 | 0.6228 | 0.1305 |
| 7.5 | 4.0 | 21.9328 | 23.9156 | 0.3212 | 44.7900 | 3.3856 | 0.0313 | 4.2325 | 0.5948 | 0.6458 | 0.1502 |
| | | | | | | | | | | | |
| | | | | | | | | | | | |

j + heat:

| Depth | Ch ² | Pd | Ag | Zr | Y | Sn | Zn | Pb | Hf | Fe |
|-------|-----------------|---------|---------|---------|--------|--------|---------|--------|--------|--------|
| 0.0 | 0.9 | 58.1842 | 21.4639 | 1.7194 | 0.0489 | 0.8556 | 17.2327 | 0.4690 | 0.0129 | 0.0134 |
| 0.5 | 0.7 | 53.2841 | 21.3151 | 3.3003 | 0.3646 | 0.8071 | 20.1434 | 0.6308 | 0.1295 | 0.0252 |
| 1.0 | 1.8 | 59.1217 | 22.2678 | 1.2274 | 0.0366 | 0.7452 | 16.2038 | 0.3895 | 0.0022 | 0.0058 |
| 1.5 | 2.8 | 67.5197 | 11.6125 | 1.3819 | 0.0793 | 1.0297 | 18.1675 | 0.1967 | 0.0052 | 0.0075 |
| 2.0 | 2.8 | 67.0234 | 12.3180 | 1.5207 | 0.0952 | 0.8286 | 18.0035 | 0.1897 | 0.0146 | 0.0063 |
| 2.5 | 2.9 | 65.5993 | 13.4062 | 2.0505 | 0.1249 | 0.6787 | 17.8749 | 0.2422 | 0.0158 | 0.0073 |
| 3.0 | 2.9 | 65.9029 | 12.9752 | 1.9959 | 0.1050 | 0.6855 | 18.0801 | 0.2327 | 0.0147 | 0.0081 |
| 3.5 | 1.5 | 56.5735 | 14.6207 | 10.4616 | 0.7781 | 0.5698 | 16.4885 | 0.3300 | 0.1489 | 0.0310 |
| 4.0 | 1.5 | 44.7497 | 20.2656 | 19.1838 | 1.4249 | 1.0360 | 12.4458 | 0.5676 | 0.2747 | 0.0519 |
| 4.5 | 2.0 | 25.9002 | 30.9279 | 31.5315 | 2.1996 | 1.4798 | 6.3980 | 1.0224 | 0.4466 | 0.0941 |
| 5.0 | 2.0 | 19.5770 | 33.0614 | 36.9044 | 2.8375 | 1.3638 | 4.4365 | 1.1617 | 0.5488 | 0.1090 |
| 5.5 | 2.2 | 18.6507 | 35.2147 | 34.1238 | 2.7214 | 2.4437 | 4.8044 | 1.4488 | 0.4809 | 0.1114 |
| 6.0 | 1.9 | 20.1430 | 35.0950 | 32.2125 | 2.5089 | 2.3700 | 5.3052 | 1.8019 | 0.4599 | 0.1036 |
| 6.5 | 2.2 | 26.6622 | 27.0711 | 31.5877 | 2.8347 | 2.3527 | 6.5001 | 2.4351 | 0.4538 | 0.1026 |
| 7.0 | 2.1 | 26.2562 | 21.2378 | 35.6894 | 2.9832 | 4.4754 | 6.1338 | 2.6030 | 0.5108 | 0.1104 |
| 7.5 | 2.6 | 19.3918 | 17.7353 | 47.2645 | 3.7166 | 4.7794 | 3.8532 | 2.4207 | 0.6879 | 0.1507 |
| 8.0 | 2.8 | 12.6992 | 15.4290 | 59.4220 | 4.6200 | 2.7467 | 2.0848 | 1.8690 | 0.9347 | 0.1946 |
| | | | | | | | | | | |
| | | | | | | | | | | |

APPENDIX F

(List of publications resulting from this thesis)

List of papers

Keuler JN, Lorenzen L, et al., August 1997, Optimizing palladium conversion in electroless palladium plating of alumina membranes, *Plating and Surface Finishing*, pp. 34-40

Keuler JN, Lorenzen L, et al., 1997, Preparing and testing electroless palladium plated alumina membranes, SAICHe Conference, Cape Town, South Africa

Keuler JN, Lorenzen L, et al., Characterising electroless plated palladium-silver alloy membranes using SEM, XRD and PIXE, Submitted to *Catalysis Today* in October 1997

Presentations

Investigation into the use of composite membranes for organic reactions – Sasol workshop (Sasolburg), March 1997

Preparation and structural characterization of palladium composite membranes – Post graduate conference (Stellenbosch), 31 May 1997

The use of Pd/Pt plated composite membranes for organic reactions – Sasol Technology Symposium (RAU, Johannesburg), 17 July 1997